

**Ph.D. Program in Civil, Chemical and Environmental Engineering**  
**Curriculum in Chemical, Materials and Process Engineering**



Department of Civil, Chemical and Environmental Engineering  
Polytechnic School, University of Genoa, Italy.

**Spent coffee grounds valorization by green and innovative extraction technologies: process optimization and product stabilization for industrial purposes**

Margherita Pettinato



SPENT COFFEE GROUNDS VALORIZATION BY GREEN AND INNOVATIVE  
EXTRACTION TECHNOLOGIES: PROCESS OPTIMIZATION AND PRODUCT  
STABILIZATION FOR INDUSTRIAL PURPOSES

BY

MARGHERITA PETTINATO

*Dissertation discussed in partial fulfillment of  
the requirements for the Degree of*

DOCTOR OF PHILOSOPHY

*Civil, Chemical and Environmental Engineering  
curriculum Curriculum in Chemical, Materials and Process Engineering,  
Department of Civil, Chemical and Environmental Engineering, University of Genoa, Italy*



April, 2019

*Adviser:*

Prof. Patrizia Perego – Department of Civil, Chemical and Environmental Engineering, University of Genoa (Italy)

*External Reviewers:*

Prof. Elmira Arab-Tehrany – Department of Biotechnology, University of Lorraine (France)

Prof. Giancarlo Cravotto – Department of Drug Science and Technology, University of Turin (Italy)

*Examination Committee:*

Prof. Renzo Di Felice – Department of Civil, Chemical and Environmental Engineering, University of Genoa (Italy)

Prof. Giovanna Ferrari – Department of Industrial Engineering, University of Salerno (Italy)

Prof. Linda Barelli – Department of Engineering, University of Perugia (Italy)

Ph.D. program in Civil, Chemical and Environmental Engineering

*Curriculum in Chemical, Materials and Process Engineering*

*Cycle XXXI*

Malgrado tutto avevo fame di un significato nella vita.  
E adesso so che bisogna alzare le vele  
e prendere i venti del destino,  
dovunque spingano la barca.  
Dare un senso alla vita può condurre a follia  
ma una vita senza senso è la tortura  
dell'inquietudine e del vano desiderio  
è una barca che anela al mare eppure lo teme.

*Edgar Lee Master*

*(George Gray, Spoon River Anthology, 1916)*

## LIST OF FIGURES

- Figure 1.** Total production of coffee according to International Coffee Organization. Trade Statistics Table <http://www.ico.org/prices/new-consumption-table.pdf> (Accessed November 2<sup>nd</sup>, 2018) 23
- Figure 2.** Number of publications per year on Spent Coffee Grounds (SCG) and related topics by Science Direct database. Document search: ■ “SCG” ; ■ “SCG + biopolymers”; ■ “SCG + adsorbent”; ■ “SCG + biofuel”; ■ “SCG + antioxidant”; ■ “SCG + carbohydrates”. 29
- Figure 3.** Chemical Structure of Chlorogenic acid  
([https://pubchem.ncbi.nlm.nih.gov/compound/Neochlorogenic\\_acid#section=Top](https://pubchem.ncbi.nlm.nih.gov/compound/Neochlorogenic_acid#section=Top)) 31
- Figure 4.** Basic structure of melanoidins (Cämmerer et al., 2002) 32
- Figure 5.** Chemical Structure of caffeine  
(<https://pubchem.ncbi.nlm.nih.gov/compound/2519#section=Top>) 33
- Figure 6.** Example of a possible solution for spent coffee grounds-based biorefinery (adapted from Mata et al., 2018) 45
- Figure 7.** Composition of lipid fraction of exhaust coffee. Concentration of methyl esters (ME) of the corresponding fatty acids is expressed as g of Fatty Acid Methyl Ester (FAME) per 100 g of extracted lipids. 55
- Figure 8.** Cumulative function  $F(d)$  of the particle size distribution of dry SCG, obtained from sieving tests. Diameter values on x label correspond to the mean diameter of each sieve opening interval. 56
- Figure 9.** Ethos E Mileston Microwave Solvent Extractor 60

- Figure 10.** Calibration curve for Folin-Ciocalteu's assay obtained from standard solutions of caffeic acid. 61
- Figure 11.** Calibration curve for total flavonoid assay obtained from standard solutions of catechin. 62
- Figure 12.** Calibration curve for ABTS<sup>•+</sup> assay obtained from standard solutions of Trolox. 64
- Figure 13.** HPLC Agilent 1100 Series 65
- Figure 14.** Graphical representation of the main steps of the study on comparison between MAE and SLE 67
- Figure 15.** Box-Behnken Design representations 68
- Figure 16.** Total polyphenol yields, expressed as mg of caffeic acid equivalent per g of dried SCG, as a function of the extraction technique (■ MAE, ■ SLE) and solvent. 75
- Figure 17.** Total flavonoid yields, expressed as mg of catechin equivalent per g of dried SCG, as a function of the extraction technique (■ MAE, ■ SLE) and solvent. 76
- Figure 18.** Antiradical power of the extract, expressed as g of DPPH (2,2-Diphenyl-1-picrylhydrazyl) per L of extract, as a function of the extraction technique (■ MAE, ■ SLE) and solvent. 77
- Figure 19.** Three-dimensional surface plots of the quadratic regression equations obtained by the experimental design coupled with RSM. Responses are reported as function of the input variables as follow: a,b) total polyphenol yield (TP, mg of caffeic acid equivalent (CAE)/g of dried SCG (DS)); b,c) total flavonoid yield (TF, mg of catechin equivalent (CE)/g of dried SCG (DS); d,e) antiradical power (ABTS, µg of Trolox equivalent (TE)/L of extract), obtained by means of the ABTS<sup>•+</sup> ( 2,2'-azino-bis(3-ethylbenzothiazoline-6-sulphonic acid) ) assay. 82

**Figure 20.** HPLC chromatogram of extract 1, obtained by MAE with the following operating conditions: Temperature=150 °C, time= 90 min and water content in the solvent=46%. 85

**Figure 21.** Chlorogenic acid spectra obtained by HPLC-DAD analysis 85

**Figure 22.** Suspected chlorogenic acid isomer or derivative spectra, classified as compound 6, obtained by HPLC-DAD analysis. 85

**Figure 23.** Suspected chlorogenic acid isomer or derivative spectra, classified as compound 7, obtained by HPLC-DAD analysis. 86

**Figure 24.** Suspected chlorogenic acid isomer or derivative spectra, classified as compound 10, obtained by HPLC-DAD analysis. 86

**Figure 25.** Cell viability of SCG extract by MTS assay. Results are mean of three measurements  $\pm$  SD. # refers to statistically significant differences among results ( $p < 0.05$ , ANOVA with Tukey's multiple comparison test). □ control, ■ 0.005 mg<sub>CAE</sub>/mL<sub>extract</sub>, ■ 0.01 mg<sub>CAE</sub>/mL<sub>extract</sub>, ▨ 0.02 mg<sub>CAE</sub>/mL<sub>extract</sub>, ▩ 0.04 mg<sub>CAE</sub>/mL<sub>extract</sub>. 88

**Figure 26.** Cell culture multi-well at the first day of treatment (a) and after 8 days of treatment (b). 88

**Figure 27.** Temperature profiles imposed during MAE tests for kinetic evaluation. —set point temperature of 150°C after 10 min; – –set point temperature of 135°C after 10 min; ----- set point temperature of 120°C after 10 min. 89

**Figure 28.** Experimental total polyphenol concentration (mg of caffeic acid equivalent (CAE)/mL of extract) over time, as a function of the set point temperature: ■ 120°C; ♦ 135°C; ▲150°C. 90

**Figure 29.** Total polyphenol concentration (mg of caffeic acid equivalent (CAE)/mL of extract) over time, as a function of the set point temperature: ■ experimental data at



120°C; ♦ experimental data at 135°C; ▲ experimental data at 150°C.; - . - . Peleg's model at 120 °C; - - - Peleg's model at 135 °C; — Peleg's model at 150°C. 91

**Figure 30.** Expected values of concentration of total polyphenols, obtained by the model equation of extraction kinetic, versus the experimental data (observed values). 96

**Figure 31.** Extraction kinetic of total polyphenols. Experimental data, obtained by means of Folin-Ciocalteu's assay, are reported as a function of time and temperature (▲ 120 °C, ● 135 °C, ■ 150 °C) and are compared with Peleg's model : ••••• at 120 °C; — — at 135 °C; — at 150 °C. Figures: 31. a) is related to a heating time of 1 min; 31. b) is related to a heating time of 10 min; 31.c) is related to a heating time of 20 min. 97

**Figure 32.** Antiradical power of the extracts, measured by means of ABTS<sup>•+</sup> (2,2'-azino-bis-3-ethylbenzthiazoline-6-sulphonic acid) assay, as a function of time and temperature: ■ 120 °C, ■ 135 °C, □ 150 °C. Figures: 32. a) is referred to a heating time of 1 min; 32. b) is referred to a heating time of 10 min; 32.c) is referred to a heating time of 20 min. TE= Trolox Equivalent; t<sub>H</sub> = heating time. 100

**Figure 33.** Extract total solids, measured by means of gravimetric method, as a function of time and temperature: ■ 120 °C, ■ 135 °C, □ 150 °C. Figures: 33. a) is referred to a heating time of 1 min; 33. b) is referred to a heating time of 10 min; 33.c) is referred to a heating time of 20 min. t<sub>H</sub> = heating time. 102

**Figure 34.** a) Büchi Mini Spray Dryer B-290; b) dimensioning scheme of Büchi Mini Spray Dryer B-290. 106

**Figure 35.** Spray-dried powder moisture as a function of the composition of the wall material, expressed as percentage of Inulin (% wt) and as a function of the inlet suspension flow rate (mL/min). 110

**Figure 36.** Product Recovery as a function of the composition of the wall material, expressed as percentage of Inulin (% wt) and as a function of the inlet suspension flow rate (mL/min). 111

**Figure 37.** Encapsulation yield (mg<sub>CAE</sub>/g dried powder) obtained from spray drying tests over inlet suspension flow rate (mL/min) and carrier composition (I, % wt). 112

**Figure 38.** Encapsulation efficiency (mg<sub>CAE</sub>/g dried powder) obtained from spray drying tests over inlet flow rate (mL/min) and carrier composition (I, % wt). 113

**Figure 39.** a) Spray-dried powder obtained using 80% of inulin and a flow rate of 7.5 mL/min; b) SEM image of spray-dried powder obtained at 160 °C, using 80% of inulin, and a flow rate of 7.5 mL/min. 113

**Figure 40.** Stainless steel stirred reactor (Parr Instruments Company) used for High Temperature and Pressure-assisted extraction tests. 116

**Figure 41.** Sterilized media for *Saccharomyces cerevisiae* (front) and *Escherichia coli* (back) 120

**Figure 42.** Supercritical Antisolvent Extraction plant scheme. Adapted from Meneses et al. (2015) 124

**Figure 43.** Scheme of SuperLip plant 126

**Figure 44.** Calibration curve for modified total polyphenol determination protocol, obtained by ethanolic standard solution of caffeic acid. 128

**Figure 45.** Total polyphenol yields obtained by High Temperature and High Pressure-assisted extraction from SCG. ■ 180 °C; ■ 150 °C; □ 120 °C. Different letters do refer to statistically significant differences among results (p<0.05, T-test for independent samples). Data are reported as mg of caffeic acid equivalent (CAE) per g of dried SCG. 131

**Figure 46.** Total flavonoids yields obtained by High Temperature and High Pressure-assisted extraction from SCG. ■ 180 °C; ▒ 150 °C; □ 120 °C. Different letters do refer to statistically significant differences among results ( $p < 0.05$ , T-test for independent samples). Data are reported as mg of catechin equivalen (CE) per g of dried SCG. 131

**Figure 47.** Antiradical power obtained by High Temperature and High Pressure-assisted extraction from SCG. ■ 180 °C; ▒ 150 °C; □ 120 °C. Different letters do refer to statistically significant differences among results ( $p < 0.05$ , T-test for independent samples). DPPH= 2,2-diphenyl-1-picrylhydrazyl. 133

**Figure 48.** Results of HPTE carried out using ethanol 54% (v/v) as solvent and at 150 °C, at three extraction times. Different letters do refer to statistically significant differences among results ( $p < 0.05$ , T-test for independent samples). Data are reported per g of dried SCG or L of extract. 134

**Figure 49.** Comparison between experimental data (■) related to total polyphenol yields and the values calculated by equation 50(□). Data are reported as mg of caffeic acid equivalent (CAE) per g of dried SCG. 136

**Figure 50.** Evaluation by Petri's dishes of the *E.coli* growth in presence of freeze-dried extract dissolved into medium by means of dimethyl sulfoxide. CFU= colony forming units. Concentrations of extract are expressed as % (w/v). 138

**Figure 51.** Evaluation by Petri's dishes of the *S.cerevisiae* growth in presence of freeze-dried extract dissolved into medium by means of dimethyl sulfoxide. CFU= colony forming units. Concentrations of extract are expressed as % (w/v). 139

**Figure 52.** Evaluation by Petri's dishes of the *S.cerevisiae* growth in presence of extract encapsulated in maltodextrins by spray drying. CFU= colony forming units. Concentrations of extract are expressed as % (w/v). 141

**Figure 53.** Comparison among the control samples Peroxide Value (PV), expressed as mg of active oxygen (AO) per kg of extra virgin olive oil (EVO). □ EVO stored in the dark

and oxygen-free; ■ EVO+pure MD (10 %, w/v) stored in the dark and oxygen-free; ▣ EVO+ 10 % (w/v) encapsulated extract stored in the dark and oxygen-free. 142

**Figure 54.** Peroxide values of the samples exposed for 3 days to sunlight and saturated with pure oxygen. Concentration of encapsulated extract = 10% (w/v). 143

**Figure 55.** Peroxide values of the samples saturated with pure oxygen and incubated in the dark for 4 days. Concentration of encapsulated extract = 10% (w/v). 143

**Figure 56.** Peroxide values of the samples saturated with pure oxygen and incubated at 40 °C for 4 and 6 days. Concentration of encapsulated extract = 10% (w/v). □ EVO stored in the dark and oxygen-free; ■ EVO stored in the dark at 40 °C and saturated with pure oxygen; ▣ EVO+encapsulated extract stored in the dark at 40 °C and saturated with pure oxygen. 144

**Figure 57.** Peroxide values of the samples exposed for 3 days to sunlight and saturated with pure oxygen. Concentration of encapsulated extract = 1% (w/v). 145

**Figure 58.** Peroxide values of the samples saturated with pure oxygen and incubated in the dark for 4 days. Concentration of encapsulated extract = 1% (w/v). 146

**Figure 59.** Peroxide values of the samples saturated with pure oxygen and incubated at 40 °C for 4 and 6 days. Concentration of encapsulated extract = 1% (w/v). □ EVO stored in the dark and oxygen-free; ■ EVO stored in the dark at 40 °C and saturated with pure oxygen; ▣ EVO+encapsulated extract stored in the dark at 40 °C and saturated with pure oxygen. 146

**Figure 60.** a) Micronized powder collected at the end of SAE process and b) filter of the SAE plant. 148

**Figure 61.** FE-SEM images of the micronized powder obtained by SAE process. 149

**Figure 62.** a) Particle size distribution of blank sample (FCO.1) of liposomes, reported as liposome fraction (% by number) as a function of diameters; b) FE-SEM image of liposomes of blank sample (FCO.1) of liposomes. 150

**Figure 63.** Particle size distributions of liposomes from SuperLip process, loaded with extract obtained by HPTE from SCG. a) Results of samples obtained at 100 bar and concentration of fed extract of — 83 ppm, — 250 ppm, and — 500 ppm; b) results of samples obtained at 200 bar and concentration of fed extract of — 83 ppm, — 250 ppm, and — 500 ppm. 152

**Figure 64.** FE-SEM images of liposomes from SuperLip process, loaded with extract obtained by HPTE from SCG. a) Sample FC1 (P=100 bar, extract concentration=500 ppm); b) sample FC2 (P=100 bar, extract concentration=250 ppm); c) sample FC3 (P=100 bar, extract concentration=83 ppm); d) sample FC4 (P=200 bar, extract concentration=500 ppm); e) sample FC5 (P=200 bar, extract concentration=250 ppm); f) sample FC6 (P=100 bar, extract concentration= 83 ppm). 153

**Figure 65.** Encapsulation efficiencies of liposomes loaded with different concentrations of extract from SCG. □ Liposomes produced at 100 bar; ■ liposomes produced at 200 bar. 154

**Figure 66.** Antiradical power evaluated by ABTS assay of liposomes loaded with different concentrations of extract from SCG. □ Liposomes produced at 100 bar; ■ liposomes produced at 200 bar. 155

**Figure 67.** Scheme of the continuous pressurized ultrasound-assisted extraction plant. 159

**Figure 68.** Three-dimensional surface plot of the regression equations for total polyphenol yields obtained by the experimental design coupled with RSM. 163

**Figure 69.** Three-dimensional surface plot of the regression equations for antiradical power (ARP) obtained by the experimental design coupled with RSM. 165

**Figure 70.** Three-dimensional surface plot of the regression equation for extract total solids (ETS) obtained by the experimental design coupled with RSM. 167

## LIST OF TABLES

<b>Table 1.</b> Chemical composition of spent coffee grounds (Ballesteros et al., 2014)	26
<b>Table 2.</b> Standard solution of methyl ester fatty acids: composition and their retention time.	49
<b>Table 3.</b> Mole fraction solubility of caffeine in three solvents as a function of temperature. Adapted from Shalmashi and Golmohammad (2010).	51
<b>Table 4.</b> Results and statistic analysis of the characterization of Spent Coffee Grounds (SCG) and roasted coffee beans (RCB). SD= standard deviation; N= number of valid tests.	52
<b>Table 5.</b> Metal concentrations in Spent Coffee Grounds. N= number of valid tests; SD= standard deviation; nd= not detected.	53
<b>Table 6.</b> Operating conditions of the extraction tests on Spent Coffee Grounds by solid-liquid extraction (SLE) and microwave-assisted extraction (MAE).	66
<b>Table 7.</b> Physical properties of methanol, ethanol and water. <sup>a</sup> (Veggi et al., 2013); <sup>b</sup> (González et al., 2004); <sup>c</sup> (Sabir et al., 1974).	67
<b>Table 8.</b> Independent variables and their levels employed in the Box Behnken Design for optimization of SCG extraction.	68
<b>Table 9.</b> Input variable values of the Box Behnken Design of experiments and experimental results in terms of: total polyphenols yield (TP), expressed as mg of caffeic acid equivalent (CAE)/g of dried SCG; total flavonoid yield (TF), expressed as as mg of catechin equivalent (CE)/g of dried SCG; antiradical power (ARP) by ABTS <sup>•+</sup> assay, expressed as $\mu\text{g}$ of Trolox equivalent (TE)/L of extract and by DPPH <sup>•</sup> assay, expressed as g of DPPH per L of extract.	78

**Table 10.** Analysis of variance table (Partial sum of squares - Type III) for Response Surface Reduced Quadratic Model of the output variable total polyphenol yield (TP). 79

**Table 11.** Analysis of variance table (Partial sum of squares - Type III) for Response Surface Reduced Quadratic Model of the output variable total flavonoid yield (TF). 80

**Table 12.** Analysis of variance table (Partial sum of squares - Type III) for Response Surface Reduced Quadratic Model of the output variable antiradical power (ARP). 81

**Table 13.** Comparison among the experimental value of dependent variables and RSM model prediction, obtained by the numerical optimization tool of Design Expert. TP: Total polyphenol yield (mg of caffeic acid equivalent (CAE)/g of dried SCG); TF: total flavonoid yield (mg of catechin equivalent (CE)/g of dried SCG); ARP: antiradical power ( $\mu\text{g}$  of Trolox equivalent (TE)/L of extract). 83

**Table 14.** HPLC analysis of the two extracts obtained using the following operating conditions: Temperature=150 °C, time=90 min, ethanol/water 54:46 (v/v) (Extract 1); Temperature=150 °C, time = 85 min, ethanol/ water 32:68 (v/v) (Extract 2). \* percentages of the total area = 7541 mAU min; \*\* percentages of the total area = 4972 mAU min 84

**Table 15.** Parameters of the proposed extraction kinetic models and comparison. \* Calculated using the mean diameter of particle size distribution. 90

**Table 16.** Values of Peleg's model coefficients for the polyphenol extraction kinetic. CAE= caffeic acid equivalent;  $1/K_1$ = initial rate of the extraction curves;  $C|_{t \rightarrow \infty}$  = polyphenol concentration at infinite time, expressed as mg of caffeic acid equivalent (CAE) per mL of extract;  $R^2$  = coefficient of determination. 92

**Table 17.** Values of the model coefficients of equation 40. 95

**Table 18.** Values of the two input variables at the corresponding design level 107

**Table 19.** Operating conditions used for experimental tests of HPTE 117

<b>Table 20.</b> Operating conditions for encapsulation of SCG extract obtained by HPTE	119
<b>Table 21.</b> Operating conditions of SAE experiments.	125
<b>Table 22.</b> Operating conditions and variables for the tests on extract encapsulation into liposomes.	127
<b>Table 23.</b> Characterization of the extract obtained by HPTE (150°C, 7.2 bar, 60 min, ethanol 54% (v/v)). CAE= caffeic acid equivalent; CE= catechin equivalent; TE= trolox equivalent; DPPH=2,2-diphenyl-1-picrylhydrazyl; ABTS= 2,2'-azino-bis(3-ethylbenzothiazoline-6-sulphonic acid); SCG=spent coffee grounds.	136
<b>Table 24.</b> Characterization of HPTE extract encapsulated into maltodextrins by spray drying.	140
<b>Table 25.</b> Characterization of SAE process feed. CAE=caffeic acid equivalent; TE=trolox equivalent.	147
<b>Table 26.</b> Micronized power characterization and liquid fraction characterization. CAE=caffeic acid equivalent; TE=trolox equivalent.	148
<b>Table 27.</b> Results of the Dynamic Light Scattering analysis on the samples of liposomes from the SuperLip process. PDI=polydispersity index.	151
<b>Table 28.</b> Independent variables and their levels employed in the Box Behnken Design for the optimization of extraction from SCG.	160
<b>Table 29.</b> Total polyphenols content of the extracts obtained by continuous pressurized ultrasound-assisted extraction. CAE=caffeic acid equivalent.	162
<b>Table 30.</b> Analysis of variance table (Partial sum of squares - Type III) for Response Surface Reduced Quadratic Model of the output variable total polyphenol yield (TP).	162



**Table 31.** Antiradical power (ARP) of the extracts obtained by continuous pressurized ultrasound-assisted extraction, evaluated by ABTS<sup>•+</sup> assay . TE=trolox equivalent. 164

**Table 32.** Analysis of variance (Partial sum of squares - Type III) for Response Surface Reduced Quadratic Model of the output variable antiradical power (ARP). 164

**Table 33.** Extract total solids (ETS) of the extracts obtained by continuous pressurized ultrasound-assisted extraction. 166

**Table 34.** Analysis of variance (Partial sum of squares - Type III) for Response Surface Reduced Quadratic Model of the output variable extract total solids (ETS). 166

**Table 35.** Comparison among the extracts obtained under the optimized operating conditions of the non-conventional extraction techniques . TP= total polyphenol yield; ARP= antiradical power; ETS= extract total solids; CAE= caffeic acid equivalent; TE= trolox equivalent; L/S= liquid to solid ratio; t<sub>H</sub>=heating time. 170

## NOMENCLATURE

a	Model parameter
A	Model parameter
AA FS	Fast sequential atomic absorption spectrometer
ABS	Absorbance
ABTS <sup>•+</sup>	2,2'-azino-bis(3-ethylbenzothiazoline-6-sulphonic acid)
AdjR <sup>2</sup>	Adjusted coefficient of determination
ANOVA	Analysis of variance
ARP	Antiradical power
atm	Atmosphere
b	Model parameter
B	Model parameter
BBD	Box-Behnken design
C	Polyphenol concentration
<i>C</i>	Model parameter
CAE	Caffeic acid equivalent
C <sub>calc</sub>	Polyphenol concentration calculated by model
C <sub>DPPH</sub>	Concentration of DPPH
CE	Catechin equivalent
C <sub>exp</sub>	Polyphenol concentration experimentally measured
CFU	Colony forming unit
CI	Confidence interval
cP	Centipoise
CPUAE	Continuous pressurized ultrasound-assisted extraction
C <sub>TF</sub>	Total flavonoid concentration
C <sub>Trolox</sub>	Concentration of Trolox Equivalent
C <sub>0</sub>	Concentration of polyphenol at t=0
C <sub>∞</sub>	Concentration of polyphenol at infinite time
d	Diameter
<i>D</i>	Diffusion coefficient
DE	Dextrose equivalent
<i>D<sub>eff</sub></i>	Apparent diffusion coefficient
df	Degree of freedom
d <sub>j</sub>	Arithmetic mean of two sieve openings
DLS	Dynamic Light Scattering
DMEM	Dulbecco's modified eagle medium
DPPH <sup>•</sup>	Radical 2,2-diphenyl-1-picrylhydrazyl
D'	Constant
E <sub>A</sub>	Activation energy
EE	Encapsulation efficiency
E <sub>F</sub>	Electric field strength
EC <sub>50</sub>	Half maximal effective concentration
ETP	Encapsulated total polyphenols
ETS	Extract total solids
EVO	Extra virgin olive oil

EY	Encapsulation yield
E'	Constant
f	frequency
F	F-statistic
FAME	Fatty acid methyl ester
FBS	Fetal bovine serum
F(d)	Cumulative function of the particle size distribution
FE-SEM	Field –emission scanning electron microscopy
FR	Flow rate
FTP	total polyphenols fed to the Superlip process
F'	Constant
g	grams
GAE	Gallic acid equivalent
GC/FID	Gas chromatograph with flame ionization detector
$\overline{g(d)}$	Mean value of the distribution as a function of diameters
GHz	Gigahertz
g'	Model parameter
h	Hour
HMF	Hydroxymethylfurfural
HPLC	High Performance Liquid Chromatography
HPLE	Hot pressurized liquid extraction
HPTE	High pressure and temperature-assisted extraction
h'	Model constant
I	Inulin concentration
I.C.	Initial condition
i'	Model constant
K	Kelvin
$K$	Constant
$K_0$	Constant
$k_{obs}$	Overall rate constant of the first order kinetic model
$k_{II}$	Second order extraction rate constant
$k_1, K_1$	Peleg's model parameter
$k_2, K_2$	Peleg's model parameter
m	Mass
M	Molarity
MAE	Microwave-assisted extraction
MD	Maltodextrins
ME	Methyl ester
mg	Milligrams
Min	Minimum
min	Minutes
mL	Milliliters
MTS	3-(4,5-dimethylthiazol-2-yl)-5-(3-carboxymethoxyphenyl)-2-(4-sulfophenyl)-2H-tetrazolium, inner salt
nm	Nanometers
P	Microwave dissipation per volume unit

P	Pressure
PLE	Pressurized liquid extraction
ppm	Parts per million
PR	Product recovery
PTFE	Polytetrafluoroethylene
PV	Peroxide value
r	Radial coordinate
R	Radius
$R^2$	Coefficient of determination
RCB	Roasted coffee beans
RCS	Reactive chlorine species
$R_g$	Universal gas constant (8.314 kJ/ mol K)
RMSD	Root mean square deviation
RNS	Reactive nitrogen species
ROS	Reactive oxygen species
RSM	Response surface methodology
SAE	Supercritical antisolvent extraction
SCG	Spent coffee grounds
SD	Standard deviation
SLE	Solid-liquid extraction
SPC	Superficial polyphenol content
T	Temperature
t	Time
TE	Trolox equivalent
TF	Total flavonoids
$T_g$	glass transition temperature
$t_H$	Heating time
$T_M$	Exact molarity of the sodium thiosulphate solution
TP	Total polyphenols
TPC	Total polyphenol content
$t_0$	Washing time
UAE	Ultrasound-assisted extraction
v	Volume
W	Watt
$W$	Water content in the solvent
wt	Weight
YPD	Yeast Extract Peptone Dextrose medium
$Y_{50}$	50% of the DPPH• radical content
$\alpha_0, \alpha_i, \alpha_{ii}, \alpha_{ij}$	Model constants
$\delta$	Dissipation factor
$\varepsilon$	particle porosity
$\varepsilon'$	Dielectric constant
$\mu\text{g}$	micrograms
$\mu\text{L}$	microliters
$\rho$	Density
$\tau$	Tortuosity

$\chi_j$   
°CMass fraction  
Celsius degree

## ABSTRACT

The valorization of agro-industrial wastes represents a huge advantage for the transformation industry and the environment. Particularly, biomasses like spent coffee grounds are largely produced worldwide by coffee-based industries and do not require any pre-treatment for their use as raw material for extraction processes. Indeed, exhaust coffee grounds are usually collected in separated containers, either in coffee shops either in vending machines and are already in powder form. Several authors, analyzing chemical composition of spent coffee grounds, demonstrated their potential use as natural source of antioxidants, which are molecules that can find several applications in food, pharmaceutical and cosmetic industries. In the first chapter of this work, a brief introduction on the biorefinery concept and proposed reuses of spent coffee grounds, based on literature data, were exposed, focusing the attention on the main valuable step of a potential biorefinery based on coffee: the recovery of high added-value compounds from exhaust coffee by green and innovative techniques and methods finalized to preserve their bioactivity.

The antioxidant activity of spent coffee grounds can be traced back to polyphenols, like chlorogenic acid and its isomers, its derivatives, and melanoidins. The antioxidant activity and type of antioxidants that are recoverable from exhaust coffee powder, as well as its chemical composition, are functions of the type of raw material (e.g. *Coffea arabica*, *Coffea canephora*), but also the brewing process used for beverage preparation. In this thesis, spent coffee grounds collected by common vending machines, were subjected to a preliminary characterization, whose results were reported in chapter 2, and to a study on different extraction techniques (solid-liquid extraction, high- pressure and temperature-assisted extraction, microwave-assisted extraction and continuous pressurized ultrasound-assisted extraction), solvents, and operating conditions.

Indeed, one of the main aims of this research project was to perform the antioxidant recovery from SCG by using green solvents as water-ethanol solutions and to improve

the extraction yields by working on the other process variables. A study on the recovery of antioxidants by microwave-assisted extraction was carried out in chapter 3, evaluating process optimization, extraction kinetics and the potential use of the extract for cosmetic purposes. For the study, both response surface modeling and kinetic studies were employed as tools for process optimization and the extracts were evaluated in terms of total polyphenol yield, total flavonoid yield and antiradical power. Chapter 5 deals with the utilization of high pressure and temperature-assisted extraction for antioxidant recovery from spent coffee grounds, while continuous pressurized ultrasound-assisted extraction results were reported in chapter 6.

Since antioxidants are subjected to loss of activity when exposed to heat, light, and oxygen, novel and green post-processing (freeze-drying and supercritical antisolvent extraction) and microencapsulation techniques were used for antioxidant activity preservation, and to enhance product features. Thus, spray drying was employed to micro-encapsulate spent coffee grounds extracts using both inulin and maltodextrins as wall materials suitable for food application purposes. Encapsulation was optimized (chapter 4) by investigating process parameters like coating agent composition, inlet temperature, feed flow rate, using response surface methodology. In addition, different preservation techniques, finalized to prevent loss of activity and improve extract bioavailability were evaluated in chapter 5, where also a novel technique, supercritical fluid-assisted liposome formation (SuperLip), was tested for the encapsulation of the produced extracts in liposomes.

## INDEX

<b>LIST OF FIGURES</b> .....	1
<b>LIST OF TABLES</b> .....	9
<b>NOMENCLATURE</b> .....	13
<b>ABSTRACT</b> .....	17
<b>INDEX</b> .....	19
<i>Chapter 1</i> .....	23
<b>INTRODUCTION</b> .....	23
1.1    BIOREFINERY CONCEPT BASED ON SPENT COFFEE GROUNDS .....	23
1.1.1    Spent coffee grounds: an agro-industrial waste?.....	23
1.1.2    Proposed reuses of spent coffee grounds .....	25
1.2    ANTIOXIDANT RECOVERY FROM SPENT COFFEE GROUNDS .....	29
1.2.1    Antioxidants .....	29
1.2.1    Bioactive molecules in spent coffee grounds .....	30
1.3    EXTRACTION TECHNIQUES FOR ANTIOXIDANT RECOVERY .....	33
1.3.1    Solid-Liquid Extraction .....	35
1.3.1    Microwave-Assisted Extraction (MAE).....	35
1.3.2    High Pressure and Temperature- assisted Extraction (HPTE).....	37
1.3.3    Ultrasound-Assisted Extraction (UAE) .....	38
1.4    POST-PROCESSING AND ENCAPSULATION OF BIOACTIVE COMPOUNDS .....	39
1.4.1    Freeze-drying.....	40
1.4.2    Supercritical Anti-Solvent technique.....	40
1.4.3    Spray drying .....	41
1.4.4    Liposomes .....	42
<i>Chapter 2</i> .....	46
<b>CHEMICO-PHYSICAL CHARACTERIZATION OF SPENT COFFEE GROUNDS</b> .....	46
2.1    ABSTRACT.....	46
2.2    MATERIAL AND METHODS.....	46
2.2.1    Spent coffee grounds.....	46
2.2.2    Moisture.....	47
2.2.3    Ashes .....	47
2.2.4    Particle size distribution .....	47
2.2.5    Lipid extraction and analysis.....	48
2.2.6    Particle real density.....	49



2.2.7	Caffeine content .....	50
2.2.8	Metal content .....	51
2.2.9	Calorific value .....	51
2.3	RESULTS AND DISCUSSION .....	52
2.4	CONCLUSIONS .....	56
<i>Chapter 3</i> .....		58
<b>MICROWAVE-ASSISTED EXTRACTION OF ANTIOXIDANTS FROM SPENT COFFEE GROUNDS</b> .....		58
3.1	ABSTRACT .....	58
3.2	MATERIAL AND METHODS .....	59
3.2.1	Analytical methods and equipments .....	59
3.2.1.1	Solid-Liquid extraction .....	59
3.2.1.2	Microwave-assisted extraction equipment .....	59
3.2.1.3	Total polyphenol content .....	60
3.2.1.4	Total flavonoid content .....	61
3.2.1.5	DPPH• assay .....	62
3.2.1.6	ABTS•+ assay .....	63
3.2.1.7	Extract total solids .....	64
3.2.1.8	High Performance Liquid Chromatography (HPLC) .....	64
3.2.1.9	Cytotoxicity evaluation .....	65
3.2.2	Preliminary comparison between MAE and SLE .....	66
3.2.3	Microwave-assisted extraction optimization by RSM .....	67
3.2.4	Kinetic study on microwave-assisted extraction .....	69
3.2.5	Study on the effects of heating steps in microwave-assisted extraction of polyphenols from SCG .....	73
3.3	RESULTS AND DISCUSSION .....	74
3.3.1	Preliminary comparison between microwave-assisted extraction and solid liquid extraction .....	74
3.3.2	Microwave-assisted extraction optimization by RSM .....	77
3.3.3	Cytotoxicity evaluation of the extract .....	87
3.3.4	Kinetic model evaluation .....	88
3.3.5	Study on the effect of heating time in MAE of antioxidants from SCG .....	91
3.3.5.1	Effects on the extraction of polyphenols .....	92
3.3.5.2	Effects on antiradical power of the extracts .....	99
3.3.5.3	Effects on global extraction .....	101

3.4	CONCLUSIONS .....	103
<i>Chapter 4</i> .....		105
<b>ENCAPSULATION OF ANTIOXIDANTS FROM MAE EXTRACTS BY SPRAY DRYING</b>		
.....		105
4.1	ABSTRACT.....	105
4.2	MATERIAL AND METHODS.....	105
4.2.1	Antioxidant extraction by microwave-assisted extraction and inlet suspension preparation.....	105
4.2.2	Spray drying apparatus and encapsulation tests.....	106
4.2.3	Analytical methods .....	107
4.2.3.1	Moisture content evaluation .....	107
4.2.3.2	Encapsulation yield.....	108
4.2.3.3	Product recovery .....	108
4.2.3.4	Encapsulation efficiency .....	109
4.2.3.5	Particle size distribution.....	109
4.3	RESULTS AND DISCUSSION .....	109
4.4	CONCLUSIONS .....	114
<i>Chapter 5</i> .....		115
<b>HIGH TEMPERATURE AND PRESSURE-ASSISTED EXTRACTION AND POST-PROCESSING GREEN TECHNIQUES FOR ANTIOXIDANT RECOVERY FROM SPENT COFFEE GROUNDS</b>		
.....		115
5.1	ABSTRACT.....	115
5.2	MATERIAL AND METHODS.....	116
5.2.1	High temperature and pressure-assisted extraction equipment.....	116
5.2.2	Evaluation of process parameters .....	116
5.2.3	Analytical methods .....	117
5.2.4	Freeze-drying.....	118
5.2.5	Encapsulation by spray drying.....	118
5.2.6	Antimicrobial activity evaluation.....	119
5.2.6.1	Microorganism preparation .....	119
5.2.6.2	Evaluation of microbial growth by Petri's dishes in presence of freeze-dried extract.....	120
5.2.6.3	Evaluation of microbial growth by Petri's dishes in presence of encapsulated extract.....	121
5.2.7	Evaluation of the lipid peroxidation inhibition .....	122

5.2.8	Supercritical Antisolvent Extraction for extract micronization .....	123
5.2.9	Encapsulation of HTPE extract in liposomes by Supercritical-assisted Liposome formation plant .....	125
5.2.9.1	Encapsulation efficiency evaluation.....	127
5.2.9.2	Antiradical power evaluation .....	129
5.2.9.3	Particle size distribution.....	129
5.2.9.4	Liposome morphology .....	129
5.3	RESULTS AND DISCUSSION .....	130
5.3.1	High Temperature and Pressure-assisted extraction .....	130
5.3.2	Freeze-dried extract antimicrobial activity .....	137
5.3.3	Analysis of encapsulated extract into maltodextrins (MD) by spray-drying .....	139
5.3.3.1	Antimicrobial activity .....	140
5.3.3.2	Evaluation of the lipid peroxidation inhibition.....	141
5.3.4	Supercritical Antisolvent extraction for extract micronization .....	147
5.3.5	Encapsulation of HTPE extract in liposomes by supercritical fluid-assisted liposome formation plant.....	149
5.4	CONCLUSIONS .....	155
Chapter 6	.....	158
<b>CONTINUOUS PRESSURIZED ULTRASOUND-ASSISTED EXTRACTION .....</b>		<b>158</b>
6.1	ABSTRACT.....	158
6.2	MATERIAL AND METHODS.....	158
6.2.1	Continuous pressurized ultrasound-assisted extraction system .....	158
6.2.2	Continuous pressurized ultrasound-assisted extractions and experimental design.....	159
6.2.3	Analytical methods .....	160
6.3	RESULTS AND DISCUSSION .....	161
6.3.1	Total polyphenol yield.....	161
6.3.2	Antiradical power.....	163
6.3.3	Extract total solids .....	165
6.4	CONCLUSIONS .....	168
<b>CONCLUSIONS.....</b>		<b>169</b>
<b>REFERENCES .....</b>		<b>173</b>

## Chapter 1

### INTRODUCTION

#### 1.1 BIOREFINERY CONCEPT BASED ON SPENT COFFEE GROUNDS

##### 1.1.1 Spent coffee grounds: an agro-industrial waste?

Spent coffee grounds (SCG) are one the main waste of the coffee-based product industry and the huge consumption of coffee in Europe (51860 in thousand 60 kg bags in 2016/2017), as well as in the entire world (157858 in thousand 60 kg bags in 2016/2017)(International coffee organization, 2017), makes the potential reuse of this biomass very interesting.

Indeed, coffee is the second largest traded commodity after petroleum (Mussatto et al., 2011c) and, according to the International Coffee Organization, the total production by all exporting countries in 2017 was of 159375 in thousand 60 kg bags, showing a continuous increasing over the last years (figure 1) as well as coffee consumption with a 1.3% average annual growth rate (Mata et al., 2018), generating enormous amounts of solid residues.

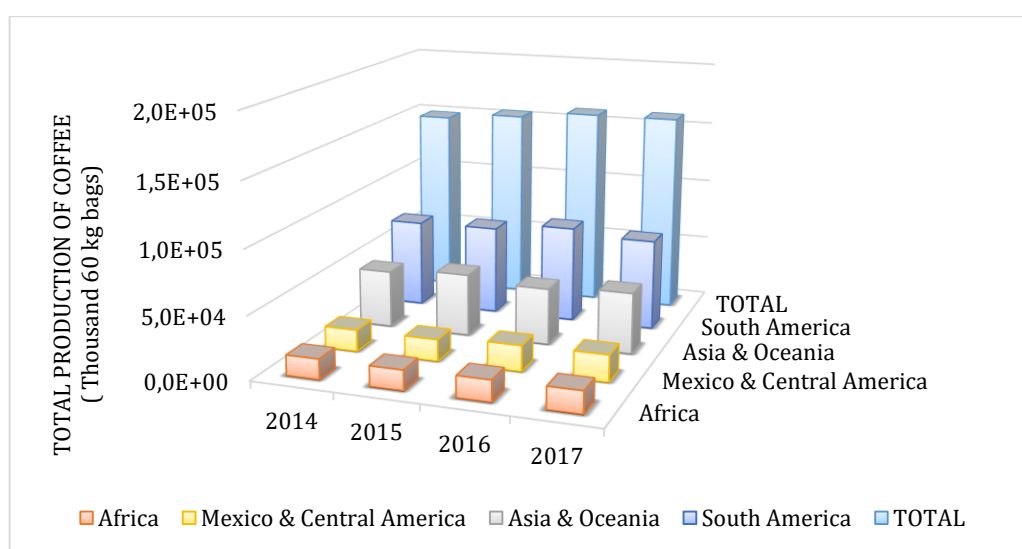


**Figure 1.** Total production of coffee according to International Coffee Organization. Trade Statistics Table <http://www.ico.org/prices/new-consumption-table.pdf> (Accessed November 2<sup>nd</sup>, 2018)

During the primary processing to obtain the green coffee, large amounts of by-products are generated, since green coffee bean of international commerce constitutes only 50-55% of the dry matter of the ripe cherry (Adams and Dougan, 1987). The main by-product from the green coffee dry processing is the coffee husk. It is made by the dried skin, pulp and parchment; from a chemico-physical point of view, it is composed by 15.0 % of moisture, 5.4 - 6.2 % of ashes, 7.0 % of protein, 0.3 % of lipids and 72.3 % of carbohydrates (24.5 % cellulose, 29.7 % hemicelluloses, 23.7 % lignin) (Murthy and Naidu, 2012). Instead, in the wet method, the main by-products are the coffee pulp and the coffee parchment husk. The former contains carbohydrates, proteins, minerals, tannins, polyphenols and caffeine (Murthy and Naidu, 2012). Another important by-product is coffee silver skin, which is a thin tegument of the outer layer of green coffee beans obtained as a residue of the roasting process and represents about 4.2 % (w/w) of coffee beans (Ballesteros et al., 2014). SCG are obtained after the brewing process and it was estimated that 650 kg of SCG per ton of green coffee bean are generated and around six millions tons per year at industrial scale, with strong national variations (Mata et al., 2018). They are the by-products that mostly are catching the attention of the scientific literature, even if several solutions for the reusing of all the previously listed residues of coffee industry were proposed in numerous papers in the last years (Anastopoulos et al., 2017; Berhe et al., 2015; Esquivel and Jiménez, 2012; Murthy and Naidu, 2012; Mussatto et al., 2011; Oliveira et al., 2008; Rodrigues et al., 2015).

As known, SCG have no any commercial value and usually are sent to compost facilities (Zuorro and Lavecchia, 2012) or discarded as solid waste, implying environmental contamination potential due to the content of caffeine, tannins and polyphenols (Mata et al., 2018). Indeed, the content of these compounds in soil can be strongly increased when SCG are applied and they resulted as toxic for several plants (Cervera-Mata et al., 2017), since are able to inhibit plant growth (Yamane et al., 2014). In addition, as reported by Fernandes et al. (2017), coffee waste may induce mutagenicity in different strains when disposed in landfills, causing DNA damage and presenting toxicity to aquatic organisms. Lastly, pollutant effects of SCG are due to the high organic load that implies a huge demand of oxygen to be degraded (Silva et al., 1998). Similarly to the case of olive mill wastewater, the high oxygen demand of SCG and the presence of

phytotoxic and antibacterial polyphenols can represent a serious pollution risk for the soil and aqueous organisms (Mekki et al., 2007). The European legislation is strongly promoting the reduction of waste generation by stimulation of innovation in recycling and reuse, but also encouraging the transformation of waste into a major, reliable source of raw materials, in order to recover energy only from non-recyclable materials and virtually to eliminate landfilling. Indeed, turning waste into a resource is one of the main aims in circular economy systems (The European Commission, 2014). At the moment being, in Europe SCG are generally incinerated or disposed in landfills and, in the last case, the rich presence of polyphenols and caffeine could represent a source of pollution (Mata et al., 2018). On the contrary, SCG reuse could reduce the environmental impact of the waste and, at the same time, provide by-products with high value for pharmaceutical, food and cosmetic industries.

#### 1.1.2 Proposed reuses of spent coffee grounds

SCG is an abundant and low cost by-product of food industry that presents the advantage of being already in powder form and its rich chemistry and physical properties make it suitable for different solutions of integrated biorefinery, according to the “zero waste approach”. Indeed, spent coffee grounds present a porous and homogenous structure with deep pores (Azouaou et al., 2010). Several surface groups have been found by Pujol et al. (2013), such as -OH groups and -NH functional groups; they observed the presence of methyl and methylene groups, (C=O) groups of aliphatic esters, C=C groups belonging to lipid, fatty acids and aromatic rings, groups attributed to chlorogenic acids as well as groups attributed to polysaccharides. An example of spent coffee grounds composition has been provided by Ballesteros, Teixeira and Mussatto (2014) and reported in table 1, but the composition could change a lot basing on the variety of coffee (Arabica, Robusta, etc.), the roasting process and the brewing method used to prepare the famous beverage (Ludwig et al., 2012; Kučera et al., 2016; Moon, Hyui Yoo and Shibamoto, 2009; Jeszka-Skowron, Stanisław and De Peña, 2016; Mussatto et al., 2011).

**Table 1.** Chemical composition of spent coffee grounds (Ballesteros et al., 2014)

Chemical compound	Composition (g/100g dry material)	Mineral elements	Composition (mg/kg dry material)
Cellulose (Glucose)	12.40±0.79	Potassium	11700±0.01
Hemicellulose	39.10±1.94	Calcium	1200±0.00
Arabinose	3.60±0.52	Magnesium	1900±0.00
Mannose	19.07±0.85	Sulfur	1600±0.00
Galactose	16.43±1.66	Phosphorus	1800±0.00
Xylose	n.d.	Iron	52.00±0.50
Lignin	23.90±1.70	Aluminum	22.30±3.50
Insoluble	17.59±1.56	Strontium	5.90±0.00
Soluble	6.31±0.37	Barium	3.46±0.05
Fat	2.29±0.30	Copper	18.66±0.94
Ashes	1.30±0.10	Sodium	33.70±8.75
Protein	17.44±0.10	Manganese	28.80±0.70
Nitrogen	2.79±0.10	Boron	8.40±1.10
Carbon/nitrogen ratio	16.91±0.10	Zinc	8.40±0.20
Total dietary fiber	60.46±2.19	Cobalt	15.18±0.05
Insoluble	50.78±1.58	Iodine	< 0.10
Soluble	9.68±2.70	Nickel	1.23±0.59
		Chromium	<0.54
		Molybdenum	<0.08
		Vanadium	<0.29
		Lead	<1.60
		Selenium	<1.60
		Gallium	<1.47
		Tin	<1.30
		Cadmium	<0.15

n.d. = not detected

The chemico-physical features of SCG led to several proposals for spent coffee grounds reusing. Sometimes, SCG is directly used in the coffee industry plants as solid fuel because of its high calorific value (about 20920 kJ/kg) (Mussatto et al., 2011c). Nevertheless, the SCG high calorific value allows the direct use of SCG for bio-syngas production, as was reported by Ramos et al. (2016), who demonstrated the feasibility of steam gasification, performed at 1 bar, temperatures between 650 and 850 °C and steam partial pressure between 0.05 and 0.3 bar. In addition, the potential of SCG as a carbon-neutral fuel for the sustainable generation of electricity in fuel cells was demonstrated, using high-temperature carbon fuel cell technology. The presence of hetero-atoms and hydrogen in SCG proved to be crucial for this purpose, leading to gasification reactions and formation of oxidizable compounds (Kourmentza et al., 2018). Biogas production was reported by several authors during the last decades by anaerobic digestion of SCG and co-digestion with other waste (Mata et al., 2018; Murthy and Naidu, 2012), as well as bioethanol production by acid, base and enzyme catalyzed hydrolysis followed by fermentation of the small sugars (mannose, galactose, glucose, arabinose, and cellobiose) (Kovalcik et al., 2018), obtained starting from great amount of carbohydrates contained in spent coffee grounds (Ballesteros et al., 2014; Burniol-Figols et al., 2016; Campos-Vega et al., 2015; Kourmentza et al., 2018; Valderez et al., 2014).

Furthermore, SCG are composed by the 10-20 % on dry weight basis of lipids (Campos-Vega et al., 2015), whose triglycerides, diterpene alcohol esters and fatty acids are the major lipid classes (Kovalcik et al., 2018). SCG oils consist predominantly of linoleic, palmitic, stearic, oleic arachidic and linolenic acids, but the composition is strongly dependent on the variety of coffee and extraction procedure. Kondamudi et al. (2008) proved that SCG can be used as raw material for oil extraction, which was converted by transesterification in biodiesel, rich in methyl esters of palmitic, linoleic and stearic acids. In addition, after oil extraction, due to the suitable Carbon to Nitrogen ratio (about 20:1) of SCG, the further application as compost was proposed by the same authors. Similarly, biodiesel from SCG was obtained also by a two-step transesterification process (Al-Hamamre et al., 2012), ultrasound-assisted process (Valderez et al., 2014) *in situ* extraction and transesterification with supercritical



methanol (Calixto et al., 2011). Bio-oil suitable for biodiesel production was also obtained by pyrolysis of SCG, according to what reported by Li et al. (2014). Biochar products between 25–40 % wt and with a calorific value of 31.9 MJ/kg were obtained by Tsai et al. (2012), who, by pyrolysis, overcame the drawbacks related to the direct use of SCG as solid fuel, which include large bulk volume, high moisture content, low energy density, hygroscopic nature, and smoke during combustion.

Moreover, coffee residues represent a promising material for metal removal, not only because are able to uptake metal species on their surface by several mechanisms, such as ion-exchange (Berhe et al., 2015; Cerino-Córdova et al., 2013; Davila-Guzman et al., 2016; Gomez-Gonzalez et al., 2016; Kaikake et al., 2007), electrostatic forces (Azouaou et al., 2010; Boonamnuyvitaya et al., 2004), complexation (Serrano-Gomez et al., 2015), chemisorption (Oliveira et al., 2008), but also because they allow an easy regeneration, as demonstrated by Davila-Guzman et al. (2016) for a fixed-bed column packed with SCG. Chavan et al. (2016), for instance, utilized SCG as active filler for the formation of bioelastomeric composite foams for water remediation; the hydrophilic foam was fabricated using the sugar leaching technique. Instead, Boudrahem, Aissani-Benissad and Aït-Amar (2009) prepared activated carbon from coffee residue by means of impregnation with zinc chloride ( $\text{ZnCl}_2$ ) at 85 °C for 7 hours, followed by mixture, drying and carbonization at 600 °C under nitrogen flow, while Kim et al. (2014) proposed the preparation of a biochar by means of heating SCG up to 400 °C for 30 minutes. A similar procedure can be carried out by putting in contact a formaldehyde solution with coffee waste, in order to avoid the desorption of color component of coffee, followed by the addition of urea, ammonium nitrate ( $\text{NH}_4\text{NO}_3$ ) and deionized water and by a thermal treatment at 600–900 °C (Serrano-Gomez et al., 2015); while Lamine et al. (2014) reported the preparation of activated adsorbent starting from coffee ground by impregnation with phosphoric acid ( $\text{H}_3\text{PO}_4$ ) and drying at 110 °C. Magnetic SCG were prepared by Safarik et al. (2012) for dyes adsorption; this new type of biocomposite materials has the great advantage of being easily separated by means of commercially available magnetic separators or strong permanent magnets.

For these reasons, several proposal for biorefineries based on spent coffee grounds were suggested by the scientific literature, since the attention on the reuse of this waste

is subjected to a continuous growth, as demonstrated by the huge increase of the publications (figure 2) during the last decades about this topic. In addition, new and more valuable applications were developed, in order to recover and employ the added-value compounds contained in SCG, before their use for energetic and environmental purposes, following the waste hierarchy.

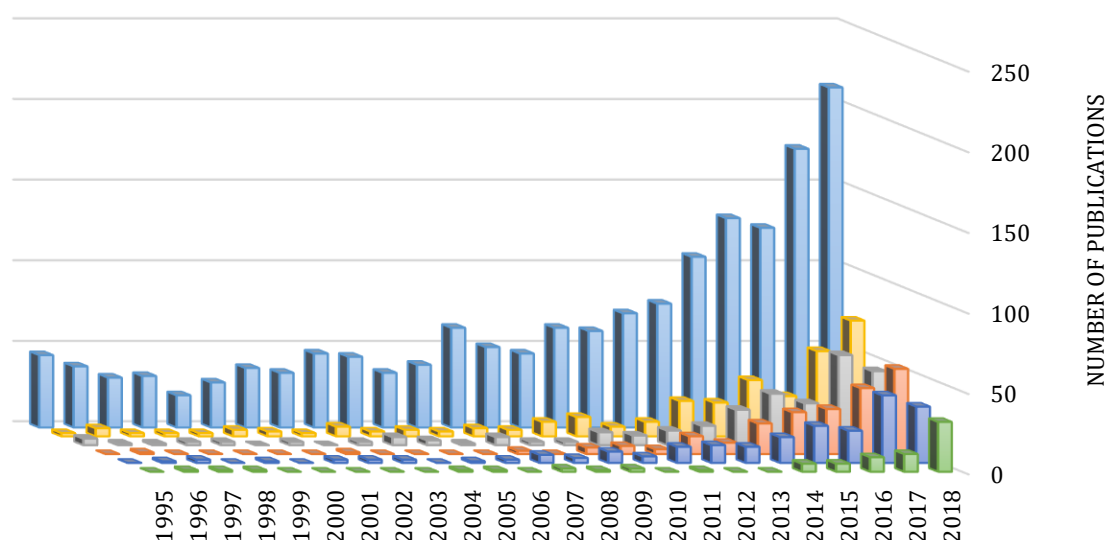


**Figure 2.** Number of publications per year on Spent Coffee Grounds (SCG) and related topics by Science Direct database. Document search: ■ “SCG” ; ■ “SCG + biopolymers”; ■ “SCG + adsorbent”; ■ “SCG + biofuel”; ■ “SCG + antioxidant”; ■ “SCG + carbohydrates” .

## 1.2 ANTIOXIDANT RECOVERY FROM SPENT COFFEE GROUNDS

### 1.2.1 Antioxidants

The term “Antioxidants” indicates substances able to significantly get slower or prevent substrate oxidation, even when they are present at low concentration. Several classes of compounds can exhibit antioxidant activity (carbohydrates, lipids, etc.), among them polyphenols are particularly interesting, being the most active dietary antioxidants

(Shahidi, 2000). The antioxidant activity of polyphenols in living species is related to the detoxification of cells from reactive oxygen species (ROS), such as superoxide radical ( $O_2^{\cdot-}$ ), hydrogen peroxide ( $H_2O_2$ ), hydroxyl radical ( $\cdot OH$ ), singlet oxygen ( $^1O_2$ ) or peroxy radicals ( $RO_2^{\cdot-}$ ), reactive nitrogen species (RNS) and reactive chlorine species (RCS), which can be generated both by exogenous chemicals or endogenous metabolic processes (Georgetti et al., 2008). Because of their structures, polyphenols can act through two different mechanisms: donation of a hydrogen atom or donation of an electron (Dugas et al., 2000; Leopoldini et al., 2011; Rice-Evans et al., 1996). In the former mechanism, the phenolic compound reacts with the free radical ( $R^{\cdot}$ ) by transferring a hydrogen atom through homolytic rupture of the O-H bond, generating the stable radical  $ArO^{\cdot}$  and  $R$  as products. The ease of formation and stability of  $ArO^{\cdot}$  strongly depends on the structural features of the  $ArOH$  compound, particularly the presence, the number and the positions of additional hydroxyl groups, which can improve the stability of the polyphenolic radical thanks to delocalization of the unpaired electron over the aromatic ring by resonance or by hyperconjugation effects (Munin and Edwards-Lévy, 2011). Phenolic acids, phenylpropanoids and flavonoids in food can be present in free form, but are often glycosylated with different sugars, especially glucose (Shahidi, 2000).

### 1.2.1 Bioactive molecules in spent coffee grounds

The antioxidant activity in SCG is chiefly ascribed to polyphenols, particularly chlorogenic acid, its isomers and derivatives (Jeszka-Skowron et al., 2016; Panusa et al., 2013), as well as Maillard reaction products (melanoidins) (Borrelli et al., 2002; Burniol-Figols et al., 2016; Kučera et al., 2016). The amount of antioxidants in the solid waste is strongly dependent on the variety of coffee (Bravo et al., 2012) and the brewing process used for beverage preparation (Ludwig et al., 2012). The strong antioxidant activity of melanoidins seems to be able to significantly inhibit lipid oxidation (Ranheim and Halvorsen, 2005); while the family of chlorogenic acid in coffee might have effects against inflammation and may reduce the risk of cardiovascular and other

inflammatory and liver diseases (Andersen et al., 2006; Bonita et al., 2007; Ranheim and Halvorsen, 2005; Wadhawan and Anand, 2016).

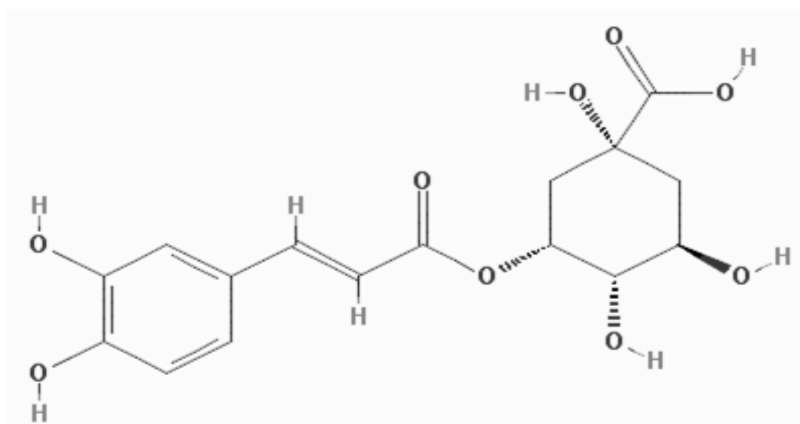


**Figure 3.** Chemical Structure of Chlorogenic acid  
([https://pubchem.ncbi.nlm.nih.gov/compound/Neochlorogenic\\_acid#section=Top](https://pubchem.ncbi.nlm.nih.gov/compound/Neochlorogenic_acid#section=Top))

Actually, chlorogenic acid constitutes a family of esters composed of transcinnamic acids, mainly caffeic acid, ferulic acid, and quinic acid, resulting in caffeoylquinic acids, and feruloylquinic acids, that may be found in several isomeric forms depending on the position of the ester link. 5-O-caffeoylquinic acid (figure 3) is the most common form and is often indicated as ‘chlorogenic acid’ (Islam et al., 2016). Isomers of chlorogenic acid are easily altered under coffee roasting conditions and high-temperature processing and are transformed into derivatives, which exhibit a range of free radical scavenging capacities (Liang et al., 2016).

Melanoidins (figure 4) are one of the major components of coffee beverages, accounting for up to 25% of dry matter (Borrelli et al., 2002). They are high molecular weight brown products, as result of the Maillard reaction and containing nitrogen; by coffee brewing only a fraction (about 33 %) of the original coffee bean protein is extracted, while the residual remains insoluble in hot water due partly to denaturation and association with cell wall arabinogalactans representing nearly 92% of the total nitrogen present in the high molecular weight melanoidins. Among them the ethanol-soluble fraction (70-80%) has the highest protein content and the lowest carbohydrate content (Moreira et al., 2012), showing an amino acid composition rich in alanine, aspartic acid/ asparagine, glutamic acid/glutamine, and glycine (Campos-Vega et al., 2015; Nunes and Coimbra, 2010). Despite all efforts, the chemical structure of coffee

brew melanoidins is still largely unknown. Carbohydrates, aminoacids, and phenolic compounds are components of coffee melanoidins but definitive conclusions have not been achieved since melanoidins have been always obtained as complex mixtures (Nunes and Coimbra, 2010). Anyway, melanoidins greatly contribute to the overall antioxidant activity of certain foods, such as roasted coffee, and may exhibit antioxidant capacity through different mechanisms, i.e., chain breaking, oxygen scavenging, or metal chelating (Borrelli et al., 2002; Daglia et al., 2000; Morales et al., 2005). In addition, melanoidins can inhibit matrix metalloproteases, can selectively modulate the bacterial population in the colon and reduce its radical stress, which is related to the development of colon cancer (Moreira et al., 2012).

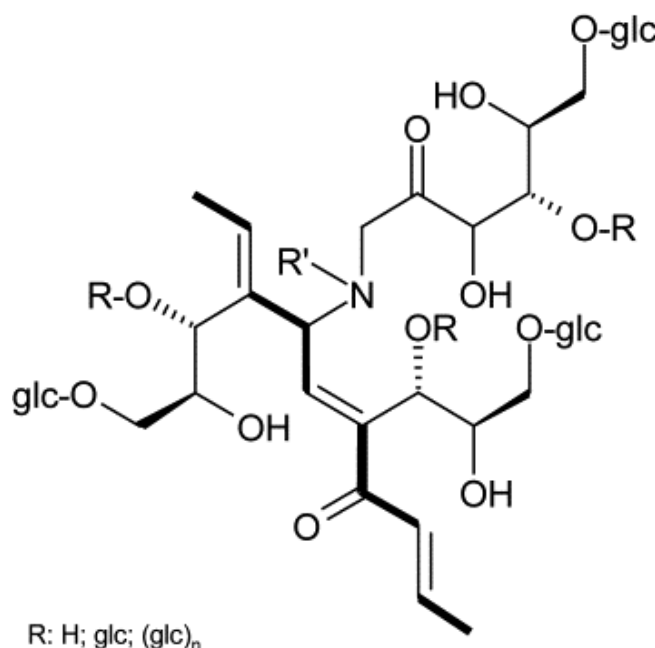


**Figure 4.** Basic structure of melanoidins (Cämmerer et al., 2002)

Caffeine (1,3,7-trimethylxanthine) is a thermostable purine alkaloid and with its catabolic products theobromine and xanthine, is a key component of coffee. Chemical structure of caffeine is reported in figure 5. George et al. (1992) reported that caffeine is an antioxidant and radioprotector against the oxic pathway of radiation damage in a wide range of cells and organisms, while Azam et al. (2003) observed that that caffeine and its metabolites may contribute to the overall antioxidant and chemopreventive properties of caffeine-containing beverages. Only in presence of high concentrations of

caffeine, theobromine, xanthine and copper ions, the alkaloids proved to be capable of binding and reducing Cu(II) to Cu(I), leading to the generation of oxygen radicals. Prasanthi et al. (2010) suggested that even very low doses of caffeine might protect against sporadic Alzheimer disease-like pathology, since they determined the effects of caffeine on amyloid- $\beta$  levels, tau phosphorylation, oxidative stress generation, and caffeine-target receptors in rabbits fed with a 2% cholesterol-enriched diet, a model system for sporadic Alzheimer disease.

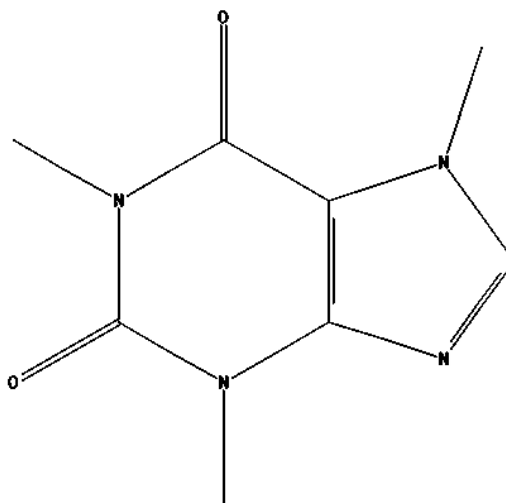


**Figure 5.** Chemical Structure of caffeine (<https://pubchem.ncbi.nlm.nih.gov/compound/2519#section=Top>)

### 1.3 EXTRACTION TECHNIQUES FOR ANTIOXIDANT RECOVERY

According to the findings about the properties of coffee constituents, several authors focused their attention on the extraction of antioxidants from spent coffee grounds. Batch solvent extraction is one of the most used technique to obtain active compounds from biomasses and plants, but in order to enhance extraction yields and to reduce the organic solvent exploitation, several non-conventional extraction techniques were proposed to replace conventional solvents, improve process selectivity and reduce the impact on the environment. An efficient definition of the principles of green extraction is given by Chemat et al. (2012), who stated that “*Green Extraction is based on the discovery and design of extraction processes which will reduce energy consumption, allows use of alternative solvents and renewable natural products, and ensure a safe and*

*high quality extract/product*", and resumed the main goals of this approach in 6 principles:

- innovation by the selection of varieties and the use of renewable plant resource, which implies the preservation of biodiversity and avoiding plant extinction due to their over-exploitation;
- use of alternative solvents and principally water or agro-solvents issued from agricultural resources;
- reduction of energy consumption by means of innovative technologies;
- production of co-products instead of waste to include the bio- and agro-refining industry;
- reduction of unit operations and favour safe, robust and controlled processes;
- production of non-denatured and biodegradable extract without contaminants.

Thus, alternative techniques such as supercritical fluid extraction were proposed as green extraction method for added-value compounds recovery from natural matrices, particularly using supercritical CO<sub>2</sub> alone or with a polar modifier (e.g. methanol, ethanol, acetone) (Da Porto and Natolino, 2017; Hatami et al., 2019; Shrigod et al., 2017; Fiori et al., 2009; Reverchon and De Marco, 2006; Ameer et al., 2017; Andrade et al., 2012). Furthermore, subcritical water extraction is receiving much attention in the field, since water polarity can be changed when water is at temperatures between its boiling and critical point and the pressure is regulated in such a way that water remains in its liquid state (Duba et al., 2015). Subcritical water extraction was utilized as alternative technique for the recovery of bioactive molecules such as curcumin (Valizadeh Kiamahalleh et al., 2016), polyphenols from winery solid waste (Aliakbarian et al., 2012; Duba et al., 2015), from rosemary plant (Ibañez et al., 2003) and from spent coffee grounds (Xu et al., 2015). Electrically-assisted extractions, as high voltage electrical discharge and pulsed electric fields, were also successfully employed for the recovery of valuable compounds from natural matrices (Donsì et al., 2010; Boussetta and Vorobiev, 2014; Boussetta et al., 2011; Roselló-Soto et al., 2015; Boussetta et al., 2009; Carullo et al., 2018).

Nevertheless, non-conventional techniques as microwave-assisted extraction, high pressure and temperature-assisted extraction and ultrasound-assisted extraction seem to be very promising for antioxidant recovery from spent coffee grounds, thus the state of the art on this topic will be discussed in the following paragraphs. Indeed, the polyphenol extraction yields could be strongly increased by the application of the listed innovative extraction techniques.

### 1.3.1 Solid-Liquid Extraction

Solid-liquid extraction (SLE) of phenolic compounds from SCG was investigated by Mussatto *et al.* (2011). The authors recognized in solvent/solid ratio, extraction time and temperature, the key factors to improve the extraction process. They also found that a combination of the organic solvent (methanol) and water contributed to create a moderate polar medium, which is particularly suitable for phenolic extraction. In addition, more eco-friendly solvents than aqueous methanol were successfully used for antioxidants extraction from SCG, and the mixture of ethanol/water was proposed as the optimal extraction solvent by several authors (Bravo *et al.*, 2013; Panusa *et al.*, 2013; Zuorro and Lavecchia, 2012, 2013).

Panusa *et al.* (2013) identified the phenolic profile of ethanol aqueous extracts from SCG, finding caffeoylquinic acids, feruloylquinic acids and quinolactones as the most abundant groups, while the amount of caffeine (in the range of 5.99–11.50 mg/g dry matter) was strongly related to the variety of coffee employed.

### 1.3.1 Microwave-Assisted Extraction (MAE)

Among the available extraction techniques, one of the most promising seems to be microwave-assisted extraction (MAE). The fundamentals of this kind of process are different from other conventional extraction methods, indeed as opposed to conventional thermal heating, in this method the heat and mass gradients work in the same direction; the heat is dissipated volumetrically inside the irradiated medium, thus



providing a fast and a uniform heating, allowing process acceleration and high extraction yields (Veggi et al., 2013).

Microwaves are electromagnetic waves with frequency from 0.3 to 3 GHz. Typically, microwave food processing uses the 0.915 and 2.45 GHz band, the last of which is used for home ovens, and both are used in industrial heating, with some limitations: the 0.915 GHz band is not available in countries outside Region 2 (Americas, Greenland and some of the eastern Pacific Islands), although frequencies of 0.43392, 0.896 and 2.375 GHz are employed outside the United States (Spigno and De Faveri, 2009). Microwave energy acts directly on the molecules via conversion into thermal energy: the energy transfer occurs by dipole rotation and ionic conduction through reversals of dipoles and displacement of charged ions present in the solute and the solvent (Veggi et al., 2013). Microwave generators are based on the principle of electron beam modulation and the Klystron and Magnetron are the most used. Energy density, defined as the microwave irradiation power per unit of extraction volume, is an important parameter in this kind of process, but the effective heating of the system strongly depends on its ability to absorb microwaves (i.e. the dielectric constant of the solvent) and on its ability to convert microwave energy in heat (dielectric loss factor) (Chan et al., 2013; Cravotto et al., 2008; Veggi et al., 2013).

The transformation of electrical energy into the thermal one is given by equation 1:

$$P = Kf\varepsilon'E_F^2 \tan\delta \quad (1)$$

In which  $P$  is the microwave dissipation per volume unit;  $K$  is a constant;  $f$  is the frequency;  $\varepsilon'$  is the dielectric constant ;  $E_F$  is the electric field strength and  $\tan\delta$  is the tangent of the dissipation factor ( $\delta$ ). Other than for its heating ability, a second effect makes microwave-assisted extraction an advantageous technique for the recovery of valuable compounds. Indeed, microwaves act by heating on tiny traces of moisture inside the cell matrix, providing the evaporation. Moisture evaporation builds intense pressure on the cell wall, which causes the release of the analytes by cell rupture (Ekezie et al., 2017). Since only few papers (Pavlovic et al., 2013; Ranic et al., 2014) , dealt with MAE of antioxidants from SCG and considering the promising potential

applications of this waste, for the best of our knowledge the topic deserves further investigations. Temperature, time, solvent composition, solid-liquid ratio, and microwave irradiation power are some of the factors which deeply affect the antioxidant extraction from natural matrices (Pavlovic et al., 2013; Ranic et al., 2014; Simić et al., 2016; Spigno and De Faveri, 2009). On one hand, high temperature and long extraction time use to promote extraction process, on the other hand they could facilitate thermal degradation of bioactive compounds (Chan et al., 2011). The most of the works on microwave-assisted extraction performed on SCG (Pavlovic et al., 2013; Ranic et al., 2014), as well as on other natural matrices (Chan et al., 2013; Sahin et al., 2017; Simić et al., 2016; Spigno and De Faveri, 2009), dealt with the analysis of extraction time and other parameters, setting up the microwave radiation power, thus temperature was not the controlled variable. In addition, the conditions able to maximize the extraction of these compounds from SCG were not established yet.

### 1.3.2 High Pressure and Temperature- assisted Extraction (HPTE)

High Pressure and Temperature-assisted Extraction, similarly to Pressurized liquid extraction or Accelerated Solvent Extraction, is a technique that utilizes liquid solvents at elevated temperature and pressure. This technique has been recognized as an efficient extraction technology to recover phenolic compounds from several matrices (Aliakbarian et al., 2011; Mariotti-Celis et al., 2018; Paini et al., 2015; Shang et al., 2017). By applying pressure during the extraction, a temperature above the boiling point can be employed while the solvent maintains the liquid state. In addition, high pressure at high temperature reduces solvent surface tension, forcing the solvent within the matrix, thus improving the analyte extraction. Furthermore, pressure on the matrix could result in disruption of matrix structure, enhancing the mass transfer of the desired compounds from the solid to the solvent (Mustafa and Turner, 2011). High temperature has a key role in enhancing the extraction process, since mass transfer coefficients are improved and solvent viscosity is decreased, leading to a deep penetration within porous matrices. In addition, high temperature increases the solubility of the analyte in the solvent and provokes, as well, breakage of bonding forces (dipole-dipole, van der

Waals, and H<sub>2</sub>-bonding), in such a way that the diffusion of desired compound to the outer surfaces of the solid matrix is facilitated (Ameer et al., 2017). On the other hand, if the high temperature is used to provide higher extraction yields, the selectivity of the process is often affected, since the amount of co-extracted analytes might be larger at higher temperatures. Furthermore, high temperatures might affect thermosensitive compounds, which could be subjected to disintegration and hydrolytic degradation (Mustafa and Turner, 2011). The high temperatures could favor also the formation of some potential human carcinogens associated with the Maillard reactions. Mussatto et al. (2011b) reported that during the extraction of sugars from SCG, furfural, hydroxymethylfurfural (HMF), acetic acid, and phenols were also found in SCG hydrolysates obtained by dilute acid hydrolysis. Particularly, HMF is considered as a good indicator of the presence of Maillard toxic compounds in thermally treated foods, since its content is directly related with the occurrence of acrylamide and other furans formation and its quantification in food matrices is significantly easier and cheaper than the other Maillard compounds. Mariotti-Celis et al. (2018) reported that the addition of ethanol as co-solvent during hot pressurized liquid extraction (HPLE) enables a decrease in the extraction temperature and this change in the HPLE operating conditions mitigated the HMF formation. However, Shang et al., (2017) demonstrated that pressurized liquid extraction could be an efficient method for the extraction of polyphenols and caffeine from SCG in a relatively short time and without toxic solvents.

### 1.3.3 Ultrasound-Assisted Extraction (UAE)

UAE is a promising technique for the green extraction of bioactive compounds. UAE advantages include versatility, simplicity, safety, rapidity, eco-friendliness, and cost-effectiveness, due to the reduced consumption of time, energy, and expensive organic solvents (Ameer et al., 2017). The extraction by ultrasounds is based on cavitation, which is induced by the pressure fluctuations generated by ultrasound waves in a liquid medium and commonly described as the formation, growth, and collapse of gas-vapour filled bubbles in a liquid. Liquid circulation currents and turbulence lead to a significant increase in the mass transfer rates (Shirsath et al., 2012) and the implosion of cavitation

bubbles can hit the surface of the solid matrix and disintegrate the cells causing the release of the desired compounds (Gil-Chávez et al., 2013).

The operational frequencies of ultrasound waves generally used for extraction purposes range from 20 kHz or above. The huge amount of energy released causes significant local temperature and pressure variations in bubbles during extraction, causing liquid solutes to leach at speeds of 280 m/s (Ameer et al., 2017). In addition, ultrasound can result in swelling of the plant material, which is able to enhance the extraction of bioactive compounds (Wijngaard et al., 2012). With the aim of enhancing the extraction efficiency in terms of yield and composition, the increase of ultrasound power, moisture reduction and temperature optimization are generally recognized as the factors that more affect the process. Nevertheless, in some cases the power variation can result in a certain selectivity of target molecules (Chemat et al., 2017). Al-Dhabi et al. (2017) studied the effects of ultrasound power on polyphenol extraction from spent coffee grounds, finding that the higher was the value of the variable the higher was extraction rate up to 250 W. By keep on increasing the power, the extraction yield was found to decrease, due to the large number of small bubbles that compromised the intensity of cavitation. On the same topic, Severini et al. (2017), who performed the extraction of phenolics from SCG using a mixture methanol/water as solvent, found that the extraction process was mainly affected by methanol/water mass ratio, followed by the length of ultrasound pulse and the extraction time.

#### 1.4 POST-PROCESSING AND ENCAPSULATION OF BIOACTIVE COMPOUNDS

SCG extracts are able to exhibit high antiradical power, which can be traced back to chlorogenic acids, its derivatives, and melanoidins. These molecules could be of great interest in cosmetic, medical and food industries, but phenolic compounds are unstable and easily degradable if exposed to light, heat and oxygen. In addition, the liquid phase is not suitable for storage, transport and preservation of the extracted molecules. Often, some compounds extracted from natural matrices show other limitations such as unpleasant taste, poor availability and also high susceptibility to processing conditions as well as gastrointestinal environments (Aguilar et al., 2016). Thus, in order to extend

extract shelf life, prevent microbial contamination and their activity loss, stabilization methods should be applied. These methods include both techniques able to perform solvent disposal, giving back a solid as product, and encapsulation methods. For what concerns the former classification, freeze-drying and supercritical antisolvent technique could be used, while microencapsulation by spray drying and supercritical liposome formation are examples of encapsulation methods.

#### 1.4.1 Freeze-drying

Freeze-drying is one of the most important techniques for the preservation of thermosensitive or unstable molecules (Munin and Edwards-Lévy, 2011). It consists in the water disposal from the sample at low temperatures via sublimation. Freeze-drying was used for the encapsulation of phenolic compounds as main technique only in few cases. For instance, Gradinaru et al. (2003) studied the thermal stability of a *Hibiscus sabdariffa* L. anthocyanin-rich extract in aqueous environment and after lyophilization with an amorphous polysaccharide (pullulan), showing that freeze-drying did not alter the properties of the extract, preserving the phenolic antioxidant activity. Similar results were obtained for the encapsulation of polyphenols from cloudberry (*Rubus chamaemorus*) using maltodextrin as coating agent (Laine et al., 2008).

Since the final product of freeze-drying is a solid powder, lyophilization is more frequently used as the final step of other encapsulation methods (Dube et al., 2010; Taylor et al., 2009)

#### 1.4.2 Supercritical Anti-Solvent technique

The Supercritical Anti-Solvent technique is characterized by the use of supercritical CO<sub>2</sub> as antisolvent: the supercritical fluid is injected in a solution of the active agent in an organic solvent, leading to a decrease in the solvation power of the organic solvent, and consequently to an oversaturation of the solution and a precipitation of the solute. This technique was successfully performed for the precipitation/encapsulation of

antioxidants from rosemary, olive leaves and green tea (Chinnarasu et al., 2015; Sosa et al., 2011; Visentin et al., 2012).

### 1.4.3 Spray drying

Encapsulation by spray drying is a well-known technique able to produce dried microparticles from a liquid extract, trapping the bioactive molecules in a coating agent. Particularly, spray drying is one of the most widely used methods for this purpose, being easy, cheap and suitable for thermosensitive products such as polyphenols (Okos et al., 2006). Particle dimension is generally around 10  $\mu\text{m}$  with a large size distribution due to the different size of the droplets during atomization. The most influent parameters on particle dimensions are nozzle geometry and the initial viscosity of the inlet suspension (Okos et al., 2006). If these variables are related to the particular device and the raw materials, other parameters can be changed in order to optimize the process. Air inlet temperature influences evaporation velocity, the moisture of the product, as well as air outlet temperature (Fazaeli et al., 2012), but Paini et al. (2015) found that the yield of microencapsulation of phenolic compounds from olive pomace has not been prejudiced by this operative parameter. Solid content of feed and the surface tension play an important role on the atomization step (Okos et al., 2006), while feed temperature and flow rate have a strong effect on the solvent evaporation: a decrease of feed temperature and an increase of its flow rate lead to a less efficient removal of the solvent and to a higher powder moisture (Fazaeli et al., 2012; Paini et al., 2015). In spray drying applications several carrier materials have been tested in order to obtain good product recovery and stability. Gum Arabic is the most common coating agent because of its high solubility and low viscosity in aqueous solution, however the fluctuating trend of its supply and cost led to move the attention toward the use of other wall materials (Carneiro et al., 2013). Maltodextrins (MD) are widely used in spray drying processes, either alone either combined with other materials, for polyphenol encapsulation (Medina-Torres et al., 2016; Paini et al., 2015a; Tolun et al., 2016). The selection of the dextrose equivalent (DE) of maltodextrins is critical for microencapsulation spray drying process. When DE increases, a higher moisture of the

product was reported because of the greater amount of hydrophilic groups in smaller molecules. In addition, DE influences also the glass transition temperature ( $T_g$ ) of the powder and consequently powder structure and stability (Fazaeli et al., 2012). Bakowska-Barczak and Kolodziejczyk (2011) did not report any DE effects on the black currant polyphenols encapsulation ability of maltodextrins. Nevertheless, maltodextrins alone lack the required interfacial properties to obtain high microencapsulation efficiencies, thus they are often used together with other wall materials, such as gum Arabic (Gharsallaoui et al., 2007). Inulin (I) is an interesting coating agent for food applications being a dietary fiber that exhibits prebiotic effects, suitable also for diabetic food (Bakowska-Barczak and Kolodziejczyk, 2011; De Barros Fernandes et al., 2014). Indeed, the current trend is to consume compounds with functional activity, so replacing conventional coating agents, such as modified starch or gum Arabic, with a healthy compounds such as inulin, that can add a higher value to the product (Zabot et al., 2016).

#### 1.4.4 Liposomes

Liposomes are vesicles formed by an external lipid double layer and an internal aqueous core, which made them useful for the entrapment, delivery, and release of water soluble, lipid-soluble, and amphiphilic materials (Fang and Bhandari, 2010). Drugs can be encapsulated into liposomes in the lipophilic and in the hydrophilic compartment, depending on their affinity with water molecules or with the lipid membrane. In addition, they are powerful drug carriers for their similarity to cell wall membranes (Trucillo et al., 2018). Another important advantage in the use of liposomes as encapsulation system is the efficient protection against digestion in the stomach, coupled with an enhanced absorption in the gastrointestinal tract, which increase bioactivity and bioavailability of the active agent (Takahashi et al., 2007). Moreover, liposomes offer the possibility to functionalize the external bilayer, leading to a more selective delivery of the active compound to the target organ.

Scientific literature reports several techniques to synthesize liposomes, like lipid film hydration, reverse phase evaporation, solvent injection, freeze thawing, sonication, French presses and extrusion (Mozafari et al., 2008; Fathi et al., 2012; Patil and Jadhav, 2014), but

some drawbacks related to the use of liposomes for novel food or pharmaceutical formulations have to be considered. Indeed, generally liposomes exhibit instability during storage, high rate of release, payload of active ingredient relatively low, if compared to other techniques and low reproducibility.

A novel process based on supercritical fluid was proposed by Santo et al. (2014), called SuperLip (Supercritical Assisted Liposome formation), for loaded liposome production. Conversely to other liposome production techniques, SuperLip allows to create first the droplet of water and, then, to surround it by one or more double layers of phospholipids. The use of supercritical carbon dioxide, in this process, allows to obtain a higher diffusion coefficient of the lipids and a lower viscosity of the medium bulk; these favorable conditions bring to a better control of liposome size distribution (Trucillo et al., 2018).

Literature reported several examples of encapsulation of pure active compounds which are present in SCG extract, such as encapsulation of chlorogenic acid in  $\beta$ -cyclodextrins and (2-hydroxypropyl)- $\beta$ -cyclodextrins by inclusion complexation (Shao et al., 2014), in chitosan nanoparticles by ionic gelation (Nallamuthu et al., 2015), in liposomes obtained by thin film drying method (Feng et al., 2016), as well as caffeine encapsulation by spray drying into sodium alginate (Bagheri et al., 2014), and caffeic acid encapsulated by inclusion complexation in hydroxypropyl- $\beta$ -cyclodextrins (Zhang et al., 2009) and  $\beta$ -cyclodextrins (Liu et al., 2016), while only few papers dealt with the encapsulation of extracts rich in antioxidants from coffee. Particularly, by means of inclusion complexation, purified green coffee extract was encapsulated in  $\beta$ -cyclodextrins (Budryn et al., 2016), as well as coffee brew (Górnas et al., 2009) and only recently Ballesteros et al. (2017) encapsulated by freeze-drying and spray drying phenolic compounds obtained from spent coffee grounds. This implies that, to the best of our knowledge, the topic deserves further investigations.

Considering the state of the art on antioxidant recovery from spent coffee grounds, one of the aim of this study was the valorization of spent coffee grounds, which was



employed as raw material for the extraction of bioactive molecules in presence of microwaves, high pressure and high temperature and ultrasounds, using eco-friendly solvents. The novelty of this work concerned the comparative study on the extraction techniques applied to polyphenol recovery from spent coffee grounds and the related optimization of the process variables. In addition, extracts were stabilized in order to preserve their bioactivity and increase their bioavailability both by techniques which provide a solid and stabilized extract as product (freeze-drying and supercritical antisolvent technique) and by methods of encapsulation (spray drying and supercritical fluid-assisted liposome formation).

These processes, could represent a first and more valuable step for a biorefinery based on coffee, such as that reported in figure 6, in which the recovery of the high added-value compounds generates a following cascade of operations that could involve the reuse of SCG extraction cake for the separations of compounds of interest for energetic purposes, such as triglycerides, and thermal transformation for the production of biofuels.

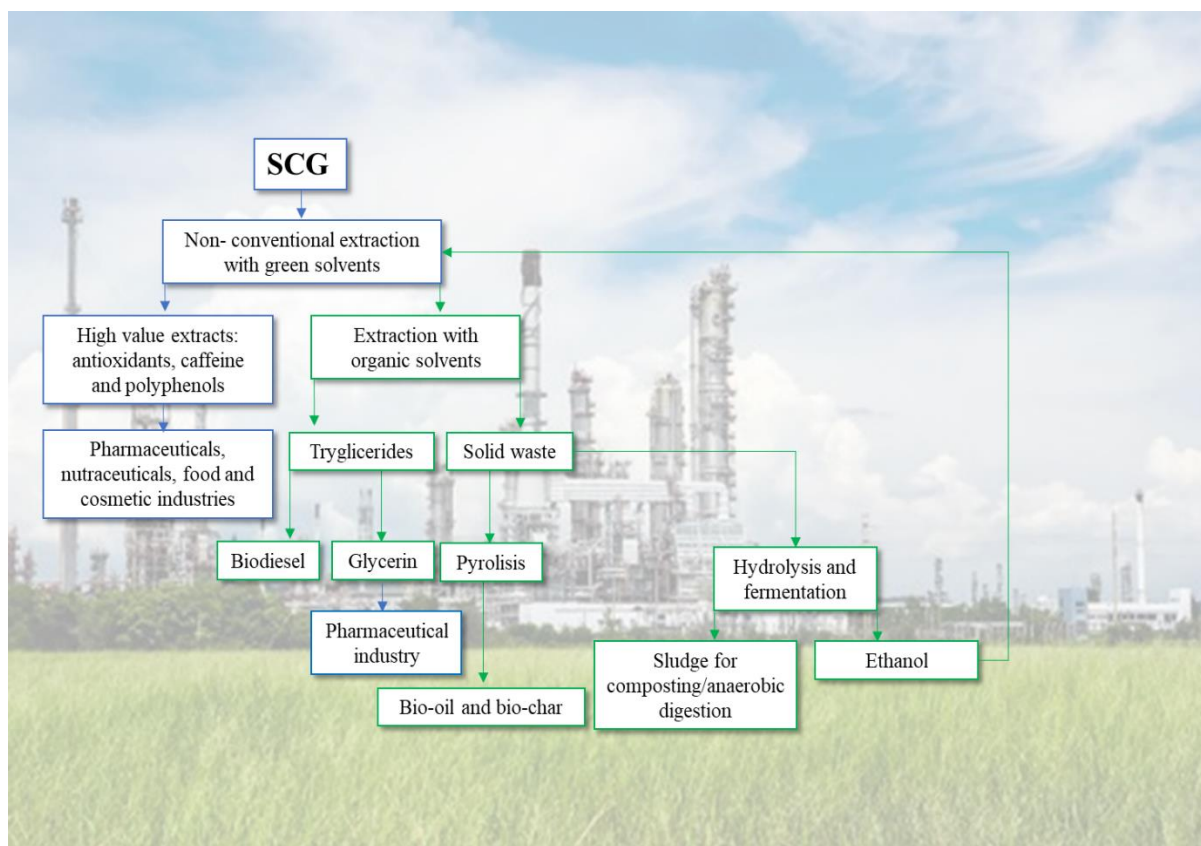


**Figure 6.** Example of a possible solution for spent coffee grounds-based biorefinery (adapted from Mata et al., 2018)

## Chapter 2

# CHEMICO-PHYSICAL CHARACTERIZATION OF SPENT COFFEE GROUNDS

### 2.1 ABSTRACT

In this section, the chemico-physical characterization of spent coffee grounds was undertaken. Being a by-product of the brewing process for espresso coffee production, SCG do not present standardized properties, which depend not only on the variety of coffee, but also on the roasting process as well as on the coffee brewing. For these reasons, SCG was characterized in terms of moisture, ashes, particle size distribution, density, mineral content and calorific value. Results demonstrated that the raw material presented a mean diameter of  $435 \pm 9 \mu\text{m}$  and a high calorific value of  $20888 \text{ J/g dried solid}$ . In addition, the obtained results allowed to establish which conditions were suitable for SCG storage (final moisture of about 6 % after drying at  $50^\circ\text{C}$  for 3 days), as well as to obtain information about the chemical composition of the material (water, ashes, caffeine and lipid content). that will be useful for further steps of the study.

### 2.2 MATERIAL AND METHODS

#### 2.2.1 Spent coffee grounds

Spent coffee grounds (SCG), were periodically collected from the daily waste production of common vending machines, available in the University of Genoa and immediately dried in oven at  $50^\circ\text{C}$  until the wet-based moisture of 6% was reached. The dried biomass was stored at room temperature and dark conditions during the experiments. The biomass was the waste of coffee brewing process, in which roasted coffee beans of *Coffea Canephora* were loaded into the vending machine and directly grinded just before the beverage preparation.

### 2.2.2 Moisture

The SCG total moisture was obtained by drying about 5 g of samples, directly collected from the vending machine at 110 °C, until constant weight was observed. Basing on the amount of water lost during drying, moisture was calculated as reported in the equation (1). The values of moisture were expressed as  $g_{\text{water}}/100 g_{\text{wet SCG}}$ .

$$\text{Moisture} = \frac{m_{\text{initial}} - m_{\text{final}}}{m_{\text{initial}}} \quad (2)$$

In equation 1,  $m_{\text{initial}}$  was the mass of wet sample at the beginning of the drying process and  $m_{\text{final}}$  was the mass of the sample at the end of the thermal treatment.

### 2.2.3 Ashes

The amount of ashes in the SCG was evaluated on dry samples, which were incinerated at 750 °C for 3 h. Ash content was finally expressed as mass of ashes per mass of dry solid.

### 2.2.4 Particle size distribution

$48.7 \pm 0.1$  g of dried biomass was subjected to sieving in order to determine the particle size distribution. The dimensions of sieve openings used for the scope were 710, 600, 500, 420, 300, 212, 106, 74  $\mu\text{m}$  (Giuliani, Tecnologie, Torino, Italy) and the operation was carried out for a shaking time of 15 min by means of a vibratory sieve shaker machine. The masses of each fraction ( $m_j$ ) were weighed and the respective range of diameters was labeled by the arithmetic mean of the two sieve openings ( $d_j$ ). The cumulative function of the undersize up to a diameter value  $d_k$  ( $F(d_k)$ ) was then built according to equation 3:

$$F(d_k) = \sum_{j=1}^{j=k} \chi_j \quad (3)$$

Where  $\chi_j$  were the mass fractions related to the single diameter interval  $d_j$ .

The generic mean value of the distribution  $\overline{g(d)}$  was determined graphically, being represented by the area under the curve  $F(d)$  versus  $g(d)$  with respect to the  $F(d)$  axis (Svarovsky, 2000), and was calculated as expressed in the discretized form of equation 4:

$$\overline{g(d)} = \int_0^1 g(d) dF = \sum_k [g(d_k) + g(d_{k-1})] \cdot [F(d_k) - F(d_{k-1})] \cdot \frac{1}{2} \quad (4)$$

### 2.2.5 Lipid extraction and analysis

In order to determine the lipid fraction in SCG,  $2.00 \pm 0.10$  g of sample, which was previously dried as reported in paragraph 2.2.1, were subjected to Soxhlet extraction using 50 mL of petroleum ether as solvent and 4 h as extraction time. After the extraction process, the complete solvent disposal of the liquid phase was performed by evaporation in calibrated laboratory ceramic capsules and the mass of recovered lipids was weighed by analytical scale. Finally, the recovery of lipid fraction was expressed as reported in equation (5).

$$\text{Lipid fraction} = \frac{m_{\text{lipids}}}{m_{\text{dried SCG}}} \quad (5)$$

The investigation on the composition of the lipid fraction in SCG was carried out via gas chromatography. The fatty acids that initially were present in the recovered oil from SCG were converted in the corresponding fatty acid methyl esters (FAME) by transesterification reaction, in order to be detected by gas chromatograph GC/FID. The procedure adopted for transesterification reaction was a modified version of the method reported by Zunin et al. (2006). Briefly, 40 mg of the lipid fraction recovered from SCG were dissolved in 8 mL of *n*-hexane, then 800  $\mu\text{L}$  of a KOH 2 N solution in methanol were added and the system was vigorously stirred with vortex for 2 min. After the reaction, the sample was centrifuged at

1619 xg (MF-20-R centrifuge, Alliance Bio Expertise, Guipry, France) for 2 min to separate methanol and 1  $\mu\text{L}$  of the supernatant was injected in a DANI 1000 Gas Chromatograph (Dani Instruments, Milan, Italy), equipped with a FID detector and a Zebron ZB-WAX column (30 m x 0.32 mm i.d. x 0.25  $\mu\text{m}$  film thickness)(Phenomenex, Auckland, New Zeland), that was used for the analysis. During the analysis both the injector and the FID were set at 250  $^{\circ}\text{C}$ , while column profile temperature was set as follow: 150  $^{\circ}\text{C}$  for 2 min, then a temperature of 175  $^{\circ}\text{C}$  was reached by a thermal ramp of 3  $^{\circ}\text{C}/\text{min}$ , which was kept constant for 1 min, followed by an increasing of temperature (3  $^{\circ}\text{C}/\text{min}$ ) up to 210  $^{\circ}\text{C}$ . This temperature was finally maintained for 7 min. Chromatograms were compared with those of methyl esters fatty acid reference solutions obtained from a standard solution with the composition reported in table 2.

**Table 2.** Standard solution of methyl ester fatty acids: composition and their retention time.

	Retention time (min)	Concentration (g/L)
Methyl ester of myristic acid	8.34	0.567
Methyl ester of palmitic acid	13.04	0.05
Methyl ester of stearic acid	18.66	0.501
Methyl ester of oleic acid	19.18	0.897
Methyl ester of linoleic acid	20.44	0.5
Methyl ester of linolenic acid	22.24	0.5

### 2.2.6 Particle real density

Particle real density of the dried biomass (about 0.5 g) was obtained by the pycnometer method using toluene as fluid, as reported by Silva et al. (1998). The pycnometer had a capacity of 15  $\text{cm}^3$  and was equipped with a thermometer immersed into the solvent. Briefly, the real density of particles ( $\rho$ ) was estimated basing on the displaced volume of liquid, as reported in equation 6:

$$\rho = \rho_{Toluene} \cdot \frac{m_2 - m_1}{m_2 - m_3} \quad (6)$$

Where:

$m_1$  was the mass of the pycnometer filled up to the reference level with toluene;

$m_2 = m_1 + \text{mass of SCG sample}$ ;

$m_3$  was the mass of the pycnometer containing the mass of the SCG sample and filled up to the reference level with toluene.

### 2.2.7 Caffeine content

Caffeine content into SCG was obtained by extraction followed by purification steps according to the reference method proposed by Mumin et al. (2006), modified as reported in this section. In order to make a comparison with the initial amount of caffeine in the roasted coffee beans, used to prepare the beverage, the same following procedure was performed also on samples of roasted coffee beans, previously milled and dried as in paragraph 2.2.1, collected from the same vending machine from which SCG were obtained. Caffeine extraction was carried out in 1 L flask, using 25 g of solid and 250 mL of deionized water as solvent. In addition, 10 g of  $\text{CaCO}_3$  were added in order to provide tannins precipitation as calcium salts. The system was stirred and maintained under boiling for 20 min, then filtered on filter paper using a Buchner funnel when the extract was still hot, thus avoiding caffeine precipitation, since its solubility in water strongly decreases with temperature (table 3).

For caffeine purification liquid-liquid extraction was employed, taking advantage of the higher solubility of caffeine in cold chloroform than in cold water (table 3). In a separatory funnel 50 mL of chloroform were added to the extract. The system was vigorously shaken and left to separate. Once separation occurred, the organic phase was recovered in a beaker, in which anhydrous  $\text{Na}_2\text{SO}_4$  was added to remove residual water and water-soluble salts that were retained in the chloroform. After 10 min the organic phase was filtered and solvent was completely evaporated. In order to eliminate impurities from the obtained solid, the dry solid obtained was dissolved in 10 mL of acetone and about 35 mL of petroleum ether. Indeed, the last one allowed the caffeine precipitation, while impurities are maintained in the solution. Finally, caffeine was separated by filtration on calibrated gootch as pure solid, dried and weighed to determine its recovery.

**Table 3.** Mole fraction solubility of caffeine in three solvents as a function of temperature. Adapted from Shalmashi and Golmohammad (2010).

T (K)	Mole fraction solubility in water ( $10^3$ )	Mole fraction solubility in ethanol ( $10^3$ )	Mole fraction solubility in chloroform ( $10^3$ )
298	$2.098 \pm 0.003$	$1.712 \pm 0.008$	$66.895 \pm 0.007$
303	$2.621 \pm 0.021$	$2.046 \pm 0.003$	$72.685 \pm 0.006$
308	$3.075 \pm 0.004$	$2.188 \pm 0.003$	$78.356 \pm 0.011$
313	$4.367 \pm 0.065$	$2.645 \pm 0.007$	$83.434 \pm 0.007$
318	$7.916 \pm 0.009$	$4.656 \pm 0.007$	$88.716 \pm 0.011$
323	$10.151 \pm 0.034$	$5.512 \pm 0.006$	$94.032 \pm 0.009$

### 2.2.8 Metal content

The investigation on metal content in SCG was performed by solid mineralization and metal species were detected by Atomic Absorption Spectroscopy.  $0.50 \pm 0.01$  g of SCG were placed in a flask and 3 mL of  $\text{HNO}_3$  and 4 mL of  $\text{H}_2\text{SO}_4$  were added to provide the digestion at room temperature. Once the reaction occurred, about 5 mL of  $\text{H}_3\text{BO}_3$  (65% w/v) were added for pH neutralization and samples were filtered on filter paper. The presence of the metal species Cu, Mn, Fe, Zn, Ca, Mg, K was assessed, since these trace elements are able to play a significant role in oxidative metabolism, being involved in metabolic pathways and in cellular defence against oxidative stress and Pb is one of the most frequent contaminant in food product (Jeszka-Skowron et al., 2016). For this purpose, a AA240FS Fast Sequential Atomic Absorption Spectrometer (VARIAN) was used to analyze the properly diluted samples.

### 2.2.9 Calorific value

Gross calorific value of SCG was determined by an automatic Mahler calorimeter (IKA C200, IKA®-Werke GmbH & Co. KG, Germany), in which about 1 g of SCG, previously reduced to a tablet by a press, was treated. The standard calorific value is then calculated from the measured calorific value, taking into consideration the moisture of the sample.



## 2.3 RESULTS AND DISCUSSION

Data related to SCG characterization are given in table 4. Experimental results were elaborated by the Statistica v 8.0 software (StatSoft, Tulsa, OK, USA). SCG samples collected from vending machines presented an average moisture of about 53 g<sub>water</sub>/100 g<sub>wet</sub> SCG, which was reduced to about 6 g<sub>water</sub>/100 g<sub>wet</sub> SCG by drying at 50 °C for 3 days in oven, in order to prevent microbial growth and to preserve the shelf-life of the raw material. The roasted coffee beans (RCB), which were collected from the same vending machine, showed a moisture of about g<sub>water</sub>/100 g<sub>wet</sub> SCG, so it is clear that only after the brewing process the waste acquired the higher value of moisture reported. Since the operations of loading and discharging of the vending machines are daily made, SCG are exposed to these conditions for up to 24 h; nevertheless, no molds, microbial contamination or evidences of perishability were noticed. Dried SCG were, then stored at room temperature in water-free plastic containers in the dark for further experiments and analyses, which revealed that the adopted storage conditions made SCG stable from a chemico-physical point of view for more than 1 year.

**Table 4.** Results and statistic analysis of the characterization of Spent Coffee Grounds (SCG) and roasted coffee beans (RCB). SD= standard deviation; N= number of valid tests.

	N	Mean	Min	Max	SD	Confidence SD -95 %	Confidence SD + 95%	Standard Error
Moisture (g/ 100 g <sub>wet</sub> SCG)	8	52.9	52.5	53.5	0.341	0.226	0.694	0.120
Ashes (g/100 g <sub>dry</sub> SCG)	4	1.43	1.31	1.55	0.098	0.055	0.366	0.049
Lipids (g/100 g <sub>dry</sub> SCG)	3	8.42	7.20	10.2	1.58	0.823	9.93	0.912
Caffeine (g/100 g <sub>dry</sub> SCG)	3	0.151	0.095	0.228	0.069	0.036	0.434	0.040
Calorific value (J/g <sub>dry</sub> SCG)	3	20888	20752	21022	135	70.3	849	77.9
Caffeine (g/100g <sub>dry</sub> RCB)	3	0.753	0.619	0.878	0.130	0.068	0.816	0.075
Moisture (g / 100 g <sub>wet</sub> RCB)	3	3.06	2.90	3.20	0.151	0.078	0.948	0.087

Ash content in SCG was found to be of 1.4 g/100 g<sub>dry</sub> SCG, which is in concordance with those reported by other authors (Pujol et al., 2013; Mussatto et al., 2011b; Campos-Vega et al., 2015; Cruz et al., 2012). The concentration of major mineral elements is shown in table 5. Calcium and potassium, are the most abundant elements, followed by magnesium, while no presence of lead was detected. Results are in agreement with other studies on elemental

composition of SCG (Ballesteros et al., 2014; Cruz et al., 2012), even if in this work lower concentrations of potassium and higher concentration of calcium were found than in the aforementioned studies, while metal concentrations resulted higher than those found by Pujol et al. (2013).

**Table 5.** Metal concentrations in Spent Coffee Grounds. N= number of valid tests; SD= standard deviation; nd= not detected.

Element (mg/g <sub>dried solid</sub> )	N	Mean	Min	Max	SD	Confidence SD -95 %	Confidence SD + 95%	Standard Error
Cu	9	0.021	0.020	0.023	0.0011	0.00072	0.0020	0.00036
Mn	9	0.017	0.016	0.018	0.0012	0.00080	0.0023	0.00039
Fe	9	0.044	0.039	0.049	0.0043	0.0029	0.0083	0.0014
Zn	6	0.023	0.022	0.024	0.001	0.00068	0.0027	0.00044
Ca	6	2.9	2.7	3.1	0.21	0.13	0.52	0.087
Mg	9	1.1	0.94	1.2	0.098	0.066	0.19	0.033
K	9	2.5	2.2	3.0	0.32	0.22	0.62	0.11
Pb	nd	nd						

In SCG the residual caffeine after the brewing process was found to be the 20 % of the initial amount exhibited by RCB and the extractable amount by the used technique was of 151 mg/100 g<sub>SCG</sub>. Caffeine recovery could be interesting since it has extensive applications in pharmacological preparations, such as analgesics, diet aids and cold/flu remedies and can be used as additive in carbonated drink. In addition its antimicrobial properties against *E. coli*, fungi and some pathogenic bacteria were documented (Muthanna and Al-Bayati, 2009). The calorific value of SCG, was confirmed to be very high and in agreement with those reported by several authors (Karmee, 2018; Pujol et al., 2013; Zuorro and Lavecchia, 2012). SCG used for this study contained about the 8 % (w/w) of lipids, which composition was evaluated by GC/FID analysis and results are shown in figure 7. Kondamudi et al.(2008) reported a coffee oil extraction yield of 10-15 %, using hexane as solvent, and variable according to the coffee variety (*Arabica* or *Robusta*), while an extraction yield between 8.6 and 15.3 % was reported by Al-Hamamre et al. (2012), depending on the solvent and the

extraction conditions employed. Saturated and unsaturated methyl esters were found in the coffee oil, particularly the main fraction of FAME consisted of ME of linoleic acid (50%), followed by ME oleic acid (21 %) , ME of palmitic acid (16 %), ME of stearic acid (13 %), ME of linolenic acid (0.7 %) and ME of myristic acid (0.5 %). Similar results were obtained by Kondamudi et al. (2008), who reported that more than 99% methyl esters fraction of coffee biodiesel was made by methyl esters of palmitic acid (51.4%), linoleic acid (40.3%), and stearic acid (8.3%). In addition, a SCG oil was extracted through ultrasound-assisted extraction by Valderez et al. (2014), who reported the following composition: 40.2% linoleic acid (C18:2), 35.9% palmitic acid (C16:0), 10.7% oleic acid (C18:1), 7.5% stearic acid (C18:0), 2.6% arachidonic acid (C20:4), 0.7% behenic acid (C22:0), 0.4% linolenic acid (C18:3) and 2.0% other fatty acids.

The oil recovered by the proposed method corresponded to the second categorization proposed by Campos-Vega et al. (2015) for SCG oils, based on their fatty acid profile, particularly the one showing low palmitic (<40%) and high linoleic (>40%) acids. SCG oil could be interesting not only for energetic purposes, but also for functional food production, since linoleic acid is an essential polyunsaturated fatty acid that can be used as food integrator (Kim et al., 2016).

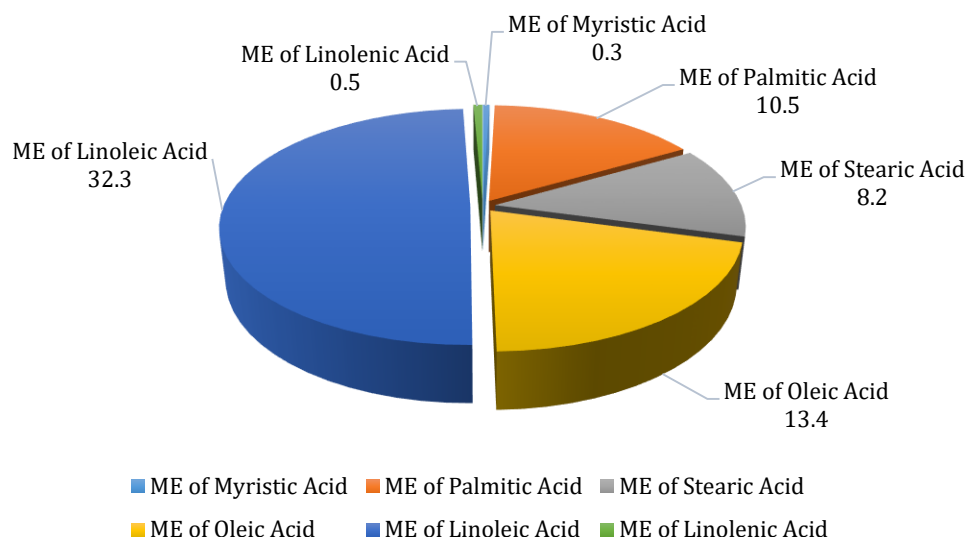


**Figure 7.** Composition of lipid fraction of exhaust coffee. Concentration of methyl esters (ME) of the corresponding fatty acids is expressed as g of Fatty Acid Methyl Ester (FAME) per 100 g of extracted lipids.

In addition, dried SCG were subjected to sieving in order to obtain the particle size distribution. Experimental results are reported as cumulative function  $F(d)$  of the undersize in figure 8. According to equation 3, the arithmetic mean diameter of the distribution was of  $435 \pm 9 \mu\text{m}$  and it was calculated as the area under the curve  $F(d)$  versus  $d$  with respect to the  $F(d)$  axis.

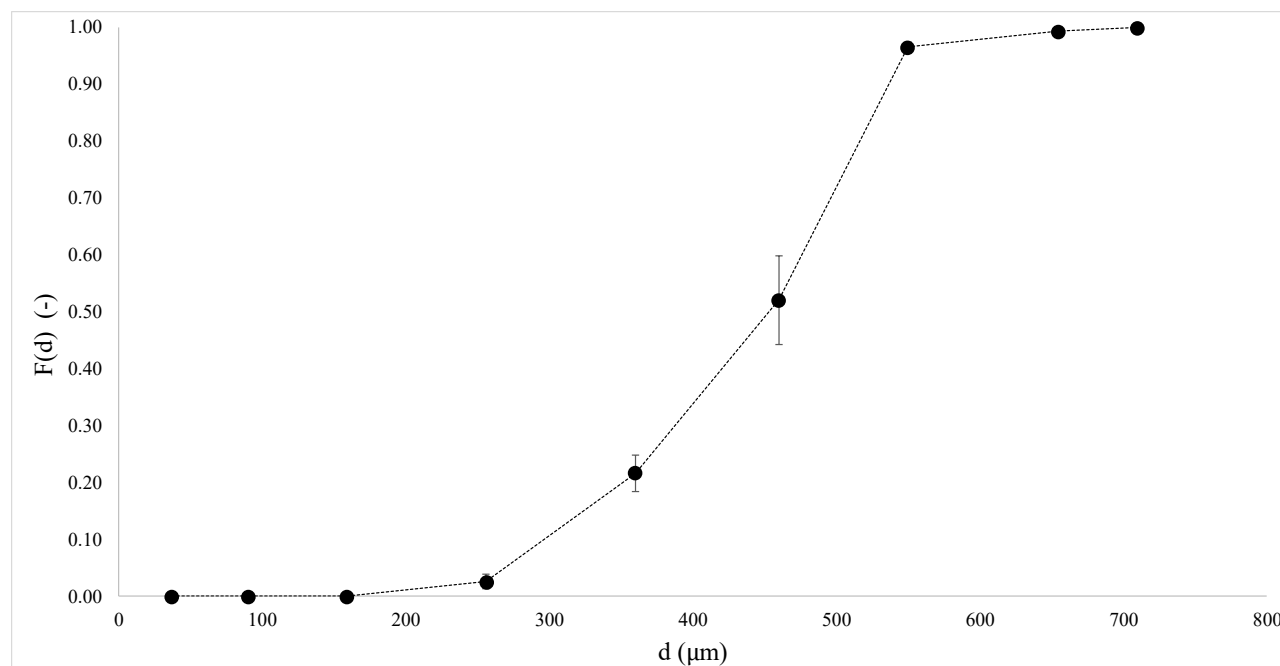


**Figure 8.** Cumulative function  $F(d)$  of the particle size distribution of dry SCG, obtained from sieving tests. Diameter values on x label correspond to the mean diameter of each sieve opening interval.

Finally, the pycnometer method was applied to investigate the particle density.  $\rho_{Toluene}$  was evaluated at the test temperature ( $22.0 \pm 0.1$  °C), basing the calculation on data reported in table 2-303 “Thermodynamic properties of toluene” of Poling et al. (2008). The observed real particle density was  $1299 \pm 32$  kg/m<sup>3</sup> and this result was in agreement with the real density of SCG found by Silva et al. (1998).

## 2.4 CONCLUSIONS

This section on SCG characterization aimed to obtain indispensable data on SCG features for further studies on the extraction of antioxidants from this raw material. Obtained data about its initial moisture at the moment of collection, confirmed that SCG, sampled in different days and periods, presented the same water content of about 53 g<sub>water</sub>/100 g<sub>wet SCG</sub>. This information allowed to establish that 3 days of drying at 50 °C provided a raw material suitable for antioxidant extraction, with a final moisture of about 6 g<sub>water</sub>/100 g<sub>wet SCG</sub>, which is stable over time under storage in the dark and at room temperature. The small average diameter of the particles makes the direct exploitation of SCG for extraction purposes possible, avoiding the

costs related to crushing and grinding. In addition, the high calorific value and the lipid content confirmed the possibility to utilize SCG for energetic purposes, and the high amount of linoleic acid and the residual caffeine suggested the potential application of SCG for food dietary supplement production and cosmetic purposes, other than for the recovery of antioxidants which is the main goal of this thesis and that will be examined in the next chapters.

*Parts of this section were already published in “Eco-sustainable recovery of antioxidants from spent coffee grounds by microwave-assisted extraction : Process optimization, kinetic modeling and biological validation” by Pettinato et al. (2019a), and partially presented as “Extraction of antioxidants from spent coffee grounds using microwave-assisted and high pressure and temperature extractions” by Margherita Pettinato, Bahar Aliakbarian, Alessandro Alberto Casazza, Pier Francesco Ferrari, Patrizia Perego, in the International congress "Green Extraction of natural products- GENP2016", Torino, Italy, 31/05/2016-01/06/2016.*

## *Chapter 3*

# **MICROWAVE-ASSISTED EXTRACTION OF ANTIOXIDANTS FROM SPENT COFFEE GROUNDS**

## **3.1 ABSTRACT**

This chapter is dedicated to the study of microwave-assisted extraction for the recovery of antioxidants from SCG. Indeed, by microwave-assisted extraction is possible to enhance antioxidant extraction yields even when eco-friendly solvents are used. To assess the real advantage in using the non-conventional extraction technique, conventional solid-liquid extraction (SLE) was performed and compared with MAE. The purposes of this study were the optimization of the antioxidant extraction process, the analysis of its kinetics, and the production of a biocompatible extract to be potentially used in cosmetics. Thus, a first optimization was carried out on the solvent composition, temperature and extraction time by response surface methodology. The extract obtained at 150 °C, 90 min of extraction time and using ethanol/water 54:46 (v/v) as solvent was tested on human keratinocytes NCTC 2544 in order to assess its biocompatibility. In addition, the kinetic of antioxidant extraction from spent coffee grounds was investigated, focusing the attention on the effects of initial thermal ramp on the total polyphenol concentration, total solids and antiradical power of the final product. The hydro-alcoholic extracts demonstrated to be very rich of antioxidants with high anti-radical power (from 0.45 to 0.88  $\mu\text{g}$  Trolox equivalent/g dried spent coffee grounds), and their quality was significantly affected by the investigated variables. Peleg's model, was successfully used to describe extraction kinetics, whose investigation revealed that 10 min of heating time at 150 °C provided the highest concentration of polyphenols, and resulted as a good compromise to perform a fast extraction with high extraction yields (43 mg Caffeic Acid Equivalent/g dried spent coffee grounds after 60 min of extraction).

## 3.2 MATERIAL AND METHODS

### 3.2.1 Analytical methods and equipments

#### 3.2.1.1 *Solid-Liquid extraction*

Extraction of antioxidants was performed on SCG, previously dried as described in the paragraph 2.2.1 of the preceding chapter. In 100 mL glass laboratory bottle, 30 mL of solvent were added to 3.0 g of SCG. In order to avoid light degradation of the polyphenols in the extract, the bottle was covered with aluminum foil. The system was left to extract for 24 h under stirring by means of a magnetic stirrer at room temperature ( $25 \pm 2$  °C). After the extraction the exhaust solid and the liquid phase were separated by centrifugation at 6000 xg (MF-20-R centrifuge, Alliance Bio Expertise, Guipry, France) for 5 min and filtration on filter paper, and stored at 4°C for further analyses.

#### 3.2.1.2 *Microwave-assisted extraction equipment*

Antioxidant-rich extracts were obtained by pouring 20 mL of solvent and 2.0 g of dried SCG into closed extraction vessels of a microwave laboratory multimodal oven (Ethos E, Milestone, Italy), equipped with an optical fiber sensor for temperature and automatic Ethos E ATC-FO temperature control (figure 9). PTFE vessels are equipped with HTC protection shield, a polypropylene segment and a ceramic thermowell in which the optical fiber can be introduced for temperature monitoring. Stirring is provided by the rotating platform. The software model 320 and the terminal allowed the control of the system.





**Figure 9.** Ethos E Mileston Microwave Solvent Extractor

During the experiments a maximum radiation power of 500 W and a cooling time of 5 min were set for each test. At the end of the extraction, the exhaust solid was separated by centrifugation at 6000 xg (MF-20-R centrifuge, Alliance Bio Expertise, Guipry, France) for 5 min and filtration on filter paper from the liquid phase, which was stored at 4°C for further analysis.

### 3.2.1.3 *Total polyphenol content*

Total polyphenol concentration in the extracts was evaluated by means of a modified Folin-Ciocalteu's assay (Swain and Hillis, 1959) and expressed as milligrams of caffeic acid per mL of the extract ( $\text{mg}_{\text{CAE}}/\text{mL}$ ). Indeed, the colorimetric assay was performed by adding to a 15 mL flask: 4.8 mL of ultrapure water, 0.2 mL of appropriately diluted sample, 0.5 mL of Folin-Ciocalteu's reagent (Sigma Aldrich, Milan, Italy) and 1.0 mL of a  $\text{Na}_2\text{CO}_3$  saturated solution; finally, a volume of 10 mL was reached by diluting with ultrapure water. The solution was shaken and left in the dark and at room temperature for 60 min. Sample absorbance at 725 nm was measured using the UV-vis spectrophotometer, model Lambda 25 (Perkin Elmer, Wellesley, MA). The total

polyphenol concentration was calculated by employing a calibration curve (equation 7), which was obtained from standard solutions of caffeic acid.

$$ABS_{725\text{ nm}} = 0.0023 \cdot C \quad (R^2 = 0.999) \quad (7)$$

where  $ABS_{725\text{ nm}}$  was the sample absorbance recorded at 725 nm and  $C$  was the concentration of total polyphenols in the liquid extract ( $\mu\text{g}_{\text{CAE}}/\text{mL}$ ).

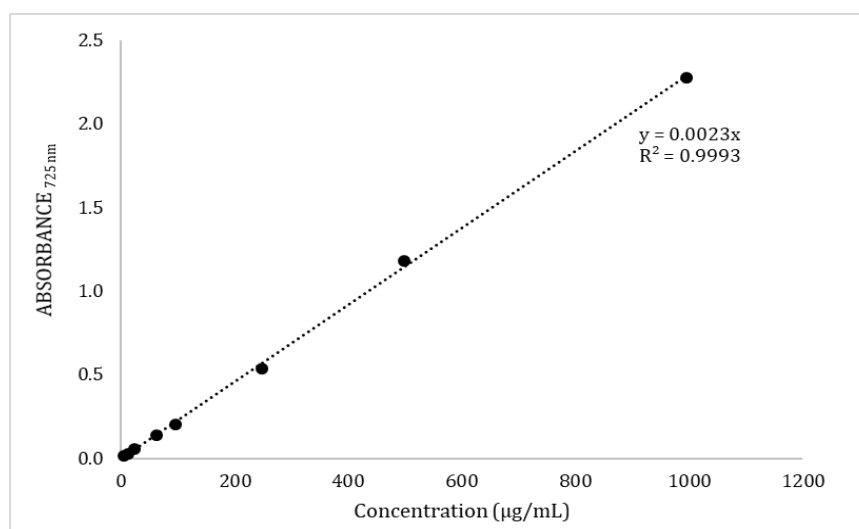


**Figure 10.** Calibration curve for Folin-Ciocalteu's assay obtained from standard solutions of caffeic acid.

#### 3.2.1.4 Total flavonoid content

Total flavonoids (TF) in the extracts were analyzed using the colorimetric assay reported by Yang et al. (2009). In a test tube, 1.25 mL of deionized water, 0.25 mL of properly diluted sample and 75  $\mu\text{L}$  of a 5%  $\text{NaNO}_2$  solution were added. After 5 min, 150  $\mu\text{L}$  of a 10%  $\text{AlCl}_3$  solution were mixed to the sample and left to react for 6 min. Finally, the sample volume was adjusted to 3 mL with 0.5 mL of a 1 M  $\text{NaOH}$  solution and 775  $\mu\text{L}$  of deionized water. The blank sample for the assay was prepared with the diluted sample and deionized water instead of all the other reagents (250  $\mu\text{L}$  of sample at the same dilution of the measurement + 2.75 mL of deionized  $\text{H}_2\text{O}$ ).

The sample absorbance was measured at 510 nm and correlated with the total flavonoid concentration ( $C_{\text{TF}}$ ,  $\mu\text{g}$  of catechin equivalent (CE) per mL of extract) by the

equation 8, which describes the calibration curve, obtained using standard solutions of catechin.

$$ABS_{510\text{ nm}} = 0.0021 \cdot C_{TF} \quad (R^2 = 0.9909) \quad (8)$$

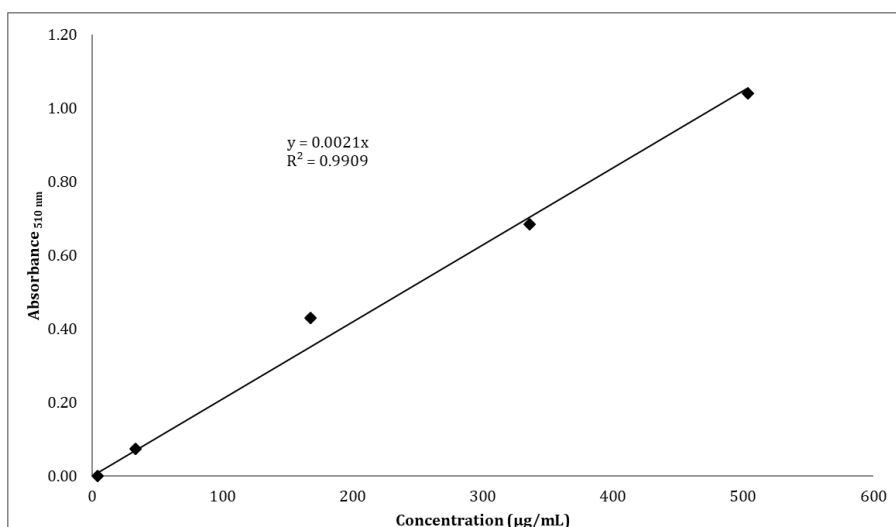


**Figure 11.** Calibration curve for total flavonoid assay obtained from standard solutions of catechin.

### 3.2.1.5 DPPH• assay

Radical-scavenging ability of the extracts was measured by means of the radical 2,2-diphenyl-1-picrylhydrazyl (DPPH•), following the methodology reported by Aliakbarian et al. (2009). The assay was carried out by preparing for each extract nine different dilutions in methanol (in the range 1:2–1:128) and 0.1 mL of them were mixed with 3.9 mL of DPPH• (Sigma Aldrich, Milan, Italy) methanolic solution ( $9.15 \cdot 10^{-5}$  mol/L). The reaction was carried out for 60 min under dark conditions and at room temperature. Sample absorbance was, then, read at 515 nm via spectrophotometer. The DPPH• concentration in the reaction medium ( $C_{DPPH}$ ) was calculated from a calibration curve, whose equation, was determined by linear regression using standard solutions of DPPH• in the range 0.003–0.044 µg<sub>DPPH</sub>/mL (equation 9).

$$ABS_{515\text{ nm}} = 0.023 \cdot C_{DPPH} \quad (R^2 = 0.999) \quad (9)$$

The initial absorbance of methanolic DPPH• solution was compared with those exhibited by the sample after the reaction and the ratio expressed as  $\mu\text{L}_{\text{extract}}/\mu\text{g}_{\text{DPPH}}$  was plotted versus the percentage of the residual DPPH• concentration after 60 min and interpolated by exponential regression (equation 10).

$$Y = a^{bx} \quad (10)$$

The ARP value was expressed as  $\text{g}_{\text{DPPH}}/\text{L}_{\text{extract}}$  and was equivalent to the reciprocal of  $\text{EC}_{50}$  (equation 11), which corresponds to the phenolic extract concentration able to reduce of 50 % the DPPH• radical content ( $Y_{50}$ ).

$$\text{EC}_{50} = \frac{\log a - \log Y_{50}}{\log b} \quad (11)$$

### 3.2.1.6 ABTS•+ assay

The antiradical power evaluation by ABTS•+ assay was performed as described by Re et al. (1999). 7 mM ABTS•+ radical solution was prepared by dissolving 0.0959 g of 2,2'-azino-bis(3-ethylbenzothiazoline-6-sulphonic acid) diammonium salt (Sigma Aldrich, Milan, Italy) in 25 mL of ultrapure water and adding 440  $\mu\text{L}$  of a 140 mM potassium persulfate solution. After 16 h under dark conditions and at 4 °C, the solution was diluted until it exhibited an absorbance of about 0.700, measured via spectrophotometer at 734 nm. Then, 50  $\mu\text{L}$  of properly diluted sample of the extract were added to 1 mL of ABTS•+ working solution and its absorbance was read by the UV-vis spectrophotometer at 734 nm. Sample absorbance was translated into ARP (expressed as  $\mu\text{g}$  of Trolox equivalent per L of extract ( $\mu\text{g}_{\text{TE}}/\text{L}$ )) by the calibration curve reported in equation 12, made by means of standard methanolic solutions of Trolox.

$$\text{ABS}_{734 \text{ nm}} = -0.3364 \cdot C_{\text{Trolox}} + 0.6239 \quad (R^2 = 0.997) \quad (12)$$

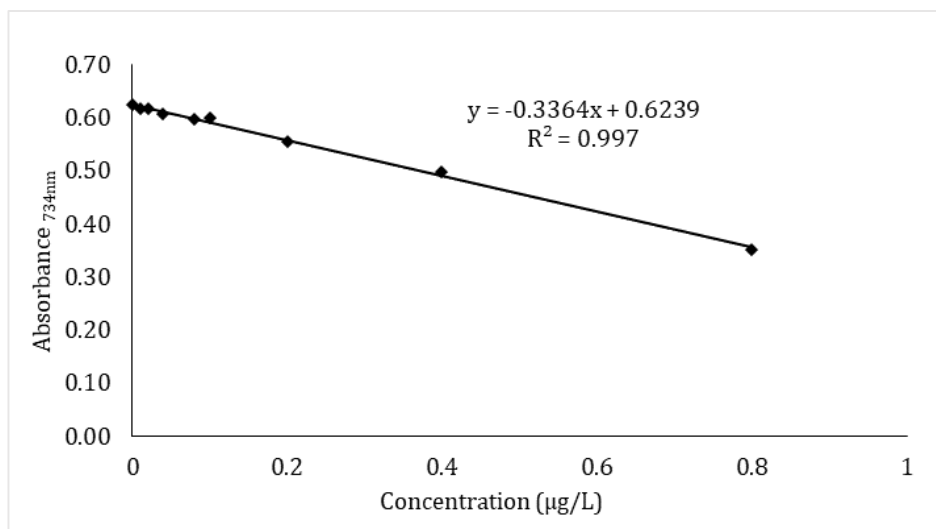


**Figure 12.** Calibration curve for ABTS\*\* assay obtained from standard solutions of Trolox.

### 3.2.1.7 Extract total solids

Extract total solids (ETS) were evaluated gravimetrically, pouring 3 mL of extract in an oven at 110 °C until constant weight was reached. ETS were finally expressed as mg of total solid per mL of extract (mg/mL).

### 3.2.1.8 High Performance Liquid Chromatography (HPLC)

HPLC Agilent 1100 Series (Palo Alto, CA) (figure 13), equipped with a C18 reverse-phase column (Model 201TP54, Vydac, Hesperia, CA) and coupled with an UV-vis Diode Array Detector was employed to investigate the phenolic composition of the extract, operating with the method reported by Casazza et al. (2012). Before the analysis, samples were filtered through a 0.20 µm membrane filter, then injected samples (20 µL) were detected at 280 nm. The mobile phase (flow rate = 1 mL/min) was composed by water/acetic acid (99:1 %, v/v) (solvent A) and methanol/acetonitrile (50:50 %, v/v) (solvent B), while the solvent gradient changed according to the following conditions: from 5% to 30% B in 25 min, from 30% to 40% B in 10 min, from 40% to 48% B in 5 min, from 48% to 70% B in 10 min, from 70% to 100% B in 5 min, isocratic at 100% B for 5 min, followed by returning to the initial conditions (10 min) and the column equilibration (12 min). Column temperature was set at 30 °C.



**Figure 13.** HPLC Agilent 1100 Series

### 3.2.1.9 Cytotoxicity evaluation

Taking into account a possible application in cosmetic formulations, SCG extract with the highest total polyphenol yield was tested at different concentrations (0.005, 0.010, 0.020 and 0.040 mg<sub>CAE</sub>/mL<sub>extract</sub>) on human keratinocytes NCTC 2544. Briefly, cells were seeded into flat-bottom 96 well-plates with a density of  $5 \times 10^3$  cells/well using DMEM supplemented with FBS and antibiotics and incubated at 37°C and 5 % CO<sub>2</sub>. SCG extract was sterilized by 0.22 µm filters (Jet Biofil, Guangzhou, China) before the cellular treatment. After 24 h of cell incubation, the extract was added to the cell culture medium and at pre-determined intervals (1, 2, 3, 7 and 8 days). 20 µL of CellTiter 96® AQueous One Solution reagent was added to each cell culture well. After incubation in dark conditions at 37°C for 1 h, time necessary to reduce yellow MTS to purple formazan, plates were read at 492 nm using a microplate reader (Tecan, Männedorf, Switzerland). Cell viability was assessed even in presence of ethanol/water (54:46 v/v) alone using the same volume of solvents that was necessary to prepare the tested SCG solutions. Results were expressed as a percentage of the control (100 %) and experiments were performed in triplicate. For data analysis, the Statistica v 8.0 software (StatSoft, Tulsa, OK, USA) was used, doing the analysis of variance (ANOVA) and the Tukey's post hoc test.

### 3.2.2 Preliminary comparison between MAE and SLE

A preliminary study on the effects of extraction technique and solvent on extract quality was undertaken by comparing the extraction yields in terms of total polyphenol content, total flavonoid content and antiradical power of the extracts, obtained utilizing solid-liquid extraction and microwave-assisted extraction. Experimental tests were carried out using methanol, ethanol (analytical grade, Sigma Aldrich, St. Louis, MO, USA), ultrapure water from a Milli-Q System (Millipore Inc., USA) and a solution ethanol/water 50:50 (v/v) as solvents.

Operating conditions used for the experiments are reported in table 6. Extractions with methanol were performed in order to have a reference, since it is one of the most used solvent for polyphenol extraction (Mussatto et al., 2011a) and chlorogenic acid presents high solubility in this alcohol (table 7). The other operating conditions were chosen basing on literature data (Casazza et al., 2010).

**Table 6.** Operating conditions of the extraction tests on Spent Coffee Grounds by solid-liquid extraction (SLE) and microwave-assisted extraction (MAE).

	Solvent	Liquid/Solid ratio (ml/g)	Extraction Time (after T <sub>set point</sub> was reached)
SLE Temperature= 25 °C	Methanol	10	24 h
	Ethanol	10	24 h
	Water	10	24 h
	Ethanol/water 50:50 , v/v	10	24 h
MAE Temperature = 110°C Heating time = 10 min maximum power = 500 W	Methanol	10	90 min
	Ethanol	10	90 min
	Water	10	90 min
	Ethanol/water 50:50 , v/v	10	90 min

**Table 7.** Physical properties of methanol, ethanol and water. <sup>a</sup> (Veggi et al., 2013); <sup>b</sup> (González et al., 2004); <sup>c</sup> (Sabir et al., 1974).

	Boiling Temperature <sup>a</sup> at 1 atm (°C)	Density <sup>b</sup> (g/cm <sup>3</sup> ) at 298.15 K	Viscosity <sup>a</sup> at 25 °C (cP)	Chlorogenic acid solubility <sup>c</sup> (g/100 mL)	Dielectric constant <sup>a</sup> $\epsilon'$ at 20 °C	Dissipation factor <sup>a</sup> $\tan\delta$ ( $\times 10^{-4}$ )
Methanol	65	0.787	0.54	15.2	32.6	6400
Ethanol	78	0.785	0.69	6.2	24.3	2500
Water	100	0.997	0.89	0.6	78.3	1570

**Figure 14.** Graphical representation of the main steps of the study on comparison between MAE and SLE

### 3.2.3 Microwave-assisted extraction optimization by RSM

The investigation on MAE operating conditions (extraction time, extraction temperature and solvent composition, expressed as water content (%) in the ethanol-water solution) was carried out by the Box-Behnken Design (BBD) (figure 15) for response surface methodology (RSM), using Design Expert software (Stat-Ease, Inc., Minneapolis, United States). Experimental design and response surface methodology are effective techniques for the simultaneous investigation on multiple process variables, identification of the most significant conditions, with minimum effort and time (Arabi et al., 2016a, 2016b; Ostovan et al., 2018; Pavlovic et al., 2013; Ranic et al., 2014).



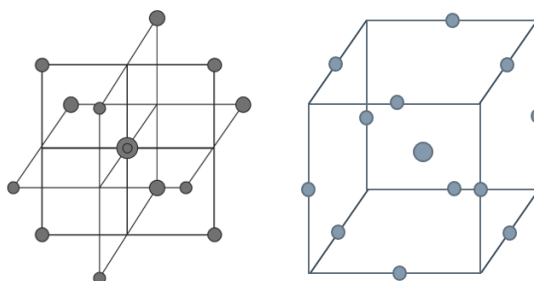


**Figure 15.** Box-Behnken Design representations

The range and levels of the three independent variables are reported in table 8. The range of temperature was chosen in order to have the lower value near the solvents boiling temperature at 1 atm, while higher temperatures than 150 °C were not considered to avoid the fast occurrence of thermal degradation and Maillard reactions.

**Table 8.** Independent variables and their levels employed in the Box Behnken Design for optimization of SCG extraction.

Independent variables		Coded levels		
		-1	0	+1
Extraction time	min	30	60	90
Water content in the solvent	%	20	60	100
Temperature	°C	90	120	150

At this early stage, the heating time (10 min) was not included in the extraction time values presented in table 8. Indeed, the extraction was considered as started only when the set point temperature was reached by the system.

TP, TF and ARP based on DPPH• and ABTS•+ assays were chosen as response variables. The fitting equation of the generic response variable  $Y$  is given in the equation 13:

$$Y = \alpha_0 + \sum_{i=1}^2 \alpha_i X_i + \sum_{i=1}^2 \alpha_{ii} X_i^2 + \sum_{i=1}^2 \sum_{j=1}^2 \alpha_{ij} X_i X_j \quad (13)$$

where  $Y$  represented the response variable,  $X_i$  and  $X_j$  were the independent variables,  $\alpha_0$  was a constant, while  $\alpha_i$ ,  $\alpha_{ii}$  and  $\alpha_{ij}$  represented the coefficients of the linear, quadratic and interactive terms of the equation.

The model adequacy was determined by means of the coefficient of determination ( $R^2$ ) and by analysis of variance (ANOVA), that was generated by Design Expert. On the basis of the data obtained by equations of fitting, the numerical optimization tool of Design Expert was used to find the optimal value of the input variables, within the investigated ranges, able to contemporary maximize the three response variables. In addition, a second optimization was carried out, in which the constraint of maximizing the water content in the solvent was added. The optimization results were experimentally verified by measuring the TP, TF, ARP and, in order to make a comparison between the extract phenolic compositions, by HPLC analysis.

### 3.2.4 Kinetic study on microwave-assisted extraction

A deeper analysis of time and temperature-dependence of TP was achieved by the study of the extraction kinetic. The experimental tests were performed at three temperatures (120 °C, 135 °C and 150 °C), employing a mixture of ethanol/water 54:46 (v/v) as solvent, and carrying on the extraction up to 130 min. In this case, also the heating time was taken into account in the extraction time computation, in such a way that the extraction behavior during the thermal ramp could be displayed.

Results were expressed as total polyphenol concentration in the extract ( $C(t)$ , mg<sub>CAE</sub>/mL) and three kinetic models were applied to represent the experimental data. Fick's law-based extraction model was investigated to characterize the extraction process. Since the extraction vessel was subjected to rotation, it was assumed that external mass resistance was negligible. Because of the nature of the heating mechanism, temperature was considered as spatially uniform in the system. Total polyphenol mass transfer in the solid matrix was considered occurring only along radial

coordinate and was function of time, but the hypothesis of time-independent diffusion coefficient was adopted. Solid particles were assumed as a pseudo-homogeneous medium with spherical shape and symmetry, and having a uniform concentration of the target compounds at the beginning ( $C_0$ ). The concentration of the solute in the solvent was only time-dependent and equal to that at the interior of the particle pores. The particle porosity and tortuosity were taken into account within the apparent diffusion coefficient. Although the extraction process involved more than one target analyte, the polyphenols were treated as a pseudo-compound and the competitive extraction of other analytes was assumed not interfering with the total polyphenol mass transfer. Under these hypothesis the mass balance in the spherical particle could be written as in the equation 14:

$$\frac{\partial C}{\partial t} = D_{eff} \cdot \nabla^2 C \quad (14)$$

Where  $C$  was total polyphenol concentration in the solid and  $D_{eff}$  was the apparent diffusion coefficient, in which particle porosity  $\varepsilon$  and channel tortuosity  $\tau$  ( $D_{eff} = D \cdot \varepsilon / \tau$ ) were included.

The equation 14 was subjected to the following initial and boundary conditions:

$$\begin{aligned} C(\forall r, t = 0) &= C_0; \\ C(r = R, t > 0) &= 0; \\ \frac{\partial C(r = 0, t > 0)}{\partial r} &= 0. \end{aligned}$$

The solution of Fick's equation could be expressed as reported by Perez *et al.* (2011) and it is shown into equation 15:

$$\frac{C(t)}{C_{\infty}} = 1 - A \exp(-Bt) \quad (15)$$

Where  $C_{\infty}$  was the concentration of total polyphenols in the solvent at  $t \rightarrow \infty$ , while A and B are shown in the equations 16 and 17:

$$A = \left(1 - \frac{C_0}{C_{\infty}}\right) \frac{6}{\pi^2} \exp(Bt_0) \quad (16)$$

$$B = \frac{D_{eff} \cdot \pi^2}{R^2} \quad (17)$$

According to the equations 15, 16 and 17 the rapid non-diffusive step of the extraction was considered into the  $C_0$ , which was the concentration reached after washing time ( $t_0$ ) in the solvent, and the simplified solution (equation 15) implies sufficient long extraction time. Model parameters A and B were evaluated as the slope and the intercept of the straight line obtained by plotting  $(1 - C(t)/C_{\infty})$  versus  $t$ .

On the other hand, the first-order model (equation 18) was commonly proposed in literature for describing the rate of antioxidant extraction from natural sources (Khan et al., 2010; Sant'Anna et al., 2012; Spigno et al., 2007; Spigno and De Faveri, 2009):

$$\frac{dC(t)}{dt} = k_{obs}(C_{\infty} - C(t)); \quad I.C.: C(t = 0) = 0 \quad (18)$$

Where  $C_{\infty}$  was the total polyphenol concentration at equilibrium,  $t$  was time, and the first order constant  $k_{obs}$  could be considered as an overall rate constant according to the steady-state model described by Spiro and Jago (1982). Integrating with the initial condition (I.C.) reported in for equation 14, the time-dependent concentration could be written as in equation 19, that easily allowed to calculate  $k_{obs}$  from experimental data, since it was the slope of the straight line obtained by plotting the  $\ln(1 - C/C_{\infty})$  versus  $t$ :

$$\ln\left(1 - \frac{C(t)}{C_\infty}\right) = -k_{obs} \cdot t \quad (19)$$

In this case,  $C_\infty$  was determined as the average value of the experimental data corresponding to the plateau in the graph  $C=f(t)$ .

As reported by Chan *et al.* (2014), another extraction model usually employed was the second-order rate law (equation 20):

$$\frac{dC(t)}{dt} = k_{II}(C_\infty - C(t))^2; \quad I.C.: C(t=0) = 0 \quad (20)$$

Where  $k_{II}$  was the second order extraction rate constant. After the integration according to the I.C.,  $k_{II}$  and  $C_\infty$  were simultaneously determined through the slope and the intercept of the straight line  $t/C(t) = f(t)$ , described by equation 21:

$$\frac{t}{C(t)} = \frac{1}{C_\infty} \cdot t + \frac{1}{k_{II} \cdot C_\infty^2} \quad (21)$$

Furthermore, the Peleg's model (Peleg, 1988) adapted to extraction process (equation 22) resulted often suitable to elaborate experimental data, as reported by several authors (Bucić-Kojić *et al.*, 2007; Dong *et al.*, 2014; Mustapa *et al.*, 2015):

$$\frac{dC(t)}{dt} = \frac{k_1}{(k_1 + k_2 \cdot t)^2}; \quad I.C.: C(t=0) = 0 \quad (22)$$

Where,  $k_1$  and  $k_2$  were the model constants,  $1/k_1$  was the initial rate ( $t = 0$ ), and  $1/k_2$  was the concentration at  $t \rightarrow \infty$ . Integration of equation 20 is reported in the equation 23 in the useful form for the parameters calculation.

$$\frac{t}{C(t)} = k_1 + k_2 \cdot t \quad (23)$$

The agreement between the proposed models and experimental data was established by means of the coefficient of determination ( $R^2$ ) and the root mean square deviation (RMSD) (equation 24):

$$RMSD = \sqrt{\frac{1}{N} \sum_{i=1}^N (C_{exp} - C_{calc})^2} \quad (24)$$

Where  $N$  was the number of experimental points of the extraction curve,  $C_{exp}$  was the experimentally observed concentration of total polyphenols and  $C_{calc}$  was the calculated concentration.

### 3.2.5 Study on the effects of heating steps in microwave-assisted extraction of polyphenols from SCG

The kinetic of antioxidant extraction from SCG was additionally investigated by focusing the attention on the effects of initial thermal ramp on the total polyphenol concentration, total solids and antiradical power of the final product. Peleg's model was used to describe extraction kinetics of polyphenols into the hydro-alcoholic extracts. Indeed, equation 22 can be written by replacing the model constants  $k_1$  and  $k_2$  with their physical meaning (equation 25):

$$\frac{dC(t, T, t_H)}{dt} = \frac{K_1(T, t_H)}{\left(K_1(T, t_H) + \frac{1}{C|_{t \rightarrow \infty}(T, t_H)} \cdot t\right)^2}; \quad I.C.: C(t=0) = 0 \quad (25)$$

Where  $K_1$  and  $C|_{t \rightarrow \infty}$  were the model constants, both of them supposed as functions of temperature ( $T$ ) and heating time ( $t_H$ ).  $1/K_1$  represented the initial rate ( $t \rightarrow 0$ ) of extraction, while  $C|_{t \rightarrow \infty}$  was the concentration at  $t \rightarrow \infty$ .

The aim was to analyze the extraction kinetic of SCG when temperature was kept under controlled conditions and to investigate the effects of heating time and temperature on extraction yields, since the former is considered as a fundamental parameter in the extraction processes, and the initial thermal ramp (i.e. heating time, once extraction temperature was fixed) could influence the product quality.

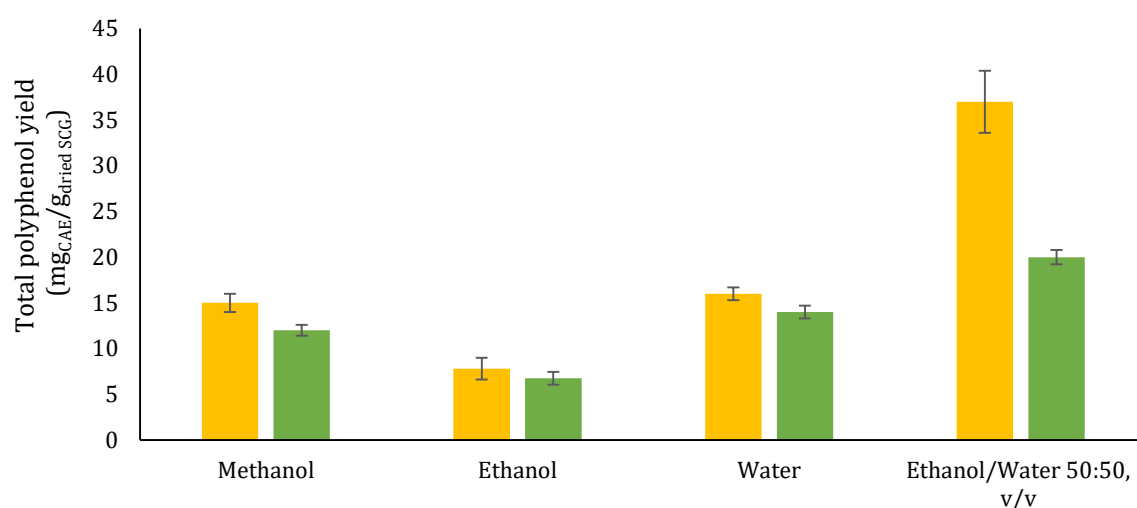
The experimental tests were performed at three different temperatures (120, 135 and 150 °C) and at three heating times (1 min, 10 min, 20 min), carrying on the extraction up to 120 min. In addition, liquid to solid ratio was of 10 mL/g dried SCG, a maximum radiation power of 500 W and a cooling time of 5 min were set for each test. Peleg's model parameters were thus evaluated from experimental curves, whose values were determined by means of the linearized form of the Peleg's model, in the same way described in the paragraph 3.2.4.

### 3.3 RESULTS AND DISCUSSION

#### 3.3.1 Preliminary comparison between microwave-assisted extraction and solid liquid extraction

Results related to the study in which conventional solid-liquid extraction and microwave-assisted extraction were compared are reported in figure 16 in terms of total polyphenol yields. Using methanol, ethanol and water as solvents no differences can be observed between MAE and SLE. Ethanol seemed to be the worst solvent for polyphenols extraction, while pure water and pure methanol allowed to extract the same amount of total polyphenols. By means of these first data, can be desumed that effectively the optimal operating conditions found in literature for MAE (110 °C and 90 min) are useful to obtain the same extraction yields that could be achieved by room temperature SLE but after 24 h. Conversely, taking into account the fourth solvent a great difference can be observed comparing the two extraction methods, indeed MAE allowed to obtain an extraction yield 75 % higher than SLE. In addition, the aqueous ethanol solution was able in both of the cases to ensure the maximum of polyphenol yields. This result highlighted the importance of the solvent composition, that combined with the right extraction technique could improve the process. The success

of the 50% ethanol solution as solvent can be traced back to the intermediate polarity, given by the mixture of the most polar investigated solvent (water) with the least one (ethanol). The major affinity of polyphenols for ethanol/water mixtures is in agreement with several cases in literature, like the extraction of polyphenols from soybean (Jokic et al., 2010) or from spent coffee grounds (Ranic et al., 2014). The use of ethanol/water mixtures as solvent can be a great advantage for the extraction from natural products since it is a safe and eco-friendly solvent, that can be also produced by fermentation from natural wastes, in agreement with the biorefinery approach.



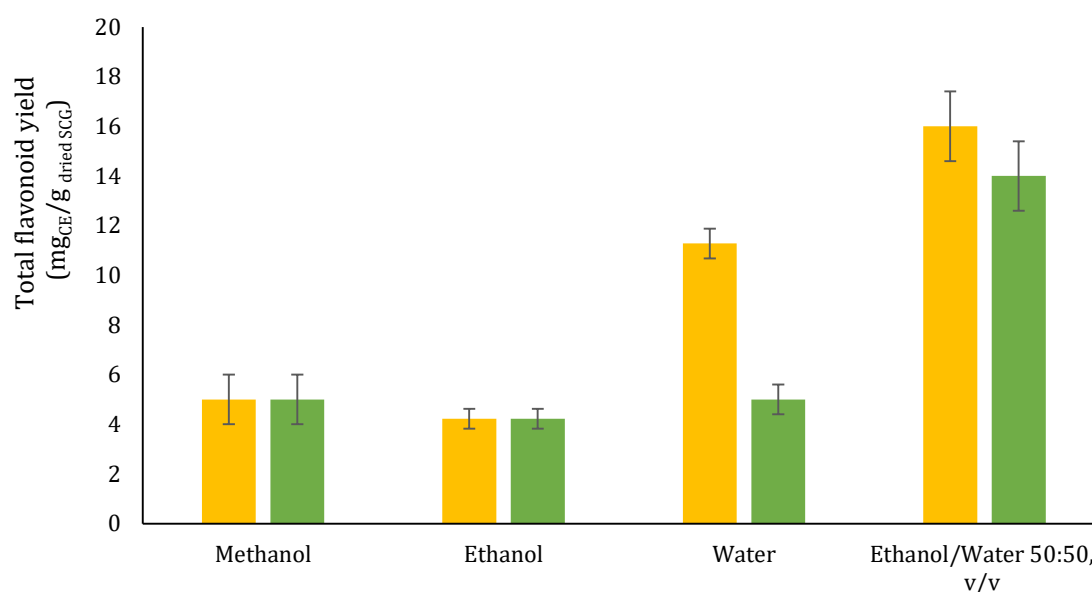
**Figure 16.** Total polyphenol yields, expressed as mg of caffeic acid equivalent per g of dried SCG, as a function of the extraction technique (■ MAE, ■ SLE) and solvent.

Figure 17 showed that total flavonoid yields followed a similar trend to that found for total polyphenols. Indeed, the only difference among the pure solvents was given by the extraction carried out with water under microwave action, since it exhibited a two folds higher yield than the one shown for SLE. The higher temperature in MAE, probably provided a more intense solubilization of flavonoids, thus a more intense difference between the yields of the two extraction techniques was found. In addition, the higher dielectric constant of water (*see table 7*) allowed to absorb a great amount of microwaves than the other solvents, increasing the effects on the flavonoid release. Nevertheless, was again the equivolumetric mixture ethanol/water the solvent that



provided the highest extraction yield, probably due to the intermediate polarity obtained by the solvent blending.

Results about antiradical power evaluation are given in figure 18. No huge differences related to the extraction technique can be observed in terms of antiradical power exhibited by the samples, exception given by the case of pure ethanol, whose extract obtained by MAE seemed to have higher scavenging potential than the SLE one. Instead, making a comparison based on the solvent, was confirmed that the mixture ethanol/water resulted as the best option, being able to ensure the highest extraction yields and the extracts with the highest antiradical power.



**Figure 17.** Total flavonoid yields, expressed as mg of catechin equivalent per g of dried SCG, as a function of the extraction technique (■ MAE, ■ SLE) and solvent.

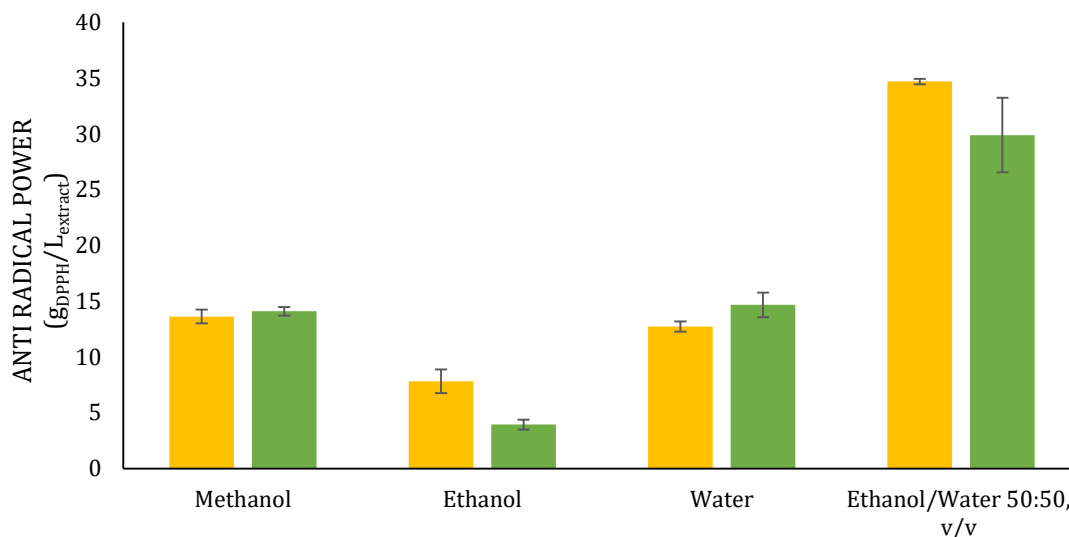


**Figure 18.** Antiradical power of the extract, expressed as g of DPPH (2,2-Diphenyl-1-picrylhydrazyl) per L of extract, as a function of the extraction technique (■ MAE, ■ SLE) and solvent.

### 3.3.2 Microwave-assisted extraction optimization by RSM

From preliminary data it could be deduced as the application of microwaves was able to make the process faster and that the ethanol/water ratio of the solvent is one of the key variable that can affect the extraction process, being directly related to the solvent polarity. For these reasons response surface methodology was used for a first screening of the process variable domain defined by temperature, ethanol/water ratio and extraction time.

The values of the input variables in the considered design space points and the experimental results in terms of response variables are presented in table 9. The experiments related to the central point were repeated three times and the total number of experiments was 15.

**Table 9.** Input variable values of the Box Behnken Design of experiments and experimental results in terms of: total polyphenols yield (TP), expressed as mg of caffeic acid equivalent (CAE)/g of dried SCG; total flavonoid yield (TF), expressed as mg of catechin equivalent (CE)/g of dried SCG; antiradical power (ARP) by ABTS<sup>••</sup> assay, expressed as  $\mu\text{g}$  of Trolox equivalent (TE)/L of extract and by DPPH<sup>•</sup> assay, expressed as g of DPPH per L of extract.

Temperature (°C)	time (min)	Water content (%)	TP (mg <sub>CAE</sub> /g)	TF (mg <sub>CE</sub> /g)	ARP ( $\mu\text{g}$ TE/L)	ARP (g <sub>DPPH</sub> /L)
120	60	60	36±3.3	12±2.4	36±3.2	25±2.8
150	30	60	44±3.7	16±1.6	48±0.7	32±3.5
150	60	20	35±2.3	15±1.2	49±2.8	28±3.0
120	90	100	19±1.4	10±0.9	33±5.4	31±8.2
120	60	60	34±2.1	17±0.7	42±1.5	23±1.4
90	60	20	21±1.2	13±0.9	29±1.2	29±4.7
90	60	100	16±2.8	8.2±2.2	22±4.2	16±4.1
120	30	100	22±0.5	10±0.7	30±2.1	21±6.0
120	60	60	37±2.9	17±1.6	41±6.1	30±1.8
90	30	60	27±0.8	12±0.9	37±3.4	25±2.3
120	30	20	26±1.7	15±1.1	33±4.6	27±3.9
150	90	60	38±2.0	21±1.9	50±0.6	23± 0.2
150	60	100	30±1.0	14±0.7	37±3.4	22±3.1
90	90	60	31±2.4	17±0.9	43±0.9	33±6.8
120	90	20	33±2.3	20±1.5	43±0.9	29±2.7

The ANOVA results for the TP (table 10) showed that the fitted RSM model (equation 24) was statistically significant ( $F=42.22$ ,  $p< 0.0001$ ) with high coefficient of determination ( $R^2=0.9769$ ) and adjusted coefficient of determination ( $\text{Adj}R^2= 0.9537$ ); not significant lack of fit was reported.

**Table 10.** Analysis of variance table (Partial sum of squares - Type III) for Response Surface Reduced Quadratic Model of the output variable total polyphenol yield (TP).

Source	Sum of Squares	df	Mean Square	F Value	p-value Prob > F	Coefficient Estimate	df	Standard Error	95% CI Low	95% CI High
Model	862.50	7	123.21	42.22	< 0.0001					
A-Temperature	338	1	338.00	115.82	< 0.0001	6.50	1	0.60	5.07	7.93
B-Time	0.5	1	0.50	0.17	0.6913	0.25	1	0.60	-1.18	1.68
C-Water Content	98	1	98.00	33.58	0.0007	-3.50	1	0.60	-4.93	-2.07
AB	25	1	25.00	8.57	0.0221	-2.50	1	0.85	-4.52	-0.48
AC	0	1	0.00	0.00	1.0000	0.00	1	0.85	-2.02	2.02
BC	25	1	25.00	8.57	0.0221	-2.50	1	0.85	-4.52	-0.48
C <sup>2</sup>	376.00	1	376.00	128.84	< 0.0001	-10.04	1	0.88	-12.13	-7.95
Intercept						35.29	1	0.65	33.76	36.81
Residual	20.43	7	2.92							
Lack of Fit	15.76	5	3.15	1.35	0.4771					
Pure Error	4.67	2	2.33							
Cor Total	882.93	14								

$$TP = -36.0 + 0.383 \cdot T + 0.466 \cdot t + 0.790 \cdot W - 2.78 \cdot 10^{-3} \cdot T \cdot t - 2.08 \cdot 10^{-3} \cdot t \cdot W - 6.27 \cdot 10^{-3} \cdot W^2 \quad (26)$$

In equation 26, T was the temperature (°C); W was the water content in the solvent mixture (%), and t was time (min). In the fitting equation, the terms that exhibited the strongest effect for the model were the linear term of temperature (F=115.82; p<0.0001), W (F=33.58; p=0.0007) and W<sup>2</sup> (F=128.84, p<0.0001), while the dependence on time resulted less significant. As depicted in figure 19-a and 19-b, the TP increased with temperature and decreased with time, while the highest values were obtained when the solvent composition was equivolumetric.

Equation 27 reports the fitted RSM model for TF:

$$TF = -1.84 + 0.0658 \cdot T + 0.0625 \cdot t + 0.149 \cdot W - 1.78 \cdot 10^{-3} \cdot W^2 \quad (27)$$

**Table 11.** Analysis of variance table (Partial sum of squares - Type III) for Response Surface Reduced Quadratic Model of the output variable total flavonoid yield (TF).

Source	Sum of Squares	df	Mean Square	F Value	p-value Prob > F	Coefficient Estimate	df	Standard Error	95% CI Low	95% CI High
Model	143.73	4	35.93	7.91	0.0038					
A-Temperature	31.21	1	31.21	6.87	0.0256	1.975	1	0.75	0.30	3.65
B-Time	28.13	1	28.13	6.19	0.0321	1.875	1	0.75	0.20	3.55
C-Water Content	54.08	1	54.08	11.90	0.0062	-2.6	1	0.75	-4.28	-0.92
C <sup>2</sup>	30.32	1	30.32	6.67	0.0273	-2.85	1	1.10	-5.31	-0.39
Intercept							16	0.81	14.20	17.80
Residual	45.45	10	4.55							
Lack of Fit	28.78	8	3.60	0.43	0.8391					
Pure Error	16.67	2	8.33							
Cor Total	189.18	14								

As reported in table 11, the TF model was significant ( $F=7.91$ ,  $p=0.0038$ ), with not significant lack of fit but the  $R^2$  and  $AdjR^2$  were not very high (0.7598 and 0.6637, respectively). Even in this case, the most significant term was W ( $p=0.0062$ ), and figure 19-c and 19-d showed that the highest yield could be obtained when the water content in the solvent mixture was slightly less than for TP. In addition, with respect to what was found for total polyphenol yield, the highest flavonoid recovery was achieved at higher time and temperatures. A behavior similar to TF was observed for what concerns the antiradical power, as reported in figures 19-e and 19-f. RSM model for ARP is given in equation 28:

$$\begin{aligned}
 ARP = 17.0 - 0.152 \cdot T - 0.0523 \cdot t + 0.692 \cdot W - 1.05 \cdot 10^{-3} \cdot T \cdot t - 1.04 \cdot 10^{-3} \cdot T \\
 \cdot W - 1.51 \cdot 10^{-3} \cdot t \cdot W + 2.07 \cdot 10^{-3} \cdot T^2 + 2.99 \cdot 10^{-3} \cdot t^2 - 4.80 \\
 \cdot 10^{-3} \cdot W^2
 \end{aligned} \quad (28)$$

**Table 12.** Analysis of variance table (Partial sum of squares - Type III) for Response Surface Reduced Quadratic Model of the output variable antiradical power (ARP).

Source	Sum of Squares	df	Mean Square	F Value	p-value Prob > F	Coefficient Estimate	df	Standard Error	95% CI Low	95% CI High
Model	834.01	9	92.67	7.50	0.0195					
A-Temperature	350.13	1	350.13	28.35	0.0031	6.62	1	1.24	3.42	9.81
B-Time	57.68	1	57.68	4.67	0.0831	2.69	1	1.24	-0.51	5.88
C-Water Content	126.70	1	126.70	10.26	0.0239	-3.98	1	1.24	-7.17	-0.79
AB	3.61	1	3.61	0.29	0.6120	-0.95	1	1.76	-5.47	3.57
AC	6.19	1	6.19	0.50	0.5106	-1.24	1	1.76	-5.76	3.27
BC	13.11	1	13.11	1.06	0.3501	-1.81	1	1.76	-6.33	2.71
A <sup>2</sup>	12.87	1	12.87	1.04	0.3541	1.87	1	1.83	-2.83	6.57
B <sup>2</sup>	26.76	1	26.76	2.17	0.2010	2.69	1	1.83	-2.01	7.39
C <sup>2</sup>	218.08	1	218.08	17.66	0.0085	-7.69	1	1.83	-12.39	-2.98
Intercept						40.06	1	2.03	34.84	45.27
Residual	61.75102	5	12.3502							
Lack of Fit	41.7424	3	13.91413	1.3908	0.4442					
Pure Error	20.00862	2	10.00431							
Cor Total	895.758	14								

ANOVA results (table 12) revealed that equation 28 was statistically significant ( $F=7.50$ ,  $p=0.0195$ ) and without significant lack of fit, while  $R^2$  and  $AdjR^2$  were of 0.9311 and 0.8070, respectively. T ( $F= 28.35$ ,  $p=0.0031$ ) and  $W^2$  ( $F=17.66$ ,  $p=0.0085$ ) were the most significant terms of the model, instead low significancy was shown by the interaction terms. Actually response surfaces related to ARP, resulted more complex than TF ones, due to the several compounds that can exhibit the antiradical power (e.g. proteins, sugars), and whose extraction could change according to the operating conditions used in the design space points.

On the other hand, ANOVA results concerning the antiradical power expressed by means of DPPH• did not show any significant trend. Thus, for extract obtained by MAE, only ABTS•<sup>+</sup> assay was used to express the extract scavenging ability.

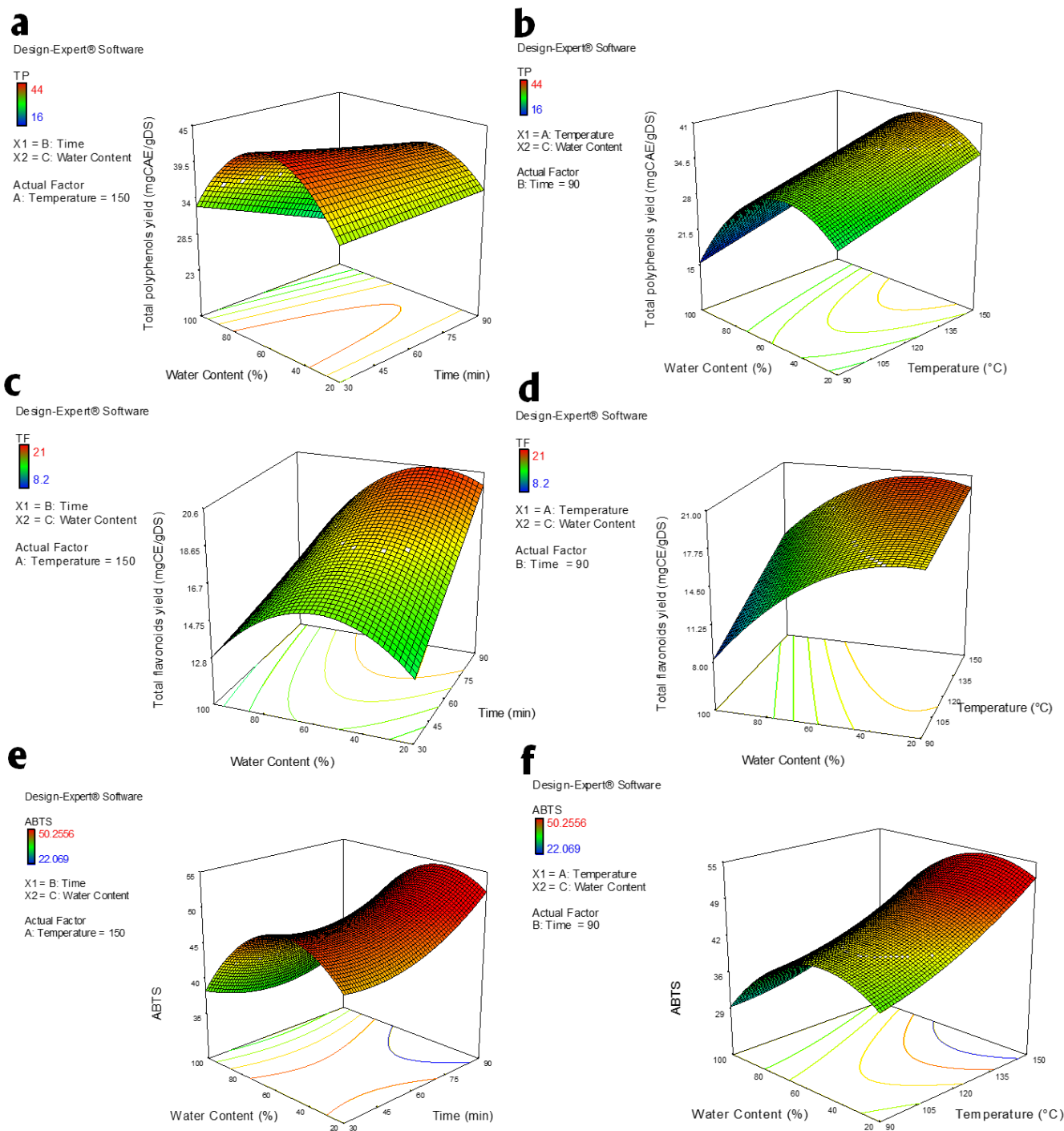


**Figure 19.** Three-dimensional surface plots of the quadratic regression equations obtained by the experimental design coupled with RSM. Responses are reported as function of the input variables as follow:  
a,b) total polyphenol yield (TP, mg of caffeic acid equivalent (CAE)/g of dried SCG (DS));  
b,c) total flavonoid yield (TF, mg of catechin equivalent (CE)/g of dried SCG (DS);  
d,e) antiradical power (ABTS,  $\mu$ g of Trolox equivalent (TE)/L of extract), obtained by means of the ABTS<sup>••</sup> (2,2'-azino-bis(3-ethylbenzothiazoline-6-sulphonic acid)) assay.

On the basis of the RSM models developed for the three response variables, two numerical optimizations led to the best values of the input variables. A first solution, able to maximize TP, TF and ARP, suggested the following operating conditions:  $T=150^{\circ}\text{C}$ ,  $t=90$  min and  $W=46\%$ . The optimization was experimentally verified and results, compared with the value predicted by the models, are shown in table 13. In the second numerical optimization, the constraint of maximizing the water content in the solvent was added. Optimized input variables presented similar values to those related to the previous optimization:  $T=150^{\circ}\text{C}$ ;  $t=85$  min;  $W=68\%$ . Results were experimentally verified and in table 13 the comparison between the experimental value and model prediction was reported.

**Table 13.** Comparison among the experimental value of dependent variables and RSM model prediction, obtained by the numerical optimization tool of Design Expert. TP: Total polyphenol yield (mg of caffeic acid equivalent (CAE)/g of dried SCG); TF: total flavonoid yield (mg of catechin equivalent (CE)/g of dried SCG); ARP: antiradical power ( $\mu\text{g}$  of Trolox equivalent (TE)/L of extract).

	Temperature ( $^{\circ}\text{C}$ )	time (min)	Water Content in the solvent (%)	TP ( $\text{mg}_{\text{CAE}}/\text{g}$ )	TF ( $\text{mg}_{\text{CE}}/\text{g}$ )	ARP ( $\mu\text{g}_{\text{TE}}/\text{L}$ )
Experimental	150	90	46	$46.0 \pm 2.9$	$16.4 \pm 1.4$	$55.8 \pm 1.8$
Model				40.4	20.4	54.0
Experimental	150	85	68	$41.0 \pm 1.6$	$20.5 \pm 1.6$	$52.1 \pm 2.1$
Model				37.8	19.2	51.0

From table 13 it can be observed as model values were very close to the experimental ones, as well as very similar were the input variable values of both of the optimizations. Obviously, the only exception was given by the water content, whose increase led to the reduction of TP and ARP as well, while TF was not affected by the operating condition variation. Moreover, HPLC analysis of the two extracts (table 14) highlighted that in both of the cases the extracted compounds had the same retention times, but the lower was the water amount in the solvent, the higher were the concentrations of caffeine and chlorogenic acid, as well as the concentration of all the phenolics as demonstrated by the total area, which was about 1.5 times higher in the case of extract 1 (7541 mAU min) with respect to extract 2 (4972 mAU min). Indeed, the compounds listed as 4,5,6,7,9,10,11,12,13 although not well defined, presented spectra very close to the one of chlorogenic acid, thus they were suspected to be its isomers or derivatives. HPLC



chromatogram of extract 1 is reported in figure 20, and spectra of chlorogenic acid (figure 21) and of compounds classified as 6, 7 and 10 are reported respectively in figures 22, 23, 24 as examples. This hypothesis was also strengthened by the phenolic profile of SCG reported by Panusa et al. (2013). Furthermore, the compounds listed as 1 and 2 remained unidentified but showed the typical spectra of polyphenol class. Thus, the conditions T=150 °C, t=90 min, ethanol/water 54:46 v/v resulted to be the best choice for antioxidant extraction from SCG.

**Table 14.** HPLC analysis of the two extracts obtained using the following operating conditions: Temperature=150 °C, time=90 min, ethanol/water 54:46 (v/v) (Extract 1); Temperature=150 °C, time = 85 min, ethanol/ water 32:68 (v/v) (Extract 2). \* percentages of the total area = 7541 mAU min; \*\* percentages of the total area = 4972 mAU min

List of compounds	Retention Time (min)	Extract 1 Area*	Concentration (mg/L)	Extract 2 Area**	Concentration (mg/L)
1 (unidentified)	17.6	13%		8%	
2 (unidentified)	19.3	6%		4%	
Chlorogenic Acid	21.3	6%	9	8%	8
4 (Chlorogenic Acid Derivative)	23.2	2%		3%	
5 (Chlorogenic Acid Derivative)	23.7	3%		2%	
6 (Chlorogenic Acid Derivative)	24.3	6%		7%	
7(Chlorogenic Acid Derivative)	24.6	10%		7%	
Caffeine	25.9	33%	32	40%	25
9 (Chlorogenic Acid Derivative)	27.1	3%		3%	
10 (Chlorogenic Acid Derivative)	27.4	6%		6%	
11(Chlorogenic Acid Derivative)	29.4	3%		4%	
12 (Chlorogenic Acid Derivative)	30.6	4%		5%	
13 (Chlorogenic Acid Derivative)	33.7	5%		5%	

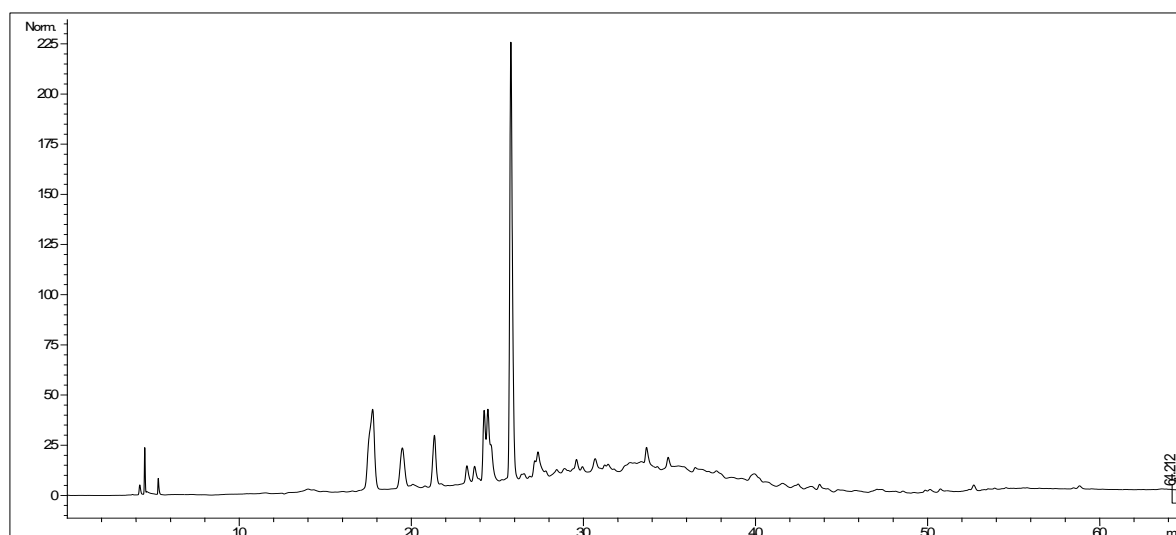


**Figure 20.** HPLC chromatogram of extract 1, obtained by MAE with the following operating conditions: Temperature=150 °C, time= 90 min and water content in the solvent=46%.

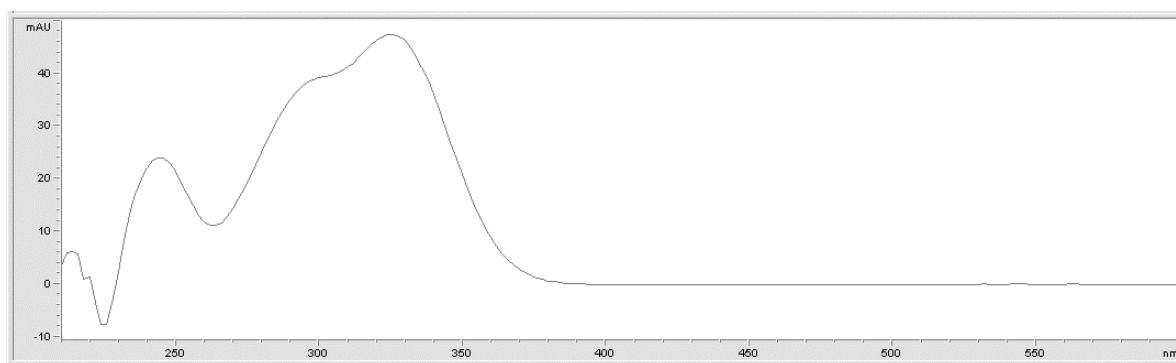


**Figure 21.** Chlorogenic acid spectra obtained by HPLC-DAD analysis

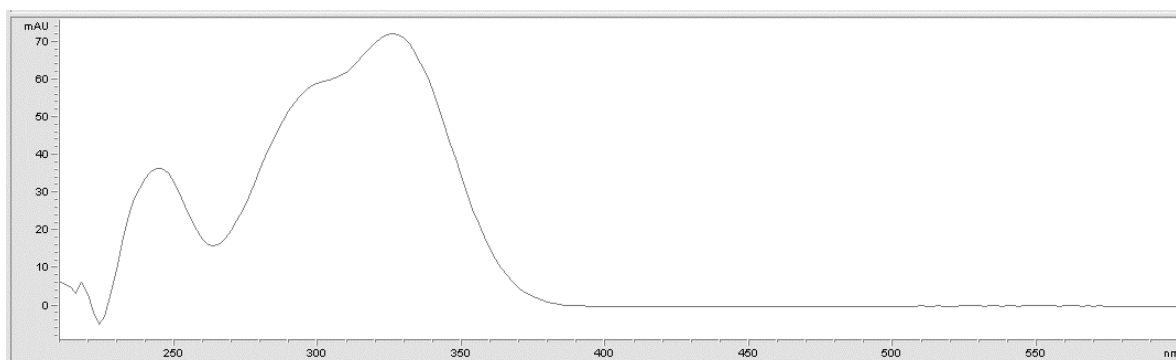


**Figure 22.** Suspected chlorogenic acid isomer or derivative spectra, classified as compound 6, obtained by HPLC-DAD analysis.

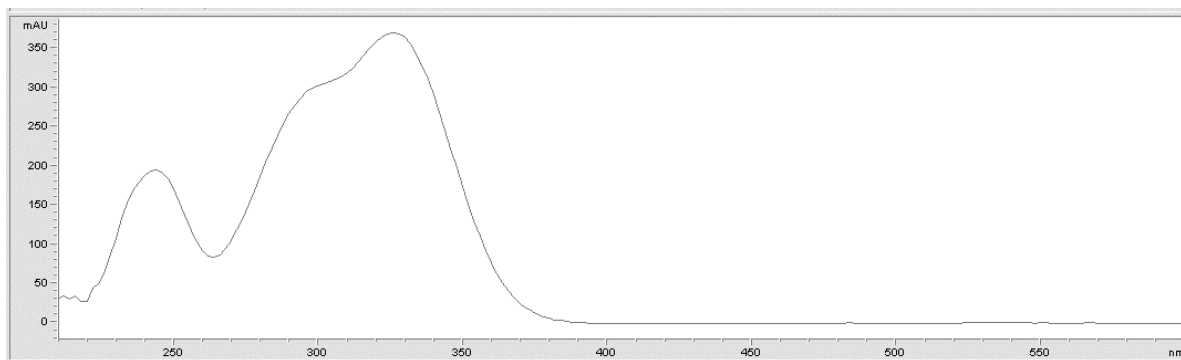


**Figure 23.** Suspected chlorogenic acid isomer or derivative spectra, classified as compound 7, obtained by HPLC-DAD analysis.

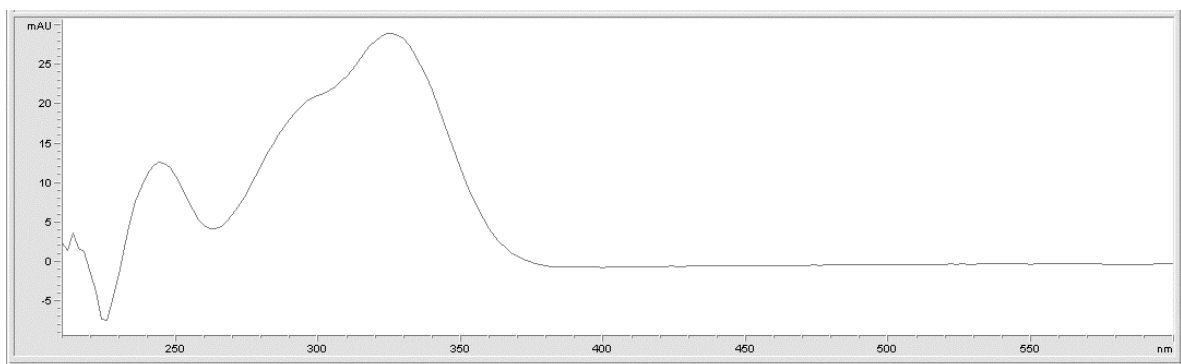


**Figure 24.** Suspected chlorogenic acid isomer or derivative spectra, classified as compound 10, obtained by HPLC-DAD analysis.

Panusa et al. (2013) studied the SLE of antioxidants from SCG collected from coffee bars, using water and a mixture of ethanol/water 60:40 (v/v) as extraction solvent and reaching an extraction yield that ranged between 6.33 and 28.26 mg<sub>GAE</sub>/g<sub>dried SCG</sub> (milligrams of Gallic Acid Equivalent/ grams of dried Spent Coffee Grounds) in 30 min. A deeper study on SLE regarding the evaluation of the effects of the extraction temperature, extraction time and liquid-solid ratio was carried out by Zuorro and Lavecchia (2013). They highlighted that the positive effect on polyphenol extraction was related to an increase of all the studied variables. They achieved a maximum yield of total polyphenols of 16.94 mg<sub>GAE</sub>/g<sub>dried SCG</sub>, working at 60°C and 180 min and with a liquid-solid ratio of 50 mL/g, using a mixture of ethanol/water 60:40 (v/v) as solvent. In addition, a study upon the comparison between the SLE, Soxhlet extraction and filter coffeemaker extraction showed that the last one could be the most effective technique when water is used as extraction solvent; moreover, substituting a mixture of

ethanol/water (60:40 v/v) for water as solvent a yield of 17.48 mg<sub>GAE</sub>/g<sub>dried\_SCG</sub> was achieved in a very short extraction time (6 min at 90°C) (Bravo et al., 2013).

The best solvent composition found in this work was in agreement with those mentioned above, in addition the used non-conventional technique provided higher extraction yields, because of the higher extraction temperature that the closed-vessel microwave-assisted extractor allowed to reach. Instead, this result apparently disagrees with the study of Pavlovic et al. (2013), who found that lower ethanol concentration (20% of ethanol at 40 s of extraction time) allowed a more selective extraction of polyphenols (368.95 mg<sub>GAE</sub>/g<sub>dried extract</sub>); indeed, if TP (based on g of dried SCG) was taken into account, it can be assessed that actually the two studies showed the same trend with high total polyphenols yields using a more equivolumetric solvent composition.

### 3.3.3 Cytotoxicity evaluation of the extract

To biologically validate SCG extract (extract 1), different concentrations (0.005, 0.010, 0.020 and 0.040 mg<sub>CAE</sub>/mL<sub>extract</sub>) over a total period of 8 days were tested on human keratinocytes NCTC 2544 through MTS assay (figure 26). Figure 25 shows all the results obtained, expressed as percentage of cell viability with respect to the control (cells not treated). It was noticed that working with 0.005, 0.010, 0.020 mg<sub>CAE</sub>/mL<sub>extract</sub> during all the period of treatment, the biocompatibility was always around 100 %, suggesting a significant ( $p < 0.05$ ) biocompatibility of the tested extract. Conversely, after just one day of treatment, it was highlighted a cytotoxic effect incubating cells with 0.040 mg<sub>CAE</sub>/mL<sub>extract</sub>. This behavior remained constant during all the period of culture. Therefore, it was possible to conclude that the maximum biocompatible concentration of SCG extract for NCTC 2544 cells was 0.020 mg<sub>CAE</sub>/mL<sub>extract</sub>.

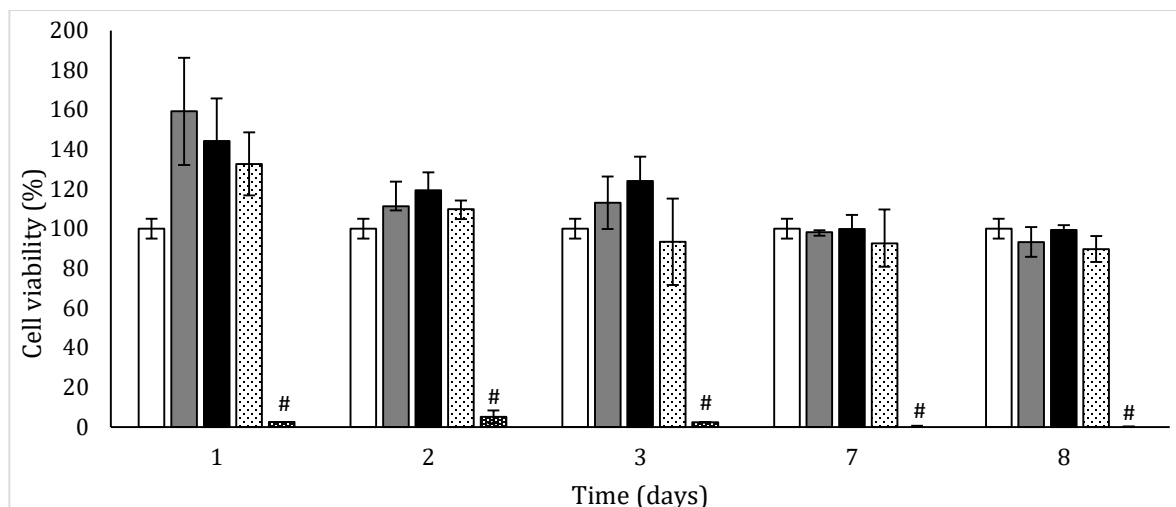


**Figure 25.** Cell viability of SCG extract by MTS assay. Results are mean of three measurements  $\pm$  SD. # refers to statistically significant differences among results ( $p < 0.05$ , ANOVA with Tukey's multiple comparison test).  $\square$  control,  $\blacksquare$  0.005 mgCAE/mLextract,  $\blacksquare$  0.01 mgCAE/mLextract,  $\square$  0.02 mgCAE/mLextract,  $\blacksquare$  0.04 mgCAE/mLextract.

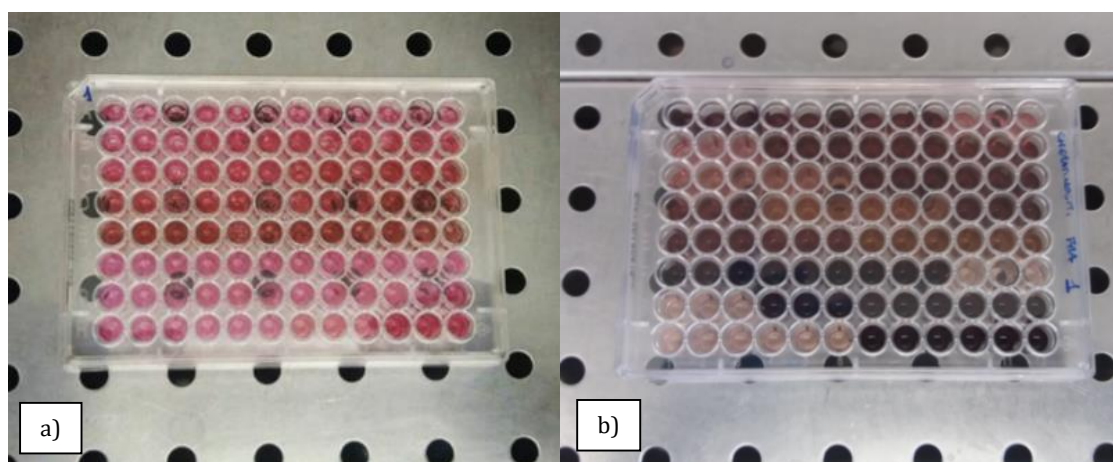


**Figure 26.** Cell culture multi-well at the first day of treatment (a) and after 8 days of treatment (b).

### 3.3.4 Kinetic model evaluation

If the best solvent composition found from experimental design was confirmed by literature, for what concern temperature is clear from table 9 that at 90 °C the extraction provided the worst performances, but further investigation deserved the temperature range from 120 °C to 150 °C. In addition, since from the response surface related to TP (figure 19-a) resulted that higher yields could be reached at shorter time, a deeper analysis was carried out in order to study the extraction kinetic, using the optimal solvent composition ethanol/water 54:46 (v/v) and taking into account also the heating period in extraction time computation. Experimental data about the

concentration of total polyphenols over time for the three investigated temperatures are reported in figure 28. Considering the temperature profile (figure 27), it can be established that the most of polyphenol extraction occurred during the thermal ramp (10 min), while, after the heating time, only a small increase in concentration was observed. This finding explained the reason why the time variable resulted as the least significant in RSM models, since the considered extraction time in that case started only when the set point temperature was reached. In addition, for the data related to the temperature of 150 °C, polyphenol concentration started decreasing after 85 min of extraction, likely due to the incoming of degradation reactions (Casazza et al., 2012). The same behavior was not highlighted at lower temperatures. Then, for the experimental data at 150 °C, the concentration-decreasing phase was not taken into account for the extraction curve modeling.

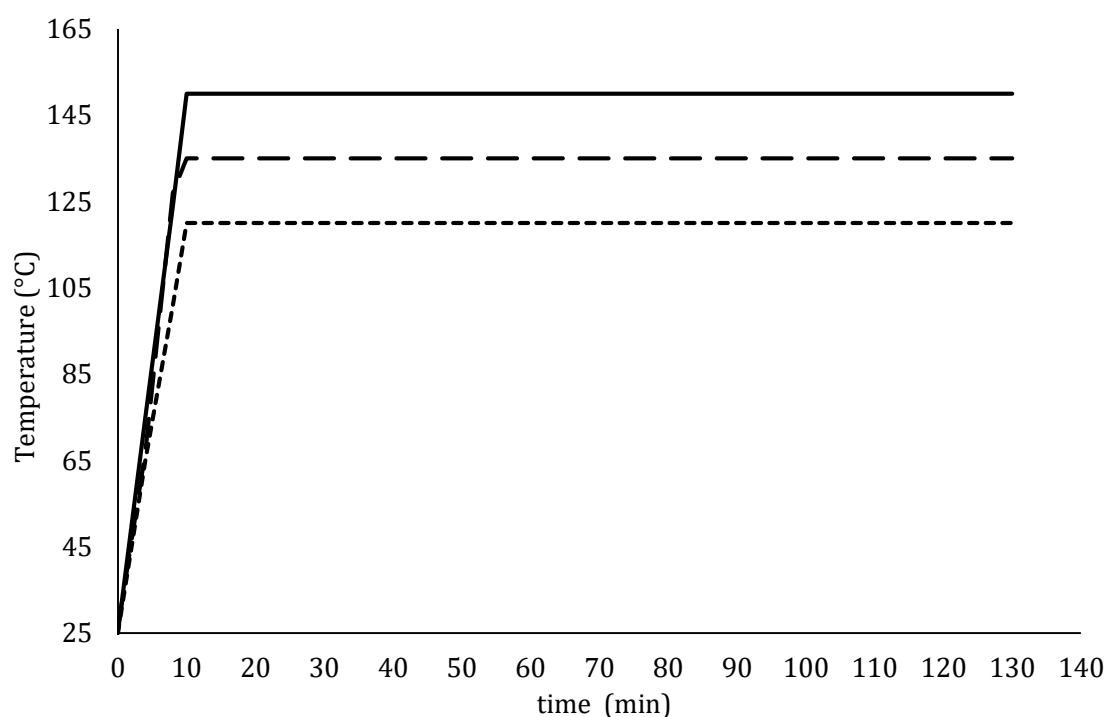


**Figure 27.** Temperature profiles imposed during MAE tests for kinetic evaluation. — set point temperature of 150°C after 10 min; — — set point temperature of 135°C after 10 min; - - - - set point temperature of 120°C after 10 min.

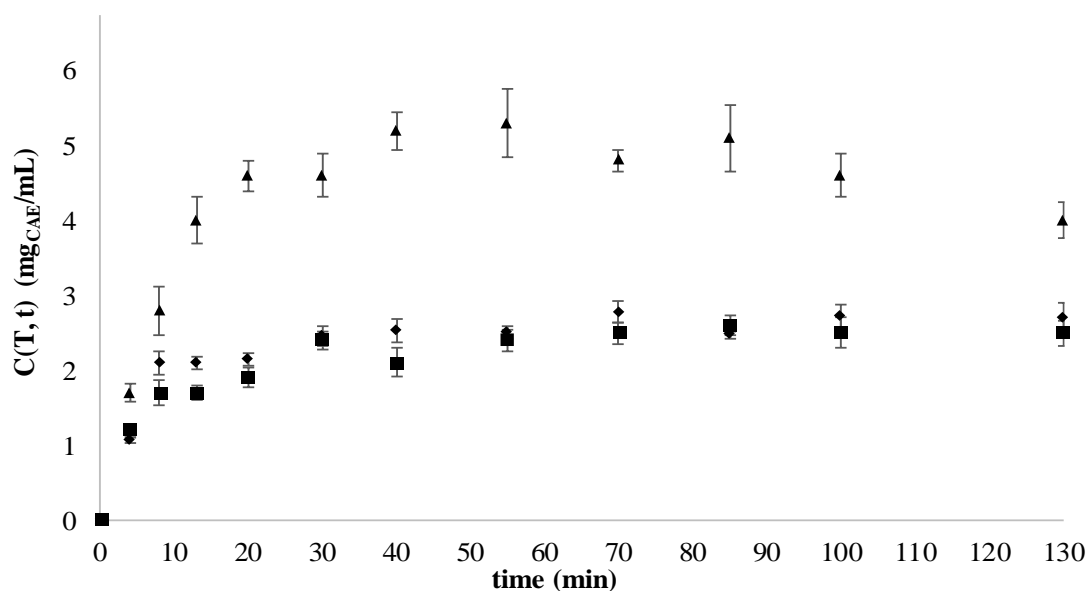


**Figure 28.** Experimental total polyphenol concentration (mg of caffeic acid equivalent (CAE)/mL of extract) over time, as a function of the set point temperature: ■ 120°C; ◆ 135°C; ▲ 150°C.

The kinetic parameters and the comparison among the proposed models are shown in table 15. On the basis of the coefficients of determination and the RSMD, Peleg's model resulted the best fitting model (figure 29) for all the investigated temperatures.

**Table 15.** Parameters of the proposed extraction kinetic models and comparison. \* Calculated using the mean diameter of particle size distribution.

	120 °C	135 °C	150°C
Fick's law-based model	A=0.5714	A=0.6468	A=1.119
	B=0.0362 min <sup>-1</sup>	B=0.0618 min <sup>-1</sup>	B=0.1224 min <sup>-1</sup>
	D <sub>eff</sub> = 2.88·10 <sup>-12</sup> m <sup>2</sup> /s *	D <sub>eff</sub> = 4.91·10 <sup>-12</sup> m <sup>2</sup> /s *	D <sub>eff</sub> = 9.73·10 <sup>-12</sup> m <sup>2</sup> /s *
	R <sup>2</sup> =0.9603	R <sup>2</sup> =0.9535	R <sup>2</sup> =0.9958
	RSMD=0.1311	RSMD=0.1909	RSMD=0.1875
I order model	K <sub>obs</sub> =0.0849 min <sup>-1</sup>	K <sub>obs</sub> =0.1031 min <sup>-1</sup>	K <sub>obs</sub> =0.1146 min <sup>-1</sup>
	R <sup>2</sup> =0.6940	R <sup>2</sup> =0.6622	R <sup>2</sup> =0.9941
	RSMD=0.2345	RSMD=0.2164	RSMD=0.1988
Peleg's model	K <sub>1</sub> = 2.196 min mL mg <sub>CAE</sub> <sup>-1</sup>	K <sub>1</sub> = 1.6957 min mL mg <sub>CAE</sub> <sup>-1</sup>	K <sub>1</sub> = 1.0575 min mL mg <sub>CAE</sub> <sup>-1</sup>
	K <sub>2</sub> = 0.3770 mL mg <sub>CAE</sub> <sup>-1</sup>	K <sub>2</sub> = 0.3582 mL mg <sub>CAE</sub> <sup>-1</sup>	K <sub>2</sub> = 0.1819 mL mg <sub>CAE</sub> <sup>-1</sup>
	R <sup>2</sup> =0.9964	R <sup>2</sup> =0.9956	R <sup>2</sup> =0.9903
	RSMD=0.1250	RSMD=0.1431	RSMD=0.3087

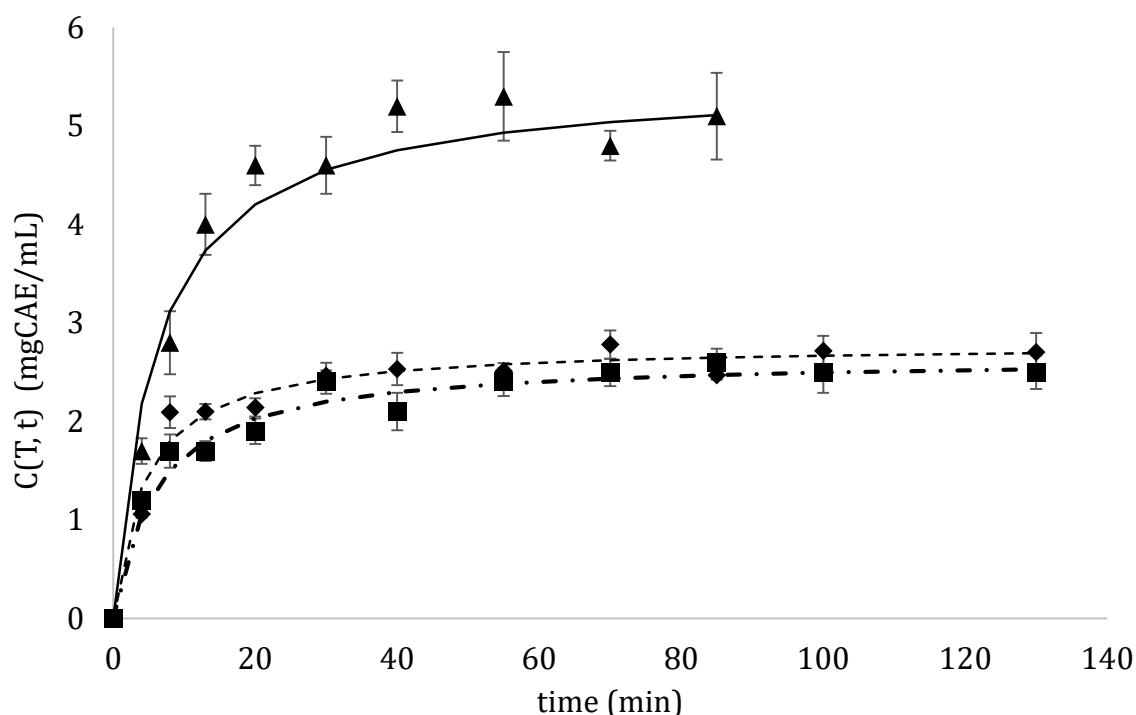


**Figure 29.** Total polyphenol concentration (mg of caffeic acid equivalent (CAE)/mL of extract) over time, as a function of the set point temperature: ■ experimental data at 120°C; ♦ experimental data at 135°C; ▲ experimental data at 150°C; - · - · Peleg's model at 120 °C; - - - Peleg's model at 135 °C; — Peleg's model at 150°C.

This step of the study confirmed that a temperature of 150°C was the best choice for TP maximization, and highlighted that at 60 min extraction curve plateau could be considered as reached, at all the investigated temperatures.

### 3.3.5 Study on the effect of heating time in MAE of antioxidants from SCG

In the previous paragraph, Peleg's model demonstrated to be more suitable to fit experimental data obtained by MAE than a diffusive model based on Fick's law and a first order kinetic, implying that the external mass transfer has an important role in the process. Thus, this section is dedicated to the investigation on the effects of initial thermal ramp on the total polyphenol concentration, total solids and antiradical power of the extract obtained by MAE. Experimental tests were, then, carried out under the same final set point temperatures considered in the previous study (120, 135 and 150



°C). In addition, three different heating time values were imposed in order to obtain a total of 9 different thermal ramps (1, 10 and 20 min).

### 3.3.5.1 Effects on the extraction of polyphenols

Experimental data (figure 31) showed that independently from the heating time ( $t_H$ ), the higher was the temperature, the higher were the extracted polyphenols, implying that even if polyphenols degradation occurred, the enhance of extraction kinetic, due to temperature increase, would be more effective. For what concerns the heating time, it was observed that its increasing led to longer time to reach the plateau. Indeed, as reported in table 16, the initial rate of the curve ( $1/K_1$ ) increased with the final set point temperature increase, while decreased with the heating time increase. Conversely, the concentration at infinite time ( $C|_{t \rightarrow \infty}$ ) was more influenced by the final temperature than by  $t_H$ , but the highest values of total polyphenol concentrations were found in correspondence of 10 min of heating time. For all the final temperatures and the heating times investigated, Peleg's model resulted adequate to describe the extraction curve, as expressed by the determination coefficients in table 16.

**Table 16.** Values of Peleg's model coefficients for the polyphenol extraction kinetic. CAE= caffeic acid equivalent;  $1/K_1$ = initial rate of the extraction curves;  $C|_{t \rightarrow \infty}$  = polyphenol concentration at infinite time, expressed as mg of caffeic acid equivalent (CAE) per mL of extract;  $R^2$  = coefficient of determination.

Final Temperature (°C)	Heating time (min)	Initial thermal ramp (K/min)	$1/K_1$ (mg <sub>CAE</sub> min <sup>-1</sup> mL <sup>-1</sup> )	$C _{t \rightarrow \infty}$ (mg <sub>CAE</sub> mL <sup>-1</sup> )	$R^2$
120	1	95.0	0.933	2.9	0.989
135	1	115	1.156	3.2	0.998
150	1	125	1.378	3.7	0.987
120	10	9.37	0.652	3.2	0.994
135	10	11.1	0.792	3.4	0.990
150	10	12.7	0.824	3.9	0.984
120	20	4.73	0.302	2.9	0.992
135	20	5.65	0.394	3.2	0.999
150	20	6.31	0.400	3.8	0.980

In order to represent numerically the dependence of model parameters on the investigated variables, a linear fitting equation was used to describe the variation of the initial rate of the extraction curve ( $1/K_1$ ) as a function of heating time ( $t_H$ ) (equation 29):

$$\frac{1}{K_1}(T, t_H) = A \cdot t_H + B \quad (29)$$

Linear regression of data provided the following equations (equations 30, 31, 32), in which  $t_H$  was the heating time:

$$\frac{1}{K_1}(393 \text{ K}, t_H) = -0.0333 t_H + 0.97252 \quad (R^2 = 0.999) \quad (30)$$

$$\frac{1}{K_1}(408 \text{ K}, t_H) = -0.0401 t_H + 1.1954 \quad (R^2 = 0.999) \quad (31)$$

$$\frac{1}{K_1}(423 \text{ K}, t_H) = -0.0513 t_H + 1.3972 \quad (R^2 = 0.989) \quad (32)$$

Determination coefficients (equations 30, 31 and 32) indicated that the chosen law of regression well described experimental data and, in these equations, the intercepts were temperature-dependent only, as well as the regression line slopes. Indeed, the intercepts correspond to the values of the initial rate of the extraction curves when heating time tends towards zero, thus the variation in the values obtained shall be only temperature-dependent. For what concerned the regression line slopes as functions of temperature, the best regression law revealed that the slope (A) was a linear function of  $1/T$  ( $K^{-1}$ ), as reported in equation 33.

$$A(T) = 99.4 \frac{1}{T} - 0.2854 \quad (R^2 = 0.974) \quad (33)$$

The determination of the temperature-dependence of the intercept (B) (equation 29) was obtained considering an Arrhenius-like law, as reported in the equation 34:

$$\ln\left(\frac{1}{K_1}(T, t_{H \rightarrow 0})\right) = \ln(B) = \ln\left(\frac{1}{K_0}\right) - \frac{E_A}{R_g \cdot T} \quad (34)$$

where  $1/K_0$  is constant ( $\text{mg}_{\text{CAE}} \text{ min}^{-1} \text{ mL}^{-1}$ ),  $E_A$  is the activation energy ( $\text{kJ/mol}$ ),  $R_g$  the universal gas constant ( $8.314 \text{ kJ/mol K}$ ), and  $T$  the absolute temperature ( $\text{K}$ ). By plotting  $\ln(B)$  versus  $1/T$  and using a linear regression of the experimental data, the following values of the parameters in the equation 11 were obtained:

$$1/K_0 = 163 \text{ mg}_{\text{CAE}} \text{ min}^{-1} \text{ mL}^{-1} \quad E_A/R_g = 2010.4 \text{ K} \quad (R^2=0.996)$$

Since the parameter  $B(T)$  was obtained by reducing heating time to zero, it could be seen as the real kinetic constant of the extraction under isothermal conditions and, in agreement with this point of view, it depends on temperature following an Arrhenius-like law.

Analogously, heating time and temperature dependence of  $C|_{t \rightarrow \infty}$  was investigated. A second order polynomial equation (equation 35) resulted to be adequate to describe the behavior of this variable respect to the heating time.

$$C|_{t \rightarrow \infty}(T, t_H) = D' t_H^2 + E' t_H + F' \quad (R^2 = 1.000) \quad (35)$$

Results of data fitting were reported as equations 36,37,38:

$$C|_{t \rightarrow \infty}(393 \text{ K}, t_H) = -0.003452 t_H^2 + 0.07311 t_H + 2.8398 \quad (R^2 = 1.000) \quad (36)$$

$$C|_{t \rightarrow \infty}(408 \text{ K}, t_H) = -0.00193 t_H^2 + 0.04444 t_H + 3.1180 \quad (R^2 = 1.000) \quad (37)$$

$$C|_{t \rightarrow \infty}(423 \text{ K}, t_H) = -0.00137 t_H^2 + 0.03294 t_H + 3.6914 \quad (R^2 = 1.000) \quad (38)$$

Coefficients  $D'$  and  $E'$  did not result as temperature-dependent, while average values of both of them provided the best data fitting:

$$D' = -0.00225 (\text{mg}_{\text{CAE}} \text{ mL}^{-1} \text{ min}^{-2}); \quad E' = 0.05016 (\text{mg}_{\text{CAE}} \text{ mL}^{-1} \text{ min}^{-1})$$

The dependence on temperature was instead found in the coefficient  $F'$ , whose relation with the final temperature was found following a second order polynomial (equation 39):

$$F'(T) = 0.0006561 T^2 - 0.5070 T + 100.76 \quad (R^2 = 1.000) \quad (39)$$

Resuming, kinetic of microwave-assisted extraction of antioxidants from spent coffee grounds could be expressed by the equation 40, whose values of the coefficients are reported in table 17:

$$C(t, T, t_H) = \frac{t}{\left( \frac{1}{\left( \frac{a}{T} + b \right) t_H + \frac{1}{K_0} e^{-E_A/(R_g T)}} \right) + \left( \frac{t}{D' t_H^2 + E' t_H + g' T^2 + h' T + i'} \right)} \quad (40)$$

**Table 17.** Values of the model coefficients of equation 40.

a	(mg <sub>CAE</sub> K mL <sup>-1</sup> min <sup>-2</sup> )	99.4
b	(mg <sub>CAE</sub> mL <sup>-1</sup> min <sup>-2</sup> )	0.2854
1/K <sub>0</sub>	(mg <sub>CAE</sub> min <sup>-1</sup> mL <sup>-1</sup> )	163
E <sub>A</sub> /R <sub>g</sub>	(K)	2010.4
D'	(mg <sub>CAE</sub> mL <sup>-1</sup> min <sup>-2</sup> )	-0.00225
E'	(mg <sub>CAE</sub> mL <sup>-1</sup> min <sup>-1</sup> )	0.05016
g'	(mg <sub>CAE</sub> mL <sup>-1</sup> K <sup>-2</sup> )	0.0006561
h'	(mg <sub>CAE</sub> mL <sup>-1</sup> K <sup>-1</sup> )	0.507
i'	(mg <sub>CAE</sub> mL <sup>-1</sup> )	100.76

The agreement between the fitting equation (equation 40) and experimental data was shown in figure 31 and expressed in terms of RMSD, reported in table 16, where the values of independent variables identify the extraction curve. In addition, in figure 30 is depicted the relationship between the experimental data (observed values) and the points calculated by using the model equation (expected values); as can be easily observed, the distribution of data point can be considered as linear.

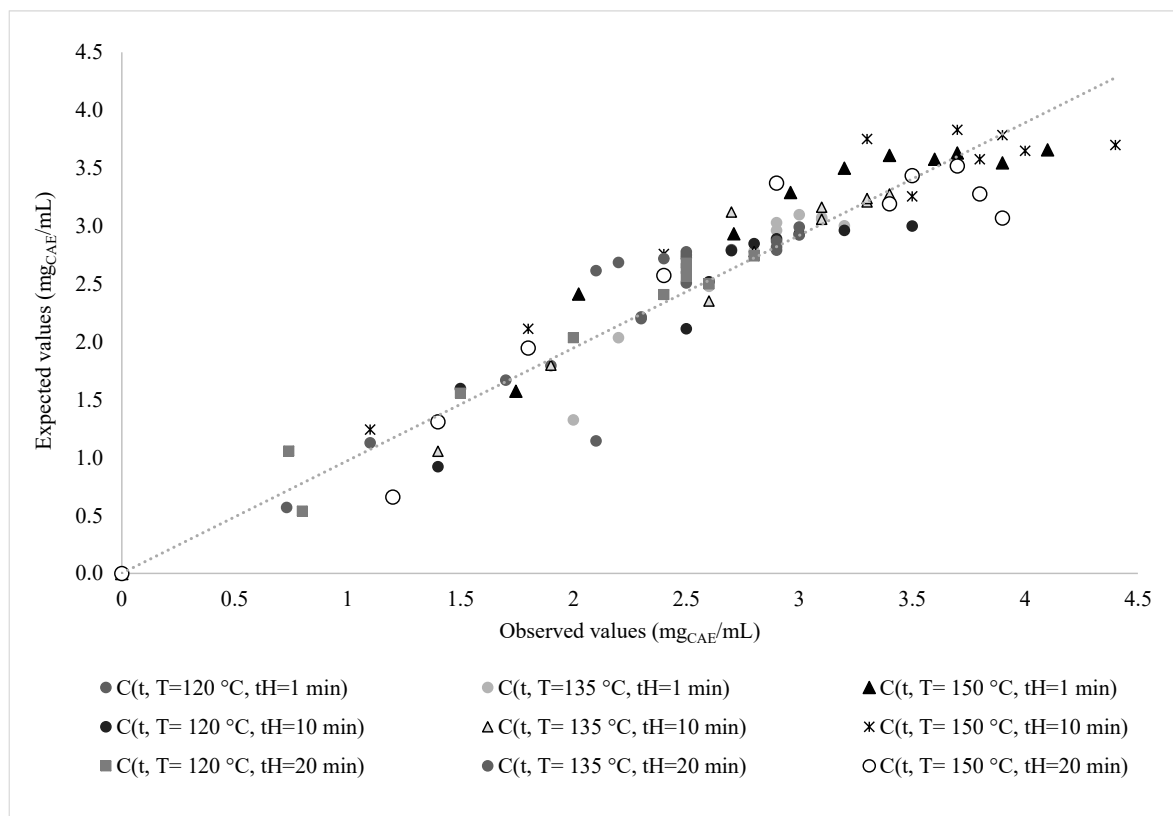


**Figure 30.** Expected values of concentration of total polyphenols, obtained by the model equation of extraction kinetic, versus the experimental data (observed values).

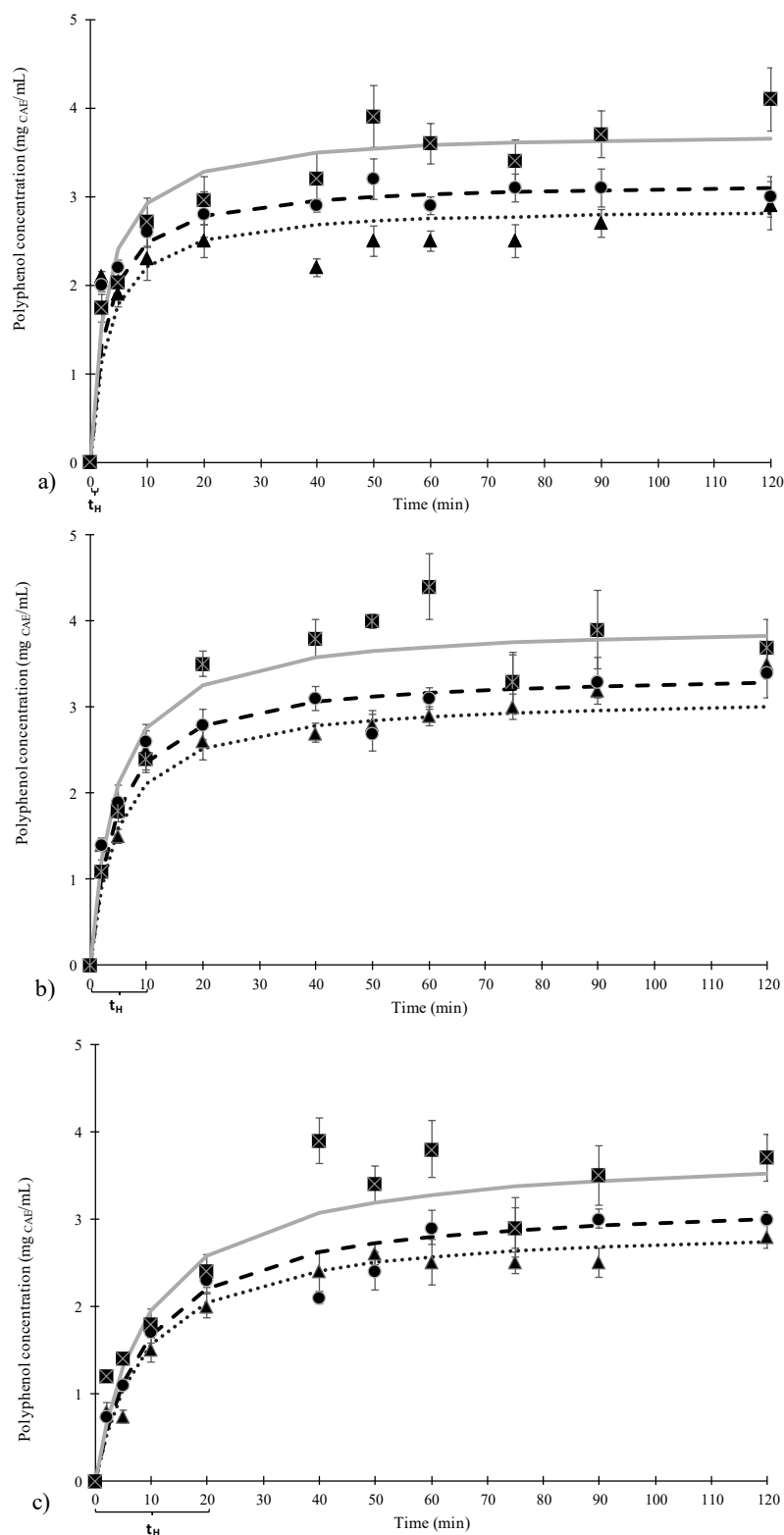


**Figure 31.** Extraction kinetic of total polyphenols. Experimental data, obtained by means of Folin-Ciocalteu's assay, are reported as a function of time and temperature (▲ 120 °C, ● 135 °C, ■ 150 °C) and are compared with Peleg's model: ..... at 120 °C; --- at 135 °C; — at 150 °C. Figures: 31. a) is related to a heating time of 1 min; 31. b) is related to a heating time of 10 min; 31. c) is related to a heating time of 20 min.

Peleg's equation resulted often a good kinetic model to describe extraction of polyphenols from natural sources, since the complexity of the natural matrices and the variety of polyphenols within them make difficult the development of useful theoretic models, and the mass transfer from the solid to the liquid phase is usually slower than a first order system kinetic. In addition, utilizing non-conventional extraction techniques, would introduce other variables to the fundamental equations. In spent coffee grounds chlorogenic, caffeic, and protocatechuic acids (Andrade et al., 2012) are the main polyphenols, but they may interact with caffeine, carbohydrates, proteins, and among themselves to produce other complex molecules that could change over time during the extraction process. In addition, the effects of microwaves on these reactions are still under evaluation. 10 min of heating time at 150 °C provided the highest amount of polyphenols in the range of time investigated, and these operating conditions seemed also a good compromise since allowed a fast extraction ( $0.65 < 1/K_1 < 0.82$  mg<sub>CAE</sub>/ml min), with high yields (around 43 mg<sub>CAE</sub>/ g dried SCG after 60 min of extraction), of molecules with high antiradical power. Longer times of extraction than 60 min, seemed to be only an energetic inefficiency since the concentration of polyphenols did not changed from 60 to 120 min, and even a  $t \rightarrow \infty$  significant variations were not highlighted by the model. Indeed, the main benefits of microwaves are expected to occur at the beginning of the process, when the dielectric properties of the solvent mixture are not decreased by the temperature (Galan et al., 2017). In addition, longer time of extraction provided more extracted total solids, consequently reducing the concentration of polyphenols in the dried extract. Total polyphenol yield obtained by means of this study demonstrated that microwave-assisted extraction is able to provide products with higher phenolic content than solid-liquid extraction (Mussatto et al., 2011a; Zuorro and Lavecchia, 2013), ultrasound-assisted extraction (Al-Dhabi et al., 2017; Andrade et al., 2012), supercritical fluid extraction (Andrade et al., 2012) and pressurized liquid extraction (Shang et al., 2017), since the great advantage of this technique was not only limited to the fast and volumetric heating, but it could also traced back to selective heating effects (Galan et al., 2017) and cell rupture mechanisms (Chan et al., 2016) that lead to an increase in extraction yield.

### 3.3.5.2 Effects on antiradical power of the extracts

Molecules which are able to exhibit ARP are several in SCG: not only polyphenols, e.g. chlorogenic acids or *p*-cumaric acid, but also melanoidins, proteins, carbohydrates, and lipids. The need to find an optimum of temperature and heating time for microwave-assisted extraction is due to the opposing effects of microwave irradiation power on the main phenomena occurring during the microwave-assisted extraction process of thermo-sensitive compounds.

Antiradical power versus extraction time, temperature, and heating time is shown in figure 32. Setting up a heating time of 1 min (figure 32.a), the greater ability to scavenge the coloured radical was found in the extracts obtained at 120 °C, which exhibited a high ARP even at very low extraction times and with a maximum around 60 min. Increasing the extraction time, the antiradical power showed a slight reduction from 88  $\mu\text{g}_{\text{TE}}/\text{L}$  to 65  $\mu\text{g}_{\text{TE}}/\text{L}$ . At  $t_{\text{H}}=1$  min, the higher was the final imposed temperature, the lower was extract antiradical power. This behaviour could be due to the really high power needed to heat the samples in a very short heating time (1 min), which likely led to a loss of the activity of the compounds extracted at 135 and 150 °C. Indeed, more intense irradiation power promotes a faster heating, consequently faster extraction, more intense wall- cell rupture and faster analyte release, but could promote reaction kinetics as well, potentially leading to undesired products or without bioactivity, so in MAE of natural antioxidants often an optimal compromise need to be found (Chan et al., 2017, 2011; Dahmoune et al., 2015; Ranic et al., 2014; Simić et al., 2016). At 120 °C, longer heating times (figures 32. b and 1.c) seemed to reduce the extraction system skill to produce extracts with antiradical power, while increased ARP were found in the extracts produced at 135 and 150 °C. From figure 32.c it can be observed that 20 min of heating time reduced the ARP of the extracts, probably because of the slower extraction kinetic. Anyway, extracts with high antiradical power were found to be obtained after only 20 min of extraction, whose values ranged from 45 to 88  $\mu\text{g}_{\text{TE}}/\text{L}$ , corresponding to extraction yields that ranged from 45 to 88  $\mu\text{g}_{\text{TE}}/100 \text{ g}_{\text{dried SCG}}$ .



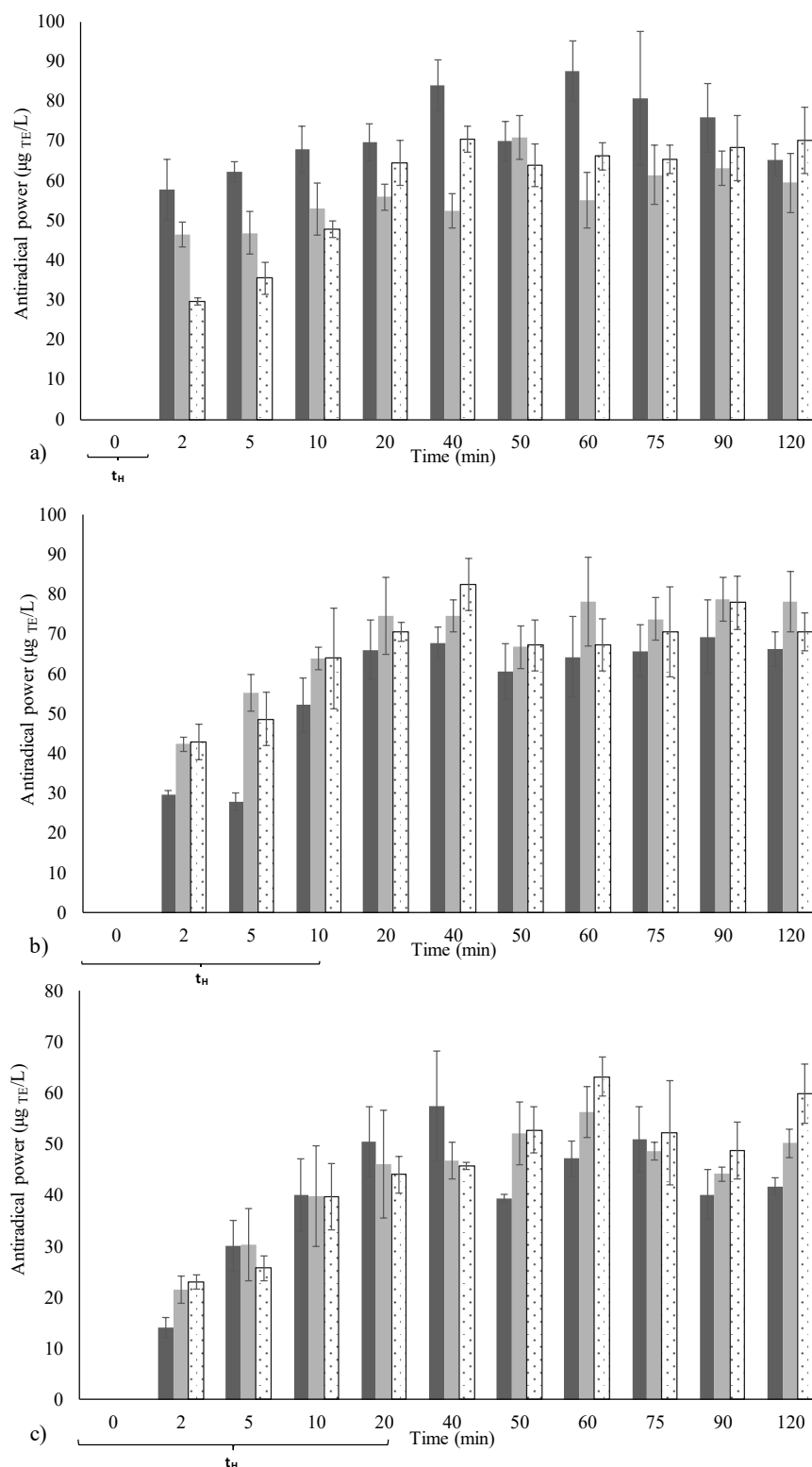


**Figure 32.** Antiradical power of the extracts, measured by means of ABTS•<sup>+</sup> (2,2'-azino-bis-3-ethylbenzthiazoline-6-sulphonic acid) assay, as a function of time and temperature: ■ 120 °C, ■ 135 °C, □ 150 °C. Figures: 32. a) is referred to a heating time of 1 min; 32. b) is referred to a heating time of 10 min; 32.c) is referred to a heating time of 20 min. TE= Trolox Equivalent;  $t_H$  = heating time.

### 3.3.5.3 *Effects on global extraction*

The effects of temperature, time, and heating time on the total amount of extracted compounds are reported in figure 33. The highest amount of extracted solids from SCG was found when the extraction was performed at 135 °C, 10 min of heating and 120 min of extraction time. For what concerns temperature effects, it was noticed a different behaviour that was heating time-dependent: very short time of heating (figure 33. a) produced an increase of extracted solids when the extraction temperature was increased from 120 to 150 °C, while for longer heating times (figure 33. b and c) the maximum of extracted solids was given by an extraction temperature of 135 °C. These results, together with the previous ones related to antiradical power, highlighted that heating time is a very important parameter in microwave-assisted extraction, which regulates not only the extraction rate and the time needed to reach a certain temperature, but has deeper effects on the extraction process, particularly on complex matrices as SCG. Comparing figure 32 and figure 33, it could be assessed that varying temperature and heating time, a modulation of the selectivity, concentration of bioactive molecules in the extract and the yield could be obtained. Of course both of these parameters are strictly connected with the imposed power (W), which is one of the most studied parameter of MAE process, but the configuration of the used extraction system (temperature-controlled system) demonstrated that more degrees of freedom are available to perform MAE, and that the variables of temperature, heating time and extraction time could be successfully used to change the quality of the extracts. For example, it can be observed that, at  $t_H=10$  min and  $t_H=20$  min (figures 32.b and c) and 135 °C, the ARP did not change after 50 min of extraction, but significantly increased the ETS (figure 33.b and c), implying that, after this time, molecules without bioactivity were extracted or partial degradation of the bioactive molecules occurred, while at the same temperature but at  $t_H=1$  min (figure 33.a) this behaviour was not observed. These findings are in agreement with what reported by Ranic et al. (2014), who, even if under different conditions, found that extract total solids and antioxidant extraction yields in MAE from spent coffee grounds did not show a concordant trend.

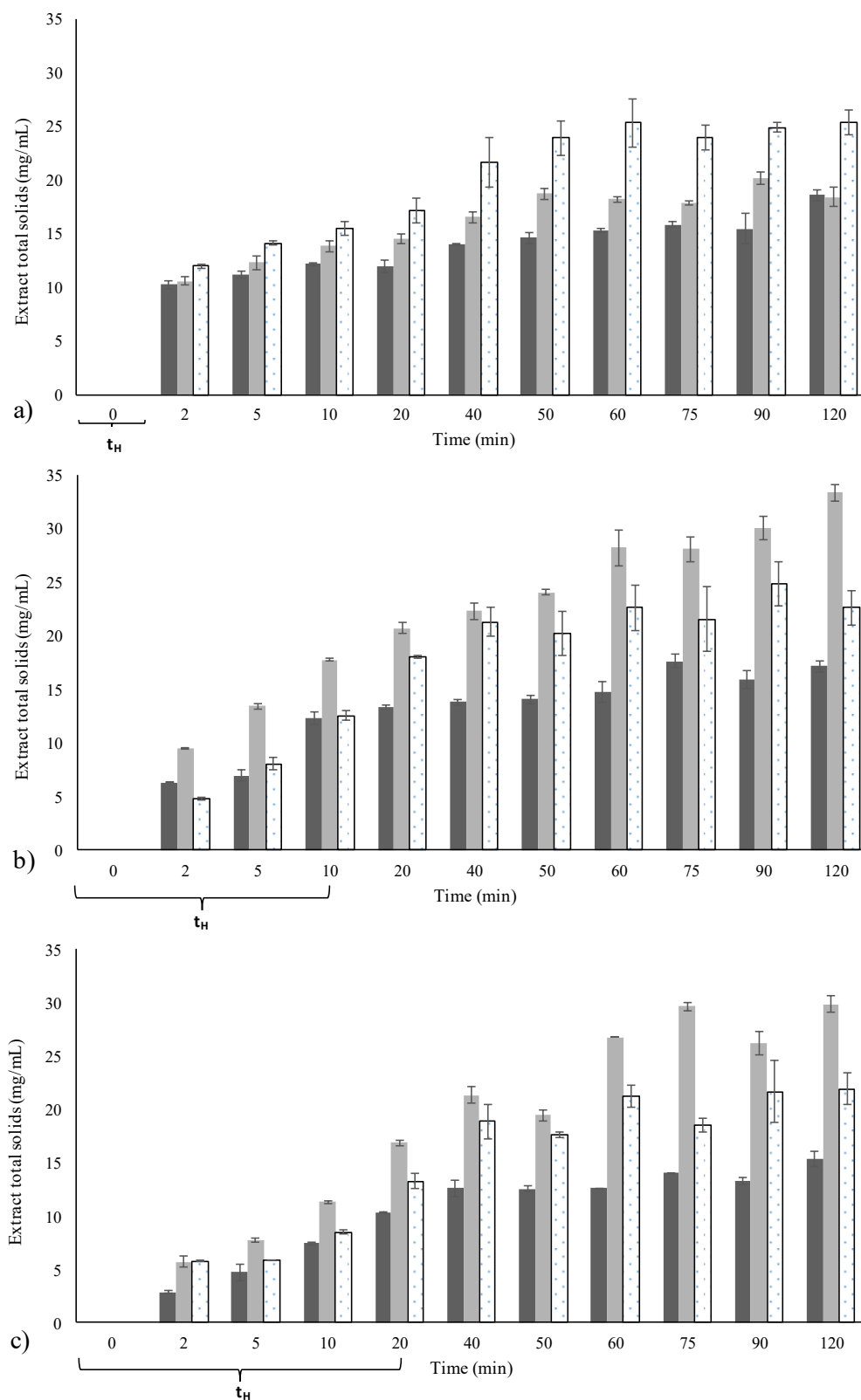


**Figure 33.** Extract total solids, measured by means of gravimetric method, as a function of time and temperature: ■ 120 °C, ■ 135 °C, □ 150 °C. Figures: 33. a) is referred to a heating time of 1 min; 33. b) is referred to a heating time of 10 min; 33.c) is referred to a heating time of 20 min.  $t_H$  = heating time.

### 3.4 CONCLUSIONS

This study applied a hybrid approach to investigate the microwave-assisted extraction of antioxidant from spent coffee grounds. Design of experiment and response surface modeling provided an overview on the microwave assisted extraction main parameters, allowing a first optimization of the solvent composition (ethanol/water 54:46 v/v) and suggesting the range of temperature and time which deserved further analysis. The optimized extract showed higher total polyphenol yield ( $46 \text{ mg}_{\text{CAE}}/\text{g}_{\text{dried SCG}}$ ) than those usually obtained by other extraction techniques and high antiradical power. In order to evaluate a possible application of this extract for cosmetic purposes, its biological validation was carried out on keratinocytes NCTC 2544 without any purification process. Results demonstrated the biocompatibility of the extract at different concentrations over a period of 8 days, and cells were not subjected to damage up to a concentration of  $0.020 \text{ mg}_{\text{CAE}}/\text{mL}$ . The combined presence of caffeine and polyphenols in the extract made it a suitable additive for cosmetics with anti-aging actions and, potentially, for pharmaceutical formulations for local dermatological treatment of skin damage related to vascular diseases. The application of Peleg's model to microwave-assisted extraction of polyphenols from spent coffee grounds allowed to deeper understand the effects of temperature, time and heating time on the extraction yields. Indeed, heating time resulted, like temperature and extraction time, an important process parameter, able to affect the antioxidant activity, the composition and the polyphenol extraction yield. Setting this parameter, together with temperature, rather than the power of microwaves, could provide an efficient method to modulate the characteristics of the product. After about 60 min, particularly setting 10 min as heating time and at  $150^\circ\text{C}$ , microwave-assisted extraction was able to provide extracts with high antioxidant activity and rich in polyphenols, that could potentially find several applications as dietary supplement, ingredient for cosmetic formulations or as additive in food packaging. Results of this study could be also applied to the extraction of polyphenols from other vegetable matrix and agro-food industry by-products, in order to achieve further process optimization and process intensification.

*Parts of this section were already published in “Eco-sustainable recovery of antioxidants from spent coffee grounds by microwave-assisted extraction : Process optimization, kinetic modeling and biological validation” by Pettinato et al. (2019a) and “The role of heating step in microwave-assisted extraction of polyphenols from spent coffee grounds” by Pettinato et al. (2019b), and partially presented as “Estrazione assistita da microonde di composti ad alto valore aggiunto da caffè esausto”, by Margherita Pettinato, Bahar Aliakbarian, Alessandro Alberto Casazza, Vincenza Calabrò, Patrizia Perego, in the National congress “GRICU 2016- Gli orizzonti 2020 dell'ingegneria chimica”, Anacapri, Italy, 12-14/09/2016.*

## *Chapter 4*

# **ENCAPSULATION OF ANTIOXIDANTS FROM MAE EXTRACTS BY SPRAY DRYING**

### **4.1 ABSTRACT**

In this study, an extract rich in phenolic compounds from spent coffee grounds was obtained by microwave-assisted extraction, using a mixture of ethanol/water 54:46 (v/v) as solvent, an operative temperature of 150 °C and an extraction time of 90 min. Encapsulation process, using inulin and maltodextrin as coating agents, has been studied by means of an experimental design and the response surface methodology was used for data treatment. Inulin/maltodextrin ratio and sample flow rate effects on encapsulation yield, efficiency and product features were evaluated. No effects of the investigated variables on the product recovery and product moisture were observed, while the best encapsulation efficiencies (63 % and 62 %) were achieved using a carrier composition of 80 % wt of inulin and at the highest inlet flow rates.

### **4.2 MATERIAL AND METHODS**

#### **4.2.1 Antioxidant extraction by microwave-assisted extraction and inlet suspension preparation**

The liquid extract used for spray drying tests was obtained from the dried SCG, whose characterization is provided in Chapter 2, and a mixture of ethanol/water (54:46 v/v) as solvent. The extraction was carried out in a professional multimode oven operating at 2.45 GHz (MicroSYNTH, Milestone, Italy) at 150°C, utilizing a solvent solid ratio (L/S) of 10 mL/g for 90 minutes. The extract was centrifuged at 6000 xg for 10 min (ALC PK131, Alberta, Canada) and filtered through a 0.45 µm filter. Then, the extract was diluted with deionized water (1:2 v/v) and stored at -18±1°C for further operations.



**Table 18.** Values of the two input variables at the corresponding design level

Variable	Level -1	Central point	Level +1
I (% wt)	20	50	80
Flow rate (mL/min)	5	7.5	10

As already reported in paragraph 3.2.3, the fitting equation of the generic response variable  $Y$  is given in the equation 13:

$$Y = \alpha_0 + \sum_{i=1}^3 \alpha_i X_i + \sum_{i=1}^3 \alpha_{ii} X_i^2 + \sum_{i=1}^3 \sum_{j=1}^3 \alpha_{ij} X_i X_j \quad (13)$$

where  $Y$  represented the response variables,  $X_i$  and  $X_j$  were the independent variables,  $\alpha_0$  was a constant, while  $\alpha_i$ ,  $\alpha_{ii}$  and  $\alpha_{ij}$  represented the coefficients of the linear, quadratic and interactive terms of the equation.

The model adequacy was determined by means of the coefficient of determination ( $R^2$ ) and by analysis of variance (ANOVA) that was generated by Design Expert.

#### 4.2.3 Analytical methods

##### 4.2.3.1 Moisture content evaluation

Moisture was determined after drying powder samples in an oven at 110 °C until a constant weight. The moisture content of microparticles was calculated based on the loss in weight between powders before and after drying, and expressed in % (g of water/g of wet sample · 100).



#### 4.2.3.2 Encapsulation yield

Encapsulation yield (EY,  $\text{mg}_{\text{CAE}}/\text{g}$  dried powder ), shown in equation 41, was determined as difference between the total phenolic content (TPC,  $\text{mg}_{\text{CAE}}/\text{g}$  WET POWDER) and superficial phenolic content (SPC,  $\text{mg}_{\text{CAE}}/\text{g}$  WET POWDER).

$$EY = \frac{(TPC - SPC)}{(1 - \text{MOISTURE})} \quad (41)$$

TPC and SPC were extracted from the powder by the methods described by (Robert et al., 2010). For total phenolic content, 200 mg of powder were destructed by adding 2 mL of methanol/acetic acid/water (50:8:42, v /v /v) and agitating using a Vortex for 1 min. Sample was, then, centrifuged at 12984 xg for 5 min and the supernatant recovered. SPC evaluation was, instead, carried out by adding 2 mL of a mixture of ethanol and methanol (1:1, v/v) to 200 mg of powder. Sample was agitated using a Vortex for 1 min and finally centrifuged at 12984 xg for 5 min and the supernatant recovered. Both of the supernatants for TPC and SPC evaluation were analyzed through a colorimetric method using the Folin–Ciocalteu’s assay, described in the paragraph 3.2.1.3. The same assay was used for the calculation of TP of the spent coffee grounds extract (EPC) before spray drying. In this case, TP yield was expressed as milligrams of equivalent caffeic acid per gram of dried biomass ( $\text{mg}_{\text{CAE}}/\text{g}_{\text{dried biomass}}$ ).

#### 4.2.3.3 Product recovery

Product recovery was calculated as reported in equation (42):

$$\text{Product recovery} = \frac{\text{mass of dried powder}}{\text{mass of coating agent+dried extract residue}} \quad (42)$$

Where dried extract residue was obtained by drying 2 mL of the diluted extract at 110°C until constant weight was reached.

#### 4.2.3.4 Encapsulation efficiency

Encapsulation efficiency was evaluated according to equation (43):

$$\text{Encapsulation efficiency} = \frac{\text{mass of encapsulated polyphenols}}{\text{mass of polyphenols in the feed}} \quad (43)$$

#### 4.2.3.5 Particle size distribution

Particle size distribution of the sample was evaluated by field –emission scanning electron microscopy (FE-SEM, mod. LEO 1525, Carl Zeiss SMT AG, Oberkochen, Germany). Before the analysis, the solid sample was treated by an advanced sputter coater (AGAR *Auto Sputter Coater* mod.108 A), which allowed to cover the dry non-conducting samples with a 250 Å layer of gold under inert atmosphere of argon and vacuum (0.05 mbar). The obtained images were analyzed by a Java-based image processing program (ImageJ, version 1.51s, National Institute of Health, USA) and output data were elaborated as reported in paragraph 2.2.4.

### 4.3 RESULTS AND DISCUSSION

Folin-Ciocalteu's assay on the diluted extract revealed an amount of total polyphenols content of  $30 \pm 0.9$  mg<sub>CAE</sub>/ g dried SCG.

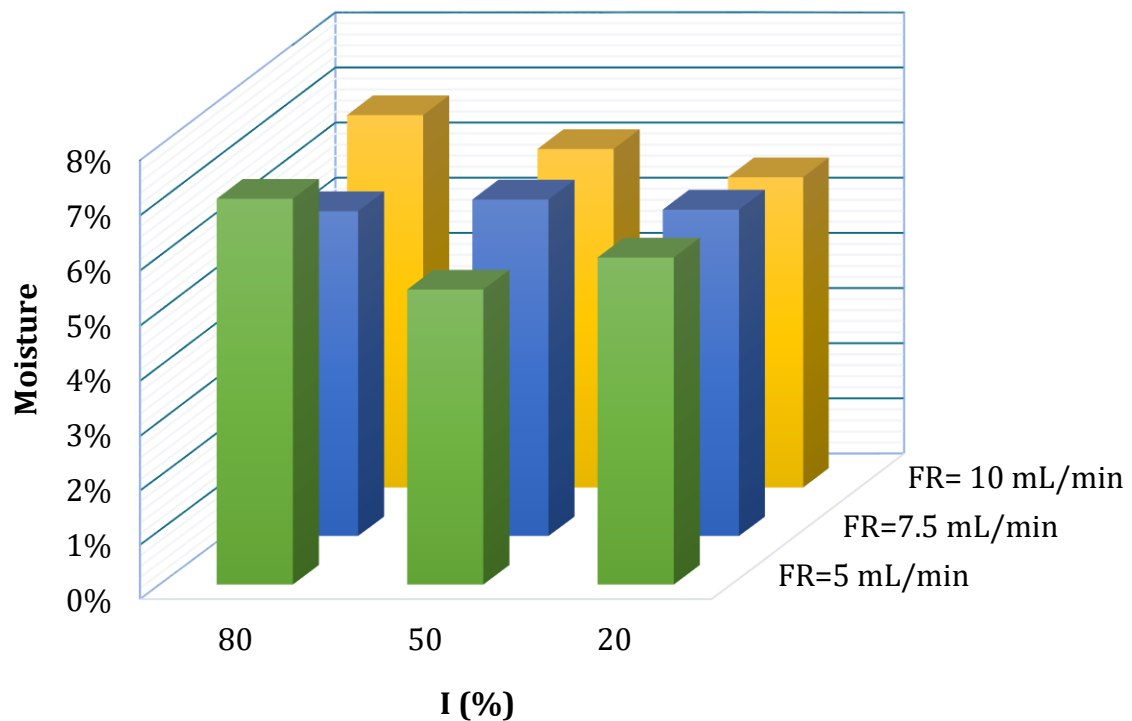
Experimental Design led to 11 tests, among them central point was repeated 3 folds. Response surface methodology showed that a polynomial fitting of the response variables resulted as not significant for what concerns the responses moisture and product recovery. Although the software Design Expert found that the data could be fitted for the variables EY (p-value 0.0442) and Encapsulation efficiency (p-value 0.0394), according to the fitting models equation (44) and equation (45) respectively, no terms of both the equations resulted as significant and the  $R^2$  (0.72 for equation (44), 0.71 for equation (45)) highlighted low accuracy.

$$EY = -0.10756 \cdot I + 2.9 \cdot \text{Flow rate} + 1.4 \cdot 10^{-3} \cdot I^2 - 0.19 \cdot \text{Flow rate}^2 \quad (44)$$

$$\text{Encapsulation efficiency} = -5.5 \cdot 10^{-3} \cdot I + 0.16 \cdot \text{Flow rate} + 7.37 \cdot 10^{-5} \cdot I^2 - 0.01 \cdot \text{Flow rate}^2 \quad (45)$$

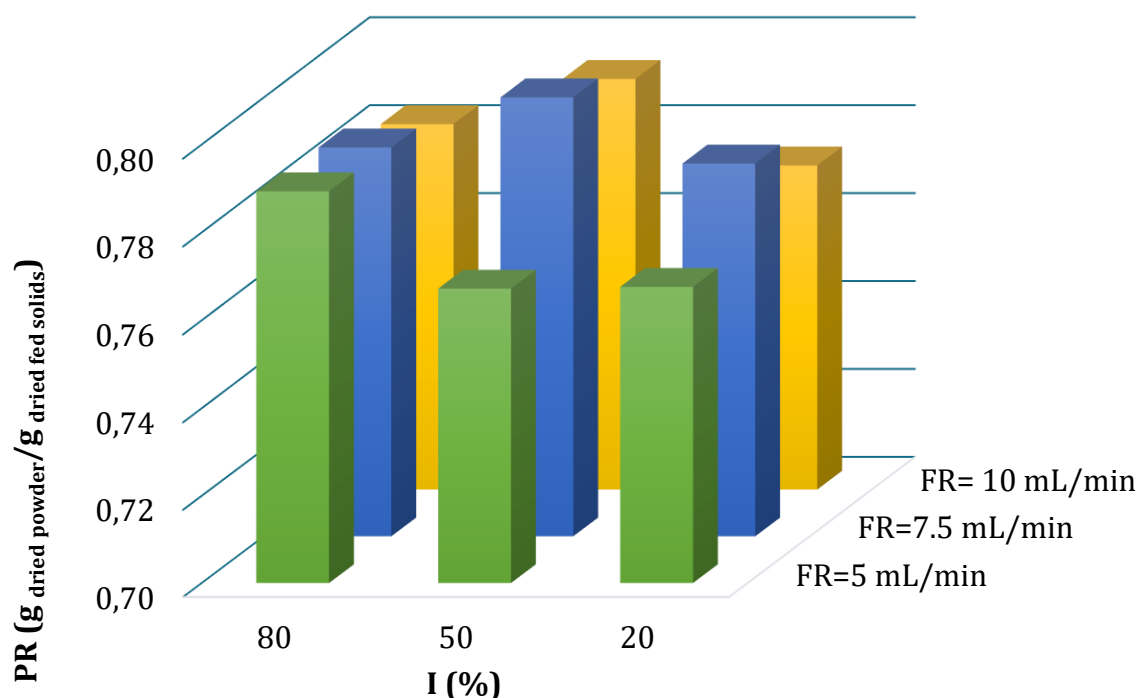
Then, it is possible to assess that the range of values of the variables and the polynomial fitting of data did not allow a good description of experimental data.

Figure 35 shows the moisture as a function of the input variables. According to software analysis, can be observed that its values ranged between 5.3 % and 7.0 %, and then it is quite constant in the considered design space.



**Figure 35.** Spray-dried powder moisture as a function of the composition of the wall material, expressed as percentage of Inulin (% wt) and as a function of the inlet suspension flow rate (mL/min).

A similar trend is reported in figure 36 for what concerns product recovery: the responses to the input variables resulted not statistically significant and all the values were around 0.79 g<sub>dried powder</sub>/g<sub>dried fed solids</sub>. Then, only the 20 % of the total load solids was lost during spray drying.



**Figure 36.** Product Recovery as a function of the composition of the wall material, expressed as percentage of Inulin (% wt) and as a function of the inlet suspension flow rate (mL/min).

Encapsulation yield is reported in figure 37. Its values ranged from 7.2 to 10.8 mg<sub>CAE</sub>/g<sub>dried powder</sub>. In this fraction the amount of superficial polyphenols was not taken into account, but only the aliquot trapped inside the particles. Total polyphenols found in the powder were 8.5-13.3 mg<sub>CAE</sub>/g<sub>dried powder</sub> and the highest values belong to the powder built with the 80% of inulin and the 20% in weight of MD. Obviously, also the highest encapsulation efficiencies (62 %, 63 %, 58 %) corresponded to the same wall material composition, but no dependence on flow rate was observed (figure 38). These results are in contrast with what was reported by De Barros Fernandes et al. (2014) for the encapsulation of rosemary essential oil. In that case, the increase of the ratio inulin/Arabic gum in the carrier led to a lower encapsulation efficiency. In addition, in the study of Bakowska-Barczak and Kolodziejczyk (2011), the inulin was less effective in encapsulation of black currant polyphenols than maltodextrins. The difference can be due to the nature of the fed extract, particularly to the presence of ethanol in the

loaded suspension of this study, and to the dissimilar operating conditions used during spray drying. Total efficiencies, which include also superficial polyphenols, for tests with inulin 80% wt were 72, 73 and 68 %. This means that about 30 % of the polyphenols loaded with the suspension were lost in the device (product loss was about 20 %) and because of the thermal treatment. Figure 39.b shows a SEM image of the particles obtained at 160°C as inlet temperature, 7.5 ml/min as flow rate and using 80% inulin as coating agent. Average Feret's diameter, calculated by the software ImageJ, of the particles depicted in the figure ranged between 0.7 to 9.3  $\mu\text{m}$ , with an average value of  $3.5 \pm 2.4 \mu\text{m}$ .

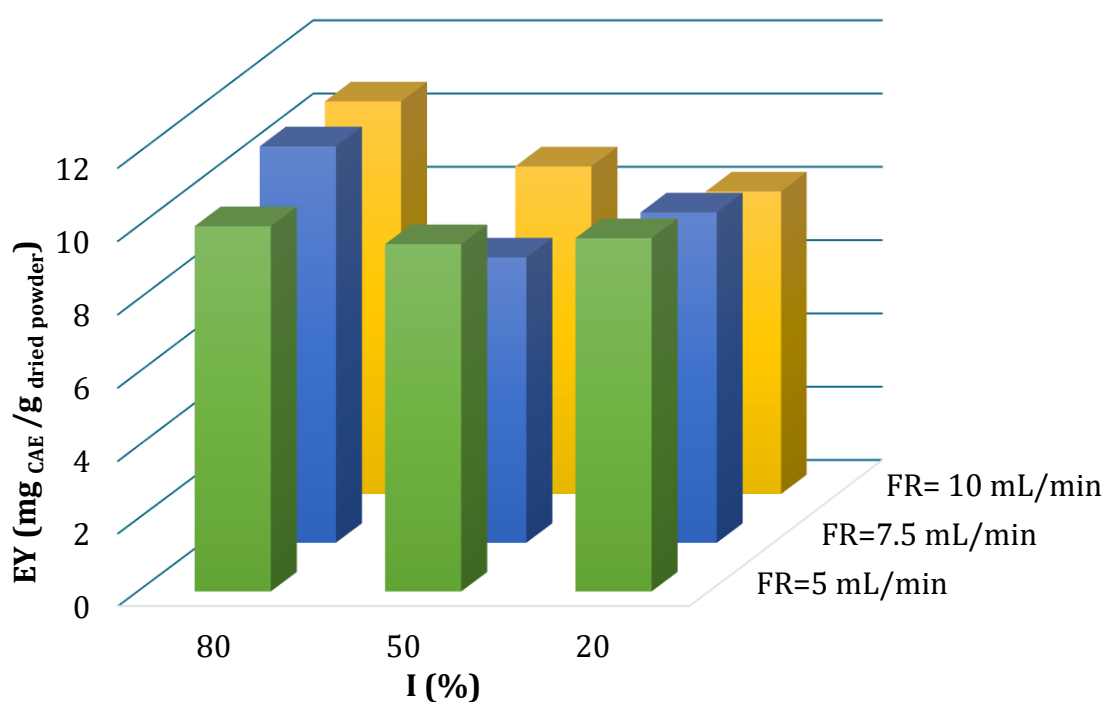


**Figure 37.** Encapsulation yield ( $\text{mg}_{\text{CAE}}/\text{g}$  dried powder) obtained from spray drying tests over inlet suspension flow rate (mL/min) and carrier composition (I, % wt).

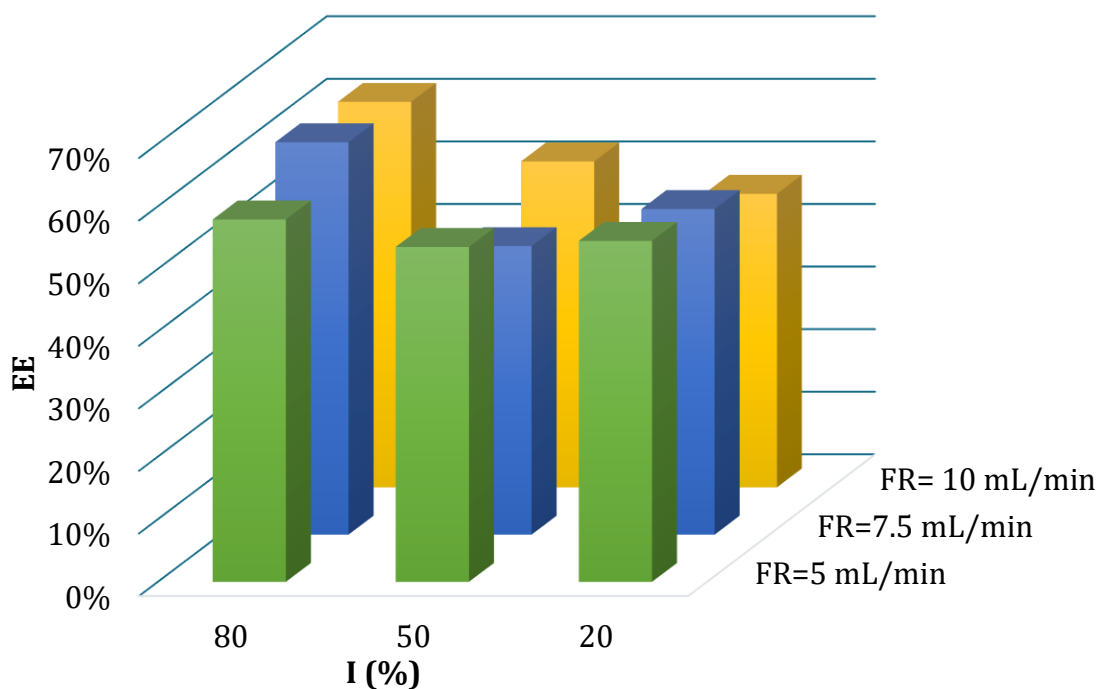


**Figure 38.** Encapsulation efficiency ( $\text{mg}_{\text{CAE}}/\text{g}$  dried powder) obtained from spray drying tests over inlet flow rate (mL/min) and carrier composition (I, % wt).

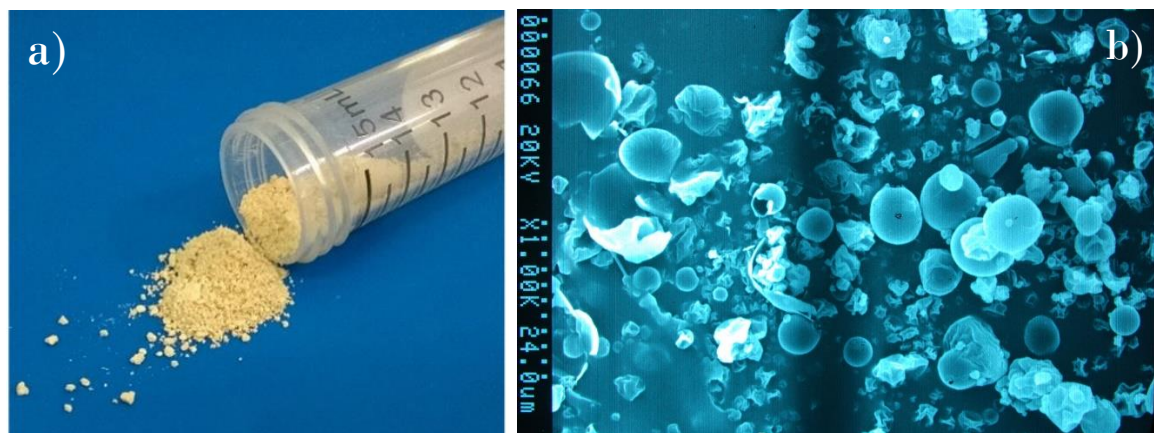


**Figure 39.** a) Spray-dried powder obtained using 80% of inulin and a flow rate of 7.5 mL/min; b) SEM image of spray-dried powder obtained at 160 °C, using 80% of inulin, and a flow rate of 7.5 mL/min.

#### 4.4 CONCLUSIONS

Encapsulation of extracted antioxidants from SCG is a necessary technique to preserve the activity of the bioactive compounds during storage. In this chapter, the effects of the variables flow rate of the feed and wall material composition on spray-dried product were analyzed. Although the response surface methodology resulted not suitable for process optimization in the range of value chosen for the input variables, the study indicated that in the range of flow rate 5-10 mL/min and varying the composition of the carrier from 20:80 to 80:20 (I:MD, wt/wt), no effects are highlighted on the product recovery and product moisture. The presence of inulin, instead, increased the polyphenols encapsulation efficiency, while flow rate seemed to be less influent on the process, in the investigated range of values. Maximum encapsulation efficiencies (63% and 62 %) were achieved using a carrier composition of 80 % wt of inulin and at the highest inlet flow rates (7.5 mL/min and 10 mL/min).

*Parts of this chapter were partially presented as “Encapsulation of Antioxidants from Spent Coffee Ground Extracts by Spray Drying” by Margherita Pettinato, Bahar Aliakbarian, Alessandro A. Casazza, Patrizia Perego, in the 13<sup>th</sup> International congress on Chemical and process engineering (ICheaP 13), 28-31 May 2017, Milan, Italy, and already published as “Encapsulation of Antioxidants from Spent Coffee Ground Extracts by Spray Drying” by Pettinato et al. (2017).*

## *Chapter 5*

# **HIGH TEMPERATURE AND PRESSURE-ASSISTED EXTRACTION AND POST-PROCESSING GREEN TECHNIQUES FOR ANTIOXIDANT RECOVERY FROM SPENT COFFEE GROUNDS**

### **5.1 ABSTRACT**

In this chapter, High Pressure and Temperature-assisted extraction (HPTE) of antioxidants from spent coffee grounds was examined. Process variables as temperature, and the related pressure, solvent and time were studied and their effects on the product were evaluated in terms of total polyphenol yields, total flavonoid yield and antiradical power. The optimized extract (obtained at 150 °C, 60 min, ethanol 54 % v/v) was then characterized and its potential application for food active packaging evaluated. Indeed, although the fabrication of the packaging was not object of this study, for the potential production of active packaging with antioxidant action, some properties of the extract should be assessed. In order to be used for this purposes, the extract was stabilized in powder form by freeze-drying and encapsulated in maltodextrins by spray drying, and antimicrobial activity and peroxidation inhibition ability of the two products were evaluated. Finally, the optimized extract obtained by HPTE was also subjected to two supercritical fluid-assisted processes: supercritical antisolvent extraction and supercritical-assisted liposome formation, which allowed to produce respectively a solid extract more rich in polyphenols ( $243 \pm 3.9 \text{ mg}_{\text{CAE}}/\text{g}_{\text{dried powder}}$ ) than freeze-dried extract ( $135.5 \pm 3.8 \text{ mg}_{\text{CAE}}/\text{g}_{\text{freeze-dried extract}}$ ) and an encapsulated extract which, differently from the one produced by spray drying, was more suitable for applications within apolar media, thus increasing the solubility of the extract in lipophilic solvents.



## 5.2 MATERIAL AND METHODS

### 5.2.1 High temperature and pressure-assisted extraction equipment

Experimental extraction tests were carried out in a stainless steel stirred reactor (Parr Instruments Company, model 350 M – 4650 Series, made of 316 stainless steel, Illinois, USA). The stirred reactor (figure 40) can work at high temperature (up to 350°C) and pressure (up to 200 bar), which are monitored by a thermocouple and a pressure gauge. The former is the sensor connected to a temperature controller (model 4840, Parr Instruments Company, Moline, USA), which allows to maintain the variable at the desired set point value by an external electrical jacket.



**Figure 40.** Stainless steel stirred reactor (Parr Instruments Company) used for High Temperature and Pressure-assisted extraction tests.

### 5.2.2 Evaluation of process parameters

An evaluation of process parameters was undertaken by performing extraction tests on dried SCG (*see paragraph 2.2.1*) at three different temperatures and using different solvents (table 19). During each test, a liquid to solid ratio of 10 mL/g was used. After the addition of the solid matrix and the solvent into the vessel, carbon dioxide was bubbled for at least 2 min in order to replace air with inert atmosphere, for

degradation reaction prevention, then the extraction under stirring (250 rpm) was carried out.

**Table 19.** Operating conditions used for experimental tests of HPTE

Solvent	Extraction Time (min)	T(°C)	P (bar)
Methanol	90	180	25
Ethanol	90	180	20
Water	90	180	13
Ethanol/Water 50:50, v/v	90	180	16
Methanol	90	150	14
Ethanol	90	150	9.6
Water	90	150	4.8
Ethanol/Water 50:50, v/v	90	150	7.2
Methanol	90	120	6.4
Ethanol	90	120	4.2
Water	90	120	2
Ethanol/Water 50:50, v/v	90	120	3.1

After the extraction, the liquid phase was separated from the solid one by filtration on filter paper and stored at 4 °C for further analyses.

### 5.2.3 Analytical methods

Extracts were evaluated in terms of total polyphenol yield (*see paragraph 3.2.1.3*), total flavonoid yield (*see paragraph 3.2.1.4*) and antiradical power (*see paragraphs 3.2.1.5 and 3.2.1.6*). Extract total solids were carried out according to procedure described in paragraph 3.2.1.7, as well as High Performance Liquid Chromatography, following the

method reported in paragraph 3.2.1.8 for HMF, caffeine and chlorogenic acid determination. In addition, caffeine content was also evaluated via UV-vis spectrophotometer. With this purpose, caffeine was separated from the liquid sample by liquid-liquid extraction, using dichloromethane (Belay et al., 2008). 1 mL of sample and 5 mL of dichloromethane were mixed for few minutes, then were placed in a separating funnel where caffeine was extracted. The process was repeated 3 times and the solvent layers combined and the absorbance read at 260 nm into quartz cuvettes. The caffeine content was, then, calculated by means of the calibration curve reported in equation (46), obtained using standard solutions of caffeine in dichloromethane.

$$ABS_{260\text{ nm}} = 25.79 \cdot C \quad R^2 = 0.998 \quad (46)$$

Where C is the concentration of caffeine (mg/mL).

#### 5.2.4 Freeze-drying

HTPE extract, obtained at 150 °C, 7.2 bar, 60 min of extraction time and using ethanol 54% (v/v) as solvent, was subjected to freeze-drying process to prevent its degradation. For this purpose, after filtration on filter paper, the liquid extract was treated in rotavapor to perform ethanol disposal and then freezed at -18 °C. Finally, extract was lyophilized using a freeze-dryer (Christ model Alpha1-2 LDplus, Osterode am Harz, Germany). Freeze-dried extract was characterized in terms of total polyphenols, total flavonoids, antiradical power and antimicrobial activity.

#### 5.2.5 Encapsulation by spray drying

The second preservation process employed on the HTPE extract (obtained at 150 °C, 7.2 bar, 60 min of extraction time and using ethanol 54% (v/v) as solvent) was encapsulated in maltodextrins (MD) (DE 16.5-19.5, Sigma-Aldrich, Milan, Italy) by spray drying (Mini Spray Dryer B-290, BÜCHI Labortechnik AG, Flawil, Switzerland). With this aim, 50 mL of liquid extract were added to 5 g of maltodextrins. The solution

was left under stirring until the complete dissolution of maltodextrin, and then was fed to spray dryer. Operating conditions used for carrying out the process are reported in table 20.

**Table 20.** Operating conditions for encapsulation of SCG extract obtained by HPTE

Aspiration rate (m <sup>3</sup> /h)	32
Feed flow rate (mL/min)	7.5
Inlet temperature (°C)	160
Maltodextrin concentration (g/L)	100

Encapsulated extract was characterized in terms of product recovery, encapsulation yield and efficiency, moisture and particle size distribution (*see paragraph 4.2.3*), antimicrobial activity and lipid peroxidation inhibition.

#### 5.2.6 Antimicrobial activity evaluation

*Escherichia coli* and *Saccharomyces cerevisiae* were employed to test the ability of freeze-dried extract and encapsulated extract in MD to inhibit microbial growth.

##### 5.2.6.1 Microorganism preparation

With this aim, *S. cerevisiae* was inoculated into Yeast Extract Peptone Dextrose (YPD) medium, made by peptone (20 g/L), yeast extract (10 g/L) and glucose (20 g/L) (Chen et al., 2011), while for *E. coli* was used Luria-Bertani medium, which was composed by tryptone (10 g/L), NaCl (10 g/L) and yeast extract (5 g/L) (Sezonov et al., 2007). Both of the media were sterilized by autoclaving at 121 °C for 20 min (figure 41). Microbial growth was carried out in an incubator (VWR, Radnor, Pennsylvania, Stati Uniti) at 37 ± 1 °C for 24 h and was recorded via spectrophotometer (model Genova, Jenway, Staffordshire, UK) by reading the optical density of the sample at 600 nm. At this stage, control sample was made by the medium without microorganism inoculum, but stored into the incubator as well as the sample with the microorganism, and exposed at the same operating conditions. After 24 h, samples were read at 600 nm and the growth in

Petri's dishes in presence of freeze-dried extract and encapsulated extract was performed.



**Figure 41.** Sterilized media for *Saccharomyces cerevisiae* (front) and *Escherichia coli* (back)

#### 5.2.6.2 Evaluation of microbial growth by Petri's dishes in presence of freeze-dried extract

The study on the antimicrobial activity of freeze-dried extract was carried out by keeping both of the microorganisms in contact with two different concentrations of freeze-dried extract ( 1% and 2 % (w/v)) and comparing the number of colony-forming units (CFU), after 24 h of incubation at 37 °C, with those of the control samples, in which microorganisms were left to grow in the same conditions but in absence of freeze-dried extract.

A first control sample was composed by solid medium and was prepared by adding 1.5 % (w/v) of agar to the YPD and Luria-Bertani media before the sterilization. Once sterilized, media were left cooling up to a temperature of about 40 °C, then microorganism inoculum into Petri's dishes was carried out.

In addition, a 40% (w/v) solution of freeze-dried extract in dimethyl sulfoxide (DMSO) (Ramalakshmi et al., 2009) was prepared, then 1.5 mL of this solution were diluted into 58.5 mL of medium (after sterilization and cooling), giving the first concentration subjected to evaluation (1 %, w/v), while 3 mL of initial solution were dissolved into 57 mL of medium (after sterilization and cooling) to obtain the concentration of 2 % (w/v).

After the addition of the extract, microorganism inoculum into Petri's dishes was carried out.

The use of DMSO was necessary to provide the dissolution of the lyophilized extract, which was not completely soluble in water, but only in ethanol 54 % (v/v). The last solvent was not suitable for the purposes of this study.

Since DMSO was used to provide the dissolution of the freeze-dried extract, a second control sample was taken into consideration in order to assess the potential effects of this compound on microbial growth. So, control sample was prepared by adding to the medium an amount of DMSO corresponding to those of the samples in which 2 % (w/v) of freeze-dried extract was added (2.94 mL of DMSO in 57.06 mL of medium). Even in this case, in the control sample the microorganism was inoculated, then the Petri's dishes were incubated for 24 h at 37 °C.

#### 5.2.6.3 *Evaluation of microbial growth by Petri's dishes in presence of encapsulated extract*

Agar plates were also used to analyze the antimicrobial activity of extract encapsulated into MD by spray-drying. With this aim, three concentrations of encapsulated extract were tested: 5, 10, 15 % (w/v). In this case, encapsulated extract was added to the liquid media (YPD for *S. cerevisiae* and Luria-Bertani for *E. coli*) in which microorganisms were left to grow for 24 h in the incubator at 37 °C. After 24 h, absorbance of the sample was read by spectrophotometer at 600 nm and the properly diluted samples were placed on the agar plates, for CFU counting after 24 h of incubation. Control samples consisted in the microorganism left to grow without any encapsulated extract and microorganism left to grow in the liquid medium in presence of pure maltodextrins (15 %, w/v) without extract.

Petri's dishes were prepared by adding 1.5 % (w/v) of agar to the YPD and Luria-Bertani media before the sterilization, while, after sterilization and cooling up to a temperature of about 40-45 °C, inoculum of the pre-incubated samples was performed.

### 5.2.7 Evaluation of the lipid peroxidation inhibition

The ability of the extract to inhibit lipid peroxidation was evaluated. Extra vergin olive oil (EVO, Carrefour-Classico) was used as food simulant and was subject to oxygen, light and temperature stress conditions to accelerate lipid peroxidation reactions, in presence and absence of extract encapsulated in maltodextrins by spray drying. Two different concentrations of encapsulated extract were tested: 10 and 1 % (w/v). Experimental tests were performed by adding encapsulated extract to 20 mL of EVO in 50 mL falcon centrifuge tube and agitating in vortex for 2 min.

Samples and operating conditions for the experimental tests are listed below:

- Control 1: EVO stored in the dark and oxygen free;
- Control 2: EVO in presence of pure coating agent (MD) at the maximum concentration (10 %, w/v ), stored in the dark and oxygen free;
- Control 3: EVO in presence of encapsulated extract (1 and 10 %, w/v) stored in the dark and oxygen free;
- EVO exposed for 3 days to sun light and saturated with pure oxygen;
- EVO in presence of encapsulated extract (1 and 10 %, w/v) exposed for 3 days to sun light and saturated with pure oxygen;
- EVO stored in the dark for 4 days and saturated with pure oxygen;
- EVO in presence of encapsulated extract (1 and 10 %, w/v) stored in the dark for 4 days and saturated with pure oxygen;
- EVO stored in the dark for 6 days at 40°C and saturated with pure oxygen;
- EVO in presence of encapsulated extract (1 and 10 %, w/v), stored in the dark for 6 days at 40°C and saturated with pure oxygen.

After the exposure to stress conditions, samples were centrifuged at 6000 xg (MF-20-R centrifuge, Alliance Bio Expertise, Guipry, France) for 5 min, separating solid from olive oil and about 3 mL of treated oil were subjected to peroxide value (PV) determination by titration, according to COMMISSION REGULATION (EEC) No 2568/91 (European

Union, 1991) on the characteristics of olive oil and olive-residue oil and on the relevant methods of analysis. Briefly, the peroxide value represents the quantity of those substances in the sample, expressed in terms of milliequivalents of active oxygen per kilogram, which oxidize potassium iodide under specified operating conditions. In a 250 mL flask, oil sample was dissolved by adding 10 mL of chloroform (Carlo Erba Reagents, Milano, Italy) and 15 mL of acetic acid (Carlo Erba Reagents, Milano, Italy). Then, 1 mL of a recently prepared potassium iodide saturated aqueous solution was added, and the sample was stirred for 1 min and left to react for 5 min in the dark. Finally, 75 mL of deionized water were added to the sample and titration was performed using a 25 mL burette with 0.002 M sodium thiosulphate solution, standardized by titration, and 1 mL of starch solution as indicator. PV was expressed in milliequivalents of active oxygen per kilogram, according to the equation 47.

$$PV = \frac{v \cdot T_M \cdot 1000}{m} \quad (47)$$

Where  $v$  is volume in mL of the standardized sodium thiosulphate solution used for the test;  $T_M$  is the exact molarity of the sodium thiosulphate solution and  $m$  is the mass in g of the test portion.

### 5.2.8 Supercritical Antisolvent Extraction for extract micronization

The third preservation process employed on the HTPe extract (obtained at 150 °C, 7.2 bar, liquid to solid ratio equal to 300 mL/30 g, 60 min of extraction time and using ethanol 54% (v/v) as solvent) was supercritical antisolvent extraction (SAE). The obtained extracts were subjected to filtration, and then ethanol disposal was performed in rotavapor at 40° C, under vacuum, before freeze-drying process, which allowed the complete removal of the solvent and an easier transportation of the extract. Indeed, this stage of the study was carried out in collaboration with the Department of Industrial Engineering of the University of Salerno. Freeze-dried extract (9.88 g) was dissolved in ethanol (300 mL) in order to prepare the feed for (SAE), and it was left under stirring for 12 h and filtered on a filter paper.



A scheme of SAE plant used for the experiment is reported in figure 42.

SAE apparatus consisted in a pumping area, a high pressure extraction vessel and a separation area. A Lewa Ecoflow pump (mod. LDC-M-2, max pressure 40.0 MPa) transported CO<sub>2</sub> from a reservoir to the extraction vessel (500 cm<sup>3</sup>), where the liquid solution was pumped by a Gilson Pump (Model 305, Gilson FR) and forced inside through an injector. The extraction vessel was equipped with a filter on the bottom with a porosity of 0.1  $\mu\text{m}$ , on which the micronized solid was collected. Downstream from the vessel a low pressure separator, made of stainless steel (AISI 316), provided solvent recovery, while CO<sub>2</sub> exited in gaseous form by the top of the separator (Martín et al., 2011). Operating conditions used in the experimental tests are reported in table 21. Feed, micronized extract and the purge were characterized in terms of total polyphenol, antiradical power, total solids and caffeine content.

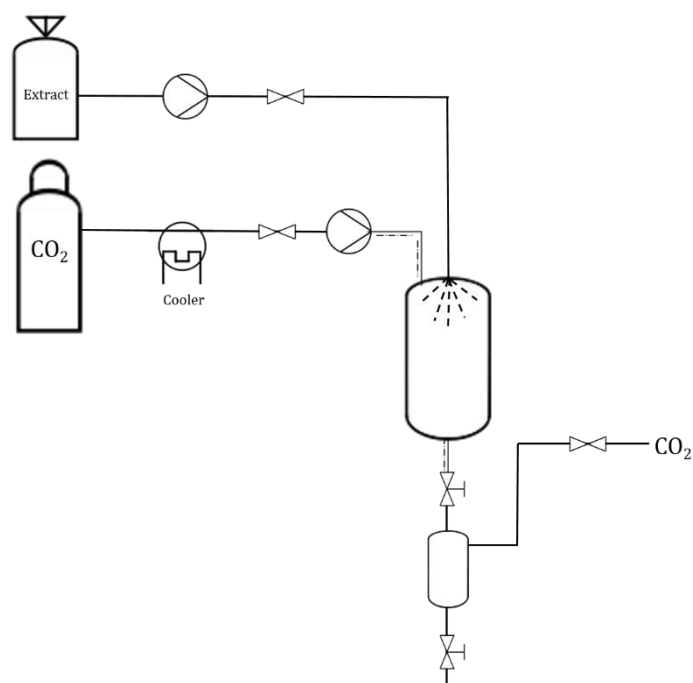


**Figure 42.** Supercritical Antisolvent Extraction plant scheme. Adapted from Meneses et al. (2015)

**Table 21.** Operating conditions of SAE experiments.

Liquid solvent loaded into the plant	Ethanol	
Solvent molecular weight	46.07	g/mol
Solvent density	789	kg/m <sup>3</sup>
Antisolvent	Carbon dioxide	
Pressure	100	bar
Pressure of the separator	25	bar
Temperature of the vessel	40	°C
Temperature of the separator	10	°C
Concentration of total solids	5.5 ± 0.04 mg/ mL	
Flow rate of CO <sub>2</sub>	16.4	dm <sup>3</sup> /min
Volume of fed solution	100	mL
Injector diameter	100	μm
Feed flow rate	1	mL/min

### 5.2.9 Encapsulation of HTPE extract in liposomes by Supercritical-assisted Liposome formation plant

Finally, encapsulation of the HTPE extract (obtained at 150 °C, 7.2 bar, liquid to solid ratio equal to 300 mL/30 g, 60 min of extraction time and using ethanol 54% (v/v) as solvent) into liposomes was carried out. Even in this case, the project was born thanks to the collaboration between the Department of Civil, Chemical and Environmental Engineering of the University of Genoa and the Department of Industrial Engineering of the University of Salerno. Similarly to what exposed in the previous paragraph, the obtained extracts were subjected to filtration, ethanol evaporation in rotavapor at 40 °C under vacuum, and freeze-drying process. Freeze-dried extract was dissolved in water, according to the tested concentrations of extract reported in table 22, and left until complete dissolution. The plant used for loaded liposomes preparation was SuperLip plant (figure 43). The plant presents three feed lines: the first one transports supercritical carbon dioxide, the second one the ethanol in which phospholipids were dissolved, and the third one the dissolved extract. CO<sub>2</sub> is fed from a storage vessel (50-60 bar, 25 °C) by a Lewa Eco pump (model LDC-M-2, Germany) to a heated saturator (S, volume equal to 0.15 dm<sup>3</sup>) together with the lipid solution in ethanol (gas to liquid ratio equal to 2.4 (w/w)), where an expanded liquid is formed. A cooler (FL300, JULABO, Seelbach, Germany) allows to cool the pump head, working at -10 °C and 15 L/min. The

ethanolic solution and the extract are pumped into the plant by Gilson pumps (model 305, Gilson, France).

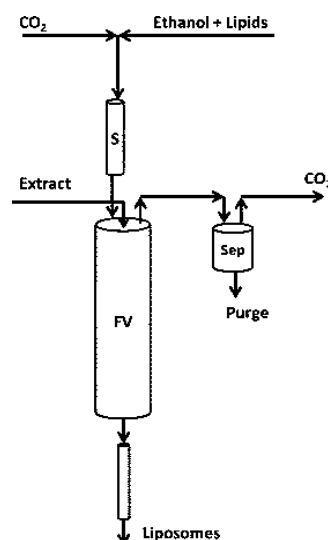


Figure 43. Scheme of SuperLip plant

Expanded liquid is continuously moved into a heated high pressure chamber of 0.5 dm<sup>3</sup>, where also the extract is nebulized by an injector. In the chamber, the expanded liquid and the extract were concurrently fed from the top; here the droplets of water, in which the extract is contained, are mixed with the expanded liquid. In the vessel, atomized droplets are covered by phospholipids on the fly. Formed liposomes precipitate towards the bottom of the chamber where a water bulk is present. Ethanol and carbon dioxide exit from the formation vessel and reach a low pressure separator, which allows to recover the ethanol as liquid, while CO<sub>2</sub> left the system as gas. Liposomes are continuously collected from the bottom of the formation vessel.

Soybean phosphatidylcholine (Sigma Aldrich, Milan, Italy) was used for liposomes fabrication, due to its wide use in food industry as emulsifying agent and dietary supplement for the reduction of cholesterol absorption (Cohn et al., 2010). In addition, it represents one of the main components of plasma membrane, contributing to regulate its fluidity, integrity and permeability (Li et al., 2006).

In table 22, operating parameters used for the tests on the SCG extract encapsulation in liposomes and the variables which was object of study are reported. Particularly, the

attention was focused on the effects of extract concentration in the feed and the pressure within the formation vessel upon product particle size distribution, antiradical power and encapsulation efficiency.

**Table 22.** Operating conditions and variables for the tests on extract encapsulation into liposomes

Operating parameters	
Lipid: phosphatidylcholine	500 mg
Solvent: Ethanol 100%	100 mL
Diluted extract volume	300 mL
Injector diameter	80 $\mu$ m
Temperature of the formation vessel	40 °C
Temperature of the saturator	40 °C
Temperature of the separator	25°C
Gas to liquid ratio	2.34
CO <sub>2</sub> flow rate	6.5 g/min
Ethanol solution flow rate	3.5 mL/min
Diluted extract flow rate	10 mL/min
Variables	
Extract concentration	500 ppm; 250 ppm; 83 ppm
Pressure of the formation vessel	100 bar; 200 bar

### 5.2.9.1 Encapsulation efficiency evaluation

The first response variable object of the study was encapsulation efficiency (%), defined according to equation 48 as the ratio between the mass of encapsulated total polyphenols (ETP) and the mass of total polyphenols fed to the process (FTP).

$$EE = \frac{m_{ETP}}{m_{FTP}} \cdot 100 \quad (48)$$

Total polyphenols were evaluated by means of a modified protocol of the Folin-Ciocalteu's assay (*see paragraph 3.2.1.3*). Briefly, in a 15 mL tube 1.5 mL of sample were added to 3.5 mL of deionized water, followed by the addition of 0.5 mL of Folin-Ciocalteu's reagent (Sigma-Aldrich, Milan, Italy), 1 mL of Na<sub>2</sub>CO<sub>3</sub> saturated solution and 3.5 mL of deionized water. After agitation by Vortex, samples were left to react in the dark for 1 hour before absorbance measurement via UV-vis spectrophotometer (model Lambda 25, Perkin Elmer, Wellesley, MA) at 725 nm. Absorbances were correlated to the concentration of caffeic acid (Sigma-Aldrich, Milan, Italy) equivalents by the calibration curve (equation 49) obtained by ethanolic standard solution and given in figure 44.

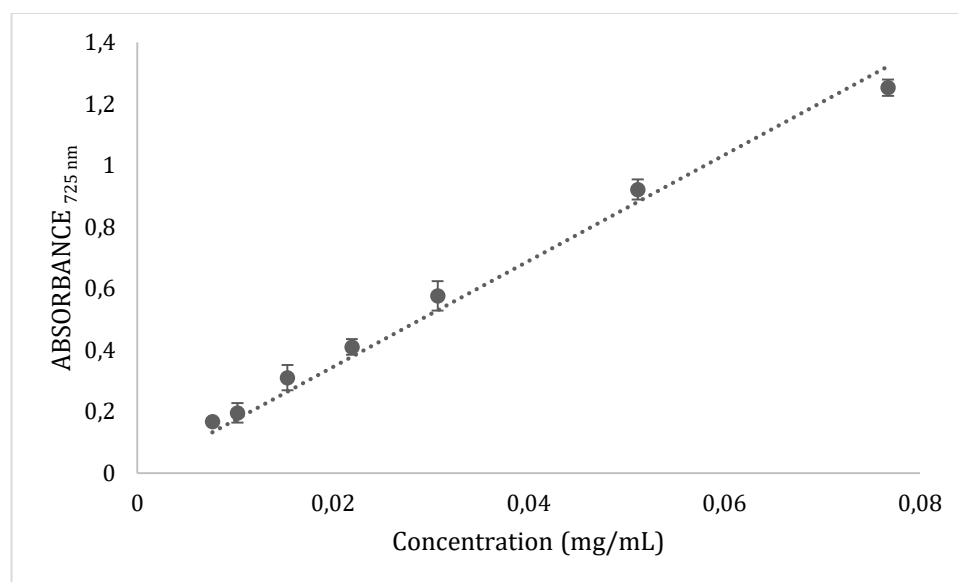


**Figure 44.** Calibration curve for modified total polyphenol determination protocol, obtained by ethanolic standard solution of caffeic acid.

$$ABS_{725\text{ nm}} = 17.2 \cdot C \quad (R^2 = 0.9862) \quad (49)$$

Where C is the caffeic acid equivalent concentration in mg/mL.

The mass of ETP was calculated using the supernatant method (Otake et al., 2006; Trucillo et al., 2018). Thus, the sample were centrifuged at 10000 rpm for 15 min at 4 °C and the supernatant was subjected to the aforementioned Folin-Ciocalteu's assay.

The  $m_{ETP}$  was then calculated as the difference between the the mass of total polyphenols fed to the plant and the mass of total polyphenols in the supernatant.

#### 5.2.9.2 *Antiradical power evaluation*

Antiradical power of loaded liposomes was evaluated by means of ABTS<sup>•+</sup> assay (see paragraph 3.2.1.6). The supernatant method (Otake et al., 2006; Trucillo et al., 2018), reported in the previous paragraph, was applied. So, the antiradical power was evaluated on the feed and the supernatant of the samples, which were centrifuged at 10731  $\times g$  for 15 min at 4 °C. Scavenging capacity of loaded liposome was obtained considering the difference between the ARP of the feed and of the supernatant and expressed as micrograms of Trolox equivalent per mass of liposomes.

#### 5.2.9.3 *Particle size distribution*

Particle size distribution of the liposomes produced by SuperLip process was analyzed by a Dynamic Light Scattering (DLS) instrument (Zetasizer, mod. 5000, Malvern Instruments Ltd). Thus, mean particle size, polydispersity index, zeta potential, and the related standard deviations were determined for each sample.

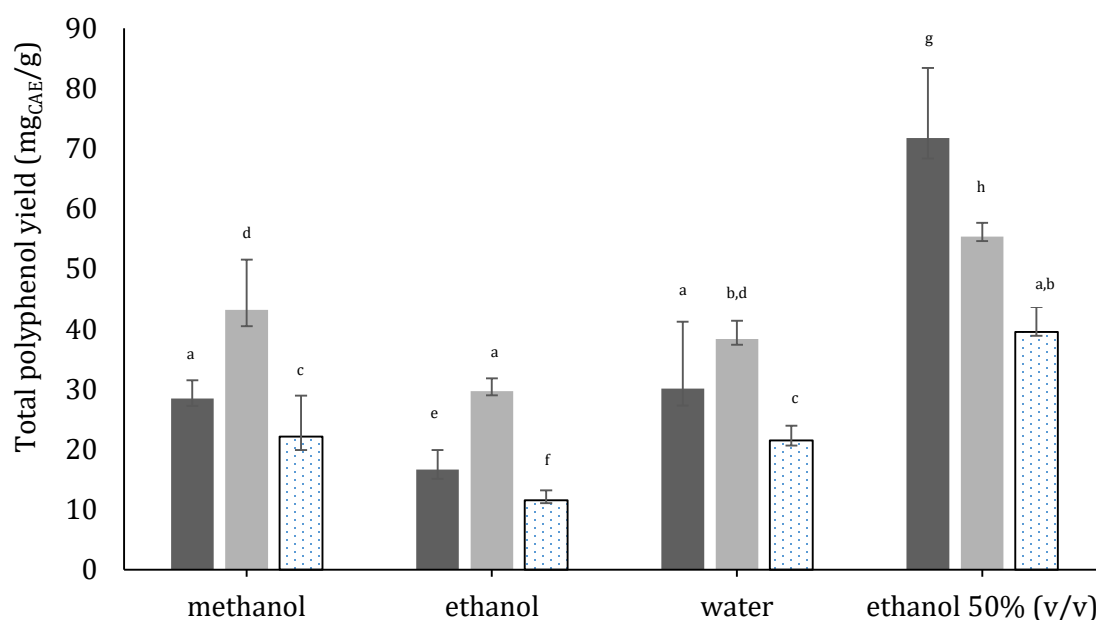
#### 5.2.9.4 *Liposome morphology*

Field –emission scanning electron microscopy (FE-SEM, mod. LEO 1525, Carl Zeiss SMT AG, Oberkochen, Germany) was employed for liposome morphology study. Before the analysis, the solid sample was treated by an advanced sputter coater (AGAR *Auto Sputter Coater* mod.108 A), which allowed to cover the dry non-conducting samples with a 250 Å layer of gold under inert atmosphere of argon and vacuum (0.05 mbar).

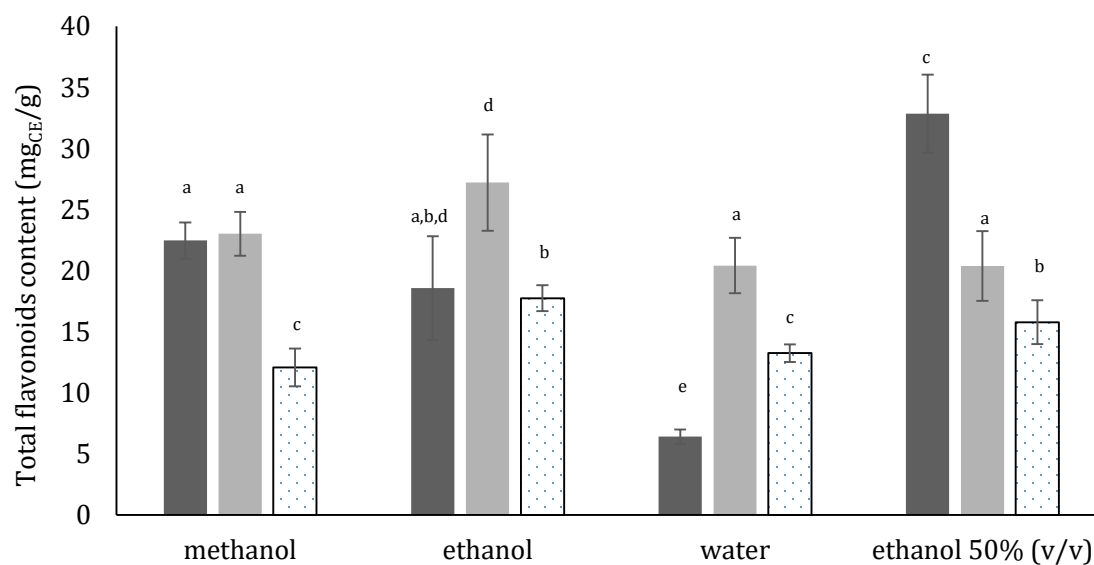
## 5.3 RESULTS AND DISCUSSION

### 5.3.1 High Temperature and Pressure-assisted extraction

Results of the study upon the effects of solvent and extraction temperature on total polyphenol yields are depicted in figure 45. As can be observed, ethanol provided the lowest extraction yields at all the temperatures, exception given for the intermediate temperature of 150 °C, which provided a result comparable with those related to the extractions performed with methanol at 180 °C, water at 180 °C, and the ethanolic solution at 120 °C. Tests, in which pure solvents were used, exhibited the highest extraction yields at 150 °C, while when the solvent was ethanol 50% (v/v) the higher was the temperature, the higher were the polyphenol extraction yields. Similarly to what found for microwave-assisted extraction, the mixture ethanol/water proved to be again the best option to achieve polyphenol extraction from SCG. This result, confirmed that independently from the extraction technique, the intermediate polarity reached by mixing the most polar solvent tested (water) and the least one (ethanol) is able to increase the affinity between the bioactive molecules and the liquid medium. These findings are in agreement with results of other authors, who found in ethanol aqueous solutions the best solvent for polyphenol extraction from SCG (Bravo et al., 2013; Panusa et al., 2013; Shang et al., 2017; Zuorro and Lavecchia, 2013), as well as for chlorogenic acid extraction from artichoke (Rabelo et al., 2016) and from *Lonicera japonica* Thunb (Zhang et al., 2008).



**Figure 45.** Total polyphenol yields obtained by High Temperature and High Pressure-assisted extraction from SCG. ■ 180 °C; ▒ 150 °C; ▤ 120 °C. Different letters do refer to statistically significant differences among results ( $p < 0.05$ , T-test for independent samples). Data are reported as mg of caffeic acid equivalent (CAE) per g of dried SCG.



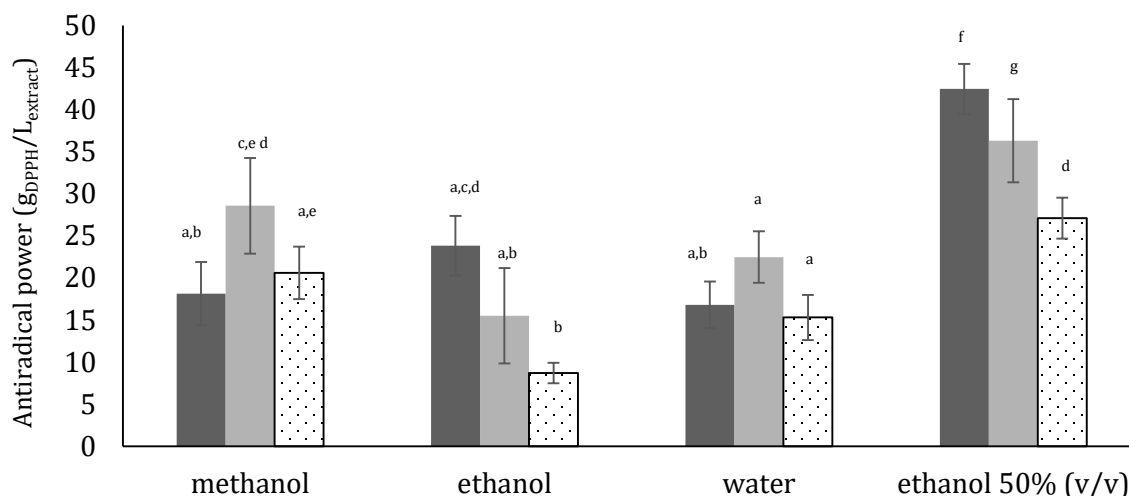
**Figure 46.** Total flavonoids yields obtained by High Temperature and High Pressure-assisted extraction from SCG. ■ 180 °C; ▒ 150 °C; ▤ 120 °C. Different letters do refer to statistically significant differences among results ( $p < 0.05$ , T-test for independent samples). Data are reported as mg of catechin equivalent (CE) per g of dried SCG.



Figure 46 resumes results related to total flavonoid yield as a function of solvent and temperature of extraction, showing a similar behaviour reported for total polyphenol yields. Indeed, even in this case, for pure solvents 150 °C was the value of temperature that ensured the highest extraction yield, whereas for ethanol 50% (v/v) solution, the higher was the temperature the higher was the yield of total extracted flavonoids.

Results about antiradical power (figure 47) reflect the trend observed for total polyphenol yield and total flavonoid yield only in the case of methanol and ethanol 50% (v/v) as extraction solvent. Conversely, the effects of temperature on the extractions carried out with pure ethanol and pure water were negligible in terms of scavenging activity of the extracts.

In HPTE, temperature and pressure are strictly related since the second one corresponded to the vapor pressure of the solvent at the set point temperature. Although pressure could theoretically enhance the solvent penetration in the porous medium and contribute to the analyte release, actually the main significant advantage is often the possibility to work at higher temperature than the solvent boiling point at atmospheric pressure. Indeed, for the extraction of polyphenols from natural matrix, often pressure did not use to show significant effects on extraction yields (Mustafa and Turner, 2011), as reported by Shang et al. (2017) for antioxidant extraction from SCG by PLE, or by Aliakbarian et al. (2012) for antioxidant extraction from winery wastes using subcritical water, and by Choi et al. (2003) for active ingredient extraction from medical plants.



**Figure 47.** Antiradical power obtained by High Temperature and High Pressure-assisted extraction from SCG. ■ 180 °C; ▒ 150 °C; ▨ 120 °C. Different letters do refer to statistically significant differences among results ( $p < 0.05$ , T-test for independent samples). DPPH= 2,2-diphenyl-1-picrylhydrazyl.

Conversely, the effects of temperature are generally significant but the outcomes are often the result of an equilibrium between the increase in extraction yield due to temperature increase and the velocity of degradation reactions that involve thermosensitive compounds like antioxidants (Mustafa and Turner, 2011).

Compared to the preliminary results from the study on SLE and MAE (*see paragraph 3.3.1*), total polyphenol yields are higher for HPTE at each temperature and solvent composition, as well as total flavonoid yields and antiradical power, demonstrating that temperature is one of the main significant variable on the extraction of bioactive molecules from SCG.

From figures 45-47, the best results seemed to be reached working with ethanol 50% (v/v) at 180 °C. But, from literature, the extractions on SCG at temperatures higher than 160 °C revealed the formation of undesired compounds, of which HMF could be a good indicator (Mussatto et al., 2011b). Indeed, a HPLC analysis of the sample extracted at 180 °C and using ethanol 50% (v/v) as solvent, revealed the presence of HMF (retention time 15 min, concentration 0.056 mg/mL). Actually the detected concentration does not represent a risk if is taken into consideration that Codex Alimentarius Standard commission set the maximum limit of HMF at 40 mg/ kg for honey (Shapla et al., 2018), but since at 150 °C no HMF was detected, and considering

that post-processing of extract could potentially increase the amount of HMF, further steps of this study will be undertaken at a maximum extraction temperature of 150 °C. Since, similarly to MAE, the other main affecting variable seemed to be solvent composition and, in order to make a comparison between the results of MAE and HPTE, an evaluation of extraction time on the process was performed using ethanol 54% (v/v) as solvent.

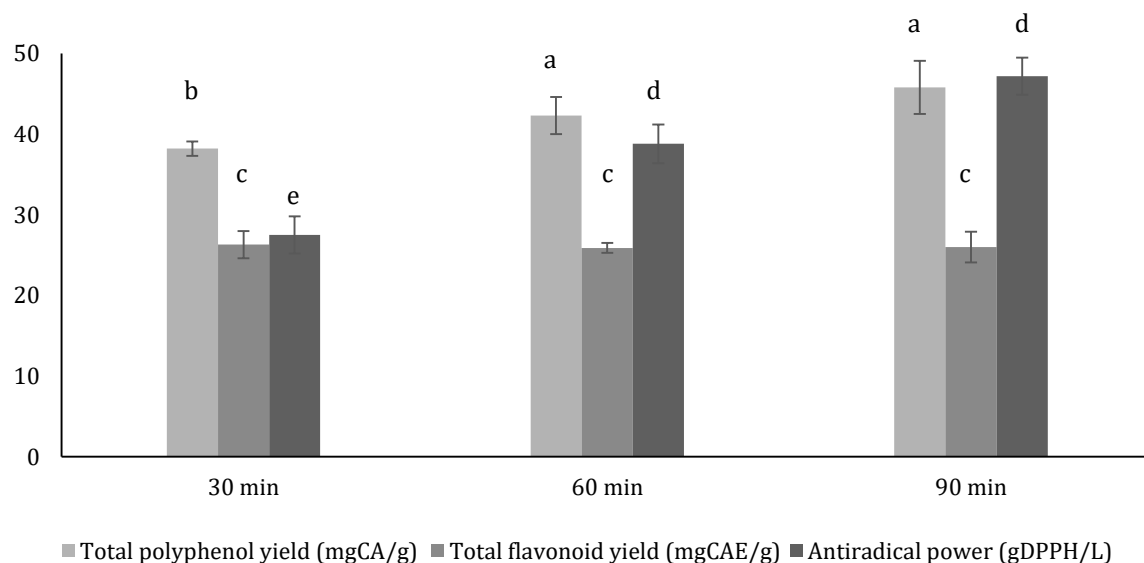


**Figure 48.** Results of HPTE carried out using ethanol 54% (v/v) as solvent and at 150 °C, at three extraction times. Different letters do refer to statistically significant differences among results ( $p < 0.05$ , T-test for independent samples). Data are reported per g of dried SCG or L of extract.

Figure 48 resumes the values of the response variables as function of time. Total polyphenol yield increased when extraction time was increased from 30 up to 60, but no variations were recorded at longer times. The same trend was observed for antiradical power, while the variable time did not affected total flavonoid yield.

As previously found for MAE, extraction kinetics appeared to reach a plateau around 60 min; longer extraction time did not provide advantages to the process.

Due to similarities found for MAE and HPTE, the kinetic extraction equation elaborated for the former one (equation 40) was used to try to describe the behavior of the extraction kinetic of HPTE. Obviously, in the equation were neglected all the parameters which were pivotal for MAE but not for HPTE. Under these considerations, equation 40 could be written as reported in equation (50).

$$C(t, T) = \frac{t}{\left( \frac{1}{\frac{1}{K_0} e^{-E_A/(R_g T)}} \right) + \left( \frac{t}{g' T^2 + h' T + i'} \right)} \quad (50)$$

The values of the kinetic parameters in equation 50 are reported in table 17. Comparing experimental data in terms of total polyphenols with the value calculated by equation 50, could be observed (figure 49) that the kinetic equation underestimated the value of the total polyphenols extracted. The reason could be found in the effects of better stirring and, above all, inert atmosphere, which in HPTE protect the antioxidants from degradation reactions and that was absent in MAE. Since the equation was built around MAE data, this effect was not taken into account in equation 50. Nevertheless, peculiar effects of microwaves on the extraction allowed to obtain an extract with a total polyphenols yield comparable to the optimized extract of HPTE.

Results proved that HPTE at 150 °C, 60 min of extraction time, using ethanol 54% (v/v) as solvent and under inert atmosphere was able to provide higher extraction yield than SLE and comparable with MAE, the last carried out at the same temperature and in the same time. The complete characterization of the extract obtained under the aforementioned operating conditions is reported in table 23. HPLC analysis carried out on the extract did not detect any presence of HMF. Similarly to what found for MAE extract, even in this case, the chromatograms showed the presence of some other polyphenols, whose spectra could be associated to isomers or derivatives of chlorogenic acid.

**Table 23.** Characterization of the extract obtained by HPTE (150°C, 7.2 bar, 60 min, ethanol 54% (v/v)). CAE= caffeic acid equivalent; CE= catechin equivalent; TE= trolox equivalent; DPPH=2,2-diphenyl-1-picrylhydrazyl; ABTS= 2,2'-azino-bis(3-ethylbenzothiazoline-6-sulphonic acid); SCG=spent coffee grounds.

Average total polyphenol yield	$43 \pm 2.3 \text{ mg}_{\text{CAE}}/\text{g}_{\text{dried SCG}} - 173 \text{ mg}_{\text{CAE}}/\text{g}_{\text{extracted solids}}$
Average total flavonoid yield	$21 \pm 2.2 \text{ mg}_{\text{CE}}/\text{g}_{\text{dried SCG}} - 84.7 \text{ mg}_{\text{CE}}/\text{g}_{\text{extracted solids}}$
Average total solid yield	$248 \pm 8.6 \text{ mg}_{\text{solids}}/\text{g}_{\text{dried SCG}} - 24.8 \text{ g}_{\text{solids}}/\text{L}_{\text{extract}}$
Antiradical power (ABTS <sup>•+</sup> assay)	$59 \pm 3 \text{ } \mu\text{g}_{\text{TE}}/\text{L}_{\text{extract}} - 2,38 \text{ } \mu\text{g}_{\text{TE}}/\text{g}_{\text{extracted solids}}$
Antiradical power (DPPH <sup>•</sup> assay)	$38.8 \pm 3 \text{ g}_{\text{DPPH}}/\text{L}_{\text{extract}} - 1.56 \text{ g}_{\text{DPPH}}/\text{g}_{\text{extracted solids}}$
Chlorogenic acid concentration	$0.58 \pm 0.02 \text{ g}/\text{L}_{\text{extract}} - 23 \text{ mg}/\text{g}_{\text{extracted solids}}$
Caffeine (from HPLC analysis)	$1.1 \pm 0.06 \text{ g}/\text{L}_{\text{extract}} - 43 \text{ mg}/\text{g}_{\text{extracted solids}}$
Caffeine (via spectrophotometer)	$2.94 \pm 0.07 \text{ g}/\text{L}_{\text{extract}} - 118 \text{ mg}/\text{g}_{\text{extracted solids}}$

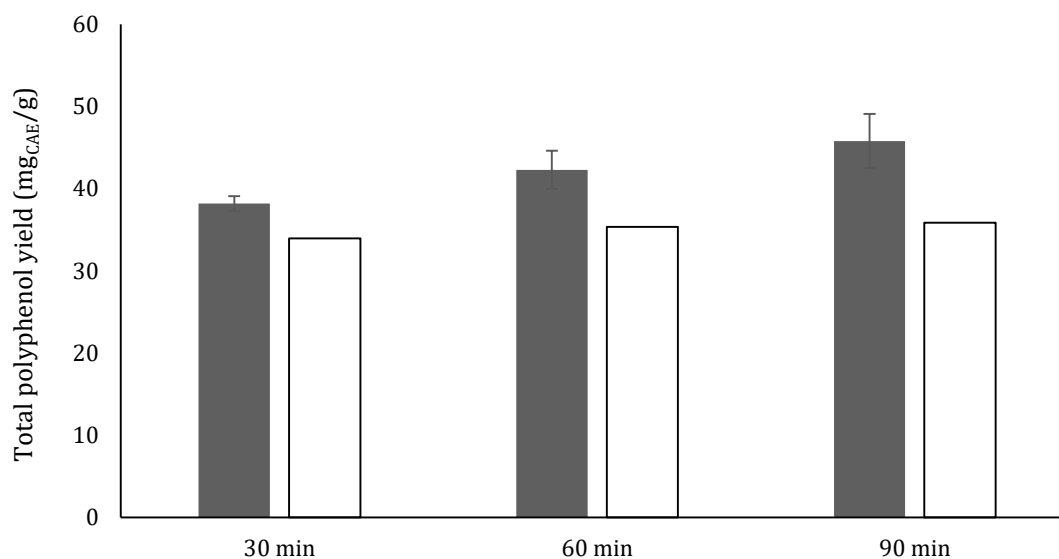


**Figure 49.** Comparison between experimental data (■) related to total polyphenol yields and the values calculated by equation 50(□). Data are reported as mg of caffeic acid equivalent (CAE) per g of dried SCG.

### 5.3.2 Freeze-dried extract antimicrobial activity

The extract characterized in table 23 was subjected to freeze-drying process and analyzed in terms of total polyphenol yield and antiradical power in order to verify the efficacy of the process to preserve the extract quality. The total polyphenol content ( $135.5 \pm 3.8 \text{ mg}_{\text{CAE}}/\text{g}_{\text{freeze-dried extract}}$ ) resulted as slightly lower than that recorded for the liquid extract, while no variation of the antiradical power was observed ( $2.36 \pm 0.05 \text{ } \mu\text{gtrolox equivalent} / \text{g}_{\text{freeze-dried extract}}$ ). Caffeine content was also determined by liquid-liquid extraction and via UV-vis spectrophotometer providing a value of  $119 \pm 5.3 \text{ mg} / \text{g}_{\text{freeze-dried extract}}$ .

The obtained product was then tested to determine its antimicrobial activity.

Evaluation of antimicrobial activity was carried out on two microorganisms (*E. coli* and *S. cerevisiae*).

The growth of *E. coli* in presence of freeze-dried extract, dissolved into medium by means of dimethyl sulfoxide, is reported in figure 50. Results showed high error due to the biological variability. Although results about the inhibition of *E. coli* growth could not be conclusive, due to the the high error of the two control samples, it can be observed that the average value of the CFU of the samples in which 1 % of freeze-dried extract was put in contact with the microorganism is 2 order of magnitude below the ones of control samples. In addition, no *E. coli* growth was observed in the samples with 2 % of freeze-dried extract.

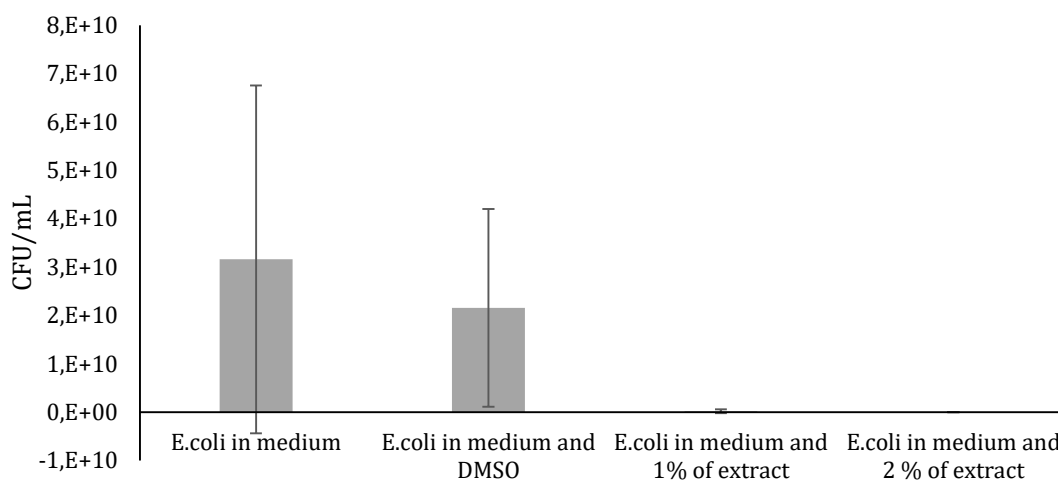


**Figure 50.** Evaluation by Petri's dishes of the *E.coli* growth in presence of freeze-dried extract dissolved into medium by means of dimethyl sulfoxide. CFU= colony forming units. Concentrations of extract are expressed as % (w/v).

Figure 51 reports experimental data concerning the *S. cerevisiae* growth in presence of freeze-dried extract. In this case, is more evident the effect of the presence of freeze-dried extract on the microorganism growth, both in the samples with 1% of extract and with 2 % of extract. Indeed, with respect to both of the control samples, the presence of extract significantly reduced the CFU observed. Particularly, when 2 % of extract was added, no CFU were recorded.

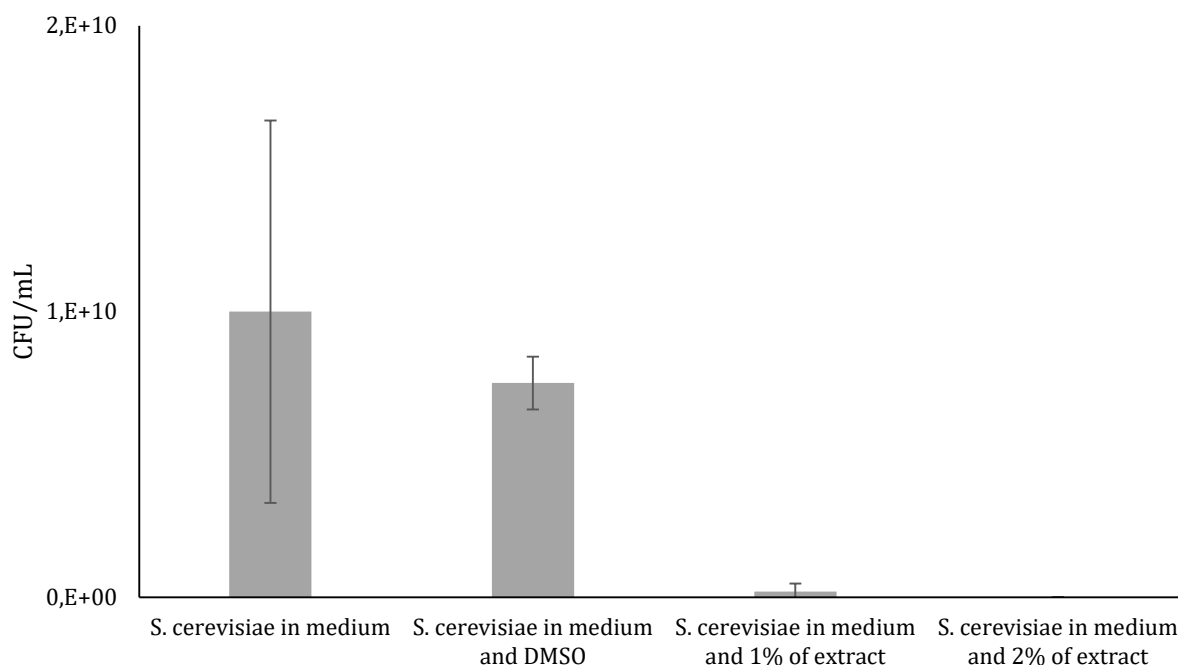


**Figure 51.** Evaluation by Petri's dishes of the *S.cerevisiae* growth in presence of freeze-dried extract dissolved into medium by means of dimethyl sulfoxide. CFU= colony forming units. Concentrations of extract are expressed as % (w/v).

### 5.3.3 Analysis of encapsulated extract into maltodextrins (MD) by spray-drying

The extract characterized in table 23, was encapsulated by spray drying process in maltodextrins in order to evaluate its potential use for packaging purposes. Indeed, one of the potential industrial applications for such extract could be the production of active packaging, in which a polymer suitable for food contact is functionalized with encapsulated solid extract to fabricate packaging with enhanced properties, allowing longer food shelf life, by protecting it from oxidation damages.

The process of microencapsulation gave back a product with the characteristics reported in table 24.



**Table 24.** Characterization of HPTE extract encapsulated into maltodextrins by spray drying.

Product recovery	$80 \pm 0.05\%$
Powder moisture	$0.114 \pm 0.002 \text{ g}_{\text{water}}/\text{g}_{\text{wet powder}}$
Encapsulation yield	$15.5 \text{ mg}_{\text{CAE}}/\text{g}_{\text{dried powder}}$
Encapsulation efficiency	$61.5 \pm 3.5\%$

The obtained product was then tested to determine its potential antimicrobial activity and its ability to inhibit lipid peroxidation.

#### 5.3.3.1 Antimicrobial activity

Agar plates inoculated with *E. coli* and *S. cerevisiae* were prepared and microorganisms were put in contact with three different concentrations of encapsulated extract: 5, 10, 15 % (w/v). For what concerned *E. coli*, even reducing the concentration of inoculated microorganisms, no inhibition of *E. coli* growth was observed.

Instead, tests carried out on *S. cerevisiae* (figure 52) showed a reduction of the average value of the CFU in samples in which 5 % and 15 % (w/v) of encapsulated extract was added, but the high error related to control samples, did not allowed to establish the significance of the results.

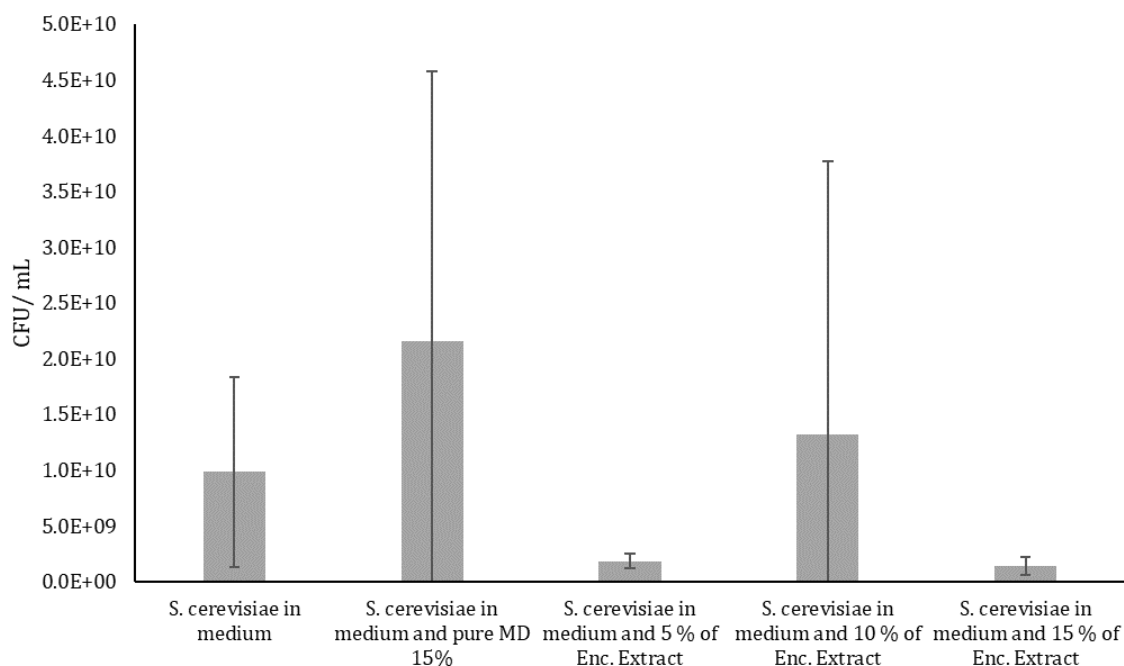


**Figure 52.** Evaluation by Petri's dishes of the *S.cerevisiae* growth in presence of extract encapsulated in maltodextrins by spray drying. CFU= colony forming units. Concentrations of extract are expressed as % (w/v).

### 5.3.3.2 Evaluation of the lipid peroxidation inhibition

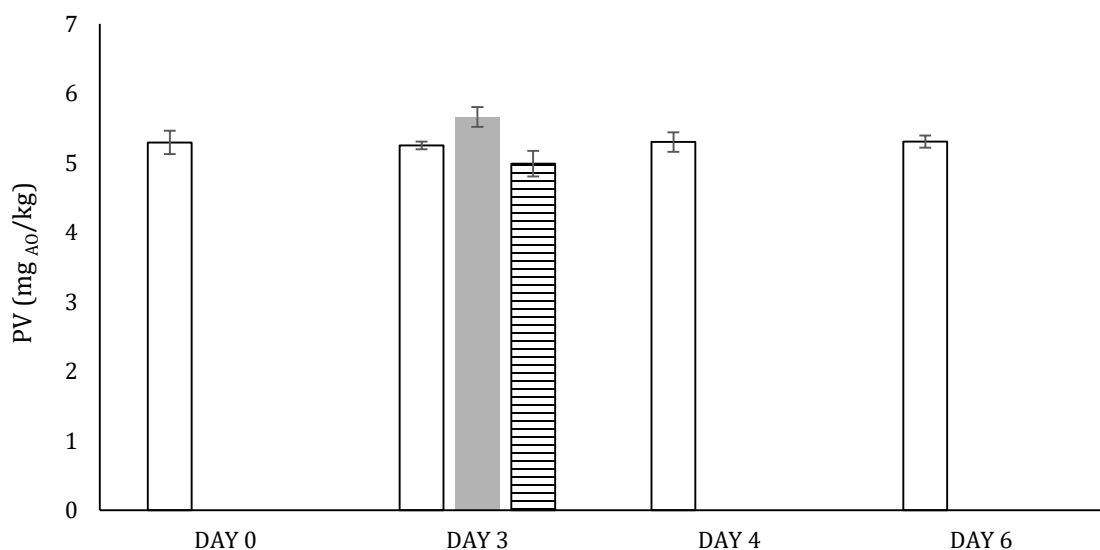
The ability of the encapsulated extract to inhibit lipid peroxidation was evaluated by measuring the peroxide value of extra virgin olive oil, subjected to lipid peroxidation under accelerated conditions. Two different concentrations of encapsulated extract were tested: 10 and 1% (w/v).

Figure 53 shows data related to control samples. Extra virgin olive oil (EVO) control sample, stored in the dark and oxygen-free, presented a constant peroxide value (PV) over time. After 3 days of incubation, PV was measured on the 3 control samples:

- EVO stored in the dark and oxygen-free;
- EVO+pure MD (10 %, w/v) stored in the dark and oxygen-free;
- EVO+ 10 % (w/v) encapsulated extract stored in the dark and oxygen-free.

Statistical analysis (T-test for Independent samples) demonstrated that there were no significant differences ( $p>0.05$ ) between the values of PV of the samples with only EVO and with encapsulated extract ( $p=0.0551$ ), while a PV slightly higher was shown by the sample in which pure MD were added ( $p=0.0036$ ). The first result imply that the

presence of encapsulated extract did not interfere with the titration method for PV determination, while the presence of only MD determine a little interference, but conservative, in the PV determination.



**Figure 53.** Comparison among the control samples Peroxide Value (PV), expressed as mg of active oxygen (AO) per kg of extra virgin olive oil (EVO). □ EVO stored in the dark and oxygen-free; ■ EVO+pure MD (10 %, w/v) stored in the dark and oxygen-free; ▨ EVO+ 10 % (w/v) encapsulated extract stored in the dark and oxygen-free.

In figure 54 are shown the PV of the sample exposed for 3 days to sunlight and saturated with pure oxygen. EVO without encapsulated extract exhibited a PV 10 times higher than EVO stored for 3 days in the dark and oxygen-free (control sample), while in the samples where encapsulated extract (10 %, w/v) was present, lipid peroxidation was prevented of 71 %.

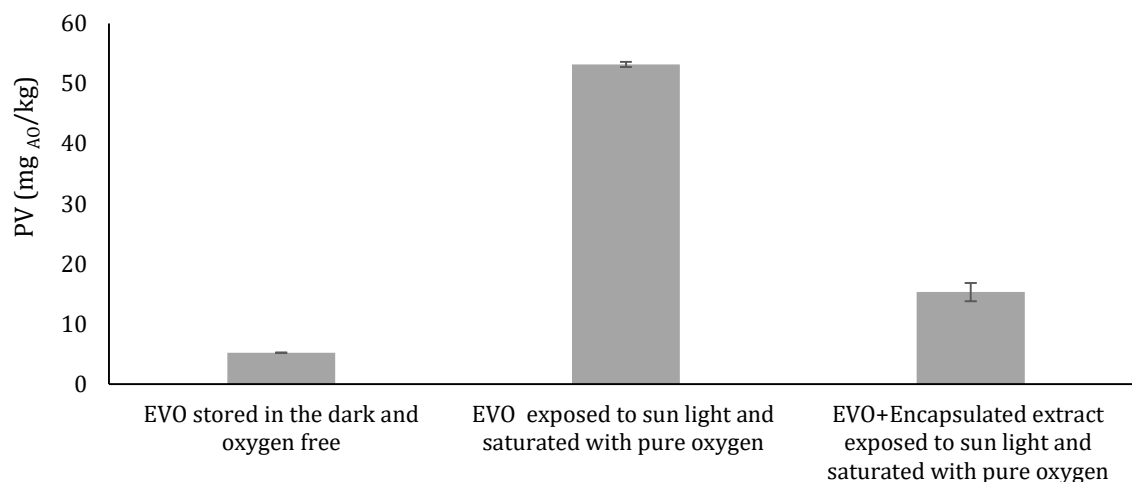


**Figure 54.** Peroxide values of the samples exposed for 3 days to sunlight and saturated with pure oxygen. Concentration of encapsulated extract = 10% (w/v).

For what concerned samples saturated with pure oxygen and stored in the dark, results are given in figure 55. After 4 days of incubation, oxygen in EVO increased its PV of 8 % compared to EVO stored in the dark and oxygen free. Conversely, in the samples where encapsulated extract (10% w/v) was present, lipid peroxidation was not observed.

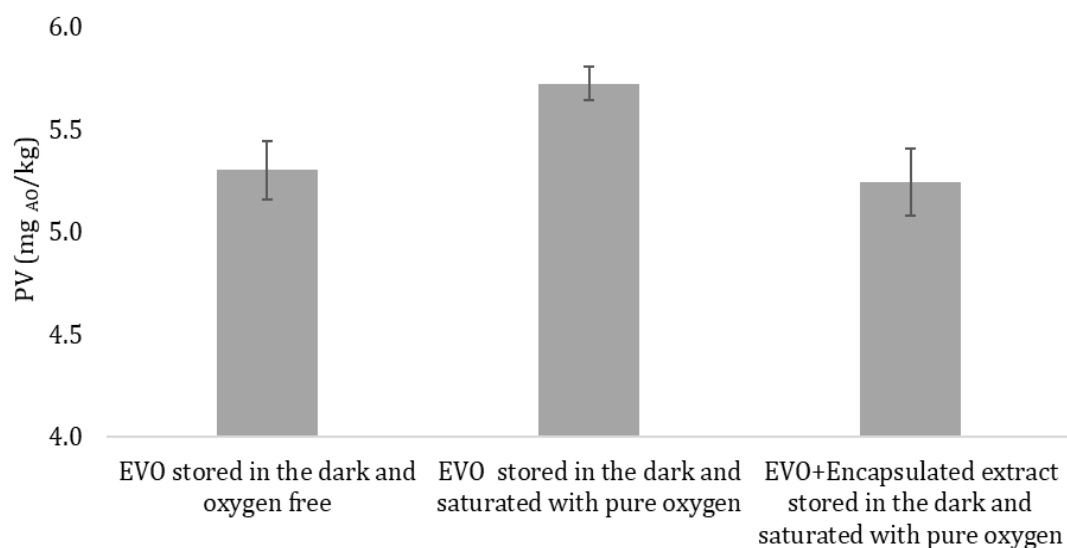


**Figure 55.** Peroxide values of the samples saturated with pure oxygen and incubated in the dark for 4 days. Concentration of encapsulated extract = 10% (w/v).

The last analyzed agent, able to accelerate lipid peroxidation, was temperature. As shown in figure 56, the effects of temperature (40 °C), were evaluated in terms of PV at 2 different times: after 4 and 6 days of incubation.

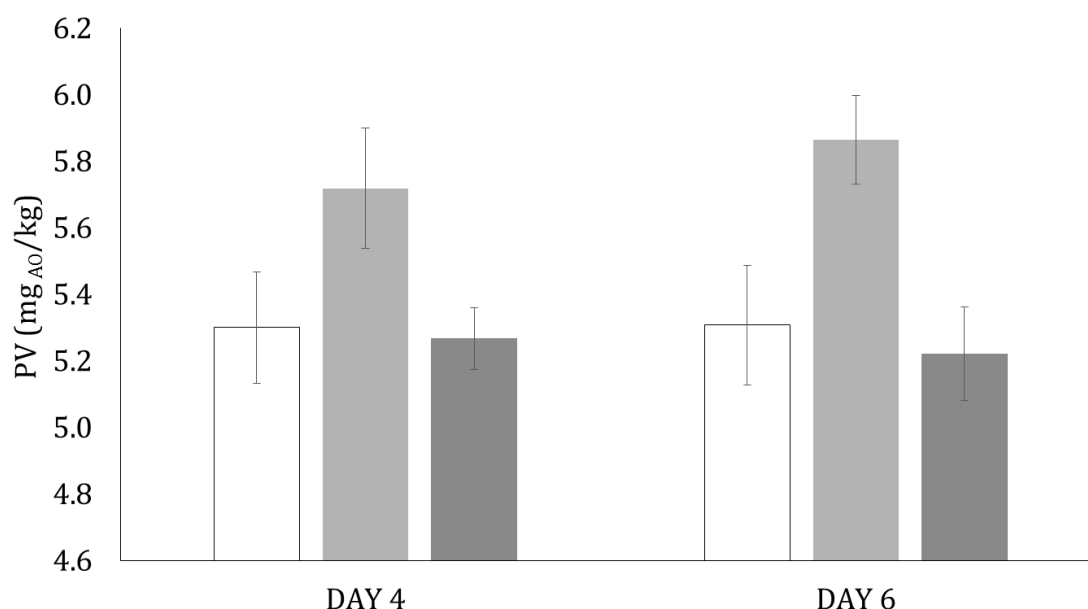


**Figure 56.** Peroxide values of the samples saturated with pure oxygen and incubated at 40 °C for 4 and 6 days. Concentration of encapsulated extract = 10% (w/v). □ EVO stored in the dark and oxygen-free; ■ EVO stored in the dark at 40 °C and saturated with pure oxygen; ■ EVO+encapsulated extract stored in the dark at 40 °C and saturated with pure oxygen.

Due to the effects of temperature and presence of oxygen, EVO reached a PV of 5.7 mg<sub>AO</sub>/kg after 4 days and of 5.9 mg<sub>AO</sub>/kg after 6 days, while the samples in which encapsulated extract was added, showed a PV equal to the one of the control sample stored in the dark and oxygen-free. Results of experimental tests highlighted that light is the factor that more influenced the increase of PV. Even if the other two tested parameters had less effect on the increase of PV, the encapsulated extract with a concentration of 10 % (w/v) prevented lipid peroxidation or significantly decreased the effect of lipid peroxidation accelerating factors.

Reducing the concentration of encapsulated extract to 1% (w/v), it was observed that when EVO was exposed to saturated oxygen and sunlight for 3 days (figure 57) its PV changed from 4.9±0.1 to 14.7±0.7 mg<sub>AO</sub>/kg, while the presence of encapsulated extract

in the sample subjected to the same conditions allowed to reduce the PV to  $10.1 \pm 0.5$   $\text{mg}_{\text{AO}}/\text{kg}$ .

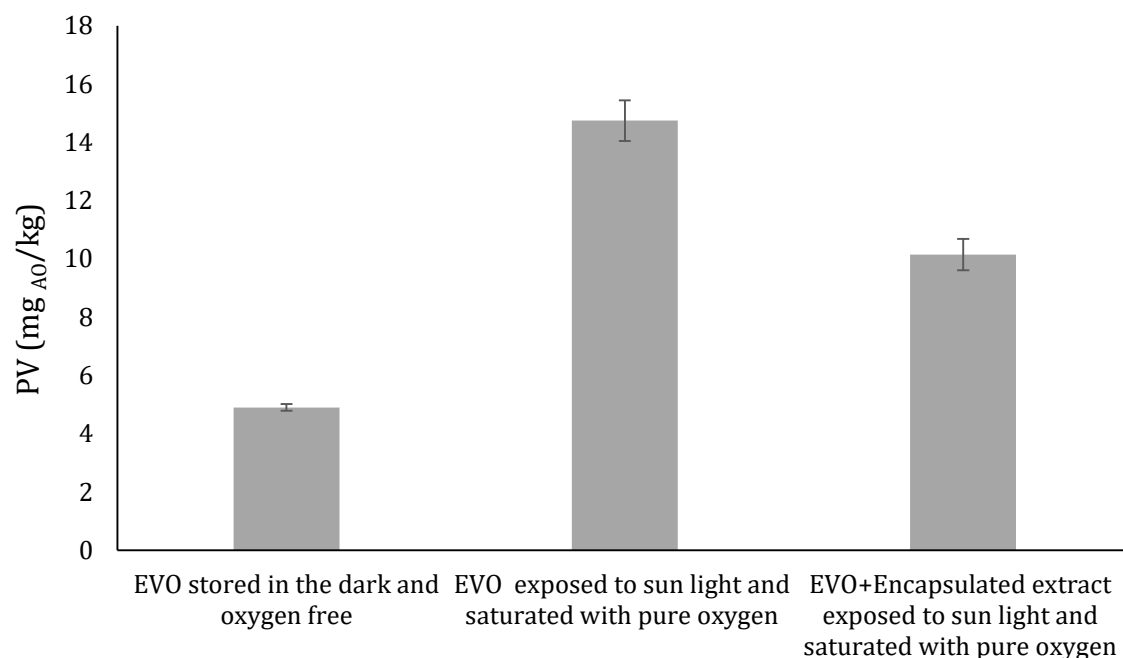


**Figure 57.** Peroxide values of the samples exposed for 3 days to sunlight and saturated with pure oxygen. Concentration of encapsulated extract = 1% (w/v).

For what concerns the tests in which pure oxygen and the combined effect of oxygen and light on the EVO were analyzed, results showed that no statistical difference ( $p > 0.05$ ) could be observed between PV of the samples of EVO stored in the dark and oxygen free and those stressed with the analyzed parameters (figures 58-59).

Nevertheless, results showed that with respect to the most effective parameter in increasing lipid peroxidation (exposure to sunlight), even a concentration of 1 % (w/v) of the encapsulated extract is able to have protective effects against lipid peroxidation. Naz et al. (2004) studied the oxidative stability of several types of oil under oxidative deterioration conditions and, analogously to what found in the present work, the presence of air-light resulted as more effective than air exposure in increasing the PV of the sample. Furthermore, the addition of antioxidants to the tested samples (caffeic,

vanillic and ferulic acids) provided a reduction of the PV in the stressed sample, and particularly caffeic acid, which is contained in the structure of chlorogenic acid, resulted to be the most active in preventing lipid oxidation.

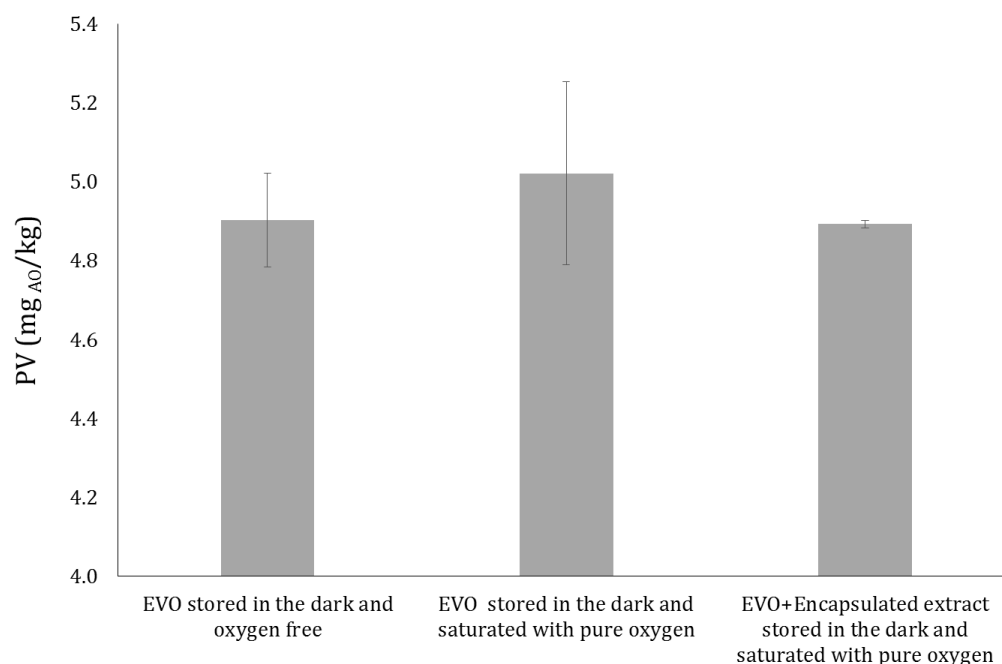


**Figure 58.** Peroxide values of the samples saturated with pure oxygen and incubated in the dark for 4 days. Concentration of encapsulated extract = 1% (w/v).

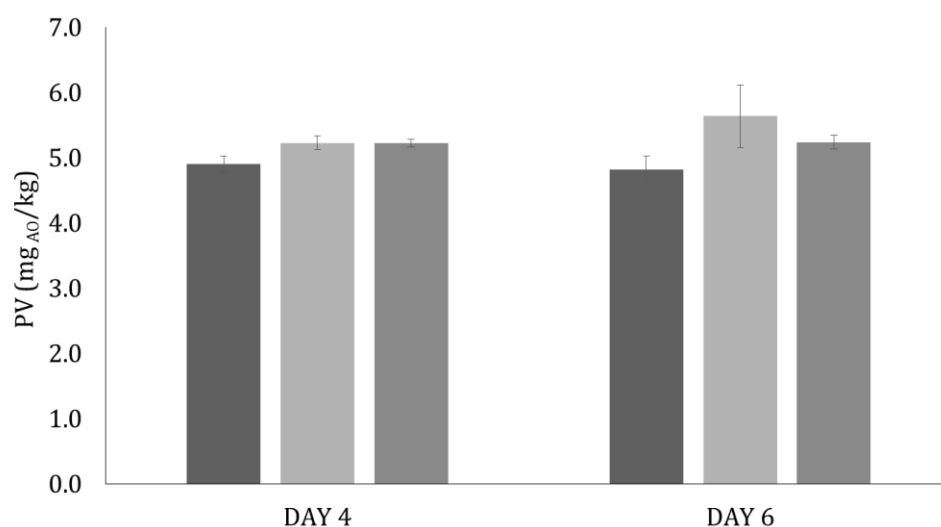


**Figure 59.** Peroxide values of the samples saturated with pure oxygen and incubated at 40 °C for 4 and 6 days. Concentration of encapsulated extract = 1% (w/v). □ EVO stored in the dark and oxygen-free; ■ EVO stored in the dark at 40 °C and saturated with pure oxygen; ■ EVO+encapsulated extract stored in the dark at 40 °C and saturated with pure oxygen.

### 5.3.4 Supercritical Antisolvent extraction for extract micronization

Freeze-dried extract obtained from HPTE, characterized in paragraph 5.3.2, was dissolved in ethanol in order to prepare the feed for supercritical antisolvent extraction, it was left under stirring for 1 night and filtered on a filter paper. Analyses on the feed solution were carried out in terms of total polyphenol content, total solids and antiradical power and results are reported in table 25. Part of the freeze-dried extract resulted as not soluble in pure ethanol, indeed the ethanolic solution presented a lower content of polyphenols, antiradical power and total solids than the initial extract obtained by HPTE (table 23).

**Table 25.** Characterization of SAE process feed. CAE=caffeic acid equivalent; TE=trolox equivalent.

total polyphenol content in the feed	$1.3 \pm 0.1 \text{ mg}_{\text{CAE}}/\text{mL}$
mass of fed total polyphenol	$388 \pm 30 \text{ mg}_{\text{CAE}}$
total solids in ethanol	$5.5 \pm 0.04 \text{ mg}/\text{mL}$
mass of total solids in ethanol	$1.65 \pm 0.012 \text{ mg}$
antiradical power in the feed	$28 \pm 1.0 \mu\text{g}_{\text{TE}}/\text{L}_{\text{EXTRACT}}$

By means of SAE process, 100 mL of inlet solution were separated in two outlets: the micronized solid ( $248 \text{ mg} \pm 2 \text{ mg}$ ) and a liquid fraction containing the solvent ( $89 \pm 3 \text{ mL}$ ). Thus, about the 11 % of the fed solvent is lost in the carbon dioxide line during the process. Characterization of the products is reported in table 26. Product recovery, expressed as recovered mass per fed mass, was of 45 %, whereas the total polyphenol recovery in the powder was of 47%. Regarding the antiradical power, the 37.5 % of the ARP exhibited by the feed was showed by the powder. The liquid phase contains not only the ethanol, but also about 3 mg of lipid-like matter, which exhibited negligible amount of total polyphenol content. Compared to the extract stabilized by freeze-drying (paragraph 5.3.2) the powder obtained by SAE presented higher concentration of total polyphenols and chlorogenic acid, as well as higher antiradical power. In addition no caffeine was detected. Thus, by SAE was produced a solid extract enriched in polyphenols, more pure and concentrated, defatted, and caffeine-free, which can find potential application in food and cosmetic industries. Indeed, caffeine was less soluble



in ethanol so, probably its content in the feed of SAE process was already lower than into freeze-dried extract. In addition supercritical carbon dioxide acted as solvent for caffeine and lipid fraction present in the feed, and the last one was collected together with ethanol in the liquid phase. Thus, this post-processing could be seen as an alternative to the process for lipid recovery from SCG (Al-Hamamre et al., 2012), since by HPTE followed by SAE process, two different fractions could be obtained: an antioxidant-rich solid powder and a lipid solution in ethanol.

**Table 26.** Micronized power characterization and liquid fraction characterization. CAE=caffeic acid equivalent; TE=trolox equivalent.

Micronized powder	
total polyphenol content	$243 \pm 3.9 \text{ mg}_{\text{CAE}} / \text{g}_{\text{dried powder}}$
antiradical power	$5.43 \pm 0.05 \text{ } \mu\text{g}_{\text{TE}} / \text{g}_{\text{dried powder}}$
caffeine content via HPLC	not detected
chlorogenic acid content	$48.6 \pm 1.3 \text{ mg} / \text{g}_{\text{dried powder}}$
Liquid fraction	
total polyphenol content	$0.198 \pm 0.03 \text{ mg}_{\text{CAE}} / \text{mL}$
antiradical power	$2.28 \pm 0.5 \text{ } \mu\text{g}_{\text{TE}} / \text{L}$
total solids	$0.034 \pm 0.02 \text{ mg} / \text{mL}$

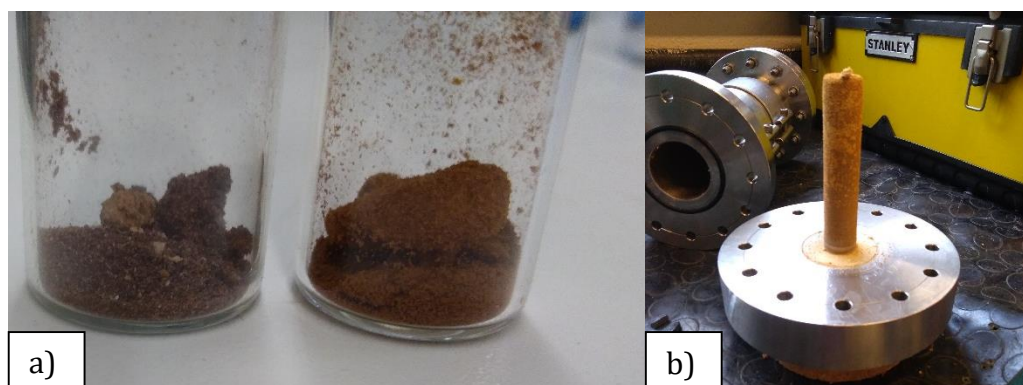


**Figure 60.** a) Micronized powder collected at the end of SAE process and b) filter of the SAE plant.

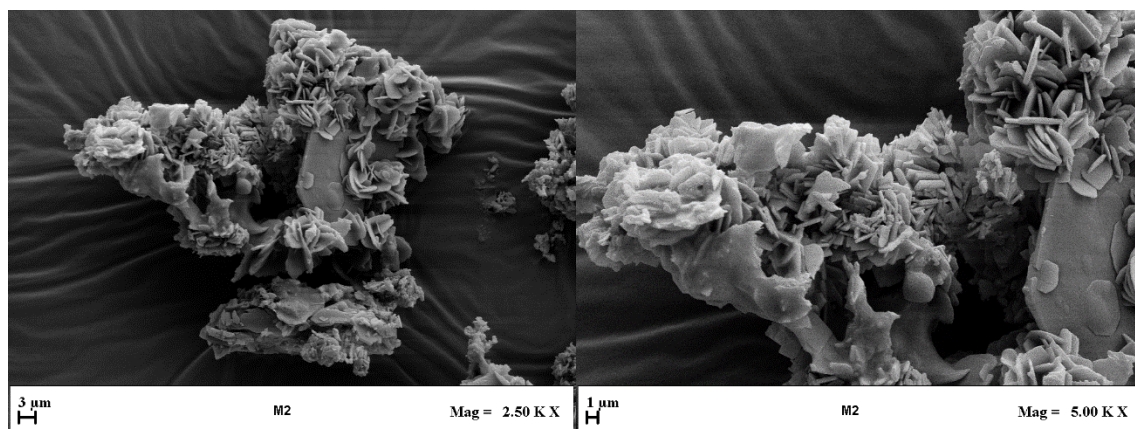


**Figure 61.** FE-SEM images of the micronized powder obtained by SAE process.

### 5.3.5 Encapsulation of HTPe extract in liposomes by supercritical fluid-assisted liposome formation plant

The last encapsulation method used to preserve and increase the bioavailability of the extract obtained by HPTe (150 °C, 7.2 bar, liquid to solid ratio equal to 300 mL/30 g, 60 min of extraction time and using ethanol 54% (v/v) as solvent) was supercritical fluid-assisted liposome formation (Superlip process).

A first explorative experiment was carried out in order to produce empty liposomes, to assess the feasibility of chosen operating conditions. In addition, these samples will be used also as blank samples for further tests. Thus, soybean phosphatidylcholine (500 mg) was dissolved in 100 mL of ethanol and fed to Superlip plant, which worked at 100 bar (blank sample FC0.1) and 200 bar (blank sample FC0.2). SEM image of FC0.1, together to the particle size distribution, were reported in figure 62, which shows that the liposomes obtained under the chosen conditions presented sub-micrometrical dimensions, spherical and regular morphology.

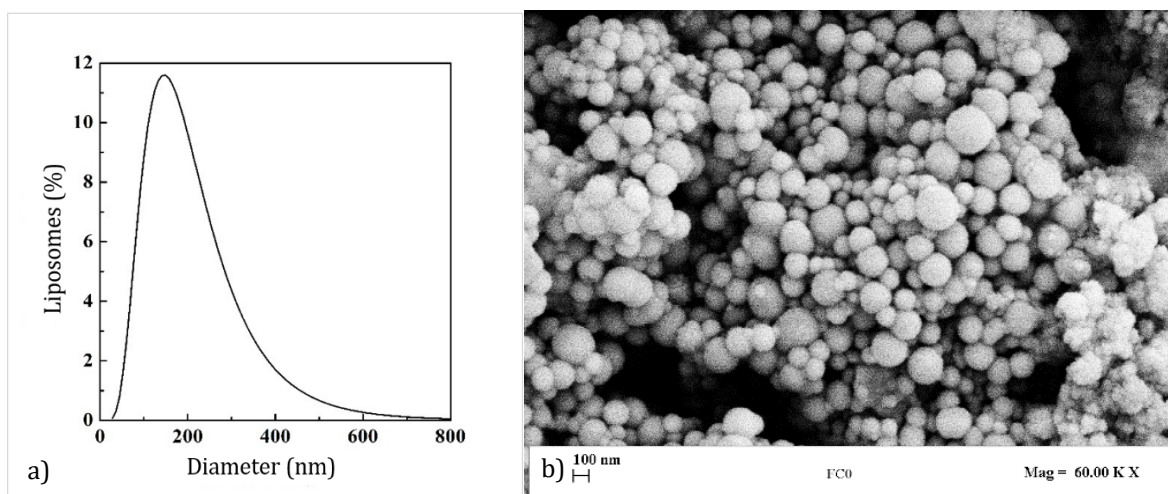


**Figure 62.** a) Particle size distribution of blank sample (FC0.1) of liposomes, reported as liposome fraction (% by number) as a function of diameters; b) FE-SEM image of liposomes of blank sample (FC0.1) of liposomes.

Results obtained from the DLS analyses performed on the samples obtained from Superlip process (table 27), confirmed that also the liposomes loaded with the extract obtained from SCG had a mean diameter below 500 nm, but no statistical differences depending on feed concentration of the extract or operating pressure were found on their average dimension. High standard deviations related to particle mean diameter and the polydispersity index indicated that the obtained liposomes did not have very narrow size distributions, as was reported in figure 63 by the particle size distributions of the samples and confirmed by SEM analyses of the same samples (figure 64). The same figure showed that liposome formation occurred in all the examined conditions. The set of test, carried out with a pressure of the formation vessel of 100 bar, produced liposomes with mean diameters that ranged between  $132 \pm 31$  and  $219 \pm 125$  nm, with particle size distributions (figure 63.a) which were essentially overlapped. Indeed, modal value of the curves showed just a small shift towards higher value when extract concentration in the feed was increased, as well as mean values. Same trend was followed by the polydispersity index. Figure 63.b resumes the particle size distributions of samples produced by using a vessel pressure of 200 bar. Differently from tests performed at 100 bar, the curves seemed less overlapped and more pronounced was the shift of the modal value toward higher values as extract concentration was increased. Polydispersity index of the curves exhibited again an increase when extract

concentration was increased, but the differences among the values were less pronounced than those found for the tests performed at 100 bar. Paini et al. (2015b) produced apigenin loaded liposomes, using rapeseed lecithin and an innovative techniques which employ sonication for liposome fabrication. Obtained liposomes presented reduced average size through sonication treatment, and final mean diameters were close to those find in the present work, but with lower polydispersity index. Very similar mean diameters and polydispersity index were exhibited by liposomes produced by SuperLip process, in which olive pomace extract was encapsulated; analogously to what found for extract obtained from SCG, mean diameter of the vesicles increased with the increase of the load of olive pomace extract (Trucillo et al., 2018).

These results are not in agreement to what found by Rafiee et al. (2017), who studied the encapsulation of phenolic compounds of pistachio green hull extract in liposomes, obtained by extrusion. They found that the entrapment of phenolic compounds probably interacts with phospholipids, having as a consequence the reduction of liposome size and an increasing of the zeta potential.

**Table 27.** Results of the Dynamic Light Scattering analysis on the samples of liposomes from the SuperLip process. PDI=polydispersity index.

Sample	Pressure in the formation vessel (bar)	Extract concentration (ppm)	Particle mean diameter (nm)	PDI	Zeta potential (mV)
FC0.1	100 bar	0	132 ± 31	0.236	-10.2
FC1		500	219 ±125	0.57	-5.42
FC2		250	205 ±102	0.5	-9.99
FC3		83	171 ±81	0.47	-12.7
FC0.2	200 bar	0	206 ± 76	0.367	-18.7
FC4		500	309 ±160	0.52	-10.4
FC5		250	239 ±117	0.49	-5.9
FC6		83	159 ±75	0.47	-12.5

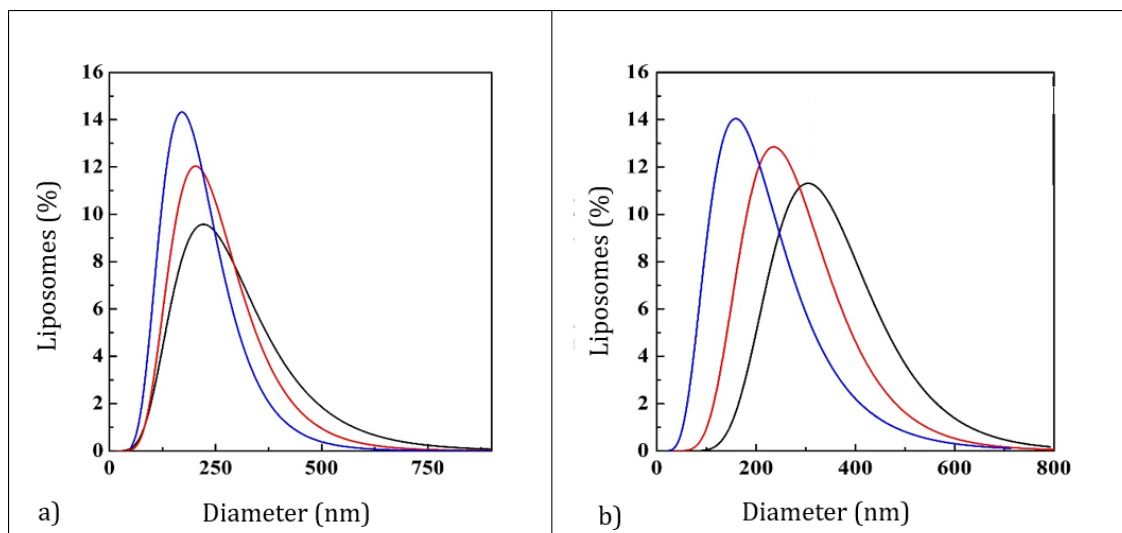


**Figure 63.** Particle size distributions of liposomes from SuperLip process, loaded with extract obtained by HPTE from SCG. a) Results of samples obtained at 100 bar and concentration of fed extract of — 83 ppm, — 250 ppm, and — 500 ppm; b) results of samples obtained at 200 bar and concentration of fed extract of — 83 ppm, — 250 ppm, and — 500 ppm.

According to table 27, all samples exhibited a negative charge, which ranged from -5.42 to -12.7 mV. Zeta potential is a good indicator of the stability of a suspension. Particularly, values of zeta potential beyond the range of -60 mV to +60 mV indicate excellent stability and good stability beyond the range of -30 mV to +30 mV, since it causes large repulsive forces, preventing aggregation; absolute values that range from 5 to 20 mV provide only short term stability, while below 5 mV fast aggregation occurs (Honary and Zahir, 2013). The values reported in table 27 are all in the range that imply short term stability, even if the indicative aforementioned intervals are strictly valid only for low molecular weight surfactants and pure electric stabilization (Honary and Zahir, 2013). Nevertheless, Trucillo et al. (2018) in a study on the encapsulation of a polyphenol-rich aqueous extract from olive pomace, reported that liposomes obtained with the same procedure described in the present work, and with zeta potential between -14.1 and -15.2 mV, resulted as stable over a period of more than 4 months.



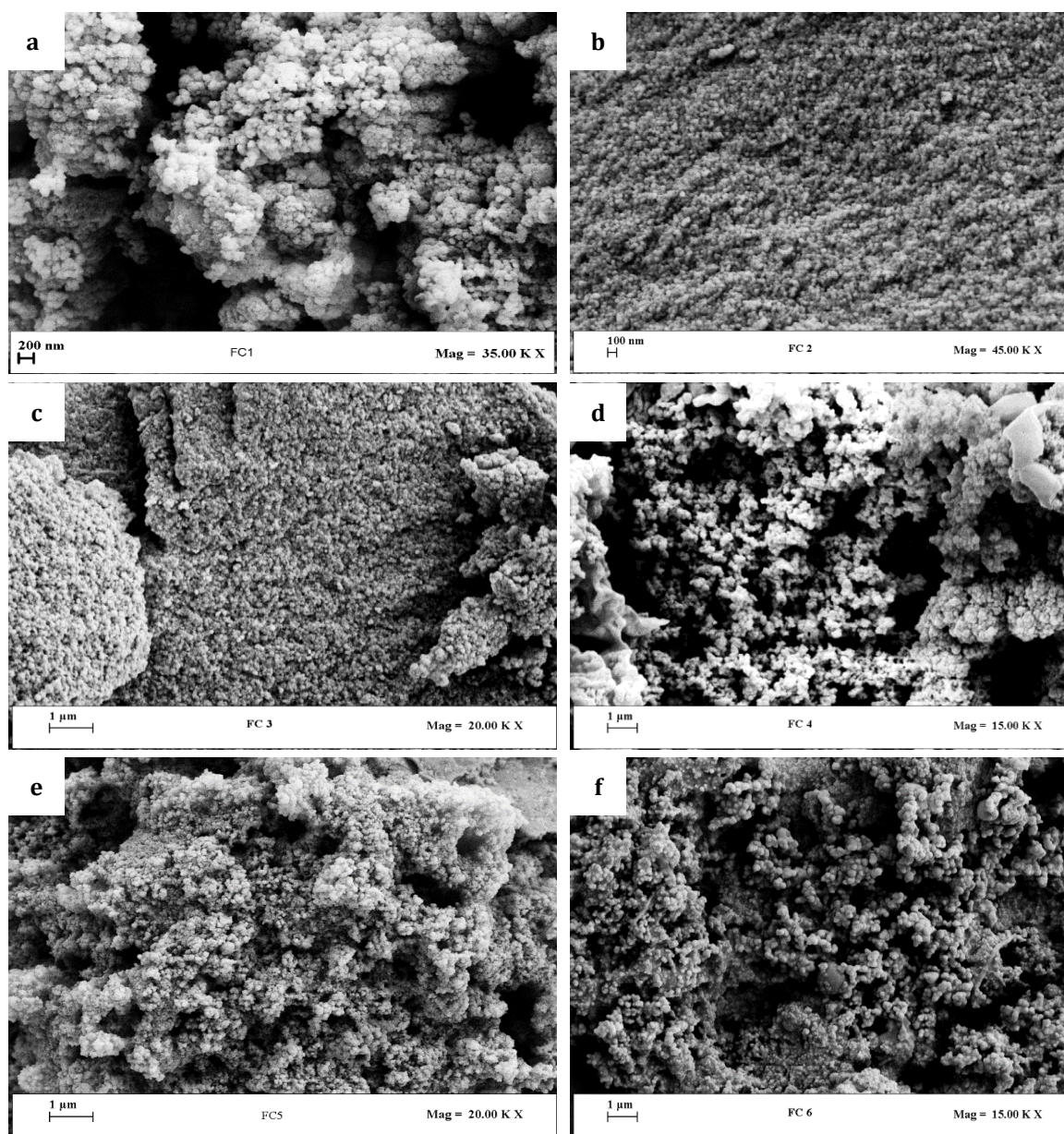


**Figure 64.**FE-SEM images of liposomes from SuperLip process, loaded with extract obtained by HPTE from SCG. a) Sample FC1 (P=100 bar, extract concentration=500 ppm); b) sample FC2 (P=100 bar, extract concentration=250 ppm); c) sample FC3(P=100 bar, extract concentration=83 ppm); d) sample FC4 (P=200 bar, extract concentration=500 ppm); e) sample FC5 (P=200 bar, extract concentration=250 ppm); f) sample FC6 (P=100 bar, extract concentration= 83 ppm).

A potential explanation of this behavior could be traced back to the pH of the final suspension of liposomes. Indeed, dissolved carbon dioxide reduce the pH of the suspension, parameter which could have significant effects on the surface charge of vesicles. Indeed, Zhou and Raphael (2007) found that unilamellar vesicles fabricated

using 1-stearoyl-2-oleoyl-phosphatidyl-choline had positive zeta potential at pH 2, while the higher was the pH, the more negative was the zeta potential recorded. Figure 65 reports the encapsulation efficiencies of the loaded liposomes, as a function of the pressure in the formation vessel and the feed extract concentration.

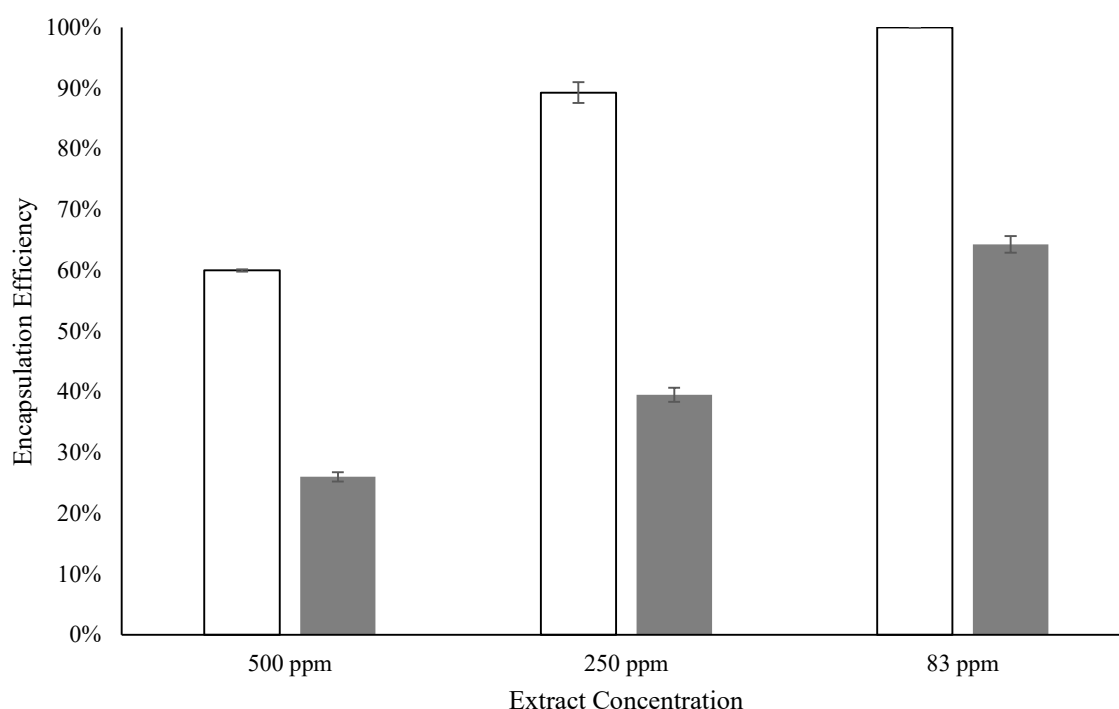


**Figure 65.** Encapsulation efficiencies of liposomes loaded with different concentrations of extract from SCG. □ Liposomes produced at 100 bar; ■ liposomes produced at 200 bar.

The encapsulation efficiencies obtained with the tested operating conditions ranged from 26 to 99 %, exhibiting strong dependence from the examined process variables. For each extract concentration, liposomes fabricated at 100 bar presented higher encapsulation efficiencies than at 200 bar. For what concerned the dependence on feed characteristics, the lower was extract concentration the higher was the encapsulation efficiency, for both the tested pressures. This trend disagrees with other results reported in literature, where the increase of phenolic concentration in the feed provided higher encapsulation efficiencies (Rafiee et al., 2017; Trucillo et al., 2018). SuperLip process operated at 100 bar, demonstrated to be an efficient method for the entrapment of polyphenols, providing encapsulation efficiencies higher than reported

by other techniques for loaded liposome production (Michelon et al., 2017; Rafiee et al., 2017; Sebaaly et al., 2015).

Evaluation of the antiradical power of the samples was performed by ABTS assay and the obtained data are given in figure 66. ARP of the loaded liposomes ranged from 1.9 to 4.9  $\mu\text{g TE/g liposomes}$ . The antiradical power of the liposomes followed the same trend of encapsulation efficiency as a function of extract concentration, while no dependence on the pressure of the formation vessel was found.

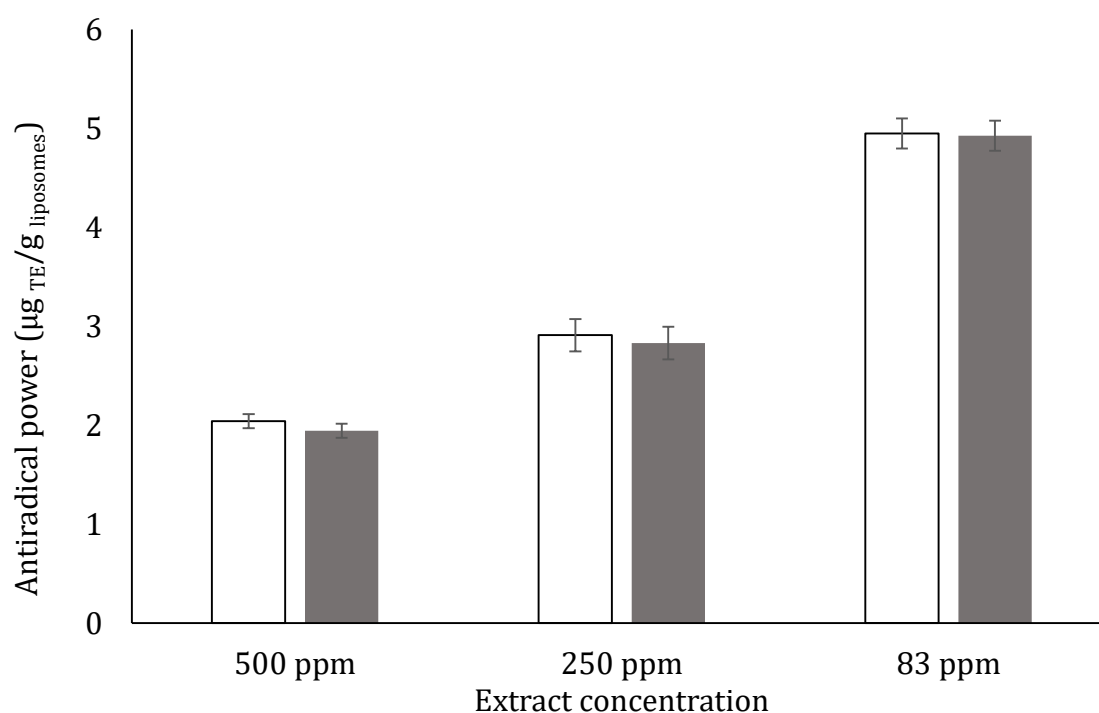


**Figure 66.** Antiradical power evaluated by ABTS assay of liposomes loaded with different concentrations of extract from SCG. □ Liposomes produced at 100 bar; ■ liposomes produced at 200 bar.

## 5.4 CONCLUSIONS

In this section, HPTE was employed to obtain antioxidant-rich extract from SCG. Process optimization allowed to obtain an extract with high total polyphenol yield (about 173  $\text{mg CAE/g extracted solids}$ ) in 60 min, using ethanol 54 % (v/v) as solvent at 150 °C, and high antiradical power (2.38  $\mu\text{g TE/g solid extract}$ ), containing a caffeine content of about 43  $\text{mg/g extracted solids}$  and chlorogenic acid content of about 23  $\text{mg/g extracted solids}$ . In



order to prevent loss of activity of the bioactive compounds and to evaluate the possibility of using the solid extract for the potential production of enhanced packaging with antioxidant properties, freeze-drying process and encapsulation by spray drying were employed. Indeed, the bioactivity of the molecules in spent coffee grounds could enhance food packaging properties, allowing longer food shelf life by protecting it from contamination and oxidation damages. So, antimicrobial activity of freeze-dried extract was tested on *S. cerevisiae* and *E. coli*, showing that at concentrations of 1 and 2 % (w/w) both of the microorganisms growths were inhibited, even if further studies must be carried out to lead to conclusive results. Less significant were the results obtained with the encapsulated extract, which did not show antimicrobial activity on *E. coli*, and only suggested some potential inhibition ability on *S. cerevisiae* growth. Even in this case, the strong biological variability led to results which need to be confirmed by further experiments. Conversely, the encapsulated extract demonstrated to act as inhibitor of lipid peroxidation, confirming its strong antioxidant activity and proved to be an excellent candidate for being incorporated in polymers for food active packaging purposes.

Finally, the extract obtained by HPTE was also subjected to two supercritical fluid-assisted processes: supercritical antisolvent extraction and supercritical fluid-assisted liposome formation. By the former, a solid powder richer in polyphenols ( $243 \pm 3.9$  mgCAE/g dried powder) than freeze-dried extract ( $135.5 \pm 3.8$  mgCAE/g freeze-dried extract) and caffeine-free was produced, together with a liquid phase made by an ethanolic solution of lipids which were co-extracted during HPTE. So, SAE could represent a good green method able to provide an extract more concentrated in polyphenols, suitable for the production of a raw material for applications in which pure polyphenols and no caffeine are needed.

By supercritical fluid-assisted liposome formation, liposomes loaded with SCG extract were produced. The study on pressure of the formation vessel and extract concentration in the feed as process variables, showed that at 100 bar higher encapsulation yields could be obtained than at 200 bar, as well as particle size distributions with modal values more shifted towards smaller diameters. So, 100 bar and 250 ppm as extract concentration, seemed to be a good compromise to obtain high

encapsulation efficiency (89 %), small liposome size (205 nm) and good antiradical power ( $2.9 \mu\text{g TE/g liposomes}$ ). Supercritical fluid-assisted liposome formation allowed to produce an encapsulated extract which represents an alternative for lipophilic media to the extract encapsulated in maltodextrins, since the coating agent of the last one is able to increase the product solubility in hydrophilic systems.

*This work was partially presented as "Extraction of antioxidants from spent coffee grounds using microwave-assisted and high pressure and temperature extractions" by Margherita Pettinato, Bahar Aliakbarian, Alessandro Alberto Casazza, Pier Francesco Ferrari, Patrizia Perego, in the International congress "Green Extraction of natural products- GENP2016", Torino, Italy, 31/05/2016-01/06/2016 and will be partially presented as "Liposome encapsulation of antioxidants from spent coffee grounds extracts" by R. Campardelli, P.Perego, M.Pettinato, E. Reverchon, P. Trucillo, in the International congress 17<sup>th</sup> European meeting on Supercritical fluids (EMSF2019), Castilla-La Mancha, Spain, 08-11/04/2019.*

## *Chapter 6*

# **CONTINUOUS PRESSURIZED ULTRASOUND-ASSISTED EXTRACTION**

### **6.1 ABSTRACT**

Continuous pressurized ultrasound-assisted extraction is a novel technique that is proposed in this chapter for the extraction of antioxidants from spent coffee grounds. Since, the effects of high temperature on extraction yields were already investigated for the two non-conventional techniques (MAE and HPTE), in this study the attention was focused on high pressure effects at relatively low temperatures and the use of ultrasounds for the recovery of polyphenols. Box-Behnken design for response surface modeling was employed for the investigation of the design space, evaluating total polyphenol yield, antiradical power and extract total solids as response variables. Results showed that pressure and on/off pulsed ratio were able to provide effects on the extraction yields, while the use of temperatures below the boiling point of the solvent (ethanol 54% (v/v)) had negligible effect on the process, even when ultrasounds are used to improve the process.

### **6.2 MATERIAL AND METHODS**

#### **6.2.1 Continuous pressurized ultrasound-assisted extraction system**

Experiments on antioxidant extraction from dried SCG were carried out by using continuous pressurized ultrasound-assisted extraction (CPUAE). As depicted in figure 67, the lab-scale plant employed for the experiments was made by a fixed bed column, packed with SCG, in which ethanol 54 % (v/v) was continuously pumped by an isocratic pump (G1310A, Agilent 1100 Series, Palo Alto, CA)), allowing the antioxidant extraction from the solid matrix.

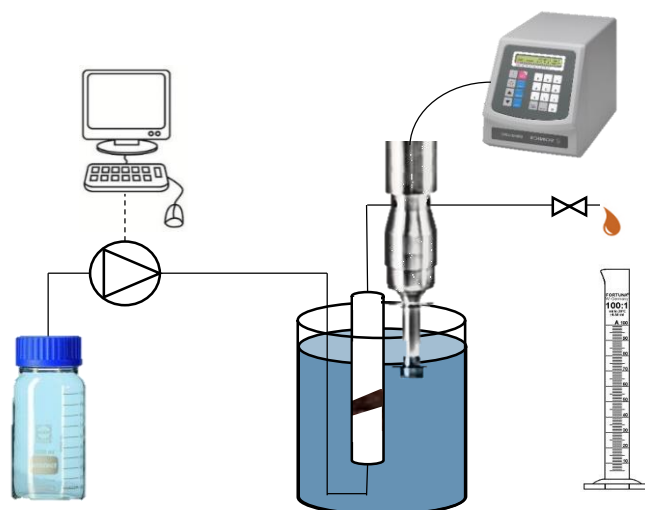


**Figure 67.** Scheme of the continuous pressurized ultrasound-assisted extraction plant.

Temperature in the stainless steel column was controlled by a thermostatic bath, in which the extraction column was submerged. In addition, a 20 kHz ultrasonic generator probe (Sonicator Vibra cell 75115, 500 Watt, Bioblock Scientific Co.) was immersed in the thermostatic bath, in order to make the SCG subjected to ultrasounds. Pressure into the column was measured by 2 manometers disposed before and after the column and controlled by the pump and by a valve at the column outlet. Furthermore, a metal filter disposed in the outlet section of the extraction column ( $0.45\ \mu\text{m}$ ) allowed the contemporary filtration of the extract, which was collected in a glass cylinder at the end of the process.

### 6.2.2 Continuous pressurized ultrasound-assisted extractions and experimental design

Extraction experiments were performed on about 1.0 g of dried SCG, using a liquid to solid ratio of 10 mL/g. The flow rate of the solvent was maintained around an average value of  $1.0 \pm 0.2$  mL/min, and the ultrasound amplitude was held constant during the experiments at a value of 40 %.

**Table 28.** Independent variables and their levels employed in the Box Behnken Design for the optimization of extraction from SCG.

Independent variables		Coded levels		
		-1	0	+1
Extraction temperature	°C	25	58	90
Pressure	bar	50	100	150
on/off pulsed ratio	min <sub>on</sub> /min <sub>off</sub>	0.5	1.25	2

The screening on the independent variables, extraction temperature, pressure and on/off pulsed ratio, was carried out by the Box-Behnken Design (BBD) (figure 15) for response surface methodology (RSM), using Design Expert software (Stat-Ease, Inc., Minneapolis, United States). The three input variables were coded into the 3 levels (-1, 0, +1 ) and the corresponding values are reported in table 28.

Total polyphenol content, antiradical power and extract total solids were chosen as response variables. The fitting equation of the generic response variable  $Y$  is reported in the equation 13 (see paragraph 3.2.3).

Significance of the chosen input variables was assessed by analysis of variance (ANOVA) that was generated by Design Expert and the fitting equation adequacy was determined by means of the coefficient of determination ( $R^2$ ).

### 6.2.3 Analytical methods

Total polyphenol content of the extracts was determined by Folin-Ciocalteu's assay (see paragraph 3.2.1.3). Radical scavenging activity was measured by means of ABTS<sup>•+</sup> assay, according to the procedure described in the paragraph 3.2.1.6, while the protocol employed for extract total solid (ETS) determination was reported in the paragraph 3.2.1.7.

## 6.3 RESULTS AND DISCUSSION

### 6.3.1 Total polyphenol yield

Experimental design provided a set of 17 tests and the central point of the design space was repeated 5 times. Table 29 reports the values in terms of total polyphenols content of the obtained extracts. Total polyphenol yields ranged from 6.2 to 18 mg<sub>CAE</sub>/g dried SCG, values that are comparable those of solid-liquid extraction of antioxidant from spent coffee grounds, instead resulted as significantly lower than those found by using MAE and HPTE. Analysis of variance on the quadratic polynomial fitting equation (table 30), demonstrated that, among the independent variables taken into consideration in this study, pressure is the only one that resulted as significant ( $p < 0.0090$ ), while no significant effects on total polyphenol yield were exhibited by temperature and on/off pulsed ratio ( $p > 0.05$ ). Particularly, the coefficient estimate in the linear function of total polyphenols yield over pressure (table 30) presented a negative value, indicating that an increasing in total polyphenol content in the extract could be found by decreasing the operative pressure. Negligible effects of pressure on the extraction of polyphenols, as already discussed in the previous chapters, were observed by several authors (Mustafa and Turner, 2011; Shang et al., 2017; Aliakbarian et al., 2012; Choi et al. 2003), but in this case, the presence of the packed-bed column implied that the higher was the pressure, the higher was the compression of the bed, which likely led to the generation of preferential pathways for the solvent, and lower extraction yields as consequence. Regression equation provided by the software produced the three-dimensional surface plot reported in figure 68, but, although the model significance ( $p = 0.0090$ ) and the not significant lack of fit ( $p = 0.5680$ ), the low  $R^2$  (0.375) did not make the equation suitable for a correct representation of the system in the selected design space.

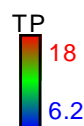
**Table 29.** Total polyphenols content of the extracts obtained by continuous pressurized ultrasound-assisted extraction. CAE=caffeic acid equivalent.

T (°C)	P (bar)	On/off pulsed ratio (min <sub>on</sub> /min <sub>off</sub> )	TP (mg <sub>CAE</sub> /g dried SCG)
25	50	1.25	14.9±1.3
90	50	1.25	18± 0.9
25	150	1.25	8.4±0.5
90	150	1.25	7.8± 0.6
25	100	0.5	9.0±0.2
90	100	0.5	11± 0.3
25	100	2	10±0.5
90	100	2	8.6±0.2
57.5	50	0.5	9.7±0.8
57.5	150	0.5	6.2± 0.2
57.5	50	2	12.6±0.3
57.5	150	2	11.9±1.0
57.5	100	1.25	6.3±0.6
57.5	100	1.25	13.3±0.5
57.5	100	1.25	10.3±0.4
57.5	100	1.25	9.5 ± 0.4
57.5	100	1.25	10.2 ± 0.4

**Table 30.** Analysis of variance table (Partial sum of squares - Type III) for Response Surface Reduced Quadratic Model of the output variable total polyphenol yield (TP).

Source	Sum of Squares	df	Mean Square	Value	p-value Prob > F	Coefficient Estimate	df	Standard Error	95% CI Low	95% CI High
Model	54.6	1	54.6	8.99	0.0090					
B-Pressure	54.6	1	54.6	8.99	0.0090	-2.6	1	0.87	-4.47	-0.75
Residual	91.1	15	6.08							
Lack of Fit	66.2	11	6.02	0.97	0.5680					
Pure Error	24.9	4	6.23							
Cor Total	145.7	16								
Intercept						10.5	1	0.60	9.18	11.73

Design-Expert® Software



X1 = B: Pressure  
X2 = C: Pulse

Actual Factor  
A: Temperature = 57.50

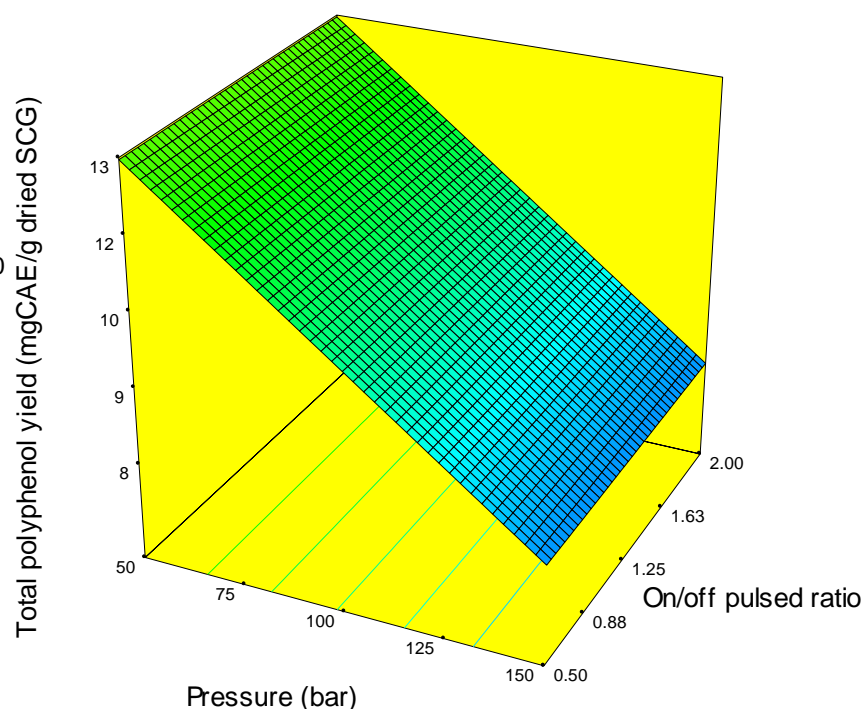


**Figure 68.** Three-dimensional surface plot of the regression equations for total polyphenol yields obtained by the experimental design coupled with RSM.

### 6.3.2 Antiradical power

Table 31 reports results concerning the antiradical power of the extracts. Obtained extracts demonstrated to exhibit lower antiradical power than extracts produced by HPTE, and even MAE carried out for few minutes showed to provide extracts with higher scavenging activity. Of course, it was an expected result, due to the lower total polyphenol content found in extracts of CPUAE.

Statistical analysis on the results from experimental design (table 32) revealed that, in agreement to what was noticed for total polyphenol content of extracts, the fitting equation for the response variables under examination was reduced to a linear one, in which the only significant term was pressure. The negative value of the coefficient estimate for pressure, indicated that total polyphenol yield and ARP followed a concordant trend. The regression equation for ARP as a function of the input variables,



represented as three-dimensional surface plot in figure 69, resulted as significant ( $p=0.0109$ ), with not significant lack of fit ( $p=0.5595$ ), but exhibited very low  $R^2$  (0.360).


**Table 31.** Antiradical power (ARP) of the extracts obtained by continuous pressurized ultrasound-assisted extraction, evaluated by ABTS<sup>•+</sup> assay . TE=trolox equivalent.

T (°C)	P (bar)	On/off pulsed ratio (min <sub>on</sub> /min <sub>off</sub> )	ARP( $\mu\text{g}_{\text{TE}}/\text{L}$ )
25	50	1.25	35 $\pm$ 1.7
90	50	1.25	33 $\pm$ 0.9
25	150	1.25	24 $\pm$ 1.6
90	150	1.25	19 $\pm$ 0.9
25	100	0.5	22 $\pm$ 0.2
90	100	0.5	23 $\pm$ 1.3
25	100	2	28 $\pm$ 2.7
90	100	2	20 $\pm$ 2.5
57.5	50	0.5	25 $\pm$ 0.5
57.5	150	0.5	14 $\pm$ 0.3
57.5	50	2	26 $\pm$ 0.9
57.5	150	2	25 $\pm$ 0.6
57.5	100	1.25	17 $\pm$ 0.9
57.5	100	1.25	28 $\pm$ 3.4
57.5	100	1.25	25 $\pm$ 0.2
57.5	100	1.25	19 $\pm$ 1.2
57.5	100	1.25	20 $\pm$ 0.9

**Table 32.** Analysis of variance (Partial sum of squares - Type III) for Response Surface Reduced Quadratic Model of the output variable antiradical power (ARP).

Source	Sum of Squares	df	Mean Square	Value	p-value Prob > F	Coefficient Estimate	df	Standard Error	95% CI Low	95% CI High
Model	175.7	1	175.69	8.4	0.0109					
B-Pressure	175.7	1	175.69	8.4	0.0109	-4.69	1	1.61	-8.13	-1.24
Residual	312.8	15	20.85							
Lack of Fit	228.4	11	20.76	0.98	0.5595					
Pure Error	84.4	4	21.10							
Cor Total	488.5	16								
Intercept						23.7	1	1.11	21.3	26.0

Design-Expert® Software

ARP  
  
 35.3547  
 13.7138

X1 = B: Pressure  
 X2 = C: Pulse

Actual Factor  
 A: Temperature = 57.50

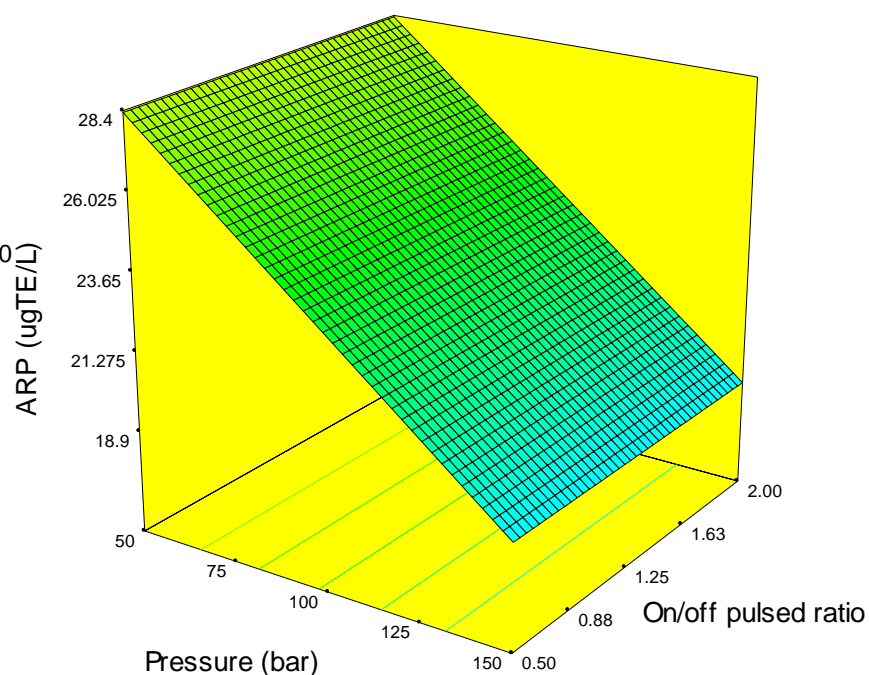


**Figure 69.** Three-dimensional surface plot of the regression equations for antiradical power (ARP) obtained by the experimental design coupled with RSM.

### 6.3.3 Extract total solids

The third response variable taken into consideration for this study was the amount of total solids, extracted during the process. In agreement with previous results, global extraction yields (table 33) by CPUAE resulted significantly lower than the ones observed for MAE and HPTE. The highest values were obtained at 50 bar, 1.25 as on/off pulsed ratio and at the two extreme temperatures (25 °C and 90 °C). By the analysis of variance (table 34) of the quadratic model of the ETS, pressure, on/off pulsed ratio and their quadratic terms resulted as the most significant, even if only for pressure and squared pressure, p-values were lower than 0.05. The three-dimensional surface plot of ETS as a function of on/off pulsed ratio and pressure is given in figure 70, where is possible to observe the non linear decreasing of the function with the increasing of the

extraction temperature, while a maximum at 1.25 was found in the non linear functionality of ETS over on/off pulsed ratio.

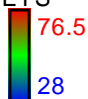
**Table 33.** Extract total solids (ETS) of the extracts obtained by continuous pressurized ultrasound-assisted extraction.

T (°C)	P (bar)	On/off pulsed ratio (min <sub>on</sub> /min <sub>off</sub> )	ETS (mg/g <sub>dried SCG</sub> )
25	50	1.25	77 ± 2.9
90	50	1.25	70 ± 2.8
25	150	1.25	36 ± 0.0
90	150	1.25	34 ± 0.0
25	100	0.5	38 ± 0.1
90	100	0.5	39 ± 10
25	100	2	34 ± 9
90	100	2	37 ± 0.0
57.5	50	0.5	48 ± 0.5
57.5	150	0.5	28 ± 1.4
57.5	50	2	48 ± 1.1
57.5	150	2	48 ± 0.74
57.5	100	1.25	31 ± 3.5
57.5	100	1.25	42 ± 11
57.5	100	1.25	44 ± 1.4
57.5	100	1.25	41 ± 2.1
57.5	100	1.25	44 ± 5.7

**Table 34.** Analysis of variance (Partial sum of squares - Type III) for Response Surface Reduced Quadratic Model of the output variable extract total solids (ETS).

Source	Sum of Squares	df	Mean Square	Value	p-value Prob > F	Coefficient Estimate	df	Standard Error	95% CI Low	95% CI High
Model	1756.24	4	439.06	6.56	0.0049					
B-Pressure	1147.21	1	1147.21	17.15	0.0014	-11.98	1	2.89	-18.28	-5.67
C- Pulsed ratio	25.2	1	25.2	0.38	0.5508	1.78	1	2.89	-4.53	8.08
B <sup>2</sup>	411	1	411	6.15	0.0290	9.87	1	3.98	1.20	18.54
C <sup>2</sup>	203	1	203	3.03	0.1073	-6.93	1	3.98	-15.60	1.74
Residual	802.7	12	66.9							
Lack of Fit	695	4	86.9	0.98	0.5595					
Pure Error	107.6	4	26.9							
Cor Total	2559	16								
Intercept						42.17	1	3.25	35.09	49.25

Design-Expert® Software

ETS  
 76.5  
 28

X1 = B: Pressure  
 X2 = C: Pulse

Actual Factor  
 A: Temperature = 57.50

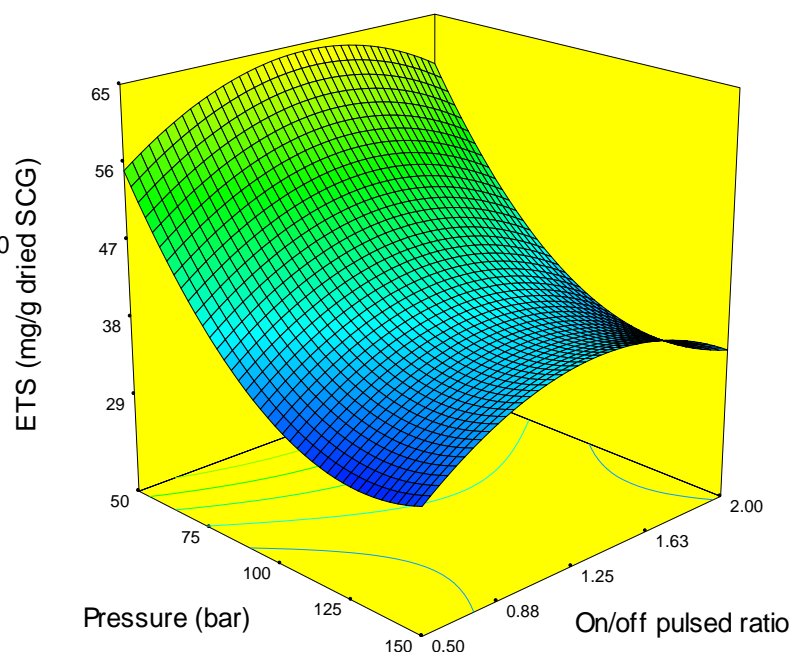


**Figure 70.** Three-dimensional surface plot of the regression equation for extract total solids (ETS) obtained by the experimental design coupled with RSM.

The different behavior of ETS from total polyphenol content and ARP, as function of input variables, indicated that the scavenging activity of the extracts could be traced back only to the polyphenols, while the rest of the extracted compounds did not contribute to the scavenging activity.

Al-Dhabi et al. (2017) studied the effects of temperature (range 30-50 °C), power (100-300 W), time (4-45 ) and solid-liquid ratio (5-30 g/mL) on ultrasound-assisted solid – liquid extraction of phenolic compounds from spent coffee grounds. Working in batch-mode, they found that higher yields (from 33.31 to 36.23 mg gallic acid equivalent/g) could be obtained at lower temperatures than 45 °C, and for a time up to 36 min and a solid to liquid ratio up to 1:05 g/mL. The main differences between the two studies could be due to the direct contact of the ultrasound probe with the solid sample, that in CPUAE was not used, since SCG was packed into the extraction column, and to the higher contact time and solid-liquid ratio used in the batch-mode.

Closer to the values obtained in the present study were the results, in terms of total polyphenol content, that were found by Severini et al. (2017). Indeed, total polyphenol yields ranged from 19.29 to 25.18 mg<sub>GALLIC ACID EQUIVALENT</sub>/g, using as operating conditions: methanol/water mass ratio between 0.49 and 1.50 (w/w), treatment time between 9 and 112 min and length of ultrasound pulse from 0.60 to 7.4 min. In addition, the central composite design (CCD) that they used, revealed that the main significant variables were methanol/water mass ratio and time length of ultrasound pulse. As a consequence, could be desumed that the extraction yield by CPUAE could be enhanced by reducing the solvent flow rate, in order to increase the contact time between solvent and solid matrix. Other options for further studies, could be the evaluation of higher solvent to liquid ratio in the process and the evaluation of the effects of power.

## 6.4 CONCLUSIONS

In this chapter, continuous pressurized ultrasound-assisted extraction was proposed as a novel technique for antioxidant extraction from spent coffee grounds. Box Behnken design was employed for the screening of the effects of temperature, on/off pulsed ratio and pressure on the total polyphenol yield, antiradical activity and extracted total solids of the extracts. Results showed that, in about 10 min, extraction yields similar to those of solid-liquid extraction, at room temperature and carried out for 24 h, were obtained. The more significant process parameter that affected the response variables was pressure. Particularly, its linear decrease, in the range of values investigated in this study, seemed to have positive effects on total polyphenol yields and antiradical power, while a more complex non-linear behaviour was showed by ETS as a function of pressure and on/off pulsed ratio. Nevertheless, continuous pressurized ultrasound-assisted extraction of polyphenols from spent coffee grounds deserves further investigations for the process optimization.

## CONCLUSIONS

In this thesis work, spent coffee grounds from common vending machines were employed as raw material for the recovery of antioxidants. Characterization of the “exhaust coffee” after beverage preparation, demonstrated that this solid can actually be a source of compounds of interest, which could find applications in several industrial fields, from food to the energetic one. Particularly, spent coffee grounds are rich of antioxidants, as proved by the study undertaken in this work, which mainly consisted in chlorogenic acid and its isomers and derivatives. In addition, green and non-conventional extraction techniques demonstrated to be suitable for the aim of this work and able to increase the extraction yields compared to the conventional solid-liquid extraction.

After an evaluation among three pure solvents (methanol, ethanol and water) and an optimization on the composition of a solvent made by ethanol/water mixtures, ethanol 54 % (v/v) was selected as the most effective for the recovery of the bioactive molecules from spent coffee grounds. Into a biorefinery concept based on coffee, this green solvent has an additional advantage, since it could be produced by fermentation from spent coffee grounds after the recovery of antioxidants. Microwave-assisted extraction (MAE), high pressure and temperature-assisted extraction (HPTE) and continuous pressurized ultrasound-assisted extraction (CPUAE) were the non-conventional extraction techniques utilized in this study. In table 35, the characteristics of the extracts obtained under the optimized operating conditions for the three non-conventional extraction techniques are summarized. Among them, continuous pressurized ultrasound-assisted extraction revealed to be the least effective, giving back extraction yields similar to solid-liquid extraction. Instead, microwave and high pressure and temperature-assisted extractions provided similar extracts with high total polyphenol yields (about 43 mg<sub>CAE</sub>/g) and very high antiradical power ( $67 \pm 6$  and  $59 \pm 3$   $\mu\text{g TE/L}_{\text{extract}}$ , respectively). In addition, from the optimization study on both of the techniques, an optimal extraction time of 60 min and a temperature of 150 °C were found.

**Table 35.** Comparison among the extracts obtained under the optimized operating conditions of the non-conventional extraction techniques . TP= total polyphenol yield; ARP= antiradical power; ETS= extract total solids; CAE= caffeic acid equivalent; TE= trolox equivalent; L/S= liquid to solid ratio;  $t_H$ =heating time.

Technique	Operating conditions	TP (mg <sub>CAE</sub> /g dried SCG)	ARP (μg <sub>TE</sub> /L <sub>extract</sub> )	ETS (mg/g dried SCG)
MAE	Temperature= 150 °C;	44± 3.8	67 ± 6	226 ± 21
	time= 60 min;			
	$t_H$ =10 min;			
	L/S= 10 mL/g;			
	solvent= ethanol 54% (v/v)			
HPTE	Temperature= 150 °C;	43 ± 2.3	59±3	248±8
	time= 60 min;			
	Pressure = 7.2 bar			
	L/S= 10 mL/g;			
	solvent= ethanol 54% (v/v)			
CPUAE	Temperature= 90 °C;	18 ± 0.9	33± 0.9	70 ± 2.8
	time= 10 min;			
	Pressure= 50 bar			
	L/S= 10 mL/g;			
	On/off pulsed ratio= 1.25			
	solvent = ethanol 54% (v/v)			

Thus, temperature proved to be the more effective parameter on the extraction of antioxidants from spent coffee grounds; in particular to reach high recoveries, temperatures above the solvent boiling point at atmospheric pressure have to be used. This finding was also confirmed by the unsatisfactory results obtained by the third extraction technique, in which a maximum temperature of 90 °C was employed. Kinetic studies, instead, revealed that extractions longer than 60 min did not significantly increase the extraction yields. Pressure has the main role of keeping solvent in liquid phase at temperatures higher than boiling point at atmospheric pressure. Indeed, if HPTE, in which temperature and pressure are intimately related, provided good results with a pressure of about 7 bar, CPUAE, in which the working pressure ranged from 50 to 200 bar, did not show considerable results. Nevertheless, in MAE an important role was also played by the heating time, related to the thermal ramp and the microwave

intensity, which affected the extraction yields and could be an important variable useful to change the extract quality, while in HPTE the inert atmosphere reduced the polyphenol degradation.

The antioxidant-rich extracts were also treated by green post-processings in order to obtain a solid product, which was more suitable for storage, transport, with longer shelf-life and, above all, able to maintain its peculiar properties. Compared to freeze-drying, supercritical antisolvent extraction was able to provide a different product, which was more concentrated in polyphenols, defatted and caffeine-free, but with product recovery lower than freeze-drying, whose solid powder maintained unchanged the activity of the liquid extract. The study on encapsulation of the extract by spray drying demonstrated the possibility to trap the extract into a wall material made by inulin/maltodextrins 80:20 (w/w), an interesting coating agent for food purposes, since the antioxidant activity of the extract could be combined to the prebiotic effects of inulin. Nevertheless, properties of the extract encapsulated in maltodextrins were tested to assess the possibility of its use for food packaging purposes. The experiments demonstrated that, even if the results on antimicrobial activity were inconclusive, the obtained powder presented high antioxidant activity, able to prevent lipid peroxidation. Finally, encapsulation on liposomes was tried, in order to increase the extract solubility in polar media, due to the drug carrier properties of the vesicles. So, a study on the operating conditions (extract concentration in the feed and pressure in the formation vessel) of supercritical fluid-assisted liposome formation process was carried out. Liposomes with sub-micrometrical dimensions were obtained in all the experiments, and 100 bar and 250 ppm as extract concentration seemed to represent the best compromise to obtain high encapsulation efficiency (89 %) and high antiradical power. The process assisted by supercritical fluids allowed to reach higher encapsulation efficiencies than encapsulation by spray drying, producing also particles a order of magnitude smaller than spray drying, but the disadvantages of the process were the use of high pressures and the low concentration of the feed, which are not present in an easy and mature process as spray drying. Nevertheless, the two types of encapsulated extract are products with different features.



In this thesis, therefore, was demonstrated that several alternative products can be obtained by using green processes from spent coffee ground extracts, with enhanced properties as a function of the applications. However, the extracts from spent coffee grounds proved to be biocompatible for cosmetic application, to be suitable for applications in food industry, in pharmaceuticals, as well as in food packaging.

## REFERENCES

- Adams, M.R., Dougan, J., 1987. Waste products, in: Clarke and Macrae (Ed.), *Coffee*. Elsevier Science Publishers LTD, New York, pp. 257–291.  
[https://doi.org/https://doi.org/10.1007/978-94-009-3417-7\\_9](https://doi.org/https://doi.org/10.1007/978-94-009-3417-7_9)
- Aguiar, J., Estevinho, B.N., Santos, L., 2016. Microencapsulation of natural antioxidants for food application – The specific case of coffee antioxidants – A review. *Trends Food Sci. Technol.* 58, 21–39. <https://doi.org/10.1016/j.tifs.2016.10.012>
- Al-Dhabi, N.A., Ponmurugan, K., Maran Jeganathan, P., 2017. Development and validation of ultrasound-assisted solid-liquid extraction of phenolic compounds from waste spent coffee grounds. *Ultrason. Sonochem.* 34, 206–213.  
<https://doi.org/10.1016/j.ultsonch.2016.05.005>
- Al-Hamamre, Z., Foerster, S., Hartmann, F., Kröger, M., Kaltschmitt, M., 2012. Oil extracted from spent coffee grounds as a renewable source for fatty acid methyl ester manufacturing. *Fuel* 96, 70–76. <https://doi.org/10.1016/j.fuel.2012.01.023>
- Aliakbarian, B., Casazza, A.A., Perego, P., 2011. Valorization of olive oil solid waste using high pressure – high temperature reactor. *Food Chem.* 128, 704–710.  
<https://doi.org/10.1016/j.foodchem.2011.03.092>
- Aliakbarian, B., Dehghani, F., Perego, P., 2009. The effect of citric acid on the phenolic contents of olive oil. *Food Chem.* 116, 617–623.  
<https://doi.org/10.1016/j.foodchem.2009.02.077>
- Aliakbarian, B., Fathi, A., Perego, P., Dehghani, F., 2012. Extraction of antioxidants from winery wastes using subcritical water. *J. Supercrit. Fluids* 65, 18–24.  
<https://doi.org/10.1016/j.supflu.2012.02.022>
- Ameer, K., Shahbaz, H.M., Kwon, J.H., 2017. Green Extraction Methods for Polyphenols from Plant Matrices and Their Byproducts: A Review. *Compr. Rev. Food Sci. Food Saf.* 16, 295–315. <https://doi.org/10.1111/1541-4337.12253>
- Anastopoulos, I., Karamesouti, M., Mitropoulos, A.C., Kyzas, G.Z., 2017. A review for coffee adsorbents. *J. Mol. Liq.* 229, 555–565.  
<https://doi.org/10.1016/j.molliq.2016.12.096>
- Andersen, L.F., Jacobs, D.R., Carlsen, M.H., Blomhoff, R., 2006. Consumption of coffee is

- associated with reduced risk of death attributes to inflammatory and cardiovascular diseases in the Iowa Womens's Health Study. *Am. J. Clin. Nutr.* 83, 1039–1046.
- Andrade, K.S., Gonálvez, R.T., Maraschin, M., Ribeiro-Do-Valle, R.M., Martínez, J., Ferreira, S.R.S., 2012. Supercritical fluid extraction from spent coffee grounds and coffee husks: Antioxidant activity and effect of operational variables on extract composition. *Talanta* 88, 544–552. <https://doi.org/10.1016/j.talanta.2011.11.031>
- Arabi, M., Ghaedi, M., Ostovan, A., 2016a. Development of dummy molecularly imprinted based on functionalized silica nanoparticles for determination of acrylamide in processed food by matrix solid phase dispersion. *Food Chem.* 210, 78–84. <https://doi.org/10.1016/j.foodchem.2016.04.080>
- Arabi, M., Ostovan, A., Ghaedi, M., Purkait, M.K., 2016b. Novel strategy for synthesis of magnetic dummy molecularly imprinted nanoparticles based on functionalized silica as an efficient sorbent for the determination of acrylamide in potato chips : Optimization by experimental design methodology. *Talanta* 154, 526–532. <https://doi.org/10.1016/j.talanta.2016.04.010>
- Azam, S., Hadi, N., Khan, N.U., Hadi, S.M., 2003. Antioxidant and prooxidant properties of caffeine, theobromine and xanthine. *Med Sci Monit* 9, 325–330. <https://doi.org/10.1002/mrm.20324>
- Azouaou, N., Sadaoui, Z., Djaafri, A., Mokaddem, H., 2010. Adsorption of cadmium from aqueous solution onto untreated coffee grounds: Equilibrium, kinetics and thermodynamics. *J. Hazard. Mater.* 184, 126–134. <https://doi.org/10.1016/j.jhazmat.2010.08.014>
- Bagheri, L., Madadlou, A., Yarmand, M., Mousavi, M.E., 2014. Spray-dried alginate microparticles carrying caffeine-loaded and potentially bioactive nanoparticles. *Food Res. Int.* 62, 1113–1119. <https://doi.org/10.1016/j.foodres.2014.05.040>
- Bakowska-Barczak, A.M., Kolodziejczyk, P.P., 2011. Black currant polyphenols: Their storage stability and microencapsulation. *Ind. Crops Prod.* 34, 1301–1309. <https://doi.org/10.1016/j.indcrop.2010.10.002>
- Ballesteros, L.F., Ramirez, M.J., Orrego, C.E., Teixeira, J.A., Mussatto, S.I., 2017. Encapsulation of antioxidant phenolic compounds extracted from spent coffee

- grounds by freeze-drying and spray-drying using different coating materials. *Food Chem.* 237, 623–631. <https://doi.org/10.1016/j.foodchem.2017.05.142>
- Ballesteros, L.F., Teixeira, J.A., Mussatto, S.I., 2014. Chemical, Functional, and Structural Properties of Spent Coffee Grounds and Coffee Silverskin. *Food Bioprocess Technol.* 7, 3493–3503. <https://doi.org/10.1007/s11947-014-1349-z>
- Belay, A., Ture, K., Redi, M., Asfaw, A., 2008. Measurement of caffeine in coffee beans with UV/vis spectrometer. *Food Chem.* 108, 310–315. <https://doi.org/10.1016/j.foodchem.2007.10.024>
- Berhe, S., Ayele, D., Tadesse, A., Mulu, A., 2015. Adsorption Efficiency of Coffee Husk for Removal of Lead ( II ) from Industrial Effluents : Equilibrium and Kinetic Study. *Int. J. Sci. Res. Publ.* 5, 1–8.
- Bonita, J.S., Mandarano, M., Shuta, D., Vinson, J., 2007. Coffee and cardiovascular disease: In vitro, cellular, animal, and human studies. *Pharmacol. Res.* 55, 187–198. <https://doi.org/10.1016/j.phrs.2007.01.006>
- Boonamnuyvitaya, V., Chaiya, C., Tanthapanichakoon, W., Jarudilokkul, S., 2004. Removal of heavy metals by adsorbent prepared from pyrolyzed coffee residues and clay. *Sep. Purif. Technol.* 35, 11–22. [https://doi.org/10.1016/S1383-5866\(03\)00110-2](https://doi.org/10.1016/S1383-5866(03)00110-2)
- Borrelli, R.C., Visconti, A., Mennella, C., Anese, M., Fogliano, V., 2002. Chemical characterization and antioxidant properties of coffee melanoidins. *J. Agric. Food Chem.* 50, 6527–6533. <https://doi.org/10.1021/jf025686o>
- Boudrahem, F., Aissani-Benissad, F., Aït-Amar, H., 2009. Batch sorption dynamics and equilibrium for the removal of lead ions from aqueous phase using activated carbon developed from coffee residue activated with zinc chloride. *J. Environ. Manage.* 90, 3031–3039. <https://doi.org/10.1016/j.jenvman.2009.04.005>
- Boussetta, N., Lebovka, N., Vorobiev, E., Adenier, H., Bedel-Cloutour, C., Lanoisellé, J.L., 2009. Electrically assisted extraction of soluble matter from chardonnay grape skins for polyphenol recovery. *J. Agric. Food Chem.* 57, 1491–1497. <https://doi.org/10.1021/jf802579x>
- Boussetta, N., Vorobiev, E., 2014. Extraction of valuable biocompounds assisted by high voltage electrical discharges: A review. *Comptes Rendus Chim.* 17, 197–203.

- <https://doi.org/10.1016/j.crci.2013.11.011>
- Boussetta, N., Vorobiev, E., Deloison, V., Pochez, F., Falcimaigne-Cordin, A., Lanoisellé, J.L., 2011. Valorisation of grape pomace by the extraction of phenolic antioxidants: Application of high voltage electrical discharges. *Food Chem.* 128, 364–370. <https://doi.org/10.1016/j.foodchem.2011.03.035>
- Bravo, J., Juaniz, I., Monente, C., Caemmerer, B., 2012. Evaluation of spent coffee obtained from the most common coffeemakers as a source of hydrophilic bioactive compounds. *J. Agric. Food Chem.* 60, 12565–12573.
- Bravo, J., Monente, C., Juániz, I., De Peña, M.P., Cid, C., 2013. Influence of extraction process on antioxidant capacity of spent coffee. *Food Res. Int.* 50, 610–616. <https://doi.org/10.1016/j.foodres.2011.04.026>
- Bucić-Kojić, A., Planinić, M., Tomas, S., Bilić, M., Velić, D., 2007. Study of solid-liquid extraction kinetics of total polyphenols from grape seeds. *J. Food Eng.* 81, 236–242. <https://doi.org/10.1016/j.jfoodeng.2006.10.027>
- Budryn, G., Zaczyńska, D., Pałecz, B., Rachwał-Rosiak, D., Belica, S., Den-Haan, H., Peña-García, J., Pérez-Sánchez, H., 2016. Interactions of free and encapsulated hydroxycinnamic acids from green coffee with egg ovalbumin, whey and soy protein hydrolysates. *LWT - Food Sci. Technol.* 65, 823–831. <https://doi.org/10.1016/j.lwt.2015.09.001>
- Burniol-Figols, A., Cenian, K., Skiadas, I. V., Gavala, H.N., 2016. Integration of chlorogenic acid recovery and bioethanol production from spent coffee grounds. *Biochem. Eng. J.* 116, 54–64. <https://doi.org/10.1016/j.bej.2016.04.025>
- Calixto, F., Fernandes, J., Couto, R., Hernández, E.J., Najdanovic-Visak, V., Simões, P.C., 2011. Synthesis of fatty acid methyl esters via direct transesterification with methanol/carbon dioxide mixtures from spent coffee grounds feedstock. *Green Chem.* 13, 1196–1202. <https://doi.org/10.1039/c1gc15101k>
- Cämmerer, B., Jalyschko, W., Kroh, L.W., 2002. Carbohydrate structures as part of the melanoidin skeleton. *Int. Congr. Ser.* 1245 269–273. [https://doi.org/10.1016/S0531-5131\(02\)00890-7](https://doi.org/10.1016/S0531-5131(02)00890-7)
- Campos-Vega, R., Loarca-Piña, G., Vergara-Castañeda, H., Oomah, B.D., 2015. Spent coffee grounds: A review on current research and future prospects. *Trends Food*

- Sci. Technol. 45, 24–36. <https://doi.org/10.1016/j.tifs.2015.04.012>
- Carneiro, H.C.F., Tonon, R. V., Grosso, C.R.F., Hubinger, M.D., 2013. Encapsulation efficiency and oxidative stability of flaxseed oil microencapsulated by spray drying using different combinations of wall materials. J. Food Eng. 115, 443–451. <https://doi.org/10.1016/j.jfoodeng.2012.03.033>
- Carullo, D., Abera, B.D., Casazza, A.A., Donsì, F., Perego, P., Ferrari, G., Pataro, G., 2018. Effect of pulsed electric fields and high pressure homogenization on the aqueous extraction of intracellular compounds from the microalgae *Chlorella vulgaris*. Algal Res. 31, 60–69. <https://doi.org/10.1016/j.algal.2018.01.017>
- Casazza, A.A., Aliakbarian, B., De Faveri, D., Fiori, L., Perego, P., 2012. Antioxidants from winemaking wastes: A study on extraction parameters using response surface methodology. J. Food Biochem. 36, 28–37. <https://doi.org/10.1111/j.1745-4514.2010.00511.x>
- Casazza, A.A., Aliakbarian, B., Mantegna, S., Cravotto, G., Perego, P., 2010. Extraction of phenolics from *Vitis vinifera* wastes using non-conventional techniques. J. Food Eng. 100, 50–55. <https://doi.org/10.1016/j.jfoodeng.2010.03.026>
- Cervera-Mata, A., Pastoriza, S., Rufián-Henares, J.Á., Párraga, J., Martín-García, J.M., Delgado, G., 2017. Impact of spent coffee grounds as organic amendment on soil fertility and lettuce growth in two Mediterranean agricultural soils. Arch. Agron. Soil Sci. 1–15. <https://doi.org/10.1080/03650340.2017.1387651>
- Chan, C.-H., See, T.-Y., Yusoff, R., Ngoh, G.-C., Kow, K.-W., 2017. Extraction of bioactives from *Orthosiphon stamineus* using microwave and ultrasound-assisted techniques: Process optimization and scale up. Food Chem. 221, 1382–1387. <https://doi.org/10.1016/j.foodchem.2016.11.016>
- Chan, C.-H., Yeoh, H.K., Yusoff, R., Ngoh, G.C., 2016. A first-principles model for plant cell rupture in microwave-assisted extraction of bioactive compounds. J. Food Eng. 188, 98–107. <https://doi.org/10.1016/j.jfoodeng.2016.05.017>
- Chan, C.-H., Yusoff, R., Ngoh, G.-C., 2014. Modeling and kinetics study of conventional and assisted batch solvent extraction. Chem. Eng. Res. Des. 92, 1169–1186. <https://doi.org/10.1016/j.cherd.2013.10.001>
- Chan, C.-H., Yusoff, R., Ngoh, G.-C., 2013. Modeling and prediction of extraction profile

- for microwave-assisted extraction based on absorbed microwave energy. *Food Chem.* 140, 147–153. <https://doi.org/10.1016/j.foodchem.2013.02.057>
- Chan, C.-H., Yusoff, R., Ngoh, G.-C., Kung, F.W.-L., 2011. Microwave-assisted extractions of active ingredients from plants. *J. Chromatogr. A* 1218, 6213–6225. <https://doi.org/10.1016/j.chroma.2011.07.040>
- Chavan, A.A., Pinto, J., Liakos, I., Bayer, I.S., Lauciello, S., Athanassiou, A., Fragouli, D., 2016. Spent Coffee Bioelastomeric Composite Foams for the Removal of Pb<sup>2+</sup> and Hg<sup>2+</sup> from Water. *ACS Sustain. Chem. Eng.* 4, 5495–5502. <https://doi.org/10.1021/acssuschemeng.6b01098>
- Chemat, F., Rombaut, N., Sicaire, A.G., Meullemiestre, A., Fabiano-Tixier, A.-S., Abert-Vian, M., 2017. Ultrasound assisted extraction of food and natural products. Mechanisms, techniques, combinations, protocols and applications. A review. *Ultrason. Sonochem.* 34, 540–560. <https://doi.org/10.1016/j.ultsonch.2016.06.035>
- Chemat, F., Vian, M.A., Cravotto, G., 2012. Green extraction of natural products: Concept and principles. *Int. J. Mol. Sci.* 13, 8615–8627. <https://doi.org/10.3390/ijms13078615>
- Chen, X., Nielsen, K.F., Borodina, I., Kielland-Brandt, M.C., Karhumaa, K., 2011. Increased isobutanol production in *Saccharomyces cerevisiae* by overexpression of genes in valine metabolism. *Biotechnol. Biofuels* 4, 1–12. <https://doi.org/10.1186/1754-6834-4-21>
- Chinnarasu, C., Montes, A., Fernández-Ponce, M.T., Casas, L., Mantell, C., Pereyra, C., Martínez de La Ossa, E.J., 2015. Precipitation of antioxidant fine particles from *Olea europaea* leaves using supercritical antisolvent process. *J. Supercrit. Fluids* 97, 125–132. <https://doi.org/10.1016/j.supflu.2014.11.008>
- Choi, M.P.K., Chan, K.K.C., Leung, H.W., Huie, C.W., 2003. Pressurized liquid extraction of active ingredients (ginsenosides) from medicinal plants using non-ionic surfactant solutions. *J. Chromatogr. A* 983, 153–162. [https://doi.org/10.1016/S0021-9673\(02\)01649-7](https://doi.org/10.1016/S0021-9673(02)01649-7)
- Cohn, J.S., Kamili, A., Wat, E., Chung, R.W.S., Tandy, S., 2010. Reduction in intestinal cholesterol absorption by various food components: Mechanisms and

- implications. *Atheroscler. Suppl.* 11, 45–48.  
<https://doi.org/10.1016/j.atherosclerosissup.2010.04.004>
- Cravotto, G., Boffa, L., Mantegna, S., Perego, P., Avogadro, M., Cintas, P., 2008. Improved extraction of vegetable oils under high-intensity ultrasound and/or microwaves. *Ultrason. Sonochem.* 15, 898–902.  
<https://doi.org/10.1016/j.ultsonch.2007.10.009>
- Cruz, R., Cardoso, M.M., Fernandes, L., Oliveira, M., Mendes, E., Baptista, P., Morais, S., Casal, S., 2012. Espresso coffee residues: A valuable source of unextracted compounds. *J. Agric. Food Chem.* 60, 7777–7784.  
<https://doi.org/10.1021/jf3018854>
- Da Porto, C., Natolino, A., 2017. Supercritical fluid extraction of polyphenols from grape seed (*Vitis vinifera*): Study on process variables and kinetics. *J. Supercrit. Fluids* 130, 239–245. <https://doi.org/10.1016/j.supflu.2017.02.013>
- Daglia, M., Papetti, A., Gregotti, C., Bertè, F., Gazzani, G., 2000. In vitro antioxidant and ex vivo protective activities of green and roasted coffee. *J. Agric. Food Chem.* 48, 1449–1454. <https://doi.org/10.1021/jf990510g>
- Dahmoune, F., Nayak, B., Moussi, K., Remini, H., Madani, K., 2015. Optimization of microwave-assisted extraction of polyphenols from *Myrtus communis* L. leaves. *Food Chem.* 166, 585–595. <https://doi.org/10.1016/j.foodchem.2014.06.066>
- Davila-Guzman, N.E., Cerino-Córdova, F.J., Loredó-Cancino, M., Rangel-Mendez, J.R., Gómez-González, R., Soto-Regalado, E., 2016. Studies of Adsorption of Heavy Metals onto Spent Coffee Ground: Equilibrium, Regeneration, and Dynamic Performance in a Fixed-Bed Column. *Int. J. Chem. Eng.* 1–11.  
<https://doi.org/10.1155/2016/9413879>
- De Barros Fernandes, R.V., Borges, S.V., Botrel, D.A., 2014. Gum arabic/starch/maltodextrin/inulin as wall materials on the microencapsulation of rosemary essential oil. *Carbohydr. Polym.* 101, 524–532.  
<https://doi.org/10.1016/j.carbpol.2013.09.083>
- Dong, Z., Gu, F., Xu, F., Wang, Q., 2014. Comparison of four kinds of extraction techniques and kinetics of microwave-assisted extraction of vanillin from *Vanilla planifolia* Andrews. *Food Chem.* 149, 54–61.



- <https://doi.org/10.1016/j.foodchem.2013.10.052>
- Donsì, F., Ferrari, G., Pataro, G., 2010. Applications of pulsed electric field treatments for the enhancement of mass transfer from vegetable tissue. *Food Eng. Rev.* 2, 109–130. <https://doi.org/10.1007/s12393-010-9015-3>
- Duba, K.S., Casazza, A.A., Mohamed, H. Ben, Perego, P., Fiori, L., 2015. Extraction of polyphenols from grape skins and defatted grape seeds using subcritical water: Experiments and modeling. *Food Bioprod. Process.* 94, 29–38. <https://doi.org/10.1016/j.fbp.2015.01.001>
- Dube, A., Nicolazzo, J.A., Larson, I., 2010. Chitosan nanoparticles enhance the intestinal absorption of the green tea catechins (+)-catechin and (-)-epigallocatechin gallate. *Eur. J. Pharm. Sci.* 41, 219–225. <https://doi.org/10.1016/j.ejps.2010.06.010>
- Dugas, A.J., Castañeda-Acosta, J., Bonin, G.C., Price, K.L., Fischer, N.H., Winston, G.W., 2000. Evaluation of the total peroxy radical-scavenging capacity of flavonoids: Structure-activity relationships. *J. Nat. Prod.* 63, 327–331. <https://doi.org/10.1021/np990352n>
- Ekezie, F.G.C., Sun, D.-W., Cheng, J.-H., 2017. Acceleration of microwave-assisted extraction processes of food components by integrating technologies and applying emerging solvents: A review of latest developments. *Trends Food Sci. Technol.* 67, 160–172. <https://doi.org/10.1016/j.tifs.2017.06.006>
- Esquivel, P., Jiménez, V.M., 2012. Functional properties of coffee and coffee by-products. *Food Res. Int.* 46, 488–495. <https://doi.org/10.1016/j.foodres.2011.05.028>
- European Union, 1991. ANNEX III. Determination of peroxide value, in: COMMISSION REGULATION (EEC) No 2568/91 of 11 July 1991 on the Characteristics of Olive Oil and Olive-Residue Oil and on the Relevant Methods of Analysis. pp. 28–29.
- Fang, Z., Bhandari, B., 2010. Encapsulation of polyphenols - A review. *Trends Food Sci. Technol.* 21, 510–523. <https://doi.org/10.1016/j.tifs.2010.08.003>
- Fathi, M., Mozafari, M.R., Mohebbi, M., 2012. Nanoencapsulation of food ingredients using carbohydrate based delivery systems. *Trends Food Sci. Technol.* 23, 13–27. <https://doi.org/10.1016/j.tifs.2014.06.007>
- Fazaeli, M., Emam-Djomeh, Z., Kalbasi Ashtari, A., Omid, M., 2012. Effect of spray drying conditions and feed composition on the physical properties of black mulberry juice

- powder. *Food Bioprod. Process.* 90, 667–675.  
<https://doi.org/10.1016/j.fbp.2012.04.006>
- Feng, Y., Sun, C., Yuan, Y., Zhu, Y., Wan, J., Firempong, C.K., Omari-Siaw, E., Xu, Y., Pu, Z., Yu, J., Xu, X., 2016. Enhanced oral bioavailability and in vivo antioxidant activity of chlorogenic acid via liposomal formulation. *Int. J. Pharm.* 501, 342–349.  
<https://doi.org/10.1016/j.ijpharm.2016.01.081>
- Fernandes, A.S., Mello, F.V., C., Filho, S.T., Carpes, R.M., Honório, J.G., Marques, M.R.C., Felzenszwalb, I., Ferraz, E.R.A., 2017. Impacts of discarded coffee waste on human and environmental health. *Ecotoxicol. Environ. Saf.* 141, 30–36.  
<https://doi.org/10.1016/j.ecoenv.2017.03.011>
- Fiori, L., De Faveri, D., Casazza, A.A., Perego, P., 2009. Grape by-products: extraction of polyphenolic compounds using supercritical CO<sub>2</sub> and liquid organic solvent—a preliminary investigation Subproductos de la uva: Extracción de compuestos polifenólicos usando CO<sub>2</sub> supercrítico y disolventes orgánicos líquidos—. *CYTA - J. Food* 7, 163–171. <https://doi.org/10.1080/11358120902989715>
- Galan, A.M., Calinescu, I., Trifan, A., Winkworth-Smith, C., Calvo-Carrascal, M., Dodds, C., Binner, E., 2017. New insights into the role of selective and volumetric heating during microwave extraction: Investigation of the extraction of polyphenolic compounds from sea buckthorn leaves using microwave-assisted extraction and conventional solvent extraction. *Chem. Eng. Process. Process Intensif.* 116, 29–39.  
<https://doi.org/10.1016/j.cep.2017.03.006>
- Georgetti, S.R., Casagrande, R., Fernandes Souza, C.R., Pereira Oliveira, W., Vieira Fonseca, M.J., 2008. Spray drying of the soybean extract: Effects on chemical properties and antioxidant activity. *LWT - Food Sci. Technol.* 41, 1521–1527.  
<https://doi.org/10.1016/j.lwt.2007.09.001>
- Gharsallaoui, A., Roudaut, G., Odile, C., Voilley, A., Saurel, R., 2007. Applications of spray-drying in microencapsulation of food ingredients : An overview. *Food Res. Int.* 40, 1107–1121. <https://doi.org/10.1016/j.foodres.2007.07.004>
- Gil-Chávez, J.G., Villa, J.A., Ayala-Zavala, J.F., Heredia, J.B., Sepulveda, D., Yahia, E.M., González-Aguilar, G.A., 2013. Technologies for extraction and production of bioactive compounds to be used as nutraceuticals and food ingredients: an

- overview. Compr. Rev. Food Sci. Food Saf. 12, 5–23.  
<https://doi.org/10.1111/1541-4337.12005>
- Gomez-Gonzalez, R., Cerino-Córdova, F.J., Garcia-León, A.M., Soto-Regalado, E., Davila-Guzman, N.E., Salazar-Rabago, J.J., 2016. Lead biosorption onto coffee grounds: Comparative analysis of several optimization techniques using equilibrium adsorption models and ANN. J. Taiwan Inst. Chem. Eng. 68, 201–210.  
<https://doi.org/10.1016/j.jtice.2016.08.038>
- González, B., Domínguez, A., Tojo, J., 2004. Dynamic viscosities, densities, and speed of sound and derived properties of the binary systems acetic acid with water, methanol, ethanol, ethyl acetate and methyl acetate at T = (293.15, 298.15, and 303.15) K at atmospheric pressure. J. Chem. Eng. Data 49, 1590–1596.  
<https://doi.org/10.1021/je0342825>
- Górnas, P., Neunert, G., Baczyński, K., Polewski, K., 2009. Beta-cyclodextrin complexes with chlorogenic and caffeic acids from coffee brew: Spectroscopic, thermodynamic and molecular modelling study. Food Chem. 114, 190–196.  
<https://doi.org/10.1016/j.foodchem.2008.09.048>
- Gradinaru, G., Biliaderis, C.G., Kallithraka, S., Kefalas, P., Garcia-Viguera, C., 2003. Thermal stability of *Hibiscus sabdariffa* L. anthocyanins in solution and in solid state: Effects of copigmentation and glass transition. Food Chem. 83, 423–436.  
[https://doi.org/10.1016/S0308-8146\(03\)00125-0](https://doi.org/10.1016/S0308-8146(03)00125-0)
- Hatami, T., Meireles, M.A.A., Ciftci, O.N., 2019. Supercritical carbon dioxide extraction of lycopene from tomato processing by-products: Mathematical modeling and optimization. J. Food Eng. 241, 18–25.  
<https://doi.org/10.1016/j.jfoodeng.2018.07.036>
- Honary, S., Zahir, F., 2013. Effect of Zeta Potential on the Properties of Nano-Drug Delivery Systems - A Review ( Part 2 ). Trop. J. Pharm. Res. 12, 265–273.  
<https://doi.org/http://dx.doi.org/10.4314/tjpr.v12i2.20>
- Ibañez, E., Kubátová, A., Señoráns, F.J., Cavero, S., Reglero, G., Hawthorne, S.B., 2003. Subcritical water extraction of antioxidant compounds from rosemary plants. J. Agric. Food Chem. 51, 375–382. <https://doi.org/10.1021/jf025878j>
- International coffee organization, 2017. World coffee consumption [WWW Document].

- URL [http://www.ico.org/trade\\_statistics.asp?section=Statistics](http://www.ico.org/trade_statistics.asp?section=Statistics) (accessed 5.16.18).
- Islam, T., Oliveira Barros De Alencar, M.V., Oliveira Ferreira Da Mata, A.M., Correia Jardim Paz, M.F., Matos, L.A., De Castro E Sousa, J.M., De Carvalho Melo-Cavalcante, A.A., 2016. Coffee: A health fuel-blot popular drinking. *Int. J. Pharm. Pharm. Sci.* 8, 1–7.
- Jeszka-Skowron, M., Stanisz, E., Paz De Peña, M., 2016. Relationship between antioxidant capacity, chlorogenic acids and elemental composition of green coffee. *LWT - Food Sci. Technol.* 73, 243–250. <https://doi.org/10.1016/j.lwt.2016.06.018>
- Jokic, S., Velic, D., Bilic, M., Ana Bucic-Kojic, Planinic, M., Tomasa, S., 2010. Modelling of the process of solid-liquid extraction of total polyphenols from soybeans. *Czech J. Food Sci.* 28, 206–212.
- Kaikake, K., Hoaki, K., Sunada, H., Dhakal, R.P., Baba, Y., 2007. Removal characteristics of metal ions using degreased coffee beans: Adsorption equilibrium of cadmium(II). *Bioresour. Technol.* 98, 2787–2791. <https://doi.org/10.1016/j.biortech.2006.02.040>
- Karmee, S.K., 2018. A spent coffee grounds based biorefinery for the production of biofuels, biopolymers, antioxidants and biocomposites. *Waste Manag.* 72, 240–254. <https://doi.org/10.1016/j.wasman.2017.10.042>
- Khan, M.K., Abert-Vian, M., Fabiano-Tixier, A.S., Dangles, O., Chemat, F., 2010. Ultrasound-assisted extraction of polyphenols (flavanone glycosides) from orange (*Citrus sinensis* L.) peel. *Food Chem.* 119, 851–858. <https://doi.org/10.1016/j.foodchem.2009.08.046>
- Kim, J.H., Kim, Y., Kim, Y.J., Park, Y., 2016. Conjugated Linoleic Acid: Potential Health Benefits as a Functional Food Ingredient. *Annu. Rev. Food Sci. Technol.* 7, 221–244. <https://doi.org/10.1146/annurev-food-041715-033028>
- Kim, M.-S., Min, H.-G., Koo, N., Park, J., Lee, S.-H., Bak, G.-I., Kim, J.-G., 2014. The effectiveness of spent coffee grounds and its biochar on the amelioration of heavy metals-contaminated water and soil using chemical and biological assessments. *J. Environ. Manage.* 146, 124–130. <https://doi.org/10.1016/j.jenvman.2014.07.001>
- Kondamudi, N., Mohapatra, S.K., Misra, M., 2008. Spent Coffee Grounds as a Versatile

- Source of Green Energy. J. Agric. Food Chem. 56, 11757–11760.  
<https://doi.org/10.1021/jf802487s>
- Kourmentza, C., Economou, C.N., Tsafrakidou, P., Kornaros, M., 2018. Spent coffee grounds make much more than waste: Exploring recent advances and future exploitation strategies for the valorization of an emerging food waste stream. J. Clean. Prod. 172, 980–992. <https://doi.org/10.1016/j.jclepro.2017.10.088>
- Kovalcik, A., Obruca, S., Marova, I., 2018. Valorization of spent coffee grounds: A review. Food Bioprod. Process. 110, 104–119. <https://doi.org/10.1016/j.fbp.2018.05.002>
- Kučera, L., Papoušek, R., Kurka, O., Barták, P., Bednář, P., 2016. Study of composition of espresso coffee prepared from various roast degrees of *Coffea arabica* L. coffee beans. Food Chem. 199, 727–735.  
<https://doi.org/10.1016/j.foodchem.2015.12.080>
- Laine, P., Kylli, P., Heinonen, M., Jouppila, K., 2008. Storage Stability of Microencapsulated Cloudberry (*Rubus chamaemorus*) Phenolics. J. Agric. Food Chem. 56, 11251–11261. <https://doi.org/10.1021/jf801868h>
- Lamine, S.M., Ridha, C., Mahfoud, H.M., Mouad, C., Lotfi, B., Al-Dujaili, A.H., 2014. Chemical activation of an activated carbon prepared from coffee residue. Energy Procedia 50, 393–400. <https://doi.org/10.1016/j.egypro.2014.06.047>
- Leopoldini, M., Russo, N., Toscano, M., 2011. The molecular basis of working mechanism of natural polyphenolic antioxidants. Food Chem. 125, 288–306.  
<https://doi.org/10.1016/j.foodchem.2010.08.012>
- Li, X., Strezov, V., Kan, T., 2014. Energy recovery potential analysis of spent coffee grounds pyrolysis products. J. Anal. Appl. Pyrolysis 110, 79–87.  
<https://doi.org/10.1016/j.jaap.2014.08.012>
- Li, Z., Agellon, L.B., Allen, T.M., Umeda, M., Jewell, L., Mason, A., Vance, D.E., 2006. The ratio of phosphatidylcholine to phosphatidylethanolamine influences membrane integrity and steatohepatitis. Cell Metab. 3, 321–331.  
<https://doi.org/10.1016/j.cmet.2006.03.007>
- Liang, N., Xue, W., Kennepohl, P., Kitts, D.D., 2016. Interactions between major chlorogenic acid isomers and chemical changes in coffee brew that affect antioxidant activities. Food Chem. 213, 251–259.

- <https://doi.org/10.1016/j.foodchem.2016.06.041>
- Liu, B., Zeng, J., Chen, C., Liu, Y., Ma, H., Mo, H., Liang, G., 2016. Interaction of cinnamic acid derivatives with  $\beta$ -cyclodextrin in water: Experimental and molecular modeling studies. *Food Chem.* 194, 1156–1163.
- <https://doi.org/10.1016/j.foodchem.2015.09.001>
- Ludwig, I.A., Sanchez, L., Caemmerer, B., Kroh, L.W., Paz De Peña, M., Cid, C., 2012. Extraction of coffee antioxidants: Impact of brewing time and method. *Food Res. Int.* 48, 57–64. <https://doi.org/10.1016/j.foodres.2012.02.023>
- Mariotti-Celis, M.S., Martínez-Cifuentes, M., Huamán-Castilla, N., Vargas-González, M., Pedreschi, F., Pérez-Correa, J.R., 2018. The antioxidant and safety properties of spent coffee ground extracts impacted by the combined hot pressurized liquid extraction–resin purification process. *Molecules* 23, 1–11.
- <https://doi.org/10.3390/molecules23010021>
- Martín, L., González-Coloma, A., Adami, R., Scognamiglio, M., Reverchon, E., Porta, G. Della, Urieta, J.S., Mainar, A.M., 2011. Supercritical antisolvent fractionation of ryanodol from *Persea indica*. *J. Supercrit. Fluids* 60, 16–20.
- <https://doi.org/10.1016/j.supflu.2011.03.012>
- Mata, T.M., Martins, A.A., Caetano, N.S., 2018. Bio-refinery approach for spent coffee grounds valorization. *Bioresour. Technol.* 247, 1077–1084.
- <https://doi.org/10.1016/j.biortech.2017.09.106>
- Medina-Torres, L., Santiago-Adame, R., Calderas, F., Gallegos-Infante, J.A., Rocha-Guzman, N.E., Nunez-Ramirez, D.M., Bernard-Bernard, M.J., Manero, O., 2016. Microencapsulation by spray drying of laurel infusions ( *Litsea glaucescens* ) with maltodextrin. *Ind. Crop. Prod.* 90, 1–8.
- <https://doi.org/10.1016/j.indcrop.2016.06.009>
- Mekki, A., Dhouib, A., Sayadi, S., 2007. Polyphenols dynamics and phytotoxicity in a soil amended by olive mill wastewaters. *J. Environ. Manage.* 84, 134–140.
- <https://doi.org/10.1016/j.jenvman.2006.05.015>
- Meneses, M.A., Caputo, G., Scognamiglio, M., Reverchon, E., Adami, R., 2015. Antioxidant phenolic compounds recovery from *Mangifera indica* L. by-products by supercritical antisolvent extraction. *J. Food Eng.* 163, 45–53.

- <https://doi.org/10.1016/j.jfoodeng.2015.04.025>
- Michelon, M., Rocha Bernardes Oliveira, D., De Figueiredo Furtado, G., Gaziola de la Torre, L., Lopes Cunha, R., 2017. Biointerfaces High-throughput continuous production of liposomes using hydrodynamic flow-focusing microfluidic devices. *Colloids Surfaces B Biointerfaces* 156, 349–357.  
<https://doi.org/10.1016/j.colsurfb.2017.05.033>
- Moon, J.-K., Yoo, S.H., Shibamoto, T., 2009. Role of roasting conditions in the level of chlorogenic acid content in coffee beans: Correlation with coffee acidity. *J. Agric. Food Chem.* 57, 5365–5369. <https://doi.org/10.1021/jf900012b>
- Morales, F.J., Fernández-Fraguas, C., Jiménez-Pérez, S., 2005. Iron-binding ability of melanoidins from food and model systems. *Food Chem.* 90, 821–827.  
<https://doi.org/10.1016/j.foodchem.2004.05.030>
- Moreira, A.S.P., Nunes, F.M., Domingues, M.R., Coimbra, M.A., 2012. Coffee melanoidins: Structures, mechanisms of formation and potential health impacts. *Food Funct.* 3, 903–915. <https://doi.org/10.1039/c2fo30048f>
- Mozafari, M.R., Khosravi-Darani, K., Borazan, G.G., Cui, J., Pardakhty, A., Yurdugul, S., 2008. Encapsulation of food ingredients using nanoliposome technology. *Int. J. Food Prop.* 11, 833–844. <https://doi.org/10.1080/10942910701648115>
- Mumin, A., Akhter, K.F., Abedin, Z., Hossain, Z., 2006. Determination and Characterization of Caffeine in Tea , Coffee and Soft Drinks by Solid Phase Extraction and High Performance Liquid Chromatography (SPE–HPLC). *Malaysian J. Chem.* 8, 45–51.
- Munin, A., Edwards-Lévy, F., 2011. Encapsulation of Natural Polyphenolic Compounds; a Review. *Pharmaceutics* 3, 793–829.  
<https://doi.org/10.3390/pharmaceutics3040793>
- Murthy, P.S., Naidu, M.M., 2012. Sustainable management of coffee industry by-products and value addition—A review. *Resour. Conserv. Recycl.* 66, 45–58.  
<https://doi.org/10.1016/j.resconrec.2012.06.005>
- Mussatto, S.I., Ballesteros, L.F., Martins, S., Teixeira, J.A., 2011a. Extraction of antioxidant phenolic compounds from spent coffee grounds. *Sep. Purif. Technol.* 83, 173–179.  
<https://doi.org/10.1016/j.seppur.2011.09.036>

- Mussatto, S.I., Carneiro, L.M., Silva, J.P.A., Roberto, I.C., Teixeira, J.A., 2011b. A study on chemical constituents and sugars extraction from spent coffee grounds. *Carbohydr. Polym.* 83, 368–374. <https://doi.org/10.1016/j.carbpol.2010.07.063>
- Mussatto, S.I., Machado, E.M.S., Martins, S., Teixeira, J.A., 2011c. Production, Composition, and Application of Coffee and Its Industrial Residues. *Food Bioprocess Technol.* 4, 661–672. <https://doi.org/10.1007/s11947-011-0565-z>
- Mustafa, A., Turner, C., 2011. Pressurized liquid extraction as a green approach in food and herbal plants extraction: A review. *Anal. Chim. Acta* 703, 8–18. <https://doi.org/10.1016/j.aca.2011.07.018>
- Mustapa, A.N., Martin, A., Gallego, J.R., Mato, R.B., Cocero, M.J., 2015. Microwave-assisted extraction of polyphenols from *Clinacanthus nutans Lindau* medicinal plant: Energy perspective and kinetics modeling. *Chem. Eng. Process. Process Intensif.* 97, 66–74. <https://doi.org/10.1016/j.cep.2015.08.013>
- Muthanna, J.M., Al-Bayati, F.A., 2009. Isolation, identification and purification of caffeine from *Coffea arabica L.* and *Camellia sinensis L.*: A combination antibacterial study. *Int. J. Green Pharm.* 52–57. <https://doi.org/10.4103/0973-8258.49375>
- Nallamuthu, I., Devi, A., Khanum, F., 2015. Chlorogenic acid loaded chitosan nanoparticles with sustained release property, retained antioxidant activity and enhanced bioavailability. *Asian J. Pharm. Sci.* 10, 203–211. <https://doi.org/10.1016/j.ajps.2014.09.005>
- Naz, S., Sheikh, H., Siddiqi, R., Sayeed, S.A., 2004. Oxidative stability of olive , corn and soybean oil under different conditions. *Food Chem.* 88, 253–259. <https://doi.org/10.1016/j.foodchem.2004.01.042>
- Nunes, F.M., Coimbra, M.A., 2010. Role of hydroxycinnamates in coffee melanoidin formation. *Phytochem. Rev.* 9, 171–185. <https://doi.org/10.1007/s11101-009-9151-7>
- Okos, M.R., Campanella, O., Narsimhan, G., Singh, R.K., Weitnauer, A., 2006. Food Dehydration, in: Heldman, Dennis R; Lund, D. (Ed.), *Handbook of Food Engineering*, Second Edition. Boca Raton, pp. 601–744. <https://doi.org/10.1201/9781420014372>
- Oliveira, W.E., Franca, A.S., Oliveira, L.S., Rocha, S.D., 2008. Untreated coffee husks as



- biosorbents for the removal of heavy metals from aqueous solutions. *J. Hazard. Mater.* 152, 1073–1081. <https://doi.org/10.1016/j.jhazmat.2007.07.085>
- Ostovan, A., Ghaedi, M., Arabi, M., 2018. Fabrication of water-compatible superparamagnetic molecularly imprinted biopolymer for clean separation of baclofen from bio-fluid samples: A mild and green approach. *Talanta* 179, 760–768. <https://doi.org/10.1016/j.talanta.2017.12.017>
- Otake, K., Shimomura, T., Goto, T., Imura, T., Furuya, T., Yoda, S., Takebayashi, Y., Sakai, H., Abe, M., 2006. Preparation of Liposomes Using an Improved Supercritical Reverse Phase Evaporation Method 2543–2550. <https://doi.org/10.1021/la051654u>
- Paini, M., Aliakbarian, B., Casazza, A.A., Lagazzo, A., Botter, R., Perego, P., 2015a. Microencapsulation of phenolic compounds from olive pomace using spray drying: A study of operative parameters. *LWT - Food Sci. Technol.* 62, 177–186. <https://doi.org/10.1016/j.lwt.2015.01.022>
- Paini, M., Daly, S.R., Aliakbarian, B., Fathi, A., Arab Tehrani, E., Perego, P., Dehghani, F., Valtchev, P., 2015b. An efficient liposome based method for antioxidants encapsulation. *Colloids Surfaces B Biointerfaces* 136, 1067–1072.
- Panusa, A., Zuorro, A., Lavecchia, R., Marrosu, G., Petrucci, R., 2013. Recovery of Natural Antioxidants from Spent Coffee Grounds. *J. Agric. Food Chem.* 61, 4162–4168. <https://doi.org/10.1021/jf4005719>
- Patil, Y.P., Jadhav, S., 2014. Novel methods for liposome preparation. *Chem. Phys. Lipids* 177, 8–18. <https://doi.org/10.1016/j.chemphyslip.2013.10.011>
- Pavlovic, M.D., Buntic, A. V, Siler-Marinkovic, S.S., Dimitrijevic-Brankovic, S.I., 2013. Ethanol influenced fast microwave-assisted extraction for natural antioxidants obtaining from spent filter coffee. *Sep. Purif. Technol.* 118, 503–510. <https://doi.org/10.1016/j.seppur.2013.07.035>
- Peleg, M., 1988. An Empirical Model for the Description of Moisture Sorption Curves. *J. Food Sci.* 53,4, 1216–1217. <https://doi.org/10.1111/j.1365-2621.1988.tb13565.x>
- Perez, E.E., Carelli, A.A., Crapiste, G.H., 2011. Temperature-dependent diffusion coefficient of oil from different sunflower seeds during extraction with hexane. *J. Food Eng.* 105, 180–185. <https://doi.org/10.1016/j.jfoodeng.2011.02.025>

- Pettinato, M., Aliakbarian, B., Casazza, A.A., Perego, P., 2017. Encapsulation of Antioxidants from Spent Coffee Ground Extracts by Spray Drying. *Ital. Assoc. Chem. Eng.* 57, 1219–1224. <https://doi.org/10.3303/CET1757204>
- Pettinato, M., Casazza, A.A., Ferrari, P.F., Palombo, D., Perego, P., 2019a. Eco-sustainable recovery of antioxidants from spent coffee grounds by microwave-assisted extraction: Process optimization, kinetic modeling and biological validation. *Food Bioprod. Process.* 114, 31–42. <https://doi.org/10.1016/j.fbp.2018.11.004>
- Pettinato, M., Casazza, A.A., Perego, P., 2019b. The role of heating step in microwave-assisted extraction of polyphenols from spent coffee grounds. *Food Bioprod. Process.* 114, 227–234. <https://doi.org/10.1016/j.fbp.2019.01.006>
- Poling, B.E., Thomson, G.H., Friend, D.G., Wilding, V.W., 2008. Physical and chemical data, in: Green, D.W., Perry, R.H. (Eds.), *Perry's Chemical Engineers' Handbook*. McGraw-Hill, New York, p. 410. <https://doi.org/10.1036/0071422943>
- Prasanthi, J.R.P., Dasari, B., Marwarha, G., Larson, T., Chen, X., Geiger, J.D., Ghribi, O., 2010. Caffeine protects against oxidative stress and Alzheimer's disease-like pathology in rabbit hippocampus induced by cholesterol-enriched diet. *Free Radic. Biol. Med.* 49, 1212–1220. <https://doi.org/10.1016/j.freeradbiomed.2010.07.007>
- Pujol, D., Liu, C., Gominho, J., Olivella, M.A., Fiol, N., Villaescusa, I., Pereira, H., 2013. The chemical composition of exhausted coffee waste. *Ind. Crops Prod.* 50, 423–429. <https://doi.org/10.1016/j.indcrop.2013.07.056>
- Rabelo, R.S., MacHado, M.T.C., Martínez, J., Hubinger, M.D., 2016. Ultrasound assisted extraction and nanofiltration of phenolic compounds from artichoke solid wastes. *J. Food Eng.* 178, 170–180. <https://doi.org/10.1016/j.jfoodeng.2016.01.018>
- Rafiee, Z., Barzegar, M., Sahari, A.M., Maherani, B., 2017a. Nanoliposomal carriers for improvement the bioavailability of high – valued phenolic compounds of pistachio green hull extract. *Food Chem.* 220, 115–122. <https://doi.org/10.1016/j.foodchem.2016.09.207>
- Rafiee, Z., Barzegar, M., Sahari, A.M., Maherani, B., 2017b. Nanoliposomal carriers for improvement the bioavailability of high – valued phenolic compounds of pistachio green hull extract. *Food Chem.* 220, 115–122. <https://doi.org/10.1016/j.foodchem.2016.09.207>

- Ramalakshmi, K., Rao, L.J.M., Takano-Ishikawa, Y., Goto, M., 2009. Bioactivities of low-grade green coffee and spent coffee in different in vitro model systems. *Food Chem.* 115, 79–85. <https://doi.org/10.1016/j.foodchem.2008.11.063>
- Ramos Pacioni, T., Soares, D., Di Domenico, M., Rosa, M.F., Moreira, R. de F.P.M., José, H.J., 2016. Bio-syngas production from agro-industrial biomass residues by steam gasification. *Waste Manag.* 58, 221–229. <https://doi.org/10.1016/j.wasman.2016.08.021>
- Ranheim, T., Halvorsen, B., 2005. Coffee consumption and human health - beneficial or detrimental? - Mechanisms for effects of coffee consumption on different risk factors for cardiovascular disease and type 2 diabetes mellitus. *Mol. Nutr. Food Res.* 49, 274–284. <https://doi.org/10.1002/mnfr.200400109>
- Ranic, M., Nikolic, M., Pavlovic, M., Buntic, A., Siler-Marinkovic, S., Dimitrijevic-Brankovic, S., 2014. Optimization of microwave-assisted extraction of natural antioxidants from spent espresso coffee grounds by response surface methodology. *J. Clean. Prod.* 80, 69–79.
- Re, R., Pellegrini, N., Proteggente, A., Pannala, A., Yang, M., Rice-Evans, C., 1999. Antioxidant Activity Applying an Improved Abts Radical Cation Decolorization Assay. *Free Radic. Biol. Med.* 26, 1231–1237. [https://doi.org/10.1016/S0891-5849\(98\)00315-3](https://doi.org/10.1016/S0891-5849(98)00315-3)
- Reverchon, E., De Marco, I., 2006. Supercritical fluid extraction and fractionation of natural matter. *J. Supercrit. Fluids* 38, 146–166. <https://doi.org/10.1016/j.supflu.2006.03.020>
- Rice-Evans, C., Miller, N.J., Paganga, G., 1996. Structure-antioxidant activity relationships of flavonoids and phenolic acids. *Free Radic. Biol. Med.* 20, 933–956. <https://doi.org/10.1103/PhysRevB.91.075109>
- Robert, P., Gorena, T., Romero, N., Sepulveda, E., Chavez, J., Saenz, C., 2010. Encapsulation of polyphenols and anthocyanins from pomegranate (*Punica granatum*) by spray drying. *Int. J. Food Sci. Technol.* 45, 1386–1394. <https://doi.org/10.1111/j.1365-2621.2010.02270.x>
- Rodrigues, F., Palmeira-de-Oliveira, A., Das Neves, J., Sarmento, B., Amaral, M.H., Oliveira, M.B.P.P., 2015. Coffee silverskin: A possible valuable cosmetic ingredient.

- Pharm. Biol. 53, 386–394. <https://doi.org/10.3109/13880209.2014.922589>
- Roselló-Soto, E., Barba, F.J., Parniakov, O., Galanakis, C.M., Lebovka, N., Grimi, N., Vorobiev, E., 2015. High Voltage Electrical Discharges, Pulsed Electric Field, and Ultrasound Assisted Extraction of Protein and Phenolic Compounds from Olive Kernel. *Food Bioprocess Technol.* 8, 885–894. <https://doi.org/10.1007/s11947-014-1456-x>
- Sabir, M.A., Sosulski, F.W., Finlayson, A.J., 1974. Chlorogenic Acid-Protein Interactions in Sunflower. *J. Agric. Food Chem.* 22, 575–578.  
<https://doi.org/10.1021/jf60194a052>
- Safarik, I., Horska, K., Svobodova, B., Safarikova, M., 2012. Magnetically modified spent coffee grounds for dyes removal. *Eur Food Res Technol* 234, 345–350. <https://doi.org/10.1007/s00217-011-1641-3>
- Sahin, S., Samli, R., Tan, A.S.B., Barba, F.J., Chemat, F., Cravotto, G., Lorenzo, J.M., 2017. Solvent-free microwave-assisted extraction of polyphenols from olive tree leaves: Antioxidant and antimicrobial properties. *Molecules* 22, 1–13.  
<https://doi.org/10.3390/molecules22071056>
- Sant’Anna, V., Brandelli, A., Marczak, L.D.F., Tessaro, I.C., 2012. Kinetic modeling of total polyphenol extraction from grape marc and characterization of the extracts. *Sep. Purif. Technol.* 100, 82–87. <https://doi.org/10.1016/j.seppur.2012.09.004>
- Santo, I.E., Campardelli, R., Albuquerque, E.C., de Melo, S.V., Della Porta, G., Reverchon, E., 2014. Liposomes preparation using a supercritical fluid assisted continuous process. *Chem. Eng. J.* 249, 153–159. <https://doi.org/10.1016/j.cej.2014.03.099>
- Sebaaly, C., Jraij, A., Fessi, H., Charcosset, C., Greige-Gerges, H., 2015. Preparation and characterization of clove essential oil-loaded liposomes. *Food Chem.* 178, 52–62. <https://doi.org/10.1016/j.foodchem.2015.01.067>
- Serrano-Gomez, J., Lopez-Gonzalez, H., Olguin, M.T., Bulbulian, S., 2015. Carbonaceous material obtained from exhausted coffee by an aqueous solution combustion process and used for cobalt (II) and cadmium (II) sorption. *J. Environ. Manage.* 156, 121–127. <https://doi.org/10.1016/j.jenvman.2015.03.013>
- Severini, C., Derossi, A., Fiore, A.G., 2017. Ultrasound-assisted extraction to improve the recovery of phenols and antioxidants from spent espresso coffee ground: a study

- by response surface methodology and desirability approach. *Eur. Food Res. Technol.* 243, 835–847. <https://doi.org/10.1007/s00217-016-2797-7>
- Sezonov, G., Joseleau-Petit, D., D'Ari, R., 2007. *Escherichia coli* physiology in Luria-Bertani broth. *J. Bacteriol.* 189, 8746–8749. <https://doi.org/10.1128/JB.01368-07>
- Shahidi, F., 2000. Antioxidants in food and food antioxidants. *Nahrung* 44, 158–163.
- Shalmashi, A., Golmohammad, F., 2010. Solubility of caffeine in water, ethyl acetate, ethanol, carbon tetrachloride, methanol, chloroform, dichloromethane, and acetone between 298 and 323 K. *Lat. Am. Appl. Res.* 40, 283–285.
- Shang, Y.F., Xu, J.L., Lee, W.J., Um, B.H., 2017. Antioxidative polyphenolics obtained from spent coffee grounds by pressurized liquid extraction. *South African J. Bot.* 109, 75–80. <https://doi.org/10.1016/j.sajb.2016.12.011>
- Shao, P., Zhang, J., Fang, Z., Sun, P., 2014. Complexing of chlorogenic acid with  $\beta$ -cyclodextrins: Inclusion effects, antioxidative properties and potential application in grape juice. *Food Hydrocoll.* 41, 132–139. <https://doi.org/10.1016/j.foodhyd.2014.04.003>
- Shapla, U.M., Solayman, M., Alam, N., Khalil, M.I., Gan, S.H., 2018. 5-Hydroxymethylfurfural (HMF) levels in honey and other food products: effects on bees and human health. *Chem. Cent. J.* 12, 1–18. <https://doi.org/10.1186/s13065-018-0408-3>
- Shirsath, S.R., Sonawane, S.H., Gogate, P.R., 2012. Intensification of extraction of natural products using ultrasonic irradiations-A review of current status. *Chem. Eng. Process. Process Intensif.* 53, 10–23. <https://doi.org/10.1016/j.cep.2012.01.003>
- Shrigod, N.M., Swami Hulle, N.R., Prasad, R. V., 2017. Supercritical fluid extraction of essential oil from mint leaves (*Mentha spicata*): Process optimization and its quality evaluation. *J. Food Process Eng.* 40, 1–9. <https://doi.org/10.1111/jfpe.12488>
- Silva, M.A., Nebra, S.A., Machado Silva, M.J., Sanchez, C.G., 1998. The use of biomass residues in the Brazilian soluble coffee industry. *Biomass and Bioenergy* 14, 457–467. [https://doi.org/10.1016/S0961-9534\(97\)10034-4](https://doi.org/10.1016/S0961-9534(97)10034-4)
- Simić, V.M., Rajković, K.M., Stojičević, S.S., Veličković, D.T., Nikolić, N., Lazić, M.L., Karabegović, I.T., 2016. Optimization of microwave-assisted extraction of total

- polyphenolic compounds from chokeberries by response surface methodology and artificial neural network. *Sep. Purif. Technol.* 160, 89–97.  
<https://doi.org/10.1016/j.seppur.2016.01.019>
- Sosa, M. V., Rodríguez-Rojo, S., Mattea, F., Cismondi, M., Cocero, M.J., 2011. Green tea encapsulation by means of high pressure antisolvent coprecipitation. *J. Supercrit. Fluids* 56, 304–311. <https://doi.org/10.1016/j.supflu.2010.10.038>
- Spigno, G., De Faveri, D.M., 2009. Microwave-assisted extraction of tea phenols: A phenomenological study. *J. Food Eng.* 93, 210–217.  
<https://doi.org/10.1016/j.jfoodeng.2009.01.006>
- Spigno, G., Tramelli, L., De Faveri, D.M., 2007. Effects of extraction time, temperature and solvent on concentration and antioxidant activity of grape marc phenolics. *J. Food Eng.* 81, 200–208. <https://doi.org/10.1016/j.jfoodeng.2006.10.021>
- Spiro, M., Jago, D.S., 1982. Kinetics and Equilibria of Tea Infusion. *J. Chem. Soc., Faraday Trans. 1* 78, 295–305. <https://doi.org/10.1039/F19827800295>
- Svarovsky, L., 2000. Characterization of particles suspended in liquids, in: Svarovsky, L. (Ed.), *Solid-Liquid Separation*. Butterworth-Heinemann, Oxford, pp. 30–65.
- Swain, T., Hillis, W.E., 1959. The phenolic constituent of *Prunus domestica*. The quantitative analysis of phenolic constituents. *J. Sci. Food Agric.* 10, 63–68.
- Takahashi, M., Inafuku, K., Miyagi, T., Oku, H., Wada, K., Imura, T., Kitamoto, D., 2007. Efficient preparation of liposomes encapsulating food materials using lecithins by a mechanochemical method. *J. Oleo Sci.* 56, 35–42.  
<https://doi.org/10.5650/jos.56.35>
- Taylor, J., Taylor, J.R.N., Belton, P.S., Amanda, M., 2009. Kafirin microparticle encapsulation of catechin and sorghum condensed tannins. *J. Agric. Food Chem.* 57, 7523–7528. <https://doi.org/10.1021/jf901592q>
- The European Commission, 2014. Communication from the commission to the European Parliament, the Council, the European economic and social committee and the committee of the regions. Towards a circular economy: A zero waste programme for Europe [WWW Document]. URL <https://eur-lex.europa.eu/legal-content/en/txt/?uri=celex%3A52014dc0398>, (accessed 5.16.18).
- Tolun, A., Altintas, Z., Artik, N., 2016. Microencapsulation of grape polyphenols using

- maltodextrin and gum arabic as two alternative coating materials : Development and characterization. *J. Biotechnol.* 239, 23–33.  
<https://doi.org/10.1016/j.jbiotec.2016.10.001>
- Trucillo, P., Campardelli, R., Aliakbarian, B., Perego, P., Reverchon, E., 2018. Supercritical assisted process for the encapsulation of olive pomace extract into liposomes. *J. Supercrit. Fluids* 135, 152–159. <https://doi.org/10.1016/j.supflu.2018.01.018>
- Trucillo, P., Campardelli, R., Reverchon, E., 2018. Production of liposomes loaded with antioxidants using a supercritical CO<sub>2</sub>-assisted process. *Powder Technol.* 323, 155–162. <https://doi.org/10.1016/j.powtec.2017.10.007>
- Tsai, W.T., Liu, S.C., Hsieh, C.H., 2012. Preparation and fuel properties of biochars from the pyrolysis of exhausted coffee residue. *J. Anal. Appl. Pyrolysis* 93, 63–67.  
<https://doi.org/10.1016/j.jaap.2011.09.010>
- Valderez Ponte Rocha, M., Brandão Lima de Matos, L.J., Pinto de Lima, L., da Silva Figueiredo, P.M., Lucena, I.L., Fernandes, F.A.N., Rocha Barros Gonçalves, L., 2014. Ultrasound-assisted production of biodiesel and ethanol from spent coffee grounds. *Bioresour. Technol.* 167, 343–348.  
<https://doi.org/10.1016/j.biortech.2014.06.032>
- Valizadeh Kiamahalleh, M., Najafpour-Darzi, G., Rahimnejad, M., Moghadamnia, A.A., Valizadeh Kiamahalleh, M., 2016. High performance curcumin subcritical water extraction from turmeric (*Curcuma longa* L.). *J. Chromatogr. B Anal. Technol. Biomed. Life Sci.* 1022, 191–198. <https://doi.org/10.1016/j.jchromb.2016.04.021>
- Veggi, P.C., Martinez, J., Meireles, M.A.A., 2013. Fundamentals of Microwave Extraction, in: Chemat, F., Cravotto, G. (Eds.), *Microwave-Assisted Extraction for Bioactive Compounds*. Springer US, New York, pp. 15–52. <https://doi.org/10.1007/978-1-4614-4830-3>
- Visentin, A., Rodríguez-Rojo, S., Navarrete, A., Maestri, D., Cocero, M.J., 2012. Precipitation and encapsulation of rosemary antioxidants by supercritical antisolvent process. *J. Food Eng.* 109, 9–15.  
<https://doi.org/10.1016/j.jfoodeng.2011.10.015>
- Wadhawan, M., Anand, A.C., 2016. Coffee and Liver Disease. *J. Clin. Exp. Hepatol.* 6, 40–46. <https://doi.org/10.1016/j.jceh.2016.02.003>

- Wijngaard, H., Hossain, M.B., Rai, D.K., Brunton, N., 2012. Techniques to extract bioactive compounds from food by-products of plant origin. *Food Res. Int.* 46, 505–513. <https://doi.org/10.1016/j.foodres.2011.09.027>
- Xu, H., Wang, W., Liu, X., Yuan, F., Gao, Y., 2015. Antioxidative phenolics obtained from spent coffee grounds (*Coffea arabica* L.) by subcritical water extraction. *Ind. Crops Prod.* 76, 946–954. <https://doi.org/10.1016/j.indcrop.2015.07.054>
- Yamane, K., Kono, M., Fukunaga, T., Iwai, K., Sekine, R., Watanabe, Y., Iijima, M., 2014. Field Evaluation of Coffee Grounds Application for Crop Growth Enhancement , Weed Control , and Soil Improvement. *Plant Prod. Sci.* 17, 93–102. <https://doi.org/10.1626/pp.17.93>
- Yang, J., Martinson, T.E., Liu, H.R., 2009. Phytochemical profiles and antioxidant activities of wine grapes. *Food Chem.* 116, 332–339. <https://doi.org/10.1016/j.foodchem.2009.02.021>
- Zabot, G.L., Silva, E.K., Azevedo, V.M., Meireles, M.A.A., 2016. Replacing modified starch by inulin as prebiotic encapsulant matrix of lipophilic bioactive compounds. *Food Res. Int.* 85, 26–35. <https://doi.org/10.1016/j.foodres.2016.04.005>
- Zhang, B., Yang, R., Liu, C.Z., 2008. Microwave-assisted extraction of chlorogenic acid from flower buds of *Lonicera japonica* Thunb. *Sep. Purif. Technol.* 62, 480–483. <https://doi.org/10.1080/00050068308255405>
- Zhang, M., Li, J., Zhang, L., Chao, J., 2009. Preparation and spectral investigation of inclusion complex of caffeic acid with hydroxypropyl- $\beta$ -cyclodextrin. *Spectrochim. Acta - Part A Mol. Biomol. Spectrosc.* 71, 1891–1895. <https://doi.org/10.1016/j.saa.2008.07.014>
- Zhou, Y., Raphael, R.M., 2007. Solution pH Alters Mechanical and Electrical Properties of Phosphatidylcholine Membranes : Relation between Interfacial Electrostatics , Intramembrane Potential , and Bending Elasticity. *Biophys. J.* 92, 2451–2462. <https://doi.org/10.1529/biophysj.106.096362>
- Zunin, P., Salvadeo, P., Boggia, R., Evangelisti, F., 2006. Sterol oxidation in meat- and fish-based homogenized baby foods containing vegetable oils. *J. AOAC Int.* 89, 441–446. <https://doi.org/10.2136/sssaj2016.06.0182>
- Zuorro, A., Lavecchia, R., 2013. Influence of extraction conditions on the recovery of



phenolic antioxidants from Spent Coffee Grounds. *Am. J. Appl. Sci.* 10, 478–486.  
<https://doi.org/10.3844/ajassp.2013.478.486>

Zuorro, A., Lavecchia, R., 2012. Spent coffee grounds as a valuable source of phenolic compounds and bioenergy. *J. Clean. Prod.* 34, 49–56.  
<https://doi.org/10.1016/j.jclepro.2011.12.003>